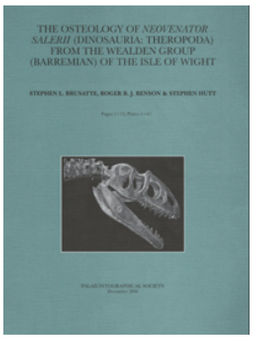

Monographs of the Palaeontographical Society

ISSN: (Print) (Online) Journal homepage: www.tandfonline.com/journals/tmps20

The Osteology of Neovenator Salerii (Dinosauria: Theropoda) From the Wealden Group (Barremian) of the Isle of Wight

Stephen L. Brusatte, Roger B. J. Benson & Stephen Hutt |

To cite this article: Stephen L. Brusatte, Roger B. J. Benson & Stephen Hutt | (2008) The Osteology of Neovenator Salerii (Dinosauria: Theropoda) From the Wealden Group (Barremian) of the Isle of Wight, Monographs of the Palaeontographical Society, 162:631, 1-75, DOI: 10.1080/25761900.2008.12452864

To link to this article: https://doi.org/10.1080/25761900.2008.12452864

Published online: 04 Nov 2024.

Submit your article to this journal

View related articles

Full Terms & Conditions of access and use can be found at
https://www.tandfonline.com/action/journalInformation?journalCode=tmps20

MONOGRAPH OF THE PALAEONTOGRAPHICAL SOCIETY

THE OSTEOLOGY OF *NEOVENATOR SALERII* (DINOSAURIA: THEROPODA) FROM THE WEALDEN GROUP (BARREMIAN) OF THE ISLE OF WIGHT

STEPHEN L. BRUSATTE, ROGER B. J. BENSON & STEPHEN HUTT

Pages 1–75; Plates 1–45

© THE PALAEONTOGRAPHICAL SOCIETY, LONDON
December 2008

Published online 04 Nov 2024

The Palaeontographical Society issues an annual volume of serially numbered publications; these may either be a single complete monograph or part of a continuing monograph.

Publication No. 631, issued as part of
Volume 162 for 2008

ISSN 0269-3445

Recommended reference to this publication:

BRUSATTE, S. L., BENSON, R. B. J. & HUTT, S. 2008. The osteology of *Neovenator salerii* (Dinosauria: Theropoda) from the Wealden Group (Barremian) of the Isle of Wight. *Monograph of the Palaeontographical Society*, London: 1–75, pls 1–45. (Publ. No. 631, part of Vol. 162 for 2008).

ABSTRACT

Neovenator salerii (Dinosauria: Theropoda), from the Early Cretaceous (Barremian) Wessex Formation (Wealden Group) of the Isle of Wight, is the most complete large theropod known from Europe. Here we present a complete description of the holotype and referred specimens, which together comprise approximately 70% of the skeleton. *Neovenator* possesses numerous autapomorphies and clearly belongs to Allosauroidea, a clade of basal tetanuran theropods that includes *Allosaurus*, *Sinraptor*, and the Carcharodontosauridae, a subgroup that contains some of the largest known theropods. Several synapomorphies support *Neovenator* as the basalmost member of Carcharodontosauridae. These are primarily features of the postcranial skeleton, indicating that large body size and the highly apomorphic skull of derived carcharodontosaurids evolved after changes to the axial and appendicular skeleton. This placement suggests that basal carcharodontosaurids were more widespread before becoming restricted to Gondwana later in their evolution.

Ostéologie de *Neovenator salerii* (Dinosauria: Theropoda) du Groupe du Wealdien (Barrémien) de l'Ile de Wight

RÉSUMÉ

Neovenator salerii (Dinosauria: Theropoda) de la Formation de Wessex (Groupe du Wealdien) du Crétacé inférieur de l'Ile de Wight, est le grand théropode le plus complet connu en Europe. Nous présentons ici une description complète de l'holotype et des spécimens rapportés à ce taxon, qui associés constituent environ 70% du squelette. *Neovenator* possède de nombreuses autapomorphies et appartient clairement aux Allosauroidea, un clade de théropodes Tetanurae basal qui inclut *Allosaurus*, *Sinraptor*, et les Carcharodontosauridae, un sous-groupe contenant certains des plus grands théropodes connus. Plusieurs synapomorphies soutiennent le placement de *Neovenator* à la base des Carcharodontosauridae. Ces dernières sont essentiellement issues du squelette postcrânien, et indiquent que la taille du corps et le crâne apomorphique des carcharodontosauridés plus dérivés a évolué après le squelette axial et appendiculaire. Ce rattachement suggère que les carcharodontosauridés basaux avaient une plus large répartition géographique avant de se restreindre au Gondwana, plus tard au cours de leur évolution. [Ronan Allain]

Die Osteologie von *Neovenator salerii* (Dinosauria: Theropoda) aus der Wealden-Gruppe (Barremium) der Isle of Wight

ZUSAMMENFASSUNG

Neovenator salerii (Dinosauria: Theropoda) aus der unterkretazischen (Barremium) Wessex-Formation (Wealden Group) der Isle of Wight ist der am vollständigsten erhaltene Theropode aus Europa. In dieser Arbeit geben wir eine vollständige Beschreibung des Holotyps und weiteren zugeordneten Materials, welche zusammen etwa 70% des Skelettes repräsentieren. *Neovenator* besitzt zahlreiche Autapomorphien und kann eindeutig den Allosauroidea zugeordnet werden, einer Gruppe basaler tetanurer Theropoden, die *Allosaurus*, *Sinraptor* und die Carcharodontosauriden umfasst. Zu den Carcharodontiden gehören einige der größten bekannten Theropoden. Verschiedene Synapomorphien bestätigen die Zuordnung von *Neovenator* als basalster Angehöriger der Carcharodontosauridae. Dabei handelt sich hauptsächlich um postcraniale Skelettmerkmale, die darauf hinweisen, dass die enorme Körpergröße und der hoch-apomorphe Schädel fortschrittlicher Carcharodontosauriden erst nach den Änderungen im Skelett des Körperstammes und der Gliedmaßen entstanden. Die Position von *Neovenator* weist darauf hin, dass basale Carcharodontosauriden zunächst eine weitere Verbreitung hatten und im Verlauf ihrer Evolution auf Gondwana beschränkt wurden. [Daniela Schwarz-Wings]

Остеология *Neovenator salerii* (Dinosauria: Theropoda) из баррэмской группы Вэлден острова Вайт

РЕЗЮМЕ

Neovenator salerii (Dinosauria: Theropoda) раннемеловой формации Вэссэкс (надгруппы Вэлден) острова Вайт в Великобритании является самым полным большим тероподом известным в Европе. В данной статье представлено полное описание голотипаи других экземпляров, рассматриваемых как *N. salerii* и вместе составляющих около 70% скелета. *Neovenator* имеет многочисленные автапоморфии и явно принадлежит Allosauroidea, кладу базальных тетанурских тероподов который также включает в себя *Allosaurus*, *Sinraptor* и Carcharodontosauridae, подгруппу, к которой принадлежат некоторые самые крупные известные тероподы. Некоторые синапоморфы показывают что *Neovenator* является самым базальным членом Carcharodontosauridae. Речь идет главным образом о признаках посткраниального скелета, указывающих, что величина тела и особенно апоморфный череп типичных кархародонтозавридов развились после изменений аксиального и аппендикулярного скелета. Это филогенетическое размещение указывает, что базальные кархародонтозавриды были широко распостранены (на других континентах), прежде чем их ареал распространения был ограничен Гондваной позже в своей эволюции. [David Marjanovic and Alexandra Snegurova]

Edited by D.K. LOYDELL

Made and printed in Great Britain
Origination by Michael Heath Print, London SE10 8PD

THE OSTEOLOGY OF *NEOVENATOR SALERII* (DINOSAURIA: THEROPODA) FROM THE WEALDEN GROUP (BARREMIAN) OF THE ISLE OF WIGHT

CONTENTS

	Page
INTRODUCTION	1
MATERIAL	2
ACKNOWLEDGEMENTS	3
GEOLOGICAL SETTING	3
HISTORY OF RESEARCH	6
SYSTEMATIC PALAEONTOLOGY	7
ANATOMICAL DESCRIPTION	10
SKULL	10
Premaxilla	10
Maxilla	12
Nasal	15
Palatine	16
Dentary	17
Dentition	18
AXIAL SKELETON	19
Atlas-axis complex	19
Axial intercentrum	19
Odontoid	21
Axis	21
Postaxial cervical vertebrae	22
Dorsal vertebrae	27
Sacral vertebrae	33
Caudal vertebrae	35
Chevrons	39
Ribs	40
Gastralia	41
APPENDICULAR SKELETON	41
Scapula-coracoid	41
Coracoid	43
Scapula	44
Pelvic girdle	44
Ilium	44
Pubis	46
Ischium	47
Femur	50
Tibia	53
Fibula	55
Pes	55
Metatarsals	56
Phalanges	59
DISCUSSION	60
PHYLOGENETIC RELATIONSHIPS OF *NEOVENATOR*	60
BIOGEOGRAPHICAL AND STRATIGRAPHICAL IMPLICATIONS	66
COMPARISON WITH OTHER WEALDEN GROUP THEROPODS	67
PATHOLOGIES OF *NEOVENATOR*	68
REFERENCES	70

INTRODUCTION

The Wealden Group of southern England has long been regarded as one of the most important Lower Cretaceous dinosaur-bearing units in the world. Dinosaur fossils have been known from the Wealden Group since at least the 1820s, and include a diverse assemblage of taxa that has formed the basis for wide-ranging anatomical, phylogenetic and palaeoecological studies. These taxa include some of the best-known British dinosaurs, such as *Baryonyx*, *Hypsilophodon*, *Iguanodon* and *Polacanthus*. Many of the Wealden dinosaurs were discovered and studied by some of the pioneering figures in British, and indeed global, palaeontology, including William Buckland, Gideon Mantell and Richard Owen. The descriptions and monographs published by these researchers helped introduce dinosaurs to both the scientific community and popular imagination, and established Great Britain as a centre of palaeontological research (Mantell 1825, 1841, 1848, 1849; Owen 1858, 1859, 1864, 1876). Today, many Wealden taxa originally described in the early–mid 1800s remain among the best-known dinosaurs worldwide.

In the past century and a half since this pioneering work, collectors and scientists have discovered several additional dinosaur taxa in the Wealden Group. More recently, within the past three decades, the Wealden Group has yielded several new theropod dinosaurs, including the spinosaurid *Baryonyx walkeri* (Charig & Milner 1986, 1997), the basal tyrannosauroid *Eotyrannus lengi* (Hutt *et al.* 2001), and the large allosauroid *Neovenator salerii* (Hutt *et al.* 1996; Text-fig. 1). The last taxon is known from the holotype (BMNH R10001, MIWG 6348) and two referred specimens (MIWG 5470, 6352) which together comprise *c.* 70% of the skeleton, making it the most complete large theropod dinosaur known from Europe. However, despite its

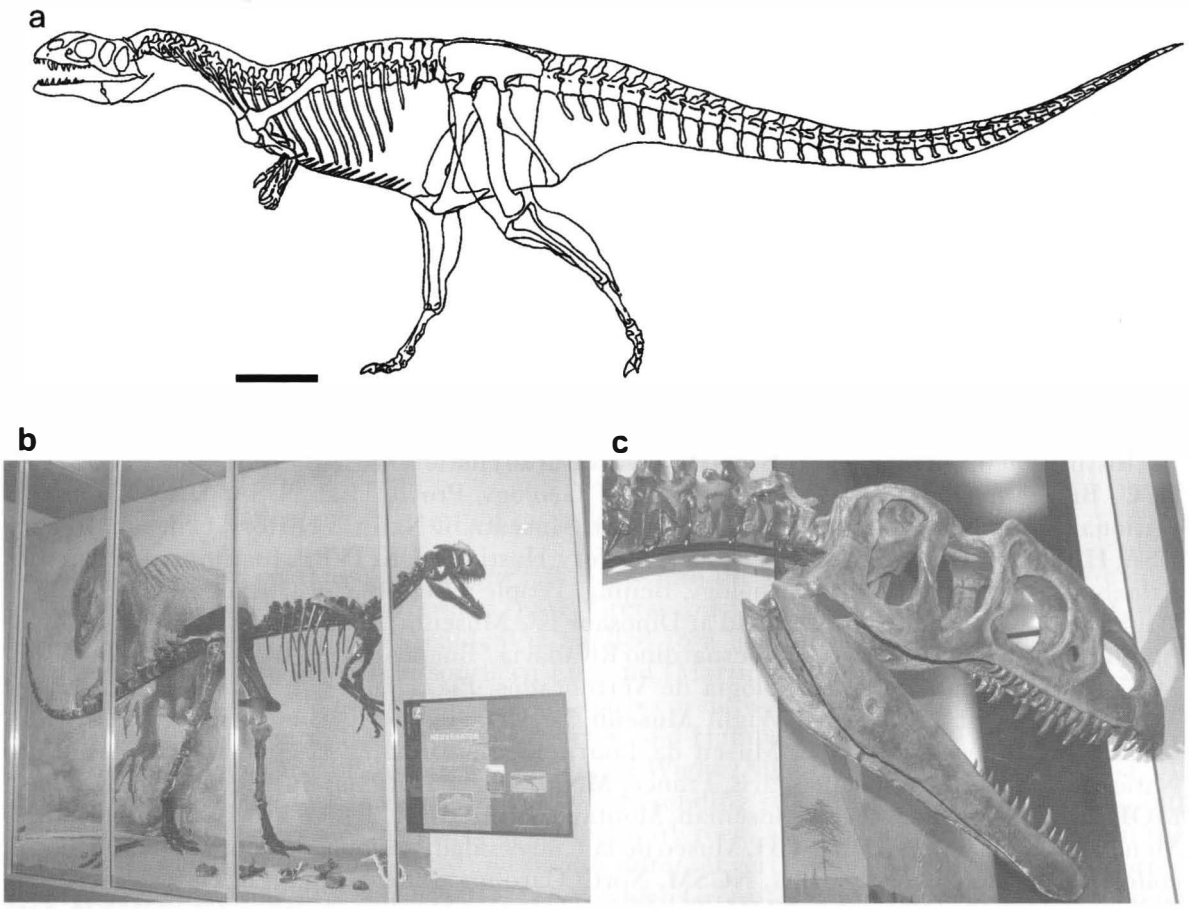

TEXT-FIG. 1. *Neovenator salerii* Hutt, Martill & Barker, 1996: **a**, reconstructed skeleton; **b**, mount of the holotype at the Dinosaur Isle Museum in Sandown; **c**, close-up of mounted skull reconstruction. Scale bar represents 0.5 m.

completeness, *Neovenator* has only been briefly described in the literature (Hutt *et al.* 1996; Naish *et al.* 2001). A more complete description formed the subject of the M.Phil. thesis of Hutt (1999), which has been distributed to many theropod dinosaur researchers, but remains unpublished. These workers have concluded that *Neovenator* is a member of Allosauroidea, a clade of basal tetanuran theropods that includes *Allosaurus* from North America and Europe, *Sinraptor* from Asia, and Carcharodontosauridae, a mainly Gondwanan subgroup which contains some of the largest theropods to have lived. However, the lack of a more complete anatomical description has hampered attempts to include this taxon in wider studies of theropod anatomy, phylogeny, and evolution. This is especially problematical, as the well-preserved skeleton of *Neovenator* possesses abundant anatomical information from a poorly known time period and biogeographical region in the evolution of theropod dinosaurs.

Here we present a monograph on *Neovenator salerii*, which includes a complete osteological description of all known specimens coupled with numerous illustrations and photographs. Based on our anatomical description and comparisons with other taxa we comment on the phylogenetic position of *Neovenator* and its importance for understanding theropod phylogeny, character evolution, biogeography, and palaeoecology. This is primarily intended to be a thorough and rigorous description of the skeletal osteology of a single theropod taxon. Along with similar recent monographs (Madsen 1976; Welles 1984; Charig & Milner 1997; Currie & Zhao 1993; Harris 1998; Madsen & Welles 2000; Brochu 2002; Sampson & Krause 2007) we aim to provide primary descriptive data that can be incorporated into wider studies of theropod evolution, especially phylogenetic analyses which frequently exclude *Neovenator* despite its completeness and biogeographical importance.

Writing this monograph necessitated considerable division of labour. SH excavated and initially described many of the specimens, and began the march toward a monograph with his 1999 M.Phil. thesis. SLB initiated and coordinated the current project. SLB and RBJB wrote the manuscript, with SLB focusing on the cranial, axial (sacral vertebrae, gastralia, and ribs), pectoral, pelvic, fibular, and pedal material and RBJB focusing on the teeth, vertebrae, femur, and tibia. RBJB photographed most of the specimens, while SH contributed the line drawings. SH is also partially responsible for the assembly and curation of the specimens, and contributed detailed knowledge of the specimen's history, provenance, and anatomy. The first two authors consider their contributions to this monograph to be equal. SLB is listed as first author because he organized the project and prepared the non-descriptive sections of the text.

MATERIAL

The material of *Neovenator salerii* described in this work includes the holotype (BMNH R10001, MIWG 6348) and two referred specimens (MIWG 5470, 6352).

Institutional abbreviations: **BMNH**, The Natural History Museum (NHM), London, UK; **BYU**, Brigham Young University Museum of Geology, Provo, Utah, USA; **DNM**, Dinosaur National Monument, Utah, USA; **FMNH**, Field Museum of Natural History, Chicago, Illinois, USA; **HASMG**, Hastings Museum and Art Gallery, Hastings, UK; **IVPP**, Institute of Vertebrate Palaeontology and Palaeoanthropology, Beijing, People's Republic of China; **IWCMS**, Isle of Wight County Museum Service (held at Dinosaur Isle Museum), Sandown, UK; **MACN**, Museo Argentino de Ciencias Naturales 'Bernardino Rivadavia,' Buenos Aires, Argentina; **MCF-PVPH**, Museo Carmen Funes, Paleontología de Vertebrados, Plaza Huincul, Neuquén, Argentina; **MIWG**, Dinosaur Isle, Isle of Wight Museum Service (formerly Museum of Isle of Wight Geology), Sandown, UK; **ML**, Museu da Lourinhã, Lourinhã, Portugal; **MNHN**, Muséum National d'Histoire Naturelle, Paris, France; **MNN**, Musée National du Niger, Niamey, Niger; **MOR**, Museum of the Rockies, Bozeman, Montana, USA; **MPM**, Museo Provincial de Mendoza, Mendoza, Argentina; **MUCPv-CH**, Museo de la Universidad Nacional del Comahue, El Chocón collection, El Chocón, Argentina; **NCSM**, North Carolina State Museum of Natural Sciences, Raleigh, North Carolina, USA; **NHM**, The Natural History Museum, London, UK; **OMNH**, Sam Noble Oklahoma Museum of Natural History, Norman, Oklahoma, USA; **OUMNH**, Oxford University Museum of Natural History, Oxford, UK; **PVL**, Paleontología de Vertebrados,

Fundación Miguel Lillo, Tucumán, Argentina; **SGM**, Ministére de l'Energie et des Mines, Rabat, Morocco; **SMU**, Southern Methodist University, Dallas, Texas, USA; **UCMP**, University of California Museum of Paleontology, Berkeley, California, USA; **UC OBA**, University of Chicago, Department of Organismal Biology and Anatomy, Chicago, Illinois, USA; **UCRC**, University of Chicago Research Collection, Chicago, Illinois, USA; **UMNH**, Utah Museum of Natural History, Salt Lake City, Utah, USA; **YPM**, Peabody Museum, Yale University, New Haven, Connecticut, USA.

ACKNOWLEDGEMENTS

We thank Martin Munt (MIWG) and Angela Milner and Sandra Chapman (NHM) for access to the holotype and referred specimens of *Neovenator*, and Darren Naish for his thorough and thoughtful review of the manuscript and discussion on Wealden Group theropods. We are grateful to Thomas Carr, Emily Rayfield, and Ron Tykoski, for commenting on earlier versions of portions of the manuscript, and to David Loydell for editorial assistance. We also thank Paul Barrett, Michael Benton, and Simon Braddy for general assistance and guidance; Paul Sereno for discussion on theropod anatomy and phylogeny; and D. R. Simons (University of Cambridge) for photographs of the teeth. For access to comparative material in their care we acknowledge numerous curators, technicians and researchers, including: Ronan Allain (MNHN), Jorge Calvo (MUCP), Juan Canale (MUCP), Sandra Chapman (NHM), Rich Cifelli (OMNH), Rodolfo Coria (MCF-PVPH), Mike Getty (UMNH), Daniel Goujet (MNHN), Pat Holdroyd (UCMP), Paul Jeffrey (OUMNH), Alejandro Kramarz (MACN), Bob Masek (UCRC), Octavio Mateus (ML), Jeff Person (OMNH), Jaime Powell (PVL), Paul Sereno (UCRC), Philippe Taquet (MNHN), Zhao Xijin (IVPP) and Xu Xing (IVPP). For hospitality in Sandown we thank Penny Newbery, Remmert Schouten, Iain MacIntyre, and the Bristol crew, and for hospitality in London SLB thanks Jud Campbell and Pete Crawford.

For finding, helping to excavate, and donating various skeletal elements of *Neovenator* we thank especially: Keith Simmonds, Penny Newbery, Nick Chase, Gabi Hullman, David Richards, Mark Lumber, David Cooper, Mick Green, Malcolm Green, Rob and Tess George, and (in alphabetical order): Jamie Anderson, Alan Brading, Paul Dix, Steffi Gabrielli, Jeremy Henwood, Pete Lawrence, Gavin Leng, Julie Mosling, Rick Penn, Glyn Rose, Jenny Simmonds and John Winch. For helping to prepare, conserve, and mould/cast the specimens we thank (in alphabetical order): Lora Apps, David Cooper, Ewan Haigh and Eric Milsom. We are especially grateful to the Salero family for allowing the long series of excavations on their land, and to Kevin Brown and the Prism Fund for providing funds to allow MIWG 6348 to remain on the Isle of Wight.

SLB is funded by a Marshall Scholarship for study in the United Kingdom. RBJB is supported by NERC studentship NER/S/A/2005/13488. Additional funding for this project was provided by the Palaeontographical Society and the Jurassic Foundation.

GEOLOGICAL SETTING

All known fossil remains of *Neovenator salerii* are from the Wessex Formation of the Wealden Group, which is regarded as Barremian (Early Cretaceous) in age (Gradstein *et al.* 2004) (Text-figs 2, 3). The general term 'Wealden' is applied to a unit of non-marine mudstones and sandstones that crops out across southern England (Martin 1828; Gallois 1965; Radley 2004, 2006a, b). Rocks of the Wealden Group succession occur in two sub-basins: the Weald Sub-basin, which comprises regions of Kent, Sussex, Surrey, and Hampshire, and the Wessex Sub-basin, which encompasses parts of Dorset and the Isle of Wight (Allen 1981; Radley 2004, 2006a, b). These sub-basins are separated by an east–west trending structural high (Allen 1975), but characterized by largely similar suites of sedimentary rock, although correlation between the two areas is sometimes problematical and slightly different vertebrate faunas have been reported from each region (Martill & Naish 2001). The Wealden Group succession is regarded as spanning from the Berriasian to the lower Aptian (Stewart *et al.* 1991), based largely on palynology (Hughes & McDougall 1989) and correlation of overlying marine strata (Rawson *et al.* 1978).

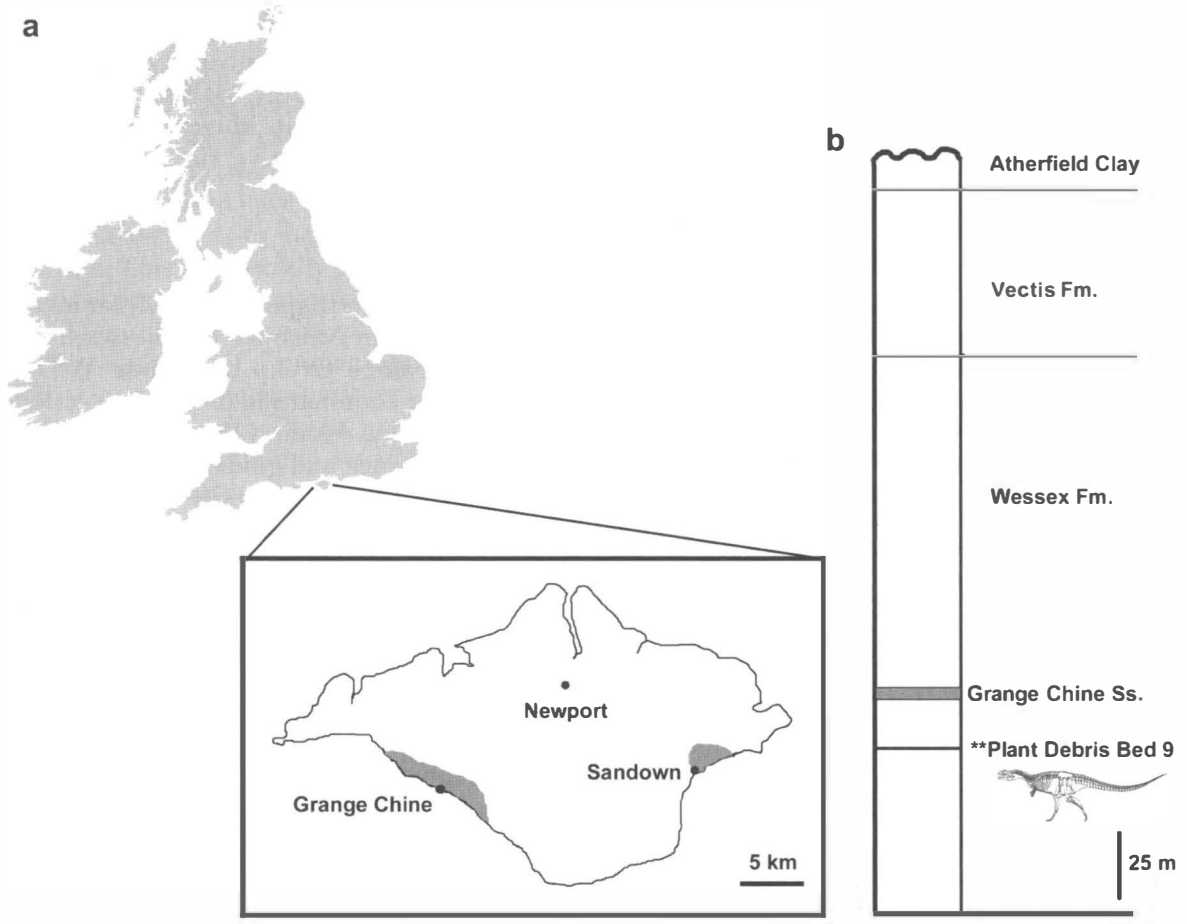

TEXT-FIG. 2. Locality and horizon for *Neovenator salerii* Hutt, Martill & Barker, 1996: **a**, map of the British Isles and an inset map of the Isle of Wight, showing where the holotype and referred specimens were discovered (Grange Chine) and where the holotype is mounted (Dinosaur Isle Museum, Sandown). Shaded grey regions on Isle of Wight map denote outcrops of the Wealden Group (Lower Cretaceous); **b**, simplified geological column of the Wealden Group succession (Lower Cretaceous) on the Isle of Wight, showing Plant Debris Bed 9, the unit in which *Neovenator* was discovered.

Palaeoecological reconstructions suggest that the sub-basins were characterized by seasonal Mediterranean-like climates during this time period, with periods of high rainfall and flooding alternating with prolonged droughts (Watson & Alvin 1996; Allen 1998).

The Wealden Group succession on the Isle of Wight (Radley 2004, 2006a) is divided into two formations: the older Wessex Formation and the overlying Vectis Formation, both of which crop out in the southern half of the island. These formations together comprise the oldest exposed rocks on the Isle of Wight, and are overlain unconformably by strata of Paleogene and Quaternary age (Martill & Naish 2001). The Wessex Formation is a thick succession of varicoloured clays and sandstones that were probably deposited within rivers, oxbow lakes, and ephemeral lakes on a coastal floodplain (Stewart 1978; Martill & Naish 2001). This formation also includes several 'plant debris beds' (Stewart 1978), which consist of a mud or clay matrix with interspersed sand, silt, plant fragments, and vertebrate fossils. These reach thicknesses of up to 2 m, can extend laterally for several hundred metres, and are thought to reflect large flood events (Stewart 1978; Insole & Hutt 1994). Approximately 180–190 m of the upper Wessex Formation are exposed on the Isle of Wight, but Stewart (1981) estimated that this formation may reach a thickness of several hundred metres. The entire exposed portion is regarded as of

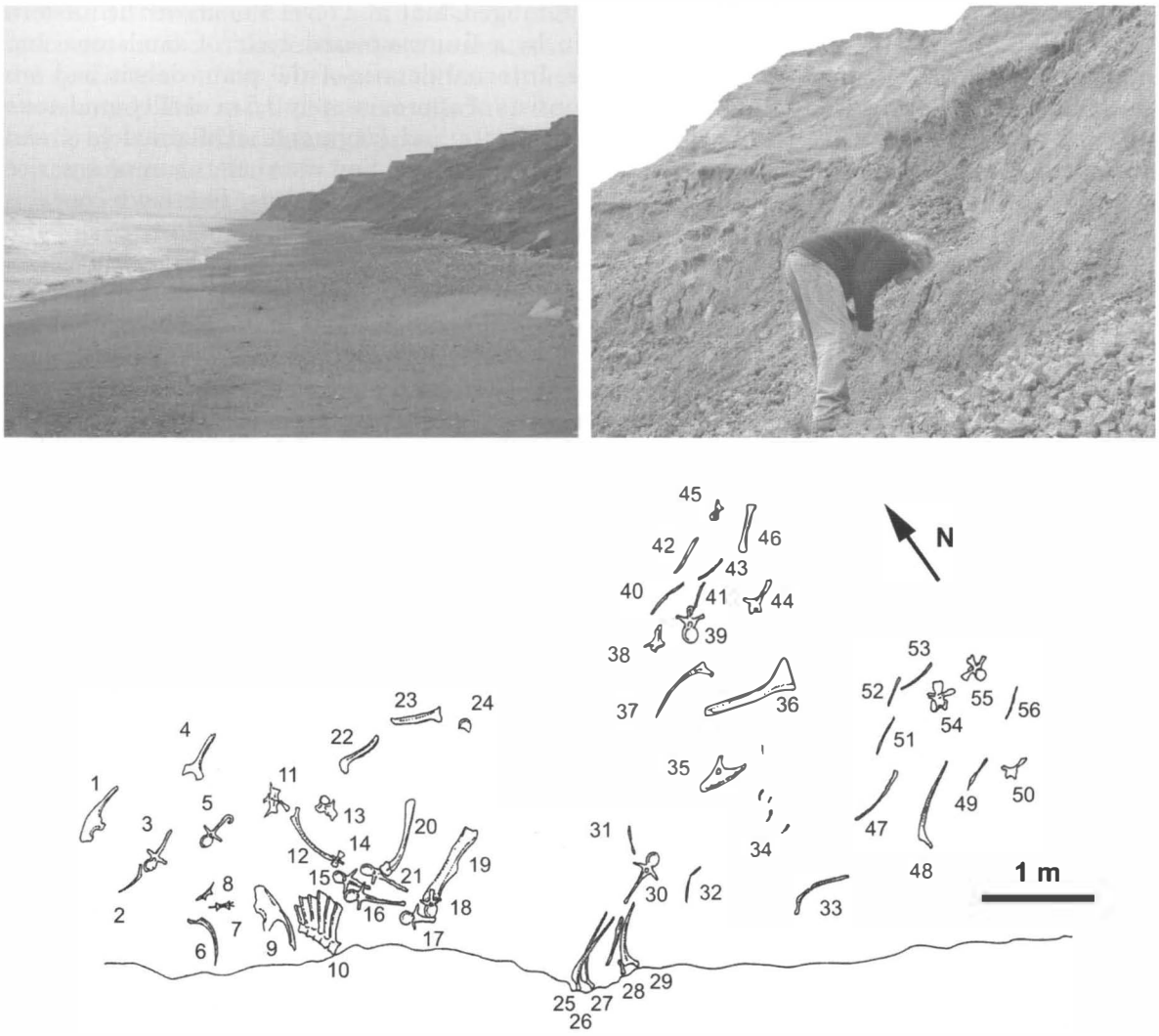

TEXT-FIG. 3. Geological setting for *Neovenator salerii* Hutt, Martill & Barker, 1996: photos of exposed Wessex Formation mudstones near the discovery site at Grange Chine along Brighstone Bay and a field map drawn during MIWG excavations in the mid 1980s.

Barremian age, and yields nearly all of the dinosaur fossils known from the Isle of Wight (Martill & Naish 2001). It is overlain by the Vectis Formation, a 70 m thick succession of lacustrine and lagoonal strata which commonly yields invertebrates and trace fossils but few dinosaur remains (Radley & Barker 1998). In turn, this formation is overlain by the Lower and Upper Greensands with Gault Clay in between, units dominated by thick sandstones and intermittent shales that reflect late Early Cretaceous sea level rise (Martill & Naish 2001).

The holotype and referred material of *Neovenator salerii* were discovered within a short distance of each other at the mouth of Grange Chine, along a beach on Brighstone Bay that is located along a 9 km stretch of Wealden strata exposed along the southwestern coast of the Isle of Wight (Hutt *et al.* 1996; Text-figs 2, 3). The holotype was discovered *c.* 17 m below the Grange Chine Sandstone of the Wessex Formation, within a plant debris bed, referred to as Plant Debris Bed 9 by Stewart (1978). This debris bed has an average thickness of 1.8 m, but varies considerably in thickness across its exposed lateral extent (*c.* 10 m locally). It is first seen in the cliff face 400 m west of Grange Chine (SZ 420817), and dips 5 degrees eastward, reaching the beach about 150 m west of Grange Chine.

The holotype was excavated *c.* 300 m west of Grange Chine at a level 4 m above the modern beach. Here, the plant debris bed is underlain by a fining-upward cycle of sandstone and mudstone and overlain by a massive mudstone. Internal details of the plant debris bed are variable, but it is largely grey in colour. Its base consists of approximately 0.5 m of silty mudstone intermixed with mudstone clasts cemented by siderite and fragments of plant debris and occasional bone. This layer is overlain by 0.5 m of mudstone and another 0.5 m of siderite concretions, above which is a *c.* 2 m thick layer of concentrated plant debris. This layer contains fossilized logs reaching lengths of 3–4 m, as well as the beautifully preserved bones of the holotype of *Neovenator salerii*, which was found associated with a partial skeleton of the ornithopod *Mantellisaurus atherfieldensis* (MIWG 6344; this specimen was previously assigned to *Iguanodon*, but see Paul 2007 for recent taxonomic revision), as well as unionid bivalves. Hutt (1999) interpreted the holotype locality as resulting from two rapid pulses of sedimentation: an initial influx of mud with small clasts resulting from a small flood, and a second deluge of mud interspersed with large tree trunks and the carcasses of both dinosaurs, resulting from a much larger flood. It is likely that the remains of *Neovenator* and *Mantellisaurus* were randomly swept together by the flood, and that their co-occurrence is not the result of an ecological interaction (e.g. predator-prey).

HISTORY OF RESEARCH

Dinosaur fossils have been known from the Isle of Wight since 1829, when William Buckland described some isolated remains of *Iguanodon* discovered along the southeast coast of the island (Martill *et al.* 2001). The first specimens of *Neovenator salerii* were discovered in the summer of 1978 by the Henwood family of Basingstroke, Hampshire, who, while holidaying along the southwest coast, noticed several dark bone fragments that had broken free of the coastal cliffs at Grange Chine after an overnight storm. Upon realizing what they had discovered, the holiday-makers borrowed spades and shovels from a local farmer and began a makeshift excavation, removing material that had been washed onto the beach and exposed during low tide. During the next several weeks David Richards, a geology student, collected additional material along the beach. Eventually, much of the material collected by Richards and the holiday-makers was reported to the Museum of Isle of Wight Geology in Sandown and the British Museum in London (BMNH; now the Natural History Museum). Dr Alan Charig of the BMNH recognized that the fragments belonged to two dinosaurs: an ornithopod, identified by him as *Iguanodon atherfieldensis*, and an unknown species of theropod. Most of the fossils were donated to the BMNH, but a lack of complete and diagnostic elements rendered the theropod specimen enigmatic until Dr William Blows recognized its uniqueness and rarity. Now catalogued as BMNH R10001, this material includes several vertebrae and pelvic fragments, which were prepared at the BMNH during the early 1980s.

This theropod material was temporarily returned to the Museum of Isle of Wight Geology (MIWG) in 1987 for further study and preparation. A few years before this time, staff from the MIWG returned to the beach at Grange Chine to collect additional remains of the '*Iguanodon*' specimen. During this excavation museum staff uncovered a single caudal vertebra from a theropod dinosaur, which was accessioned into the collections of the MIWG and given the specimen number MIWG 6348. Subsequently, museum staff joined with local fossil collectors Keith and Jenny Simmonds to undertake a more complete excavation of the site, which yielded additional fossils of the theropod dinosaur. The new material included portions of the skull (both premaxillae, left maxilla, right nasal, right palatine, several isolated teeth), as well as six presacral vertebrae; 22 caudal vertebrae; several chevrons, ribs, and gastralia; the left scapula and coracoid; and parts of both hind limbs. The right femur was collected from the site after a cliff fall by Mark Lumber, and elements of the left pes were collected by Gabi Hullman and later by Rob and Tess George. Further study revealed that these theropod remains belonged to the same individual as the specimens already donated to the British Museum (BMNH R10001).

Scientific study of the theropod material, including the portions in the BMNH and the MIWG, was directed by Stephen Hutt of the MIWG beginning in the late 1980s. Hutt, along

with Keith Simmonds and Gabi Hullman, published a preliminary paper on the history of the specimens and certain features of the anatomy in 1990 (Hutt *et al.* 1990). The authors regarded the specimens only as Theropoda indet., although certain features shared with 'megalosaurids' were noted. The specimens were officially designated the holotype of a new taxon, *Neovenator salerii*, by Hutt, Martill, and Barker (1996). *Neovenator* was described as a close relative of the North American *Allosaurus* and the first allosaurid theropod known from Europe, a conclusion reinforced by Hutt's (1999) unpublished M.Phil. thesis. One year after the publication of the original paper, Dr David Cooper, a pathologist and amateur fossil collector, discovered the first caudal vertebra of the holotype washed up on the beach near the excavation site. Soon after, on Christmas Day, 1998, Hutt and Penny Newbery discovered the left femur and the right tibia of the holotype specimen. In the wake of these new discoveries, the BBC sponsored a five-day excavation in 2001, but it failed to yield any definitive material belonging to *Neovenator*. However, subsequent to this excavation a single pedal phalanx (IV-4) from the holotype was collected along the beach. It appears as if material from the holotype has been mostly collected, but it is possible that additional fragments, especially of smaller bones, remain to be discovered.

Additional material referred to *Neovenator* was discovered near the type locality, but belongs to a different individual. This material, designated MIWG 6352, includes several vertebrae and portions of the pelvis belonging to a single individual, and was discovered in 1987 by Jenny Simmonds. She was originally drawn to several vertebrae eroding out of a sandy mudstone close to the type locality, and further excavation revealed additional remains of a theropod. A full-scale excavation was launched by the MIWG, and after a brief interruption by poor weather the team unearthed a set of crushed but nearly complete conjoined pubes with a greatly enlarged pubic boot. Originally, Hutt *et al.* (1990) regarded this theropod as a separate species from what would eventually become the holotype of *Neovenator salerii*, as it was thought that the holotype individual possessed a very small pubic boot. However, the identification of the supposed pubic boot of the holotype as an ischial boot and the recognition of several *Neovenator* autapomorphies in the new theropod led Hutt (1999) to refer MIWG 6352 to *Neovenator salerii*.

The second referred specimen of *Neovenator*, two vertebrae from a single individual (MIWG 5470), was collected in 1985 by Hutt, Martin Munt, and Robin Reid from a site within Plant Debris Bed 11 (Stewart 1978) *c.* 500 m west of the holotype locality.

Currently, all specimens of *Neovenator salerii* are held at the Dinosaur Isle Museum in Sandown (MIWG) and The Natural History Museum in London (BMNH/NHM). Much of the type specimen is mounted for public display at the MIWG, with unknown elements (including much of the skull) based on the closely related *Allosaurus*. Some material of the referred specimen MIWG 6352 is also displayed at the MIWG (Text-fig. 1).

SYSTEMATIC PALAEONTOLOGY

Dinosauria Owen, 1842
Saurischia Seeley, 1888
Theropoda Marsh, 1881
Tetanurae Gauthier, 1986
Allosauroidea Marsh, 1878

Genus NEOVENATOR Hutt, Martill & Barker, 1996

Diagnosis. Allosauroid theropod possessing the following autapomorphies: premaxilla with accessory interpremaxillary peg and socket articulation in the dorsal region of the symphysis; maxilla with large maxillary fenestra approximately one sixth the length of the maxillary tooth row; transverse expansion of the anterior articular surface of the axial intercentrum; lateral foramina on the anterior surface of the odontoid; small single foramen on the lateral surface of the axial neural spine; fusion of the cervical ribs to the posterior cervical vertebrae; camellate internal texture exposed externally on parapophyseal facets of eighth and ninth cervical vertebrae; ventral surfaces of anterior dorsal vertebrae developed as sharp ridges, not inset from the lateral surface of the centra; hypapophyses of anterior dorsal vertebrae developed as low mound-like eminences; curved flanges emerging laterally from pre- and postzygapophyseal facets

of posterior dorsal vertebrae; scapula-coracoid glenoid fossa that is wider mediolaterally than long anteroposteriorly; shelf adjacent to the preacetabular notch on the medial surface of the ilium; distal ischial boot in which the left and right ischia are conjoined anteriorly but diverge posterolaterally; femoral head oriented anteromedially and inclined proximally; robust ridge on the external surface of the lesser trochanter of the femur; thumbprint-shaped depression on posterior surface of femoral shaft lateral to the proximal end of the fourth trochanter; proximodistally short, notch-like extensor groove and almost flat anterior surface of distal end of femur; suboval rugosity on medial surface of distal tibia; anteroposteriorly pinched proximal portion of the lateral malleolus of the distal tibia; ventral spine on anterolateral crest of fibular condyle of tibia; concave lateral surface of metatarsal II for articulation with metatarsal III; and pedal unguals with groove on extensor surface.

Type species. *Neovenator salerii* Hutt, Martill, & Barker 1996, figs 2–4.

Neovenator salerii Hutt, Martill, & Barker, 1996 Plates 1–45; Text-figs 1, 3, 5–25, 27

1990	Theropoda indet./?Megalosauridae; Hutt, Simmonds & Hullman, figs 1–6.
1994	?Allosauridae ?n.g., n.sp. (Hutt *et al.*, 1990); Insole & Hutt, table 1.
1996	*Neovenator salerii* Hutt, Martill & Barker, p. 635, figs 2–4.
2001	*Neovenator salerii* Hutt, Martill and Barker, 1996; Naish, Hutt & Martill, p. 258, pls 37–39, pl. 40, figs 1, 2, text-figs 9.9–9.25.
2003	*Neovenator salerii*; Naish, fig. 5.
2004	*Neovenator salerii* Hutt, Martill, et Barker; 1996; Holtz, Molnar & Currie, table 4.1, figs 4.5A, 4.11, 4.17C, 4.18A, 4.19B.

Diagnosis. As for *Neovenator*.

Type material. Holotype, MIWG 6348 (left and right premaxillae; left maxilla; right nasal; right palatine; left dentary; isolated teeth; cervical, dorsal, and caudal vertebrae; ribs; chevrons; gastralia; left scapula; left coracoid; left ischium; left and right femora; left and right tibiae; left metatarsals II–V; left pedal phalanges II-1, II-2, III-4, IV-1–IV-5; right pedal phalanges IV-3 and III-4) and BMNH R10001 (cervical, dorsal, sacral, and caudal vertebrae; left and right ilium; left and right pubes; left and right ischia). Figured by Hutt *et al.* (1990, figs 1, 3–6; 1996, figs 2–4), Naish *et al.* (2001, pls 37–39, pl. 40, figs 1, 2, text-figs 9.9–9.25), Naish (2003, fig. 5) and Holtz *et al.* (2004, figs 4.5A, 4.11, 4.17C, 4.18A, 4.19B). From Grange Chine, Brighstone Bay, Isle of Wight, England, United Kingdom, in the Wessex Formation, Wealden Group, Barremian, Lower Cretaceous. Some of the type material in the MIWG was erroneously referred to as MIWG 6438 by Hutt *et al.* (1990, p. 139), due to a mistaken switching of the numbers 3 and 4 (i.e., this material is properly MIWG 6348). The left dentary is catalogued as BMNH R10001 by Hutt (1999) and Martill & Naish (2001), but has never been accessioned to the BMNH (S. Chapman, pers. comm.). It may be a MIWG specimen but its whereabouts are currently unknown (see below).

Referred material. MIWG 5470 (ninth cervical vertebra and eighth dorsal vertebra) and MIWG 6352 (second and fifth dorsal centra; seventh dorsal neural arch; second, third and fourth sacral centra; isolated sacral centrum and neural arch; left ilium; left and right pubes; left ischium; chevron; ribs; axial fragments). Both also from Grange Chine, Brighstone Bay, Isle of Wight, England, United Kingdom, in the Wessex Formation, Wealden Group, Barremian, Lower Cretaceous.

Distribution. Currently *Neovenator salerii* is known only from the Wessex Formation on the Isle of Wight, United Kingdom. Demonstrably referable material has not been reported from elsewhere within the Wealden Basin.

Discussion. We prefer a conservative approach to referring additional material to *Neovenator salerii*, based on the presence of clear autapomorphies seen also in the holotype.

MIWG 5470, an associated ninth cervical vertebra and eighth dorsal vertebra, is referred to *Neovenator salerii* based on the presence of two autapomorphies: camellate parapophyseal facet of the ninth cervical vertebra and lateral flanges on the postzygapophyses of the eighth dorsal vertebra. This referral is corroborated by the camellate internal structure of the neural arches and centra, a feature not unique to *Neovenator* among theropods but unknown in other Wealden

Group theropods. Additionally, the vertebrae of MIWG 5470 do not differ in any substantial way from the corresponding vertebrae of the holotype of *Neovenator*.

MIWG 6352, which comprises several vertebrae, additional axial material and pelvic elements all associated and belonging to a single individual, is referred to *Neovenator salerii* based on the presence of three axial autapomorphies: ventral surface of the anterior dorsal centra developed as a sharp ridge that is not inset from the lateral surfaces of the centrum, hypapophysis developed as a mound-like eminence anteriorly on the ventral surface of the second dorsal vertebra, and incipient development of lateral flanges of the postzygapophyses of the seventh dorsal neural arch. This referral is corroborated by the camellate internal structure of the presacral vertebrae and the fact that none of the elements differs in any substantial way from the corresponding elements (when known) in the holotype.

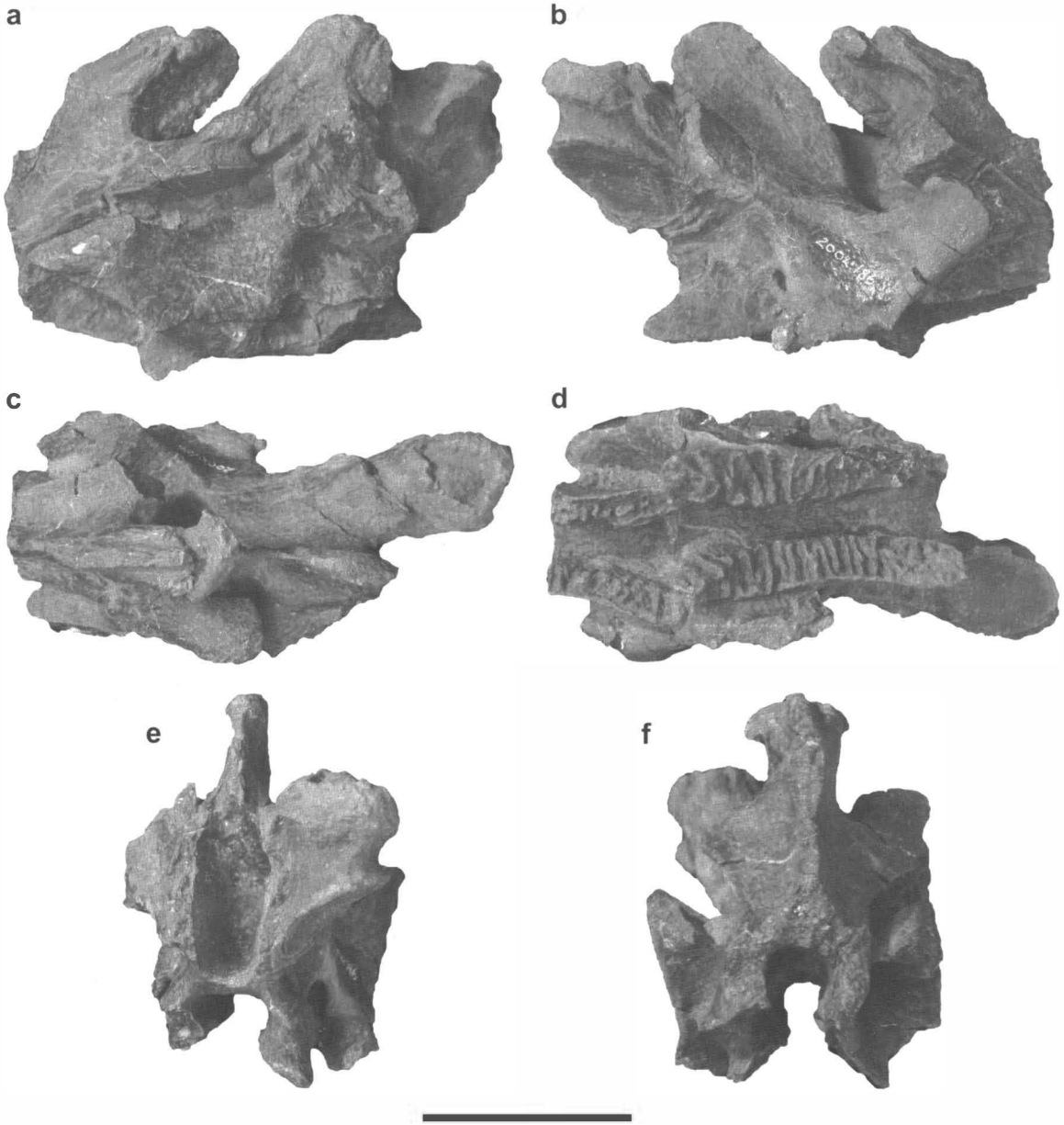

TEXT-FIG. 4. Theropoda indet., possibly *Neovenator salerii* Hutt, Martill & Baker, 1996; two articulated anterior cervical vertebral neural arches (IWCMS 2002.186). **a**, left lateral view; **b**, right lateral view; **c**, dorsal view; **d**, ventral view; **e**, anterior view; **f**, posteror view. Scale bar represents 50 mm.

Additional material has been referred to *Neovenator salerii* both in the literature and in the collections of Dinosaur Isle (Museum of Isle of Wight Geology). Hutt (2001) referred a pedal phalanx from the Wessex Formation of Brighstone Bay (MIWG 4199) to *Neovenator*. However, this element cannot be confidently assigned to *Neovenator* due to the absence of autapomorphies on the non-ungual pedal phalanges, and thus is regarded as Theropoda indet. A distal end of a metatarsal (IWCMS 2000.1108) and an isolated tooth (MIWG 5121) are assigned to *Neovenator* in the displays at Dinosaur Isle, but also cannot be confidently referred due to lack of clear autapomorphies. Both are here regarded as Theropoda indet. Finally, a collection of associated remains, including fragments of vertebrae and long bones (IWCMS 2002.186), is referred to *Neovenator* in the collections of Dinosaur Isle (Text-fig. 4). These elements cannot be referred to *Neovenator* based solely on autapomorphies. However, two articulated anterior cervical neural arches display camellate pneumaticity, which is seen in a range of theropods but only *Neovenator* among known Wessex Formation theropods. Unfortunately, the anterior cervicals apart from the atlas-axis complex are unknown in *Neovenator*, precluding definitive comparison.

Description. Approximately 70% of the skeleton is represented by the holotype and referred material of *Neovenator salerii*. All of this material is described below. The current description focuses on the holotype, but also includes details from the referred material, especially for those elements that are better represented in the referred specimens.

ANATOMICAL DESCRIPTION

SKULL

Only a limited amount of cranial material is known for *Neovenator*, but this is all well-preserved and nearly complete (Pls 1–4; Text-figs 5–8). All elements belong to the holotype, and consist of left and right premaxillae, a left maxilla, a right nasal, a right palatine and the anterior fragment of a left dentary (all MIWG 6348). The shapes and sizes of the different major cranial openings are mostly unknown, but the external naris was large as in other allosauroids, with a long axis measuring 138 mm. Hutt *et al.* (1996) and Rauhut (2003) considered a large external naris to be autapomorphic of *Neovenator*, but when compared to a standard measure (such as the anteroposterior length of the ventral margin of the premaxilla or the maxilla) the external naris of *Neovenator* is of similar size to those of most other allosauroids (e.g. Madsen 1976; Currie & Zhao 1993), but noticeably larger than in *Acrocanthosaurus* (Currie & Carpenter 2000).

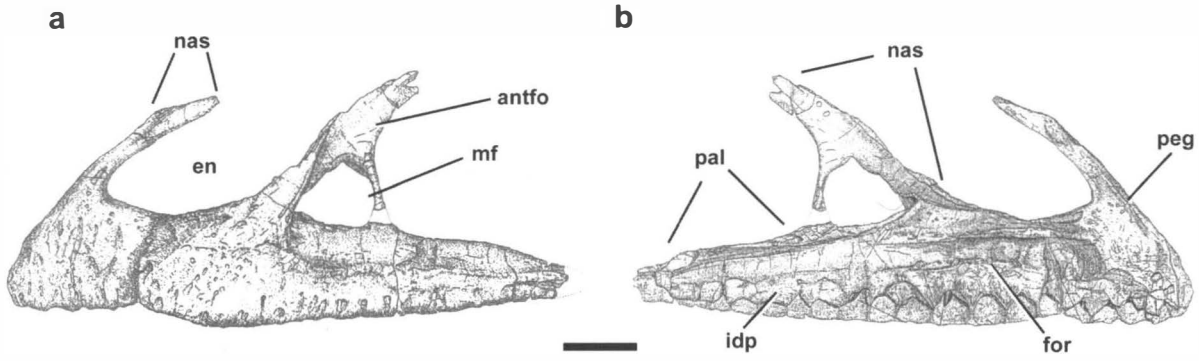

TEXT-FIG. 5. *Neovenator salerii* Hutt, Martill & Barker, 1996; left premaxilla and maxilla (MIWG 6348): **a**, lateral view; **b**, medial view. Abbreviations: **antfo**, antorbital fossa; **en**, external naris; **for**, foramen; **idp**, interdental plates; **mf**, maxillary fenestra; **nas**, articulation with the nasal; **pal**, articulation with the palatine; **peg**, peg and socket accessory articulation between the premaxilla and maxilla. Scale bar represents 50 mm.

Premaxilla. Complete left and right premaxillae are known (Table 1; Pl. 1; Text-fig. 5). The premaxillary body is longer than high in *Neovenator* as it is in *Allosaurus* (Madsen 1976), *Dubreuillosaurus* (Allain 2002) and *Sinraptor* (Currie & Zhao 1993; Gao 1998), not higher than

TABLE 1. Skull measurements

Premaxilla (MIWG 6348, left element)
Length (anteroposterior) of ventral margin along the tooth row: 87 mm
Depth (dorsoventral) of posterior margin: 70 mm
Length (dorsoventral) of nasal ascending process: 107 mm
Length (anteroposterior) of maxillary process: 23 mm

Maxilla (MIWG 6348, left element)
Length (anteroposterior) of ventral margin along the tooth row: 300 mm*
Length (anteroposterior) of anterior ramus: 85 mm
Depth (dorsoventral) of anterior ramus: 75 mm

Nasal (MIWG 6348, right element)
Length (anteroposterior): 328 mm*
Height (dorsoventral)[1]: 46 mm
Thickness (dorsoventral) of medial process: 9 mm

[1]: Immediately posterior to where premaxillary and maxillary processes diverge from main body.
*denotes incomplete measurement due to broken surfaces

long as it is in *Acrocanthosaurus* (Currie & Carpenter 2000), *Ceratosaurus* (Madsen & Welles 2000), *Giganotosaurus* (MUCPv-CH-1) and *Torvosaurus* (Britt 1991) or square as it is in *Monolophosaurus* (IVPP 84019: Zhao & Currie 1993). The anterior margin is inclined caudodorsally as in *Acrocanthosaurus* and *Giganotosaurus*, not subvertically straight as in *Allosaurus*, *Ceratosaurus*, *Monolophosaurus*, *Sinraptor* and many other theropods.

The surfaces for contact with the maxilla, nasal and opposing premaxilla are preserved. The symphysis for the opposing premaxilla is anteroposteriorly long and flat. The anterodorsal region of the symphysis is braced by an autapomorphic peg-and-socket structure located anteroventral to the external naris: the left premaxilla is marked by a ridge oriented parallel to the anterior margin of the element, which becomes a groove ventrally. These correspond to a dorsal groove and ventral ridge on the right premaxilla (Text-fig. 5b). Accessory premaxillary articular structures such as this are not known in any other theropod (e.g. Madsen 1976; Britt, 1991; Currie & Zhao 1993; Madsen & Welles 2000; Currie & Carpenter 2000; Allain 2002). The premaxillary articulation with the maxilla is complex and takes the form of a deep anteroposteriorly extending groove on the medial surface ventral to the external naris, which receives the anteromedial process of the maxilla. Dorsal to this groove is a posteriorly projecting tab, the maxillary process of the premaxilla, which fits onto the dorsal surface of the anterior ramus of the maxilla to strengthen the articulation. The maxillary process is dorsally placed as in most large theropods, not located ventrally and abutting the interdental plates as in *Sinraptor* (Currie & Zhao 1993). The nasal process of the premaxilla is broad and flat dorsally, and would have braced against the dorsomedial surface of the premaxillary process of the nasal.

The lateral surface of the premaxilla is highly rugose and ornamented with numerous foramina, many of which are set within shallow grooves. These are much larger and more densely packed anteriorly and ventrally along the tooth row. A single large foramen opens ventrally into a deep, posterodorsally oriented groove at the base of the nasal process in both left and right premaxillae. A similar foramen is present in *Dubreuillosaurus* (Allain 2002) and *Torvosaurus* (Britt 1991), in which it is located on the premaxillary body ventral to the nasal process, but is absent in *Acrocanthosaurus* (NCSM 14345), *Allosaurus* (Madsen 1976), *Ceratosaurus* (Madsen & Welles 2000), *Dilophosaurus* (UCMP 37303), *Majungasaurus* (Sampson & Witmer 2007), '*Megalosaurus*' *hesperis* (Waldman 1974) and *Sinraptor* (Currie & Zhao 1993; Gao 1998). There is no subnarial foramen between the premaxilla and maxilla (Text-fig. 5a), unlike the condition in *Allosaurus* (Madsen 1976), and the external naris is not bordered anteroventrally by a broad fossa. The subnarial process is short, and consequently the maxilla contributes broadly to the margin of the external naris.

Medially, the interdental plates are fused into a single lamina as in all allosauroids except *Sinraptor* (Currie & Zhao 1993; Gao 1998). These increase in height posteriorly, from a

dorsoventral depth of 10 mm immediately above the second alveolus to 29 mm above the fifth alveolus. Dorsally the interdental plates are bordered by a groove for the dental lamina; this groove angles strongly posterodorsally in concert with the increasing height of the plates. Between the lamina and the deep groove for the maxilla is a distinct rounded depression with a diameter of 23 mm. A similar depression is present in *Dubreuillosaurus* (MNHN 1998-13 RJN 1; Allain 2002) and *Majungasaurus* (Sampson & Witmer 2007), but the corresponding region is flat in most other theropods (e.g. *Allosaurus*, *Torvosaurus*). Comparison with *Sinraptor* is difficult due to the ventrally placed maxillary process, which abuts the interdental plates and thus does not demarcate a broad area dorsal to the dental groove. Anterior to the maxillary process on the medial surface is a deeply excavated, anteroposteriorly oriented groove that terminates anteriorly in a foramen, a feature present in most large theropods.

The premaxillary tooth row contains five alveoli, a condition otherwise known only in *Allosaurus* among theropods. The first two alveoli are noticeably smaller than the remaining three (Table 2). No functional or nearly erupted teeth are present.

Maxilla. The left maxilla is nearly complete, missing only a small portion posteriorly in the vicinity of the jugal articulation (Table 1; Pl. 2; Text-fig. 5). The maxillary body (=main body of some authors) tapers posteriorly as in most theropods, and is not of approximately equal depth throughout its length as it is in abelisaurids (Sampson & Witmer 2007). The maxilla contributes to the external naris as in *Afrovenator* (Sereno *et al.* 1994), *Carcharodontosaurus* (Brusatte & Sereno 2007), *Monolophosaurus* (Zhao & Currie 1993), *Torvosaurus* (Britt 1991) and spinosaurids (Sues *et al.* 2002). As in many other basal tetanurans there is a distinct anterior ramus that projects from the maxillary body anterior to the ascending ramus. This ramus is separated from the nasal process by a concave region that formed the maxillary contribution to the floor of the external naris. The anterior ramus is longer anteroposteriorly than deep dorsoventrally as in *Afrovenator* (Sereno *et al.* 1994), *Dubreuillosaurus* (Allain 2002), *Monolophosaurus* (Zhao & Currie 1993), *Torvosaurus* (Britt 1991) and spinosaurids (Sereno *et al.* 1998). In contrast, the ramus is deeper than long in *Acrocanthosaurus* (Currie & Carpenter 2000) and *Carcharodontosaurus* (Sereno *et al.* 1996), and is absent altogether in *Sinraptor* (Currie & Zhao 1993; Gao 1998). The condition in *Allosaurus* is variable: Rauhut (2003) scores this taxon for an elongated ramus (based on DNM 2560 and MOR 693, neither of which we have observed), but specimens we have observed (e.g. BYU 7255126) and those figured by Madsen (1976) exhibit a ramus that is deeper than long, and closely approximating a square. The condition in *Mapusaurus* is also variable: one specimen (MCF-PVPH-108.115) exhibits a short and deep anterior ramus whereas another (MCF-PVPH-108.169) lacks the ramus altogether.

The surfaces for contact with the premaxilla and nasal are preserved. When viewed laterally, the premaxillary articular surface is subvertical for most of its length as in *Allosaurus*, not caudodorsally inclined as in *Acrocanthosaurus* (Currie & Carpenter 2000), *Carcharodontosaurus* (Sereno *et al.* 1996; Brusatte & Sereno 2007), *Giganotosaurus* (MUCPv-CH-1), *Eocarcharia* (Brusatte & Sereno 2006; Sereno & Brusatte 2008), *Mapusaurus* (Coria & Currie 2006) and *Sinraptor* (Currie & Zhao 1993; Gao 1998). Dorsally this contact develops a semioval notch on the lateral surface of the maxilla for reception of a rugose lateral swelling of the premaxilla (Text-fig. 5a). Additional bracing is provided by a thin lappet of the maxilla that extends slightly laterally over the posterior surface of the premaxilla. The maxilla contacts the nasal via a 122 mm long groove on the dorsal surface of the ascending ramus (= nasal process of some authors). In dorsal view this articulation is sinuous, as it first curves laterally and then angles medially where the ascending ramus meets the main body. Here it fans out to become continuous with the dorsal surface of the anterior ramus where the maxilla contributes to the external naris.

The lateral surface of the maxilla is rugose, similar to the condition in abelisaurids (e.g. *Carnotaurus*: MACN-CH 894), *Giganotosaurus* (MUCPv-CH-1) and *Mapusaurus* (MCF-PVPH-108.115), but unlike those of most theropods, in which the lateral surface is generally smooth. This surface is also rugose in *Carcharodontosaurus*, in which the rugosity is developed as distinctive, dorsoventrally oriented grooves and ridges (Brusatte & Sereno 2007). The lateral surface of the maxilla of *Neovenator* is pierced by numerous foramina, which are especially concentrated on the

anterior ramus ventral to the external naris and immediately above the tooth row. The foramina immediately above the tooth row are large, measuring 5–9 mm in diameter, and open ventrally into deep grooves. The ascending ramus rises from the maxillary body posterodorsally at approximately 45 degrees. It is marked by a minor inflection at midlength but not the distinct step seen in some basal tetanurans (e.g. *Afrovenator*: Sereno *et al.* 1994; *Dubreuillosaurus*: Allain 2002). The lateral lamina of the ascending ramus slightly overhangs the anterior margin of the antorbital fossa before fanning out dorsally to form the lateral margin of the nasal articulation. This lamina overhangs the fossa to a similar extent in *Allosaurus* (Madsen 1976; Holtz *et al.* 2004), but the overhang is much reduced or absent in other allosauroids (e.g. Currie & Zhao 1993; Sereno *et al.* 1996; Currie & Carpenter 2000; Sereno & Brusatte 2008).

The antorbital fossa extends onto the lateral surface of the maxillary body as in most theropods. The extent and strength of the fossa is intermediate between the ventrally extensive and sharply defined fossae of most specimens of *Allosaurus* (Madsen 1976), *Eocarcharia* (Sereno & Brusatte 2008) and *Sinraptor* (Currie & Zhao 1993) and the reduced fossae of *Acrocanthosaurus* (Currie & Carpenter 2000), *Carcharodontosaurus* (Sereno *et al.* 1996; Brusatte & Sereno 2007), *Giganotosaurus* (MUCPv-CH-1) and *Mapusaurus* (Coria & Currie 2006), which are shallow and make only a minor contribution to the lateral surface of the main body. This latter condition is also present in *Torvosaurus* (Britt 1991), spinosaurids (Sereno *et al.* 1998) and abelisaurids (Lamanna *et al.* 2002). The anterior margin of the fossa is slightly rounded ventrally, but is more similar in shape to the squared-off margin of *Afrovenator* (Sereno *et al.* 1994), *Dubreuillosaurus* (Allain 2002), *Eocarcharia* (Sereno & Brusatte 2008) and coelophysoids (Colbert 1989) than the smoothly rounded condition of other allosauroids (e.g. *Allosaurus*: Madsen 1976; *Sinraptor*: Currie & Zhao 1993). Additionally, the fossa is bordered by a distinct raised rim that thins and flattens out posteriorly as in most theropods.

Two accessory antorbital openings pierce the fossa in *Neovenator*. The more anterior promaxillary fenestra (foramen of some authors) is small and teardrop-shaped, and leads anteriorly into what appears to be a deep and medially closed recess in the anterior ramus of the maxilla (promaxillary recess of Witmer 1997) whose internal details are unknown. This foramen is completely obscured in lateral view by the lateral lamina, as in *Allosaurus* (Witmer 1997) and *Giganotosaurus* (MUCPv-CH-1). In contrast, the promaxillary fenestrae of *Acrocanthosaurus* (NCSM 14345; Currie & Carpenter 2000), *Eocarcharia* (Sereno & Brusatte 2008) and *Sinraptor* (Currie & Zhao 1993; Witmer 1997) are broadly visible in lateral view. The second opening, the maxillary fenestra, is a large triangular opening that leads medially into a large maxillary antrum whose medial surface was possibly enclosed by a wall of bone similar to the condition in *Allosaurus* (Madsen 1976), *Carcharodontosaurus* (SGM-Din 1) and other theropods (Witmer 1997). What may be broken margins of this wall are present on the medial surface of the ascending ramus and the main body, including what is likely the base of the postantral pillar (pila postantralis of Witmer 1997). This fenestra is 62 mm long anteroposteriorly at its base and 50 mm dorsoventrally deep at its centre, and separated from the antorbital fenestra by a narrow pillar of bone (the pila interfenestralis of Witmer 1997). The margins of the fenestra are broken but the opening was clearly larger than in other theropods; the anteroposterior axis of the fenestra of *Neovenator* is approximately one fifth of the length of the maxillary tooth row, whereas in other allosauroids the maxillary fenestra measures approximately one tenth to one fifteenth of the length of the tooth row (Madsen 1976; Currie & Zhao 1993; Coria & Salgado 1995; Sereno *et al.* 1996; Currie & Carpenter 2000; Coria & Currie 2006; Sereno & Brusatte 2008). In addition, other allosauroids also possess a much thicker pila interfenestralis. Rauhut (2003) considered a narrow pila interfenestralis to be a distinct autapomorphy of *Neovenator*, but this is probably correlated with the enlarged maxillary fenestra. There is no pneumatic excavation (excavatio pneumatica of Witmer 1997) on the ascending ramus as is present in *Acrocanthosaurus* (NCSM 14345), *Eocarcharia* (Sereno & Brusatte 2008) and *Sinraptor* (Currie & Zhao 1993; Witmer 1997), and to a lesser extent *Allosaurus* (Witmer 1997) and *Ceratosaurus* (Witmer 1997).

On the medial surface, the interdental plates are fused into a continuous lamina as in most allosauroids, neoceratosaurs (Rauhut 2003) and *Torvosaurus* (Britt 1991), not unfused as in

Sinraptor (Currie & Zhao 1993; Gao 1998) and other basal tetanurans (e.g. *Afrovenator*: UC OBA 1; *Dubreuillosaurus*: Allain 2002; *'Megalosaurus' hesperis*: Waldman 1974). They decrease in depth posteriorly, beginning with a depth of 40 mm at the level of the first alveolus and shortening to a depth of 4 mm above the fifteenth alveolus. The interdental plates are not as deep dorsoventrally relative to their basal width as in *Carcharodontosaurus* (Brusatte & Sereno 2007), *Giganotosaurus* (MUCPv-CH-1), and *Mapusaurus* (Coria & Currie 2006), but more comparable to the depth seen in *Allosaurus* (Madsen 1976), *Sinraptor* (Currie & Zhao 1993) and *Eocarcharia* (Sereno & Brusatte 2008). They are slightly rugose and bear numerous foramina, but are not ornamented by discrete striations as they are in abelisaurids. Vertical depressions are present on the interdental plates between alveoli, indicating that the crypts for replacement teeth extend throughout the main body of the maxilla.

TABLE 2. Alveolus measurements (MIWG 6348, left elements) in mm.

Premaxilla (left element)	Mesiodistal length	Labiolingual width
Alveolus 1	11	5
Alveolus 2	12	6
Alveolus 3	16	9
Alveolus 4	17	10
Alveolus 5	18	5
Maxilla		
Alveolus 1	16	16
Alveolus 2	23	16
Alveolus 3	26	17
Alveolus 4	28	18
Alveolus 5	26	14
Alveolus 6	25	10
Alveolus 7	22	10
Alveolus 8	20	7
Alveolus 9	20	8
Alveolus 10	20	6
Alveolus 11	19	6
Alveolus 12	18	7
Alveolus 13	21	5
Alveolus 14	16	5
Alveolus 15	14	5

Dorsally, the interdental plates are bordered by a groove for the dental lamina. This groove is pierced by a suprainterdental plate foramen above each alveolus. The foramina decrease in size posteriorly and several are confluent with tooth replacement pits, where replacement teeth are exposed lingual to the erupted tooth as in most theropods (Edmund 1960), not directly above the erupted tooth as in crocodyliforms, avians and troodontids (Norell & Hwang 2004). The region above the dental groove bears a medial maxillary shelf, which is excavated posteriorly by a deep longitudinal groove for articulation with the palatine. This groove tapers anteriorly and terminates at the level of the ninth alveolus. Above the level of the sixth alveolus the medial shelf gives rise to an anterodorsally inclined ridge that expands medially to become the anteromedial process for articulation with the vomer and opposing maxilla. In anterior view this process is directed strongly medially and appears subhorizontal rather than arched dorsomedially as it is in *Carcharodontosaurus iguidensis* (Brusatte & Sereno 2007). However, the anterior end of the anteromedial process is abraded and probably originally curved anteroventrally, as it does in basal tetanurans generally. The dorsal surface of the process is marked by a groove for articulation with the vomer, and a wide notch lateral to the process receives the maxillary process of the premaxilla.

The tooth row contains 15 alveoli, and it is likely that an additional one or two alveoli were located on the missing posterior end of the maxilla (Table 2). The estimated length of additional alveoli was taken into account in the above comparisons using the maxillary tooth row as a

comparator. No functional or nearly erupted teeth are present. The lateral wall of the alveolar row, formed by the maxillary body, extends substantially further ventrally than the medial margin, formed by the interdental plates.

Nasal. A nearly complete right nasal is preserved, lacking the distal (=anteroventral) end of the maxillary process, the posterior tips of the frontal and prefrontal articulation, and some of the medial surface for articulation with the opposing nasal (Table 1; Pl. 3; Text-fig. 6). This element has been crushed transversely, resulting in a dorsal surface that appears to slope strongly medially and a lateral surface that is pushed slightly dorsally. This bone was misidentified as a left nasal by Naish *et al.* (2001, pl. 37), who included a figure originally published by Hutt *et al.* (1996) in which the right nasal is reversed to complete a skull reconstruction in left lateral view.

Surfaces for contact with the premaxilla, maxilla, and lacrimal are preserved. The premaxilla is contacted via a flattened region on the medial surface of the premaxillary process. The maxillary process is broken distally, but the detailed structure of the articulation with the maxilla is evident on the ventral surface of the nasal. Here, a shallow groove on the ventral surface extends posteriorly from the base of the maxillary process, sweeps medially to the antorbital fossa, and continues posteriorly to form an elongated contact for the ascending ramus of the maxilla. The lacrimal contact surface consists of a deeper longitudinal groove on the ventral surface of the bone, which begins lateral to the maxillary articulation and medial to the antorbital fossa and continues posteriorly, ultimately terminating in a broken surface. Unfortunately, details of the articulation with the frontal, prefrontal, and most of the opposing nasal are unclear due to breakage. However, a small region of the contact for the opposing nasal is visible on the medial surface posteriorly, but is too badly damaged to describe in detail.

The external surfaces of the nasal are rugose, similar to those in abelisaurids (e.g. *Carnotaurus*: MACN-CH 894; *Majungasaurus*: FMNH PR 2100) and *Carcharodontosaurus* (Sereno *et al.* 1996). The rugosity in *Neovenator* is slightly weaker than that of *Carcharodontosaurus* (SGM-Din 1), and in both of these taxa the rugosity is much less strongly developed than in *Giganotosaurus* (MUCPv-CH-1) and *Mapusaurus* (Coria & Currie 2006), in which numerous excresences, up to several centimetres in size, are present along the dorsal surface of the nasal. The dorsolateral margin of the nasal in *Neovenator* is marked by a prominent rugose ridge that separates the dorsal and lateral surfaces along the entire length of the nasal. Naish *et al.* (2001) regarded this crest

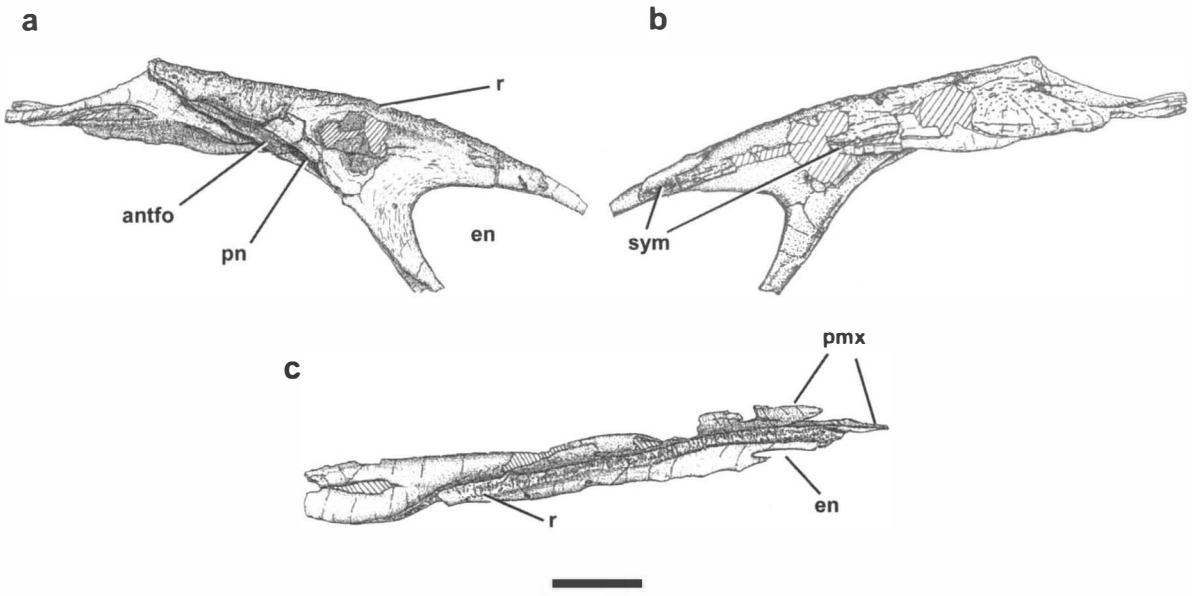

TEXT-FIG. 6. *Neovenator salerii* Hutt, Martill & Barker, 1996; right nasal (MIWG 6348): **a**, lateral view; **b**, medial view; **c**, dorsal view. Abbreviations: **antfo**, antorbital fossa; **en**, external naris; **pmx**, articulation with the premaxilla; **pn**, pneumatopore; **r**, ridge; **sym**, medial symphysis. Scale bar represents 50 mm.

as a 'characteristic feature' of *Neovenator*, but it is also present in *Allosaurus* (e.g. UMNH VP 9162). The width of the dorsal surface is relatively constant across the length of the bone, and does not appear to expand posteriorly as in *Allosaurus* (Madsen 1976) and *Sinraptor* (Currie & Zhao 1993), although breakage in *Neovenator* renders this comparison incomplete. In lateral view, the posterodorsal margin of the external naris is formed by the bifurcating premaxillary and maxillary processes of the nasal, which also enclose a broad lateral fossa that borders the naris posterodorsally. The lateral surface tapers posteriorly and shows no signs of the strong crest that overhangs the lateral surface in *Allosaurus* (Madsen 1976) and *Sinraptor* (Currie & Zhao 1993).

The antorbital fossa extends onto the lateral surface of the nasal, as it does in allosauroids (*Allosaurus*, *Carcharodontosaurus*, *Giganotosaurus*, *Mapusaurus*, *Sinraptor*: Sereno *et al.* 1996), *Cryolophosaurus* (Smith *et al.* 2007), *Dilophosaurus* (Smith *et al.* 2007) and *Monolophosaurus* (Zhao & Currie 1993), but not other basal tetanurans (including *Acrocanthosaurus*: NCSM 14345). A crest-like extension of the dorsal surface of the nasal overhangs the nasal antorbital fossa, and transverse compression has forced this crest ventrally, so that it obscures the antorbital fossa in lateral view. The same crest is oriented ventrolaterally in carcharodontosaurids such that the antorbital fossa is only visible in ventral view, and it is not clear if the original condition in *Neovenator* was more similar to the carcharodontosaurid condition or to that in *Allosaurus* (Madsen 1976) and *Sinraptor* (IVPP 10600; Currie & Zhao 1993), in which the crest is oriented laterally and the antorbital fossa is clearly visible in lateral view. The nasal contribution to the antorbital fossa is limited in extent relative to those of *Allosaurus* and *Sinraptor*, measuring only 140 mm anteroposteriorly and 13 mm transversely at its midpoint. A limited nasal antorbital fossa is characteristic of carcharodontosaurids, including *Carcharodontosaurus* (SGM-Din 1), *Giganotosaurus* (MUCPv-CH-1) and *Mapusaurus* (Coria & Currie 2006). In *Neovenator* the nasal antorbital fossa is pierced by a single large pneumatopore that extends deeply into the bone, suggesting that much of the nasal is hollow. Similar pneumatopores are known in other allosauroids, and are often variable in number. Two are seen in *Sinraptor* (*S. dongi*: Currie & Zhao 1993; *S. hepingensis*: Gao 1998) and *Giganotosaurus*, whereas one, two, or three such openings may be present in *Allosaurus* (Currie & Zhao 1993).

Palatine. An incomplete, tetaradiate right palatine is known from the holotype (MIWG 6348), missing the distal ends of the jugal, medial, vomeropterygoid, and maxillary processes (Pl. 3; Text-fig. 7). The preserved portion is 114 mm long anteroposteriorly and 23 mm dorsoventrally deep in the waisted region of the main body between the divergences of the various processes. This element was originally identified as a skull fragment in the collections of the MIWG, and has not been reported in any previous publication.

The numerous processes of the palatine are poorly preserved, but certain details are apparent. Anteriorly, the vomeropterygoid process is broken but its preserved base indicates that it projected anterodorsally from the main body. The maxillary process extends anteriorly as a small tapering projection on the anteroventral margin of the bone, and its divergence from the vomeropterygoid process demarcates the internal narial choana. The preserved region of the posterodorsally trending jugal process is marked by a deep groove for articulation with the jugal. The diverging jugal and medial processes delimit the palatine fenestra, the margins of which are mostly broken in *Neovenator*. The ventral surface of the maxillary process is marked by two longitudinal grooves for articulation with the maxilla.

In lateral view, a deep fossa marks the palatine pneumatic recess immediately anterior to where the jugal and medial processes emerge. It is deeper anteriorly and becomes shallower posteriorly, eventually merging with the lateral surface of the ventral jugal process. A similar large pneumatic recess is present in *Acrocanthosaurus* (Harris 1998) and *Sinraptor* (Currie & Zhao 1993), but is not seen in *Allosaurus* (Madsen 1976). The pneumatic fossa of *Neovenator* does not appear to contain any internal pneumatopores such as those present in *Sinraptor* and possibly *Acrocanthosaurus*, although damage obscures this region in the latter taxon (SMU 74646 3-24: Harris 1998). Dorsally the fossa is overhung by a robust ridge that trends posterodorsally onto the jugal process and tapers posteriorly. In *Neovenator* a small pneumatopore pierces the lateral surface immediately posterior to the divergence of the vomeropterygoid and maxillary

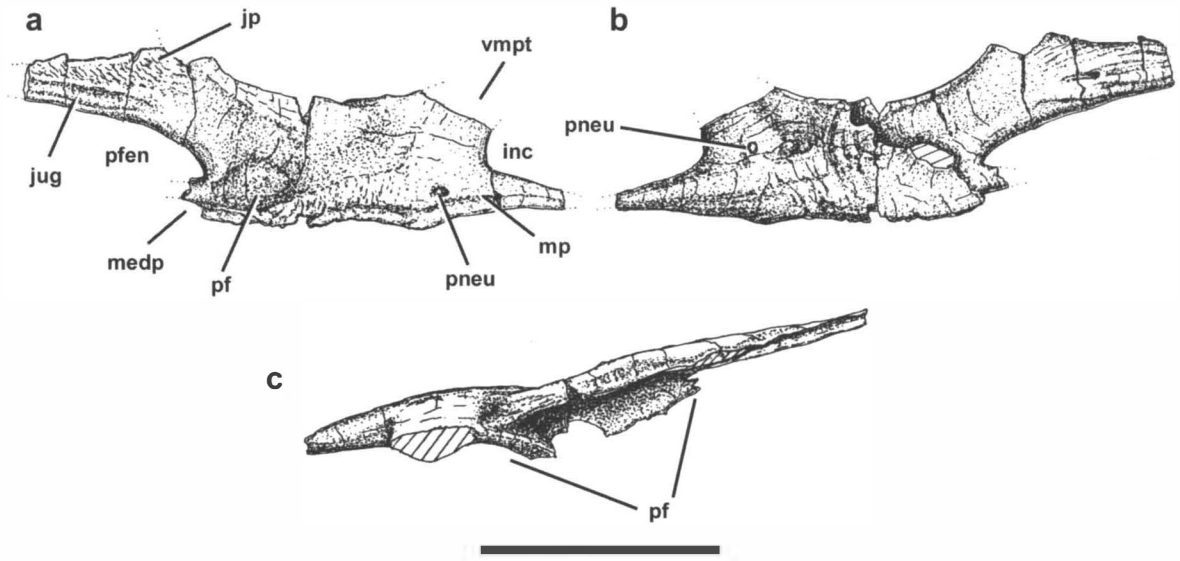

TEXT-FIG. 7. *Neovenator salerii* Hutt, Martill & Barker, 1996; right palatine (MIWG 6348): **a**, lateral view; **b**, medial view; **c**, dorsal view. Abbreviations: **inc**, internal narial choana; **jp**, jugal process; **jug**, articulation for jugal; **medp**, medial process; **mp**, maxillary process; **pf**, pneumatic fossa; **pfen**, palatine fenestra; **pneu**, pneumatic opening; **vmpt**, vomeropterygoid process. Scale bar represents 50 mm.

processes, and two pneumatopores are present medially on the base of the vomeropterygoid process. Pneumaticity is also apparent in dorsal view, where a deep fossa is present between the diverging medial and jugal processes. This fossa continues posteriorly onto the medial surface of the jugal process.

Dentary. A partial left dentary is known from the holotype (MIWG 6348; Text-fig. 8), which unfortunately could not be located during the course of the present study. We currently regard this specimen as lost, but it may be uncovered in the collections of The Natural History Museum or the Dinosaur Isle Museum at a later date. Fortunately, the dentary has been figured in various published works (Hutt *et al.* 1996; Naish *et al.* 2001) and briefly described in the M. Phil. thesis of Hutt (1999), and the following description is based on these sources as well as examination of a cast in the MIWG collection.

The left dentary is nearly complete, measuring 235 mm in anteroposterior length and 68 mm in maximum dorsoventral height. Portions of 13 alveoli are preserved. The dorsal margin of the dentary is relatively straight, whereas the ventral margin is straight posteriorly but becomes rounded anteriorly. Thus, the anterior end is not squared-off as in many carcharodontosaurids (*Acrocanthosaurus*, *Carcharodontosaurus*, *Giganotosaurus* and *Tyrannotitan*: Brusatte & Sereno 2007), but is more similar to the broadly rounded condition in *Allosaurus* (Madsen 1976), *Sinraptor* (Currie & Zhao 1993; Gao 1998) and most other theropods. Additionally, unlike many carcharodontosaurids, there is no projecting flange (dentary 'chin') on the anteroventral margin. The dentary is straight in dorsal view as in *Acrocanthosarus* (NCSM 14345) and most basal theropods. However, in most other allosauroids the dentary curves anteromedially (e.g. *Allosaurus*, *Carcharodontosaurus* and *Giganotosaurus*: Brusatte & Sereno 2007).

Laterally, the surface of the dentary is generally smooth, not heavily textured and scoured by deep neurovascular tracts as it is in *Carcharodontosaurus* (Brusatte & Sereno 2007), and is pierced by numerous neurovascular foramina. The largest foramina are located ventral to the alveolar margin and form a linear series set into a longitudinal groove. This groove immediately parallels the alveolar margin anteriorly but deflects ventrally at the level of the fifth alveolus, such that posterior foramina are located approximately 30 mm ventral to the tooth row. Such a ventrally deflected row of primary vascular foramina is present also in *Carcharodontosaurus*

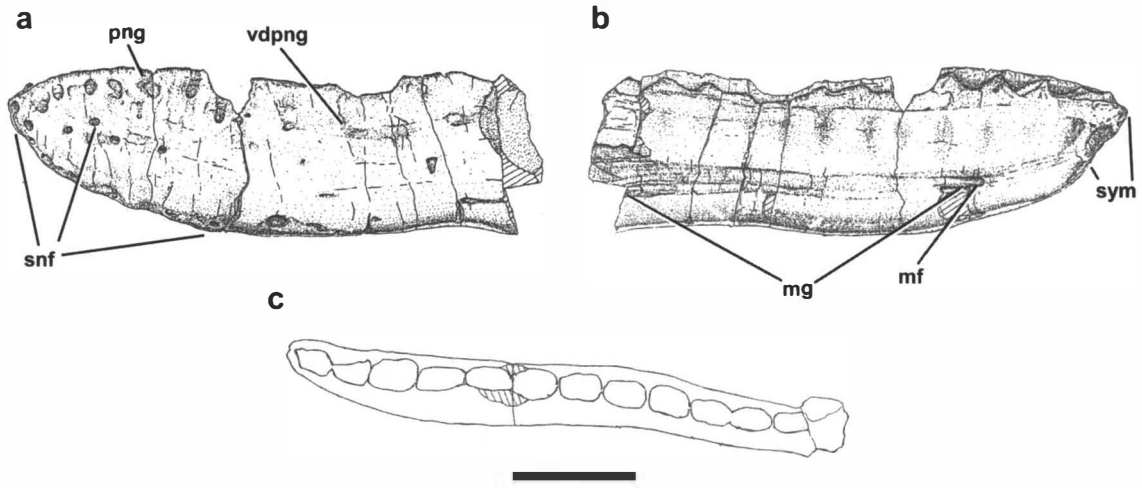

TEXT-FIG. 8. *Neovenator salerii* Hutt, Martill & Barker, 1996; left dentary (MIWG 6348): **a**, lateral view; **b**, medial view; **c**, dorsal view. Abbreviations: **mf**, Meckelian foramen; **mg**, Meckelian groove; **png**, primary neurovascular groove; **snf**, secondary neurovascular foramina; **sym**, symphysis; **vdpng**, ventral deflection of the primary neurovascular groove. Scale bar represents 50 mm.

(Brusatte & Sereno 2007) and *Giganotosaurus* (Calvo & Coria 2000), and differs from the more horizontal and elevated groove present in *Allosaurus* (Madsen 1976), *Sinraptor* (IVPP 10600; Currie & Zhao 1993) and most other theropods. Additionally, a second series of smaller foramina is present anteriorly ventral to the main series, while a third series parallels the anterior margin of the dentary. Many of these foramina open dorsally via well-defined exit grooves.

In medial view, the interdental plates are completely fused together, similar to those in the premaxilla and maxilla. Ventral to the fused plates is a thickened medial band, which housed the dental lamina in a groove along its dorsal surface. Further ventral to this band is the Meckelian groove, which begins as a dorsoventrally deep groove posteriorly and becomes progressively shallower anteriorly before passing into the Meckelian foramen *c.* 5 mm posterior to the symphysis at the level of the third alveolus. Only a single Meckelian foramen is present as in *Giganotosaurus* and *Mapusaurus*, not two foramina as in *Allosaurus*, *Sinraptor* and basal tetanurans in general (Benson *et al.* 2008). The mesial dentary symphysis is small and limited to the anterodorsal corner of the medial surface. It is *c.* 30 mm deep and 10 mm long, and projects slightly medially. Such a contact probably resulted in a relatively weak union between the conjoined dentaries, unlike the case in *Allosaurus* and carcharodontosaurids (Brusatte & Sereno 2007), which possess a well-defined and dorsoventrally high symphysis. Additionally, there is no pronounced articular brace in the ventral region of the symphysis, as has been described in *Carcharodontosaurus* (Brusatte & Sereno 2007). There is a slightly raised rugosity in this region in *Neovenator* and other basal theropods (e.g. *Dubreuillosaurus*: MNHN 1998-13 RJN 22), which may be homologous to the greatly enlarged and rugose brace of *Carcharodontosaurus*.

In dorsal view, the alveoli are arranged in a slight sinuous curve, which may be slightly exaggerated by crushing. No erupted dentary teeth are visible, but replacement teeth are evident in alveoli 3, 5, 7 and 12. On average the alveoli are smaller than the maxillary alveoli. The lateral surface of the dentary expands laterally to accommodate the third alveolus, which is the largest of the dentary alveoli. An enlarged third dentary alveolus is also present as in most spinosauroids and basal theropods such as *Dilophosaurus* (Rauhut 2003), but is otherwise only present in *Acrocanthosaurus* among allosauroids (NCSM 14345).

Dentition. Although the premaxillae, maxilla and dentary do not contain any erupted teeth, several isolated theropod teeth were found with the holotype specimen (MIWG 6348, BMNH R10001; Pl. 4). These teeth come in varying sizes and morphologies, representing fully erupted adult teeth, partly developed replacement teeth, and teeth from more anteriorly in the jaw, perhaps the premaxilla, which are anteroposteriorly shortened (Pl. 4). In general these teeth are typical of theropod teeth, as they are recurved, serrated, and blade-like. However, they are

unlike the teeth of derived carcharodontosaurids (*Carcharodontosaurus*: SGM-Din 1, Sereno *et al.* 1996; Benton *et al.* 2000; Brusatte & Sereno 2007; Brusatte *et al.* 2007; *Giganotosaurus*: MUCPv-CH-1; *Mapusaurus*: Coria & Currie 2006), which are transversely thin, broad in lateral view, and only slightly recurved. Contra Brusatte *et al.* (2007), numerous enamel wrinkles are present on the mesial and distal carinae of labial and lingual surfaces of the teeth, continuing across the labial and lingual surfaces as visible bands. These are unlike the enamel wrinkles of some carcharodontosaurids (*Carcharodonotosaurus*: SGM-Din 1; *Giganotosaurus*: MUCPv-CH-1; *Mapusaurus*: Coria & Currie 2006), which are restricted to the regions of the tooth immediately adjacent to the carinae and continue across the labial and lingual surfaces only as shallow and often indistinguishable bands. For a more general overview of the morphology and systematic importance of enamel wrinkles, see Brusatte *et al.* (2007).

In *Neovenator*, the distal carina continues to the base of the tooth and is situated to one side of the midline, giving the tooth an asymetrical cross section. The mesial carina is positioned centrally, and continues approximately one third of the way to the base of the tooth. Serrations are present continuously over the apex of the tooth, a character once thought to be unique to *Acrocanthosaurus* (Harris 1998) but now known in a wide array of theropods. Very short grooves (interdental sulci of Smith 2007) continue onto the surface of the crown from between the serrations on both the mesial and distal surfaces of the teeth. These grooves are oriented parallel to the emergent axes of the denticles, and thus perpendicular to the carinae. Detailed measurements of the teeth of MIWG 6348 were published by Sweetman (2004).

Axial skeleton

The majority of the axial column is preserved in the holotype (Table 3), including the axis with the axial intercentrum and odontoid (MIWG 6348), most of the cervical and dorsal series (BMNH R10001 and MIWG 6348), and twenty-three caudal vertebrae representing anterior, middle and posterior parts of the caudal series (MIWG 6348 and BMNH R10001) (Pls 5–29; Text-figs 9–17). The atlas, the atlantal intercentrum, the third and fourth cervical vertebrae, and the third, eleventh and fifteenth dorsal vertebrae are not known. Additionally, five chevrons are known from the holotype (MIWG 6348): one from the anterior part of the caudal series, three from the posterior part of the middle of the series, and one from the posterior part. Fragments of ribs (MIWG 6348) and several gastral elements are also represented in the holotype (MIWG 6348). Several dorsal vertebrae and a single ninth cervical vertebra are known from the referred specimens (MIWG 5470, 6352).

The neural arch is attached to the centrum in all preserved holotype and referred vertebral elements, indicating that the specimens represent mature or subadult individuals, close to adult body size. Irmis (2007) commented that the distal caudal vertebrae of MIWG 6348 exhibited fully closed neurocentral sutures, whereas those of the dorsal vertebrae were open. Open sutures are also present in the cervical vertebrae. The junction between the two vertebral components is consistently marked by a swollen ridge and scored by fine transverse striations. The internal structure of the presacral vertebrae is camellate (terminology after Britt 1993), consisting of a complex network of small chambers. This morphology is clearly visible wherever the centra or neural arches of these elements are broken. A similar condition is present in the pneumatic presacral axial elements of derived allosauroids, including *Acrocanthosaurus* (Harris 1998) and derived carcharodontosaurids (e.g. *Giganotosaurus*: MUCPv-CH-1), as well as certain other theropod groups including neoceratosaurs (e.g. *Carnotaurus* and *Ceratosaurus*: Britt 1993; *Ekrixinatosaurus*, MUCPv-294). This condition is also present in a potential allosauroid taxon (MPM 1) preliminarily described by Alcober *et al.* (1998). In other basal tetanurans the internal structure of pneumatic vertebrae is generally camerate, consisting of a small number of large internal chambers (e.g. *Allosaurus*, *Piatnitzkysaurus*, *Sinraptor* and *Torvosaurus*: Britt 1993).

Atlas-axis complex

Axial intercentrum. The axial intercentrum is preserved in articulation with the odontoid and the axis, to which it is fused (Pl. 5; Text-fig. 9). This element is wedge-like, as it is longer anteroposteriorly along the ventral margin than dorsally, and as a consequence the anterior surface is posterodorsally inclined. The intercentrum occupies approximately half of the anterior

TABLE 3. Vertebral measurements (MIWG 6348, BMNH R10001) in mm; * = crushed or distorted; i = incomplete element; e = total measurement estimated.

Specimen Number	Specimen identification	Antero-posterior length of centrum[1]	Minimum transverse width of centrum	Dorso-ventral height of anterior surface of centrum	Medio-lateral width of anterior surface of centrum	Dorso-ventral height of posterior surface of centrum	Medio-lateral width of posterior surface of centrum	Dorso-ventral height of neural spine[2]	Minimum antero-posterior breadth of neural spine
MIWG 6348	Axis	58	21	44	45	45	72	44*	--
BMNH R10001	Cervical 5	62	40	44	47	57	?	61e	?
MIWG 6348	Cervical 6	76	41	55	58*	71	--	74e	--
BMNH R10001	Cervical 7	73	39	53	64	54*	35	57e	38?
MIWG 6348	Cervical 8	66	40	45	64	53*	69	76	29
MIWG 6348	Cervical 9	75	41	57	57	64	--	71	--
BMNH R10001	Dorsal 1	71	50	59	84	73	78	88	22
BMNH R10001	Dorsal 2	62	54	71	72	66e	?	82	?
BMNH R10001	Dorsal 5	87	43	79	65	78	?	76	?
BMNH R10001	Dorsal 6	77	41	75	78	84	69	83	46
BMNH R10001	Dorsal 7	93	31	83	81	88	76	86	54
BMNH R10001	Dorsal 8	89	45	92	87	95	76	94	49
MIWG 6348	Dorsal 9	92	51	99	89	106	88	104	54
MIWG 6348	Dorsal 10	95	48	103	101	105	80i	104	62
BMNH R10001	Dorsal 12	115	51	106	99	107	104	104*	60
BMNH R10001	Dorsal 13	117	49	108*	104e	113*	103	104*	59
MIWG 6348	Dorsal 14	110	47*	108e	107e	114e	--	111e	--
MIWG 6348	Caudal 1	109	60	104	101	114		102	--
MIWG 6348	Caudal 2	99	69	95	107	88	126	95	56
MIWG 6348	Caudal A (3)	105	55	93	89	89	114	83	59*
MIWG 6348	Caudal B (4)	109	48	87	83	82	105i	74	60
MIWG 6348	Caudal C (5)	107	43	78	70	74	95i	72	67
MIWG 6348	Caudal D (6)	107	30*	71	71	69	82i	66	48
MIWG 6348	Caudal E (?7)	106	43	73	70	69e	--	65	--
MIWG 6348	Caudal F (?9)	--	--	--	--	--	--	--	--
MIWG 6348	Caudal G (?14)	103	39	61	64	59	90i	60	25
MIWG 6348	Caudal H (?17)	103	39	58	60	55	62i	59	
MIWG 6348	Caudal I (?18)	102	40	53	59	54e	--	57	--
MIWG 6348	Caudal J (?21)	94	39	51	59	50e	82i	56	24
MIWG 6348	Caudal K (?22)	95	36	47	57	47	--	54	--
MIWG 6348	Caudal L (?25)	91	39	44	51	44	--	52	--
MIWG 6348	Caudal M (?26)	92	39	44	52	47	67	52	?
MIWG 6348	Caudal N (?27)	88	38	39	50	41	--	50	--
MIWG 6348	Caudal O (?28)	81	34	36	48	37	--	59	--
MIWG 6348	Caudal P (distal)	79	31	30	44	28	--	43	--
MIWG 6348	Caudal Q (distal)	77	28	27	35	27	--	36	--
MIWG 6348	Caudal R (distal)	75	26	26	34	26	--	35	--
MIWG 6348	Caudal S (distal)	73	24	25	31	24	--	32	--
MIWG 6348	Caudal T (distal)	71	22	22	30	22	--	31	--
MIWG 6348	Caudal U (distal)	68	21	21	28	20	--	27	--

[1]: not including anterior articular surface
[2]: measured parallel to the long axis of the spine from the dorsal surface of the transverse processes

articular surface of the axial centrum ventral to the odontoid, as is the case in *Dilophosaurus* (UCMP 37302) and *Sinraptor* (Currie & Zhao 1993), but not *Allosaurus* (Madsen 1976), *Ceratosaurus* (UMNH VP 5278) or *Giganotosaurus* (MUCPv-CH-1), in all of which the axial intercentrum is slightly larger relative to the odontoid. The axial intercentrum of *Neovenator* has a crescentric outline in anterior view (Text-fig. 9). The anterior surface is slightly concave and is wider transversely than the posterior surface and the odontoid, giving the entire axial complex a bell-shaped outline in anterior view. An expanded anterior articular suface of the axial intercentrum is not present in other allosauroids (*Acrocanthosaurus*: Harris 1998; *Allosaurus*:

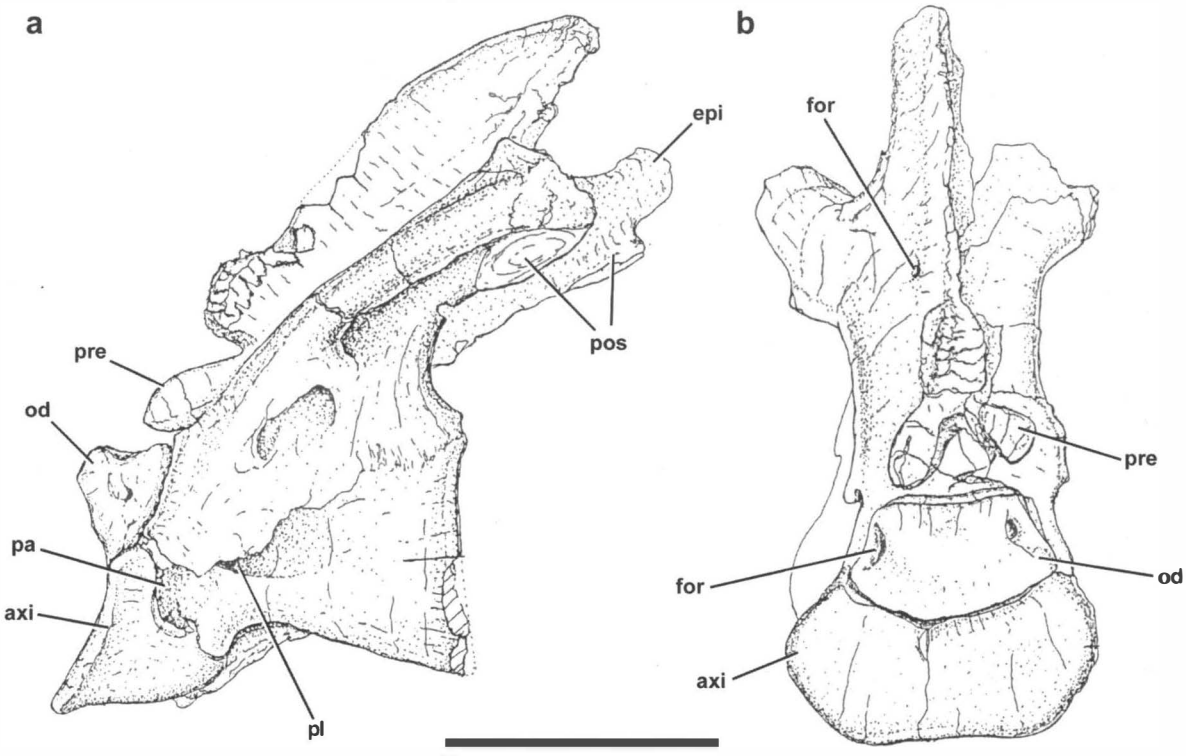

TEXT-FIG. 9. *Neovenator salerii* Hutt, Martill & Barker, 1996; atlas-axis complex (MIWG 6348): **a**, left lateral view; **b**, anterior view. Abbreviations: **axi**, axial intercentrum; **epi**, epipophysis; **for**, foramen; **od**, odontoid; **pa**, parapophysis; **pl**, pleurocoel, **pos**, postzygapophysis; **pre**, prezygapophysis. Scale bar represents 50 mm.

Madsen 1976; *Giganotosaurus*: MUCPv-CH-1; *Sinraptor*: Currie & Zhao 1993) or more basal theropods (*Ceratosaurus*: UMNH VP 5278; *Dilophosaurus*: UCMP 37302) and is an autapomorphy of *Neovenator*.

In *Giganotosaurus* (MUCPv-CH-1) and *Sinraptor* (Currie & Zhao 1993) the ventral margin of the axial intercentrum is inclined anterodorsally, unlike the situation in *Allosaurus*, *Carnotaurus*, *Ceratosaurus*, *Dilophosaurus* and *Piatnitzkysaurus* (Currie & Zhao 1993) in which the ventral margin of the intercentrum is horizontal and forms a continuous line with the ventral margin of the axial centrum. In *Neovenator* the ventral margin of the axial intercentrum is gently inclined anterodorsally, a similar condition to that present in *Acrocanthosaurus* (Harris 1998).

Odontoid. The odontoid is a smoothly rounded knob of bone fused to the dorsal half of the anterior articular face of the axial centrum (Pl. 5; Text-fig. 9). The dorsal surface is truncated and slightly concave. A single foramen is located laterally on either side of the anterior surface (Text-fig. 9). Such foramina are absent in other allosauroids (*Acrocanthosaurus*: Harris 1998; *Allosaurus*: Madsen 1976; *Sinraptor*: Currie & Zhao 1993) and theropods in general. However, small depressions are present in the same position as the odontoid foramina of *Neovenator* in *Dilophosaurus* (UCMP 37302), *Giganotosaurus* (MUCPv-CH-1), *Monolophosaurus* (IVPP 84019) and *Piatnitzkysaurus* (PVL 4073). As they are absent in other basal tetanurans, these foramina are an autapomorphy of *Neovenator*.

Axis. The axis is well-preserved but crushed, resulting in compression of the right side of the centrum and left postzygapophysis anteroposteriorly (Pl. 5; Text-fig. 9). The right transverse process has been crushed medially against the lateral surface of the centrum and the left diapophysis has been broken off.

The articular surfaces of the centrum are vertical and are approximately as high as wide,

similar to the situation in most basal theropods (e.g. *Allosaurus*: Madsen 1976; *Dilophosaurus*: UCMP 37302; *Giganotosaurus*: MUCPv-CH-1). In contrast, the articular surfaces of the axial centrum of *Acrocanthosaurus* are substantially higher than they are wide (Harris 1998). The anterior articular surface is obscured by the odontoid and axial intercentrum but is offset ventrally relative to the posterior articular surface, which is strongly concave. The ventral surface of the centrum is transversely convex; on the left side the ventral surface appears to be transversely concave between the parapophyses, but this is the result of crushing. Although a weak longitudinal ridge is present on the ventral surface posteriorly, it is not as strongly developed as it is in some allosauroids (*Acrocanthosaurus*: Harris 1998; *Giganotosaurus*: MUCPv-CH-1) and more basal theropods (*Ceratosaurus*: UMNH VP 5278; *Dilophosaurus*: UCMP 37302). A ventral ridge is absent in the axes of *Allosaurus* (Madsen 1976) and *Sinraptor* (Currie & Zhao 1993).

The parapophyses are situated just ventral to midheight of the centrum adjacent to the anterior articular surface. They are subcircular depressions on the lateral surface of the centrum, 10 mm in diameter, and are not raised on pedicles as are the parapophyses of more posterior axial elements. A suboval pleurocoel penetrates the lateral surface of the centrum posterodorsal to the parapophysis. The left pleurocoel is situated within a shallow fossa that extends further posteriorly than does the pleurocoel itself.

The prezygapophyses are small compared to those of more posterior presacral axial elements. They are thin flanges that emerge anteroventrally from the anterior surface of the neural arch on both sides of the anterior opening of the neural canal. The dorsal surfaces of these flanges are inclined laterally and form the articular facets; they are not distinct from the bodies of the prezygapophyses (as they are in other elements of the axial series) and are weakly convex proximodistally. The postzygapophyseal facets are large, comparable in size to those of the postaxial cervicals. They emerge posterodorsally and diverge laterally, such that they are widely separated dorsal to the posterior opening of the neural canal, although this separation has been reduced by crushing. The postzygapophyseal facets face posteroventrally with a slight lateral inclination. Pronounced epipophyses are present on the dorsal surfaces of the postzygapophyses and extend past the posterior level of the facets, curving slightly laterally. The epipophyses are wider transversely than high dorsoventrally.

Only the right diapophysis is preserved. It is directed posteroventrally, although it was probably oriented more laterally prior to crushing, and the diapophyseal facet is situated posterodorsal to the pleurocoel. The diapophysis is connected to the postzygapophysis by a robust postzygodiapophyseal lamina, and a low posterior centrodiapophyseal lamina connects the postzygodiapophyseal lamina to the posterior neural arch pedicle. The latter lamina separates the infrapostzygopophyseal fossa posterodorsally from the infradiapophyseal fossa. The deepest parts of the infradiapophyseal fossa are occupied by matrix. There is no anterior centrodiapophyseal lamina.

The neural spine is triangular in lateral view and is transversely thin, although it thickens posteriorly. The apex of the spine is positioned posterodorsally. Some rugosity for ligament attachment is developed along the anterior edge of the spine, but this rugosity does not form a distinct ridge as it does in more posterior elements of the presacral series. A similar, more distinct, rugosity is present posteriorly between the spinopostzygapophyseal laminae. The base of the neural spine projects anteriorly as a rounded eminence that overhangs the anterior opening of the neural canal and extends past the anteriormost level of the anterior surface of the centrum. A small pneumatic foramen is present on the lateral surface of the neural spine dorsal to the right diapophysis (Pl. 5). The corresponding region on the right side is obscured by the base of the postzygapophysis. Multiple larger foramina are present laterally on the axial neural spine of *Acrocanthosaurus* (Harris 1998), but are absent in other allosauroids (*Allosaurus*: Madsen 1976; *Giganotosaurus*: MUCPv-CH-1; *Sinraptor*: Currie & Zhao 1993) and theropods in general (e.g. *Ceratosaurus*: UMNH VP 5278; *Dilophosaurus*: UCMP 37302). Therefore, a small single foramen on the lateral surface of the neural spine is an autapomorphy of *Neovenator*.

Postaxial cervical vertebrae. Based on comparison with the cervical series of *Allosaurus* (Madsen 1976), *Sinraptor dongi* (Currie & Zhao 1993) and *Sinraptor hepingensis* (Gao 1998), the known

cervical elements of the holotype *Neovenator* can be identified as the fifth to ninth elements of the cervical series (Pls 5–7; Text-figs 10, 11). Additionally, the single cervical element of referred specimen MIWG 5470 is identified as the ninth cervical (Pl. 26). Unfortunately, there is little consensus over identification of cervical vertebrae in theropods (Brochu 2002; e.g., the contrasting systems of Welles 1983 and Currie & Zhao 1993) and the identification criterion is often not made explicit (e.g. Madsen 1976). As the morphology of ribs corresponding to vertebrae in the pectoral region of the axial column is not known, we have arbitrarily designated the first nine presacral vertebrae as cervical vertebrae and subsequent vertebrae as dorsal vertebrae to make the present description comparable with previous information regarding *Neovenator* (e.g. Hutt *et al.* 1996) as well as with the descriptions of other authors who have used this system.

In the holotype (BMNH R10001 and MIWG 6348) the fifth cervical vertebra is preserved, but is missing the neural spine and right pre- and postzygapophyses. The centrum of the sixth cervical vertebra is preserved with the base of the neural arch, but the ventral portion of the rim of the posterior articular surface is damaged. This element has been crushed transversely, and the left side has been sheared anteriorly relative to the right. The seventh cervical vertebra is complete but distorted, with the dorsal portion sheared to the left side relative to the posterior portion. The centrum and neural arch of the eighth cervical vertebra are preserved. The left parapophysis, the distal portion of the left transverse process, the transverse process, and both zygapophyses of the right side have been broken off and are missing. The neural arch has been sheared anteroventrolaterally to the right relative to the centrum. The centrum of the ninth cervical vertebra is almost complete, with some damage to the ventral part of the rim around the posterior articular surface. The neural arch is incomplete: the extremities of the transverse processes and neural spine as well as the postzygapophyses and the portion of the right lateral wall of the arch just dorsal to the neurocentral suture are missing. Finally, the ninth cervical vertebra of one of the referred specimens (MIWG 5470) is represented by only a neural arch, which lacks the right pre- and postzygapophyses and the tip of the neural spine.

The cervical centra are constricted medially, though to a much lesser extent than those of the dorsal and caudal vertebrae, and have articular surfaces that are slightly wider than high. They are therefore similar in proportion to those of *Allosaurus* (Madsen 1976), but differ from those of *Carcharodontosaurus* (Stromer 1931; Sereno *et al.* 1996; Brusatte & Sereno 2007), which are significantly dorsoventrally compressed. In all five cervical elements the anterior articular surface is offset dorsally relative to the posterior surface. This offset is a general character of dinosaurs (Sereno 1991), but is substantially reduced in some carcharodontosaurids (*Acrocanthosaurus, Giganotosaurus*: Brusatte & Sereno 2008) and spinosaurids (*Baryonyx*: Charig and Milner 1997). The most extreme condition is seen in *Carcharodontosaurus*, in which offset between the two faces is essentially absent (Sereno *et al.* 1996; Brusatte & Sereno 2007). Within the cervical series of *Neovenator* the offset is strongest in the seventh presacral vertebra and becomes weaker anteriorly and posteriorly in the presacral series.

The centra of all of the preserved cervical vertebrae are opisthocoelous: the anterior articular surface is convex and ball-like and the posterior surface is deeply concave. Rauhut (2003) found strongly opisthocoelous cervical vertebrae to be a synapomorphy of his Carnosauria (which includes Allosauroidea and Spinosauroidea) and convergently present in some basal coelurosaurs (e.g. *Compsognathus*). The anterior surface of the centrum is not a smooth hemisphere but is irregular and hummocky, and is surrounded by a distinct flattened rim, similar to the rim around the anterior articular surfaces of the cervical vertebrae of some other basal tetanurans (*Afrovenator*: UC OBA 1; *Allosaurus*: Madsen 1976; *Baryonyx*: Charig & Milner 1997; *Megaraptor*: MUCPv 341; *Streptospondylus*: MNHN uncatalogued; *Torvosaurus*: Britt 1991). However, this rim is absent in some allosauroids (*Acrocanthosaurus*: OMNH 10146; *Carcharodontosaurus*: SGM Din 3; *Mapusaurus*: Coria & Currie, 2006; *Sinraptor*: Currie & Zhao 1993).

The ventral surfaces of the centra are broad, gently rounded transversely and convex, except anteriorly between the parapophyses where they are transversely concave. The convexity of the ventral surface is greatest in the ninth cervical vertebra, and in this element the anterior concave region is reduced to a gentle longitudinal groove confined to the anterior portion of the centrum.

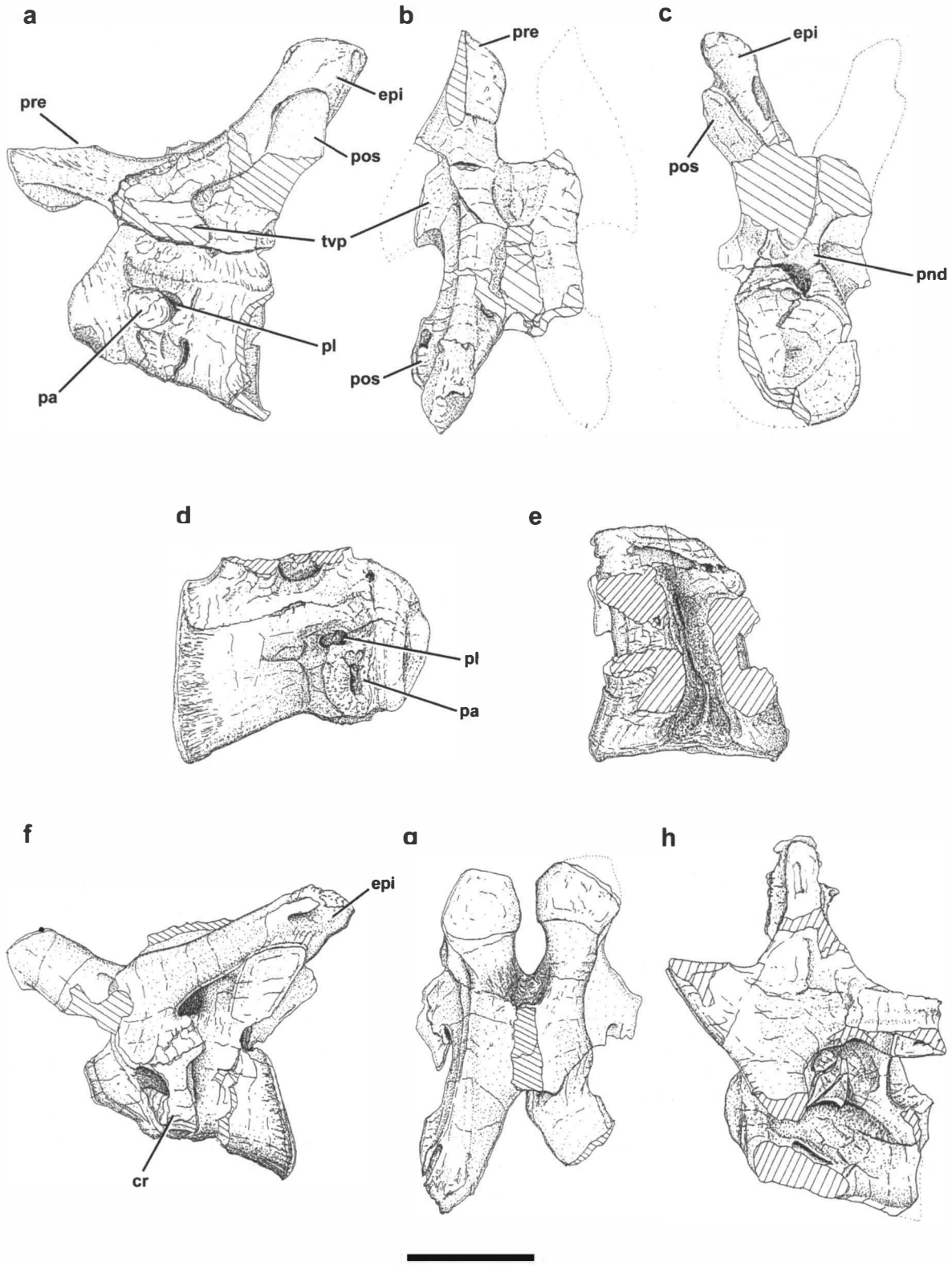

TEXT-FIG. 10. *Neovenator salerii* Hutt, Martill & Barker, 1996; cervical vertebrae: **a**, cervical 5 in left lateral view; **b**, cervical 5 in dorsal view; **c**, cervical 5 in posterior view; **d**, cervical 6 in right lateral view; **e**, cervical 6 in dorsal view; **f**, cervical 7 in left lateral view; **g**, cervical 7 in dorsal view; **h**, cervical 8 in left lateral view. Abbreviations: **cr**, cervical rib; **epi**, epipophysis; **pa**, parapophysis; **pl**, pleurocoel; **pnd**, pneumatic depression; **pos**, postzygapophysis; **pre**, prezygapophysis; **tvp**, transverse process. Scale bar represents 50 mm.

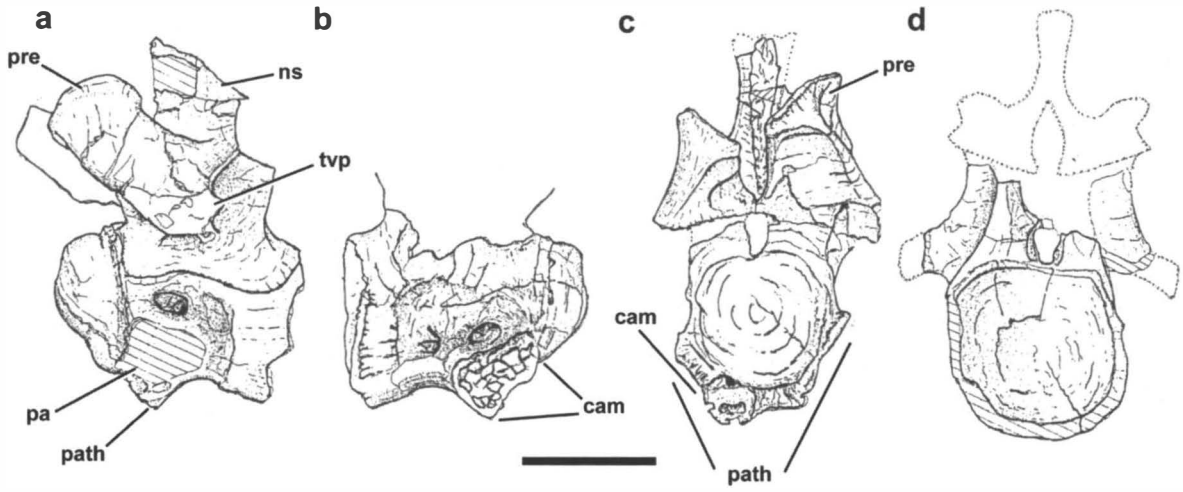

TEXT-FIG. 11. *Neovenator salerii* Hutt, Martill & Barker, 1996; cervical vertebra 9: **a**, left lateral view; **b**, right lateral view; **c**, anterior view; **d**, posterior view. Abbreviations: **cam**, camellate internal structure of parapophysis; **ns**, neural spine; **pa**, parapophysis; **path**, pathology; **pre**, prezygapophysis; **tvp**, transverse process. Scale bar represents 50 mm.

The parapophyses of all cervical vertebrae are situated anteroventrally on the lateral surfaces of the centra. In the fifth and sixth cervical vertebrae they are slightly raised on low pedicles and have semicircular, slightly concave parapophyseal facets finished with a smooth articular surface. In the seventh cervical vertebra the ribs are fused to the parapophyses and diapophyses and the articular surfaces are not visible (Pl. 6). Small foramina are present on the contact between the rib and the parapophysis, and where the proximal portion of the rib is broken a pneumatic, camellate, internal structure is visible. Fusion of at least some of the cervical ribs to the vertebral rib facets occurs in several theropod groups, although the situation is often confused in the literature. Numerous authors have used fusion of the ribs to the cervical centra as a character in cladistic analyses: Carrano *et al.* (2002) scored such fusion as present in *Ceratosaurus*, *Coelophysis*, *Elaphrosaurus* and *Syntarsus*; Harris (1998) scored fusion as present in Tyrannosauridae, Troodontodiae and Ornithomimosauria; and Tykoski & Rowe (2004) scored it as being present in *Majungasaurus*, *Masiakasaurus*, *Noasaurus*, Ornithischia and *Procompsognathus*. However, this type of fusion does not occur in mature specimens of other allosauroids (*Allosaurus*: Madsen 1976; *Giganotosaurus*: MUCPv-CH-1; *Sinraptor*: Currie & Zhao 1993) and may be an autapomorphy of *Neovenator* among allosauroids. In the eighth and ninth cervical vertebrae the parapophyseal facets are larger than those of preceding vertebrae, more irregular in shape, only weakly raised on pedicles, and lack a smooth articular surface. Instead, the surface of the parapophyseal facets in these posterior cervical elements has an irregular, camellate surface structure within which a complex network of small chambers is visible. This may indicate invasion of the space between the rib and the centrum by pneumatic diverticulae, and possibly incipient fusion of the cervical rib to the parapophysis as in the seventh cervical vertebra. This condition does not appear to be the result of erosion or pathology, and whatever the case, external exposure of the camellate internal texture on the parapophyseal facet of posterior cervical vertebrae is not known in any other basal tetanuran and is an autapomorphy of *Neovenator*.

An oval pleurocoel penetrates the lateral surface of the centrum immediately posterodorsal to the parapophysis in all cervical vertebrae. The pleurocoels of the seventh and eighth cervical vertebrae are dorsoventrally compressed and slit-like. On the right sides of the sixth and ninth elements a smaller second pleurocoel is present posteroventral to the first. On the left side of these two elements a small suboval fossa is present in place of the more posterior pleurocoel. This is quite distinct from the posterior pleurocoel of non-tetanuran theropods (e.g. *Ceratosaurus*: UMNH VP 5278; *Dilophosaurus*: UCMP 37302), as it is not situated near the posterior articular surface of the centrum. The situation is more similar to the case in some carcharodontosaurid

cervical vertebrae (e.g. *Giganotosaurus*: MUCPv-CH-1; *Tyrannotitan*: Novas *et al.* 2005), in which a large single pleurocoel situated anteriorly on the lateral surface of the centrum is divided in two by an anterodorsally inclined ridge. Division of the pleurocoel is absent in all but the most anterior carcharodontosaurid dorsal vertebrae and is not consistently present in the cervical vertebrae, occurring on only a proportion of the cervical elements of a single individual, and with a bias towards the left or right side (*Giganotosaurus*: MUCPv-CH-1). The cervical pleurocoels of *Acrocanthosaurus* have undivided openings, but pleurocoels similar to the divided pleurocoels of carcharodontosaurids are consistently present on both sides of the dorsal centra (OMNH 10146).

The cervical zygapophyseal facets are larger than those of the dorsal and caudal vertebrae. The prezygapophyses emerge anteriorly from the base of the transverse process in the fifth and sixth cervical vertebrae but emerge anterolaterally in the eighth and ninth elements. They are well-separated across the midline dorsal to the neural canal, especially in the more posterior elements of the cervical series. The prezygapophyseal facets face dorsomedially and the prespinal fossa originates as a suboval recess between the facets, bounded laterally by the spinoprezygapophyseal lamina. These laminae are low and robust in the fifth through eighth elements and become less prominent in the ninth.

The postzygapophyses of the cervical vertebrae are discrete processes that emerge from the posterior region of the neural arch at the base of the transverse process. Only the left postzygapophysis of the fifth element is preserved. It is directed almost strictly dorsally from the posterior portion of the base of the transverse process and has a slight posterolateral inclination. A long, stout epipophysis emerges dorsally from the dorsal surface of the postzygapophysis and may have approached the dorsal height of the broken neural spine. The peripheral surface of the epipophysis is rugose distally (= posterodorsally), as it is in successive cervical epipophyses. The postzygapophyses of the seventh and eighth cervical vertebrae are robust, posterodorsolaterally directed processes. The epipophysis of the seventh cervical vertebra is well-developed and overhangs the postzygapophyses posteriorly, but is not as strongly developed as is that of the fifth cervical vertebra. The epipophysis of the eighth cervical vertebra is reduced compared to those of earlier cervical vertebrae and takes the form of a rugose posterodorsal protuberance that does not extend past the posterior limit of the postzygapophysis. The left postzygapophyseal facet of the fifth cervical vertebra faces posterolaterally and is only slightly ventrally inclined, whereas those of the seventh and eighth elements face ventrolaterally. The postspinal fossa originates as a deep oval recess between the postzygapophyses and is bounded laterally by the spinopostzygapophyseal laminae. These laminae are robust and well-developed where they are known. Small but distinct triangular pneumatic recesses are present ventromedial to the postzygapophyses in all known cervical vertebrae. Similar but weaker recesses are also present ventromedial to the prezygapophyses of all cervical vertebrae except for the ninth. Pronounced epipophyseal-prezygapophyseal laminae, connecting the epipophyses to the lateral edges of the prezygapophyseal facets, are present on the dorsal surfaces of the neural arches in the fifth and seventh cervical vertebrae but are absent in the eighth.

The transverse processes have dorsoventrally thin, sheet-like, triangular bases that develop into rod-like processes distally (= laterally). They are ventrolaterally directed and become more laterally directed posteriorly in the cervical series. Well-developed posterior centrodiapophyseal laminae and weaker, but also pronounced, anterior centrodiapophyseal laminae support the transverse processes ventrally. Both types of lamina are more prominent in more posterior elements of the cervical series. The infradiapophyseal and infrapostzygapophyseal fossae are deep, and contain pneumatic foramina that lead into the neural arch. These foramina are present in the deepest recesses of the fossae, and are most clearly visible on the left side of the ninth cervical vertebra, which has been thoroughly prepared. Such foramina are also evident in the infradiapophyseal fossae of the seventh and fifth cervicals. However, in the fifth cervical it is clear that no foramina were present in the infrapostzygapophyseal fossa. Unfortunately, it is impossible to determine the exact morphology of all pneumatic structures in an imperfectly preserved and incompletely prepared specimen such as this without the use of three-dimensional scanning techniques such as computed tomography. The infraprezygapophyseal fossa is small but

deep in more posterior elements of the cervical series. The presence of foramina within this fossa cannot be determined, as this region has not been thoroughly prepared in any of the cervical vertebrae.

The neural spines of the cervical vertebrae are anteroposteriorly narrow, transversely thick, and rod-like. Squared rugose ridges originating within the pre- and postspinal fossae continue dorsally along the anterior and posterior surfaces of the spines and terminate ventral to the dorsalmost point of the spine body. The neural spine of the seventh cervical vertebra is inclined posteriorly, while that of the eighth element is inclined anteriorly and that of the ninth element is vertical.

Dorsal vertebrae. Twelve dorsal vertebrae are known from the holotype specimen (Pls 8–13; Text-figs 12–14). Based on comparisons with *Allosaurus* (Madsen 1976), *Sinraptor dongi* (Currie & Zhao 1993) and *Sinraptor hepingensis* (Gao 1998), these elements correspond to the first and second, the fourth to the tenth, and the twelfth to the fourteenth dorsal vertebrae. The eighth dorsal vertebra of MIWG 5470 is also preserved, missing only the distal portions of the prezygapophyses, the left transverse process and the neural spine (Pl. 26). Parts of several dorsal vertebrae of MIWG 6352 are preserved: the centrum and base of the neural arch of the second; the centrum of the fifth; and the neural arch of the sixth, which is missing the majority of the left side and the distal half of the neural spine (Pls 27, 28).

Most of the dorsal vertebrae of the holotype are well-preserved and undistorted, although cracking of the bone surface is widespread. The first dorsal vertebra is complete, with minor damage to the right parapophysis. The second dorsal vertebra preserves the base of the neural

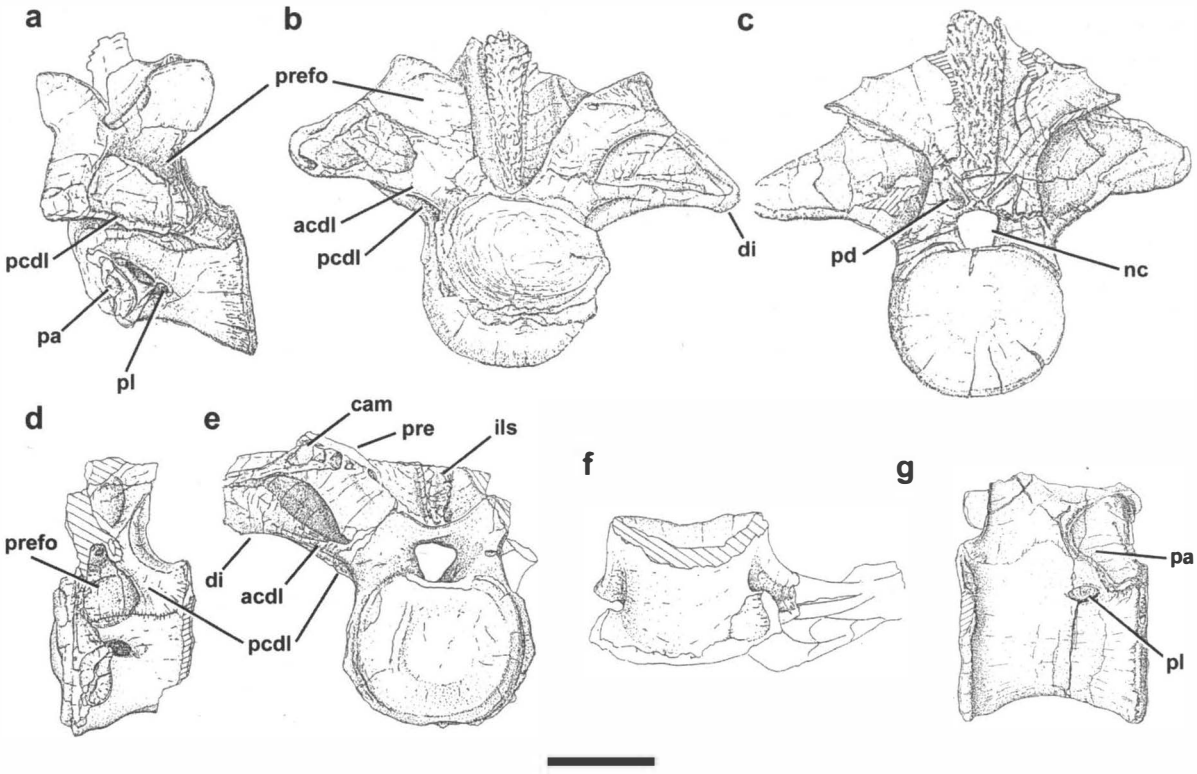

TEXT-FIG. 12. *Neovenator salerii* Hutt, Martill & Barker, 1996; dorsal vertebrae: **a**, dorsal 1 in left lateral view; **b**, dorsal 1 in anterior view; **c**, dorsal 1 in posterior view; **d**, dorsal 2 in left lateral view; **e**, dorsal 2 in anterior view; **f**, dorsal 2 in ventral view; **g**, dorsal 5 in right lateral view. Abbreviations: **acdl**, anterior centrodiapophyseal lamina; **cam**, camellate internal structure; **di**, diapophysis; **ils**, interspinous ligament scars (ridge); **nc**, neural canal; **pa**, parapophysis; **pcdl**, posterior centrodiapophyseal lamina; **pd**, pneumatic depression; **pl**, pleurocoel; **prefo**, prezygapophyseal fossa. Scale bar represents 50 mm.

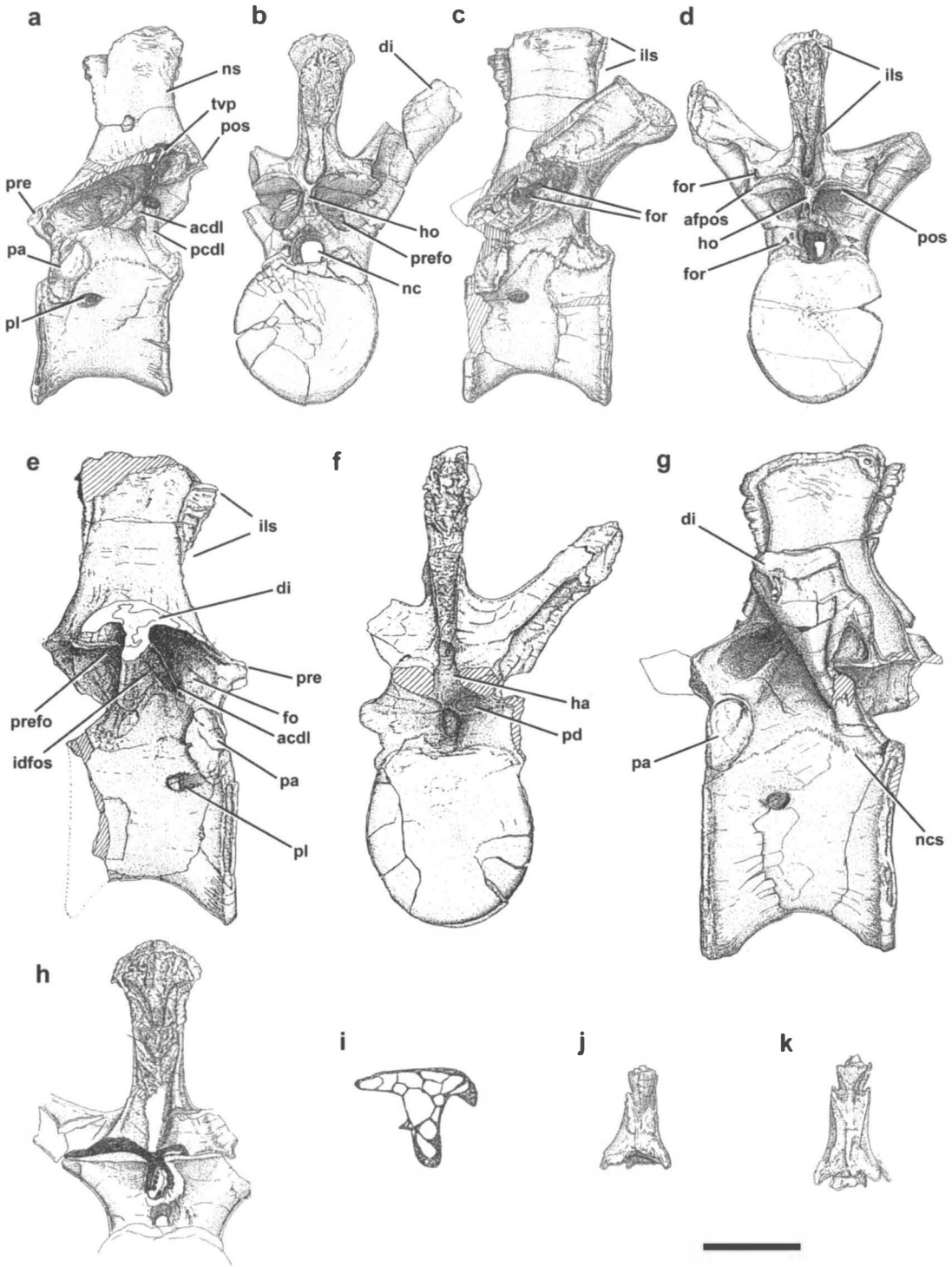

TEXT-FIG. 13. *Neovenator salerii* Hutt, Martill & Barker, 1996; dorsal vertebrae: **a**, dorsal 6 in left lateral view; **b**, dorsal 6 in posterior view; **c**, dorsal 7 in left lateral view; **d**, dorsal 7 in posterior view; **e**, dorsal 8 in right lateral view; **f**, dorsal 8 in anterior view; **g**, dorsal 9 in left lateral view; **h**, dorsal 9 neural spine in posterior view; **i**, dorsal 9 right transverse process in cross sectional view; **j**, dorsal 6 neural spine in dorsal view; **k**, dorsal 7 neural spine in dorsal view. Abbreviations: **acdl**, anterior centrodiapophyseal lamina; **afpos**, accessory flange on the postzygapophysis; **di**, diapophysis; **fo**, fossa; **for**, foramen; **ha**, hypantrum; **ho**, hyposphene; **idfos**, infradiapophyseal fossa; **ils**, interspinous ligament scars (ridge); **nc**, neural canal; **ncs**, neurocentral suture; **ns**, neural spine; **pa**, parapophysis; **pcdl**, posterior centrodiapophyseal lamina; **pd**, pneumatic depression; **pl**, pleurocoel; **pos**, postzygapophysis; **pre**, prezygapophysis. Scale bar represents 50 mm.

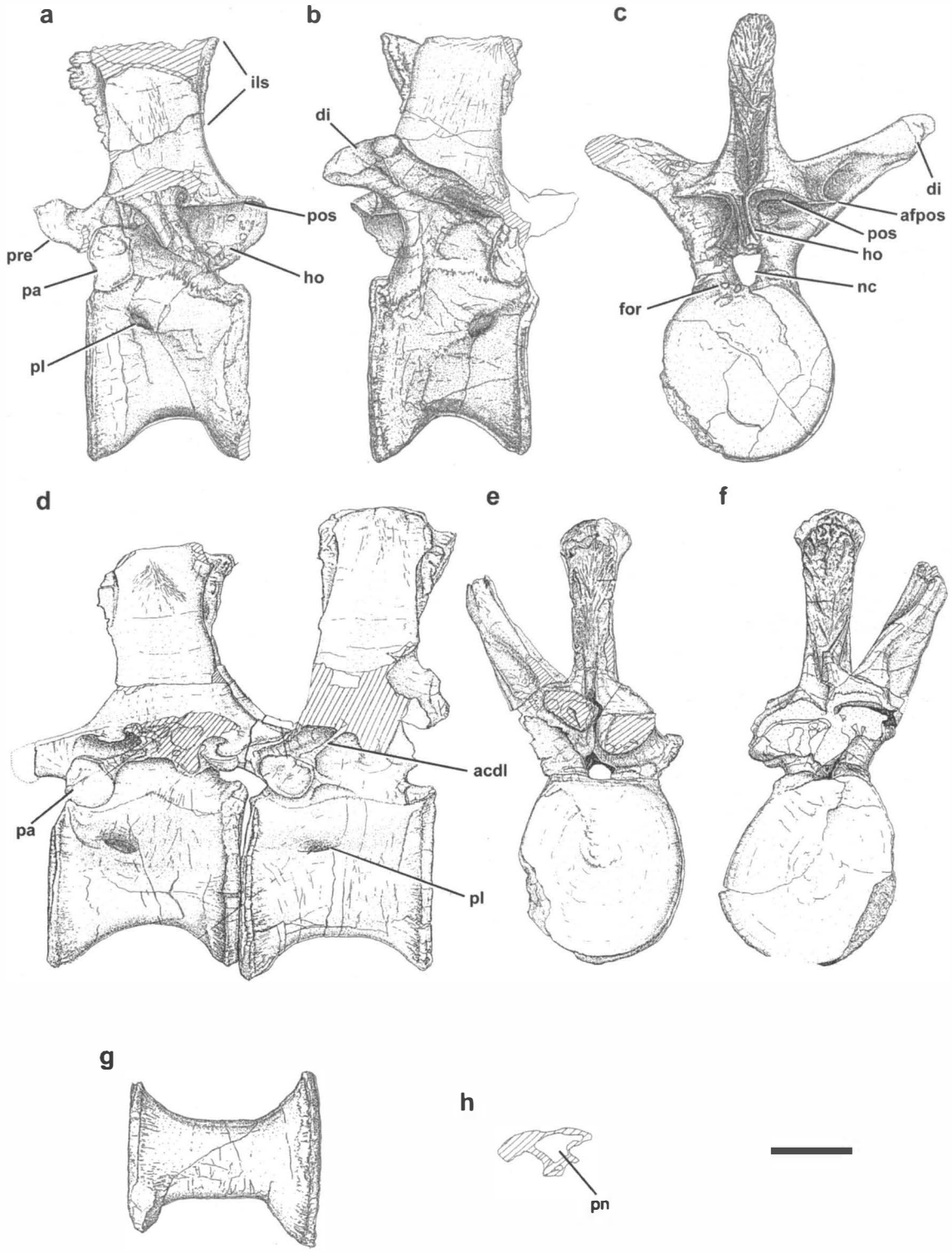

TEXT-FIG. 14. *Neovenator salerii* Hutt, Martill & Barker, 1996; dorsal vertebrae: **a**, dorsal 10 in left lateral view; **b**, dorsal 10 in right lateral view; **c**, dorsal 10 in posterior view; **d**, dorsals 12 and 13 in left lateral view; **e**, dorsal 12 in anterior view; **f**, dorsal 12 in posterior view; **g**, dorsal 12 in ventral view; **h**, dorsal 12 left transverse process in cross sectional view. Abbreviations: **acdl**, anterior centrodiapophyseal lamina; **afpos**, accessory flange on the postzygapophysis; **di**, diapophysis; **for**, foramen; **ho**, hyposphene; **ils**, interspinous ligament scars (ridge); **nc**, neural canal; **pa**, parapophysis; **pl**, pleurocoel; **pn**, pneumatic cavity; **pos**, postzygapophysis; **pre**, prezygapophysis. Scale bar represents 50 mm.

arch, part of the right transverse process and prezygapophysis, and most of the centrum. The ventral portion of the posterior articular surface is damaged. The fourth dorsal vertebra is known only from parts of the transverse processes. The fifth dorsal vertebra consists of the centrum, the base of the neural arch, and the right transverse process. The left side of the fifth centrum has been crushed inwards. The sixth dorsal vertebra is almost complete, although the prezygapophyses and left transverse process have been broken off. The seventh dorsal vertebra is missing the prezygapophyses and the distal end of the right transverse process. The left transverse process has been broken and set posteriorly to its original position. The seventh dorsal vertebra has also been deformed, as the left side has been sheared posteriorly relative to the right. The eighth dorsal vertebra is missing the right transverse process and the anterior tips of the prezygapophyses, and is also slightly broken and deformed such that the anterior surface of the centrum faces anterolaterally. A fragment of a tooth root is present adhering to the anterior surface of the eighth dorsal centrum. The ninth dorsal vertebra is very well preserved but has undergone plastic deformation; the centrum has been twisted relative to the neural arch and the left transverse process has been reoriented so that it emerges dorsolaterally with no posterior inclination. The left transverse process of the tenth dorsal vertebra has been broken away. The twelfth dorsal vertebra has been strongly deformed; the right side has been sheared dorsally relative to the left, which is particularly evident from the orientations of the transverse processes. The anterior tips of the prezygapophyses have been broken away. The posterior tips of the postzygapophyses have been broken away and are preserved with the thirteenth dorsal vertebra and the anterior tips of the prezygapophyses of the thirteenth dorsal vertebra adhere to the region below the postzygapophyses of the twelfth dorsal vertebra. The centrum and base of the neural arch of the thirteenth dorsal vertebra, including the left transverse process, are preserved. The element has been distorted so that the vertical axis is inclined dorsolaterally to the right.

In many aspects of their morphology the first two dorsals are transitional between vertebrae of the cervical series and more posterior dorsal elements. For example, these two elements, particularly the second, are anteroposteriorly short relative to more posterior elements; the articular surfaces of the centra are lower dorsoventrally than they are wide mediolaterally; and these vertebrae are gently opisthocoelous, with the anterior surface of the centrum gently convex and the posterior surface gently concave. In the cervical vertebrae, the articular surfaces are strongly opisthocoelous and lower than they are wide, while in more posterior dorsals the articular surfaces are higher than they are wide and amphicoelous. Because the first two dorsals have this transitional morphology, they are described here independently of the remaining dorsal vertebrae.

The anterior surface of the first dorsal centrum is strongly offset dorsally relative to the posterior surface of the centrum, while that of the second dorsal is slightly offset ventrally. The ventral surface of the first dorsal vertebra is broad and gently convex except for anteriorly, where it is slightly depressed between the parapophyses. The ventral surface of the second dorsal centrum is pinched into a broad rounded ridge, which terminates anteriorly in a low mound-like eminence (Pl. 8, fig. 11). This ridge is low relative to the prominent and transversely narrow ventral keels of the posterior cervical and anterior dorsal vertebrae of the majority of basal tetanurans (*Afrovenator*: UC OBA 1; *Allosaurus*: Madsen 1976; *Baryonyx*: BMNH R9951; *Sinraptor*: Currie & Zhao 1993; *Torvosaurus*: Britt 1991) and much less distinct than the stout ventral ridge of some carcharodontosaurids (*Giganotosaurus*: MUCPv-CH-1; *Mapusaurus*: MCF-PVPH-108.82). Low ventral ridges, similar to those of *Neovenator*, are also present on the ventral surfaces of the posterior cervical and anterior dorsal vertebrae of neoceratosaurs (*Carnotaurus*: MACN-CH 894; *Ceratosaurus*: UMNH VP 5278). However, the ventral surfaces of neoceratosaur vertebrae are much broader than those of tetanurans and thus have a very different overall morphology. The anterior ends of the ventral keels of many basal tetanurans are transversely expanded to form a hypapophysis (e.g. *Lourinhanosaurus*: ML 370; *Torvosaurus*: Britt 1991) but these are easily distinguishable from the low mound-like eminences present in the corresponding position in *Neovenator* vertebrae. Thus, a weak ventral ridge terminating anteriorly in a low mound-like eminence on the ventral surfaces of the anterior dorsal vertebrae is an autapomorphy of *Neovenator*.

The parapophyses of the first two dorsal vertebrae are raised on low pedicles, are dorsoventrally long, and have semicircular outlines in lateral view. They are situated at approximately midheight on the lateral surfaces of the centra adjacent to the anterior articular surfaces, and they approach, but do not contact, the neurocentral suture dorsally. Deep suboval pleurocoels are situated on the lateral surfaces of the centra immediately posterodorsal to the parapophyses. The left pleurocoel of the first dorsal vertebra is subdivided internally by a thin, anterodorsally inclined ridge, and is more similar to the subdivided pleurocoels present on some cervical vertebrae than the single, undivided pleurocoels of more posterior elements in the dorsal series. However, on the right side of the same element a single undivided pleurocoel is present, and a shallow fossa occupies the position of the posterior pleurocoel on the left side.

The neural arches of the first and second dorsal vertebrae are anteroposteriorly short and the zygapophyses are widely spaced across the midline. The transverse processes emerge laterally and are dorsoventrally high and anteroposteriorly thin, tapering distally and curving ventrolaterally along their length. The prezygapophyseal facets are situated on the dorsal surfaces of the transverse processes and face dorsomedially. The postzygapophyses are oriented ventrolaterally. Those of the first dorsal vertebra are marked by low rugose epipophyses on the dorsal surfaces, but incomplete preservation precludes the identification of these structures on the second dorsal vertebra. The zygapophyseal facets are large compared to those of more posterior dorsal vertebrae, and comparable in size to those of the cervical vertebrae. Prominent anterior and posterior centrodiapophyseal laminae support the transverse processes ventrally; the posterior lamina is slightly thicker than the anterior one. The centroprezygapophyseal lamina is situated on the anterior surface of the base of the neural arch and is low and transversely wide. These three laminae bound the deep infraprezygapophyseal, infradiapophyseal and infrapostzygapophyseal fossae. Unlike the condition in more posterior dorsal vertebrae, the infraprezygapophyseal fossa is only visible in anterior view, entering posteromedially into the base of the transverse process. Foramina that penetrate the surface of the bone are clearly visible in the depths of the right infradiapophyseal fossa of the first dorsal vertebra and the right infrapostzygapophyseal fossa of the second dorsal vertebra.

Broad rugose ridges are present on the anterior and posterior surfaces of the anteroposteriorly short and rod-like neural spines, originating in the pre- and postspinal fossae and continuing to the dorsal end of the neural spine. Deep pneumatic recesses, which are absent in more posterior dorsal vertebrae but present in the cervical vertebrae, are present ventrolateral to the postspinal fossae of the first and second dorsal vertebrae. In the second dorsal vertebra the recess on the right side is markedly shallower than that on the left. An additional pair of depressions, not present in the cervical vertebrae, is present on the posterior surface of each of the posterior neural arch pedicles of the first and second dorsal vertebrae. These are located on either side of the posterior opening of the neural canal, and occupy the same position as the posterior neural arch foramina of more posterior dorsal vertebrae.

The remaining dorsal vertebrae are more homogeneous in their overall morphology and are less similar to the cervical vertebrae than are the first two dorsal vertebrae. They are characterized by centra that are higher than wide with biconcave articular surfaces, of which the anterior surface is more weakly concave than the posterior surface; small zygapophyseal facets; and tall, anteroposteriorly broad neural spines. The ventral surface of the fifth dorsal vertebra is pinched into a sharp ventral ridge. A low tuber, similar to the mound-like eminence on the ventral surface the second dorsal centrum, is present at the anterior end of this ridge. A similar ventral ridge that lacks an anterior tuber is present on the sixth and seventh dorsal centra, with that of the seventh expressed more subtly. The ventral surfaces of more posterior dorsals are evenly rounded. A single, undivided, suboval pleurocoel is present in the anterodorsal region of each side of all known dorsal centra, and presumably all presacral vertebrae were pleurocoelous. The parapophyses are raised on low pedicles, and that of the fifth dorsal vertebra is located in the anterodorsal corner of the lateral surface of the neural arch. A distinct ventral lobe is present on the parapophysis of the fifth dorsal vertebra and extends onto the anterodorsal part of the lateral surface of the centrum. This lobe is reduced in successively more posterior elements of the series, but is not absent until the tenth dorsal vertebra, in which the parapophysis has a subcircular outline.

The prezygapophyses of dorsal vertebrae emerge anteriorly from the base of the neural arch and are oriented parallel to each other along their lengths. This results in a narrow cleft between the prezygapophyses, the hypantrum, which accommodates the hyposphene of the preceding vertebra. Small suboval depressions are present on the sixth to the ninth dorsal vertebrae ventromedial to the prezygapophyses on the anterior surface of the neural arch on either side of the anterior opening of the neural canal. These structures may also have been present in more anterior dorsals in which this region is not preserved, although they are clearly absent in the first and second dorsal vertebrae. There is a bias in the strength of the expression of these depressions, favouring the left side. For instance, the left depression of the sixth dorsal is much deeper than the corresponding structure on the right, and the eighth dorsal is marked by a shallow depression on the left but no such feature is present on the right. However, this bias does not hold across the column, as such a depression is only present on the right side of the ninth dorsal vertebra, although it is very small and shallow. The prezygapophyseal facets face dorsally with a slight anterior inclination, and those of the thirteenth dorsal vertebra (which are attached to the postzygapophyses of the fourteenth dorsal vertebra) continue onto the dorsal surfaces of ventrolaterally curving lateral flanges that emerge from the lateral surface of the prezygapophyses (Pl. 13, fig. 5). These flanges are developed laterally into swollen processes that may also have been present in more posterior dorsal vertebrae.

The transverse processes of the dorsal vertebrae are dorsoventrally thin and anteroposteriorly broad, with rectangular outlines in dorsal view. They emerge dorsolaterally from the neural arch and are slightly posterolaterally backswept. The transverse processes are supported ventrally by both anterior and posterior centrodiapophyseal lamina. The anterior centrodiapophyseal lamina is moderately well-developed in the fourth dorsal vertebra, but reduced to a low sharp ridge that is only present on the left side in the fifth dorsal vertebra and expressed as a broader low ridge in more posterior elements of the dorsal series. The prominent posterior centrodiapophyseal lamina continues laterally along the ventral surface of the transverse process as a robust longitudinal ridge. In the ninth and subsequent dorsal vertebrae the posterior centrodiapophyseal lamina is a sharp, narrow ridge that contacts the parapophysis anteroventrally and becomes increasingly prominent posteriorly along the dorsal series. The centroprezygapophyseal lamina is a short, robust buttress between the parapophysis and prezygapophysis. The infradiapophyseal fossa is shallow relative to the infraprezygapophyseal and infrapostzygapophyseal fossae in known dorsal vertebrae, except for the first and second. It increases in depth with increasing prominence of the anterior centrodiapophyseal lamina, but is never especially deep and never contains foramina that penetrate the surface of the bone. The infraprezygapophyseal and infrapostzygapophyseal fossae are generally broad and very deep. Where these fossae are well-preserved and adequately prepared, foramina can often be observed penetrating the surface of the bone.

The neural spines have subrectangular outlines in lateral view and are transversely thick relative to those of most non-allosauroid basal tetanurans (*Afrovenator*: UC OBA 1; *Eustreptospondylus*: OUMNH J.13558; *Lourinhanosaurus*: ML 370; *Torvosaurus*: Britt 1991) and *Sinraptor* (IVPP 10600; Currie and Zhao 1993). The pre- and post-spinal fossae are present as deep grooves on the anterior and posterior surfaces of the spine, originating between the zygapophyses. Thick, rugose ridges are present within these fossae and likely represent interspinous ligament scars. The anterior ridge is generally more strongly developed than the posterior ridge, and both increase in prominence posteriorly along the dorsal series. The neural spines of the dorsal vertebrae of *Allosaurus* have a similar thickened morphology with prominent anterior and posterior ridge-like rugosities (Madsen 1976). The dorsal neural spines of *Acrocanthosaurus* (OMNH 10146) and derived carcharodontosaurids (*Giganotosaurus*: MUCPv-CH-1; *Mapusaurus*: MCF-PVPH-108.84) are even broader transversely but are excavated by deep longitudinal troughs on the lateral surfaces and lack anterior and posterior rugosities. In other basal tetanurans (*Afrovenator*: UC OBA 1; *Lourinhanosaurus*: ML 370; *Piatnitzkysaurus*: PVL 4073; *Sinraptor*: IVPP 10600, Currie & Zhao 1993; *Torvosaurus*: Britt 1991) the dorsal neural spines are transversely thinner and the anterior and posterior rugosities are also much thinner, much less prominent, and absent in the ventral portion of the spine.

The postzygapophyses are known from the sixth dorsal vertebra and more posterior elements of the series. The postzygapophyseal facets are extended laterally by curving accessory flanges emerging from the lateral surfaces of the postzygapophyses (Text-figs 12–14). These accessory flanges are reduced anteroposteriorly to miniature tabs in the twelfth dorsal vertebra. They are absent in other allosauroids (*Acrocanthosaurus*: OMNH 10146; *Allosaurus*: Madsen 1976; *Giganotosaurus*: MUCPv-CH-1; *Sinraptor* Currie & Zhao 1993) and unknown in other basal tetanurans (e.g. *Afrovenator*: UC OBA 1; *Piatnitzkysaurus*: PVL 4073; *Torvosaurus*: Britt 1991) and theropods in general (e.g. *Ceratosaurus*: UMNH VP 5278; *Dilophosaurus*: UCMP 37302), and are thus an autapomorphy of *Neovenator*. The postzygapophyses of the dorsal vertebrae are in contact at their ventromedial corners, forming the ventral border of the postspinal fossa. From here they extend ventrally as a pair of thin parallel laminae to form tall, sheet-like hyposphenes. The hyposphenes of the dorsal vertebrae of *Acrocanthosaurus* (OMNH 10146), *Allosaurus* (YPM 4944), derived carcharodontosaurids (*Giganotosaurus*: MUCPv-CH-1; *Mapusaurus*: MCF-PVPH-108.84) and abelisaurids (e.g. *Carnotaurus*: MACN-CH 894) are similar to those of *Neovenator*. However, those of basal tetanurans in general (*Piatnitzksaurus*, PVL 4073; *Sinraptor* Currie & Zhao 1993; *Torvosaurus*: Britt 1991) and basal neoceratosaurs (*Ceratosaurus*: UMNH VP 5278) consist of two ventrolaterally diverging laminae that give the hyposphene a triangular outline in posterior view. Foramina are present on the posterior surfaces of the neural arch pedicles ventrolateral to the hyposphene in the seventh through to the tenth dorsal vertebrae. Foramina are present on the left neural arch pedicle only in the fifth and sixth dorsal vertebrae.

Sacral vertebrae. Fragmentary sacral material is known from the holotype (BMNH R10001; Pl. 14; Text-fig. 15), but much better preserved elements are represented in the referred specimen, MIWG 6352 (Pl. 29; Text-fig. 15). These include portions of the centra of the articulated second, third and fourth sacral vertebrae, as well as an isolated centrum that is either the first or fifth sacral, and an isolated neural arch. Unfortunately, these isolated fragments were found apart from the articulated region, precluding definitive identification. Thus, the articulated second through fourth sacral vertebrae will form the basis of the description below.

The second and third sacral vertebrae are fused, but with a clear suture visible between the elements. In contrast, the sacral vertebrae of *Acrocanthosaurus* (Harris 1998) and *Sinraptor* (Currie & Zhao 1993) are unfused, whereas fusion is variable in *Allosaurus* (Madsen 1976). The lack of fusion between the third and fourth sacrals may indicate that MIWG 6352 is a subadult (Rauhut 2005), consistent with the smaller size of the specimen compared to the holotype. Immaturity may also explain the unfused sacral vertebrae in *Sinraptor* (Currie & Zhao 1993). Only the centrum is known for the second and fourth sacral vertebrae, and the preserved region of the neural arch on the third sacral includes only a small portion of its base. Thus, details of the sacral neural arches are largely unknown for *Neovenator*. The anterior articular surface of the second sacral vertebra and the posterior surface of the third sacral are both shallowly concave, whereas the fourth sacral is characterized by a convex anterior face and a concave posterior articular surface.

The articulation for the third sacral rib is shared by the second and third sacral vertebrae, and rises laterally from the dorsal margin of their centra. A groove is present posteriorly on the offset platform of this articulation as in *Condorraptor* (Rauhut 2005). Details of the articulations of the second and fourth sacral ribs are largely obscured. However, the base of the articulation for the second rib is preserved on both sides of the second sacral, and projects laterally from the anterior margin of the centrum near where this vertebra would have met the first sacral. It is not possible to determine whether the first sacral contributed to this articulation as in *Allosaurus* (Madsen 1976), *Sinraptor* (Currie & Zhao 1993) and other theropods. The ventral base of the articulation for the fourth sacral rib may be preserved on the posterodorsal margin of the third sacral, but it is difficult to discern additional details.

The sacral centra are not excavated laterally by pleurocoels, as is also the case in *Allosaurus* (Madsen 1976), *Sinraptor* (Currie & Zhao 1993) and the basal carcharodontosaurid *Tyrannotitan* (Novas *et al.* 2005). In contrast, more derived carcharodontosaurids (e.g. *Acrocanthosaurus*: Harris 1998; *Mapusaurus*: Coria & Currie 2006) possess sacral pleurocoels, often on multiple elements

(Harris 1998). Dorsally, a smooth groove for the floor of the neural canal is visible on the fourth sacral vertebra, but obscured by breakage in the second and third elements. Ventrally, the second and fourth sacral vertebrae are smooth and lack a keel or depression, but the ventral surface of the third sacral centrum is marked by a groove. This groove is triangular; it is pointed and deep anteriorly and fans out and becomes shallower posteriorly. A similar groove is present in *Condorraptor* but is much shallower (Rauhut 2005).

The isolated neural arch does not clearly articulate with any of the centra, and cannot be positively assigned to a specific sacral, as its morphology differs from each of the well-described sacral arches of *Allosaurus* (Madsen 1976). The sacral series of other allosauroids are largely incomplete, precluding comparison. However, since it is an unfused element with obvious postzygapophyses, it is likely that this neural arch belonged to either the first, fourth or fifth sacral. It is unlikely that it belongs to the first sacral, as the transverse processes rise dorsolaterally, not strongly laterally as they do in the first sacral of *Allosaurus*. Additionally, the transverse processes of the first sacral in *Allosaurus* are marked by an attachment surface for the first sacral rib, which is not seen in this fragment. In fact, no attachment surface for a sacral rib is apparent on this fragment, consistent with the morphology of the fourth sacral vertebra of *Allosaurus*. However, unlike the fourth sacral neural arch of *Allosaurus*, this fragment almost completely encloses the neural canal, whereas the corresponding element in *Allosaurus* makes little contribution to the canal.

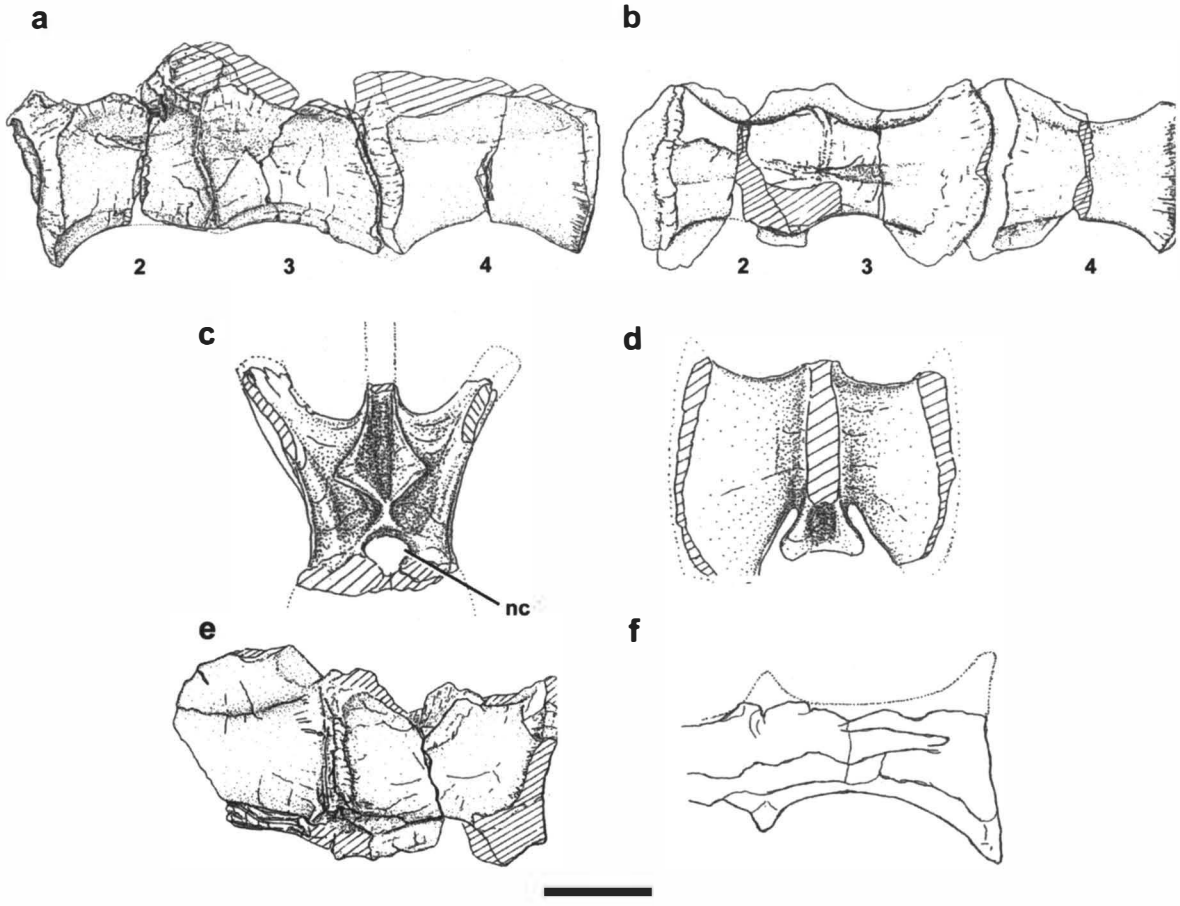

TEXT-FIG. 15. *Neovenator salerii* Hutt, Martill & Barker, 1996; sacral vertebrae (BMNH R10001 and MIWG 6352): **a**, sacrals 2, 3, and 4 (MIWG 6352) in left lateral view; **b**, sacrals 2, 3, and 4 (MIWG 6352) in dorsal view; **c**, unidentified sacral neural arch (MIWG 6352) in posterior view; **d**, unidentified sacral neural arch (MIWG 6352) in dorsal view; **e**, sacrals 5 and 6 (BMNH R10001) in left lateral view; **f**, sacrals 5 and 6 (BMNH R10001) in dorsal view. Abbreviation: **nc**, neural canal. Scale bar represents 50 mm.

The sacral neural arch fragment of *Neovenator* is 90 mm long anteroposteriorly and 70 mm wide mediolaterally at its base. The width expands to 125 mm at the tips of the transverse processes, which are 112 mm above the base. The neural spine is broken at its base, but it must have projected dorsally as a mediolaterally thin sheet. The transverse processes extend dorsolaterally, gradually expanding anteroposteriorly towards their distal ends. The anterior surface is abraded, obscuring most details of its morphology. However, there is clearly a broad fossa that extends onto the anterior surface of the transverse process.

In posterior view, the postzygapophyses face ventrolaterally. The postspinal fossa is a suboval recess that originates between the postzygapophyses and continues dorsally along the posterior surface of the neural spine, similar to the situation in the dorsals and anterior caudals. A short hyposphene is abraded but is clearly similar to those in the dorsal and anterior caudal vertebrae. It is somewhat shorter dorsoventrally than those in the dorsals, but similar in size to the hyposphenes of the anterior caudals. The neural canal is teardrop-shaped, measuring 21 mm mediolaterally and 23 mm dorsoventrally at its midpoint. In lateral view, the posterior margin of the transverse process is marked by a posterodorsally curving ridge, above which is a smooth fossa. Posteriorly to this ridge, the bone surface is highly rugose. There is no evidence of a pleurocoel ventrally where the arch would have met the centrum, nor is there any sign of the camellate internal structure that characterizes cervical and dorsal vertebrae.

The fragmentary holotype sacral material (BMNH R10001) includes pieces of at least three and possibly four centra, two of which preserve the base of the neural arch. These specimens are all extensively crushed and badly weathered, and similar in overall morphology to MIWG 6352. The most noticeable difference involves sacral fusion: while MIWG 6352 exhibits fusion only between sacrals two and three, the holotype is characterized by at least two fused contacts. Unfortunately, the identification of individual sacral vertebrae is complicated by the distorted and fragmentary nature of the specimen, so it is unclear which sacrals are fused. The presence of two zones of fusion is consistent with the larger size of the holotype compared to MIWG 6352.

Caudal vertebrae. Twenty-two vertebrae from the caudal series of the holotype (MIWG 6348) are known (Pls 15–23; Text-fig. 16). They have been arranged in order of descending size of the centrum using numbers to designate position of the first and second caudal vertebrae and the letters A–U for more distal vertebrae for which exact position in the caudal series is not known. They do not form an uninterrupted succession from anterior to posterior. The position of each element in the series has been estimated by comparison with those of *Allosaurus* (Madsen 1976).

Most of the anterior caudal vertebrae have been crushed or damaged, and certain parts, especially of the centra, have been broken and shifted relative to each other. In these elements, parts of the bone surface have been damaged or are missing, and have been restored in white plaster. These are minor effects that have not affected the gross character of the vertebrae except where noted below. More posterior elements of the caudal series have better preservation of the bone surface and often show little in the way of cracking or damage.

The first caudal vertebra has been strongly abraded by beach rolling and is missing all extremities of the neural arch. The second caudal vertebra is the best preserved of the anterior caudal vertebrae, as it is almost complete and shows only minor distortion. The right prezygapophysis and posterodorsal tip of the neural spine of the third element in the series (caudal A) have both been broken off. There has also been significant post-burial distortion of the specimen: the right side of the centrum has been sheared posteriorly relative to the left side and the transverse processes have been reoriented so that the right process is directed posteriorly at a high angle and the left has a strong dorsal inclination. The fourth caudal vertebra (caudal B) is undistorted. The right transverse process has been broken off and the left has been broken and reattached so that it is directed more posteriorly than it would have been originally. The fifth caudal vertebra (caudal C) is undistorted but is missing the distal portion of the left transverse process and anterior tip of the right prezygapophysis. The right prezygapophysis has been broken and reattached during preparation so that it is directed more dorsally than it would have been originally. The centrum of the sixth caudal vertebra (caudal D) has been transversely crushed so that parts of the bone surface are broken or caved in and the posterior articular surface is

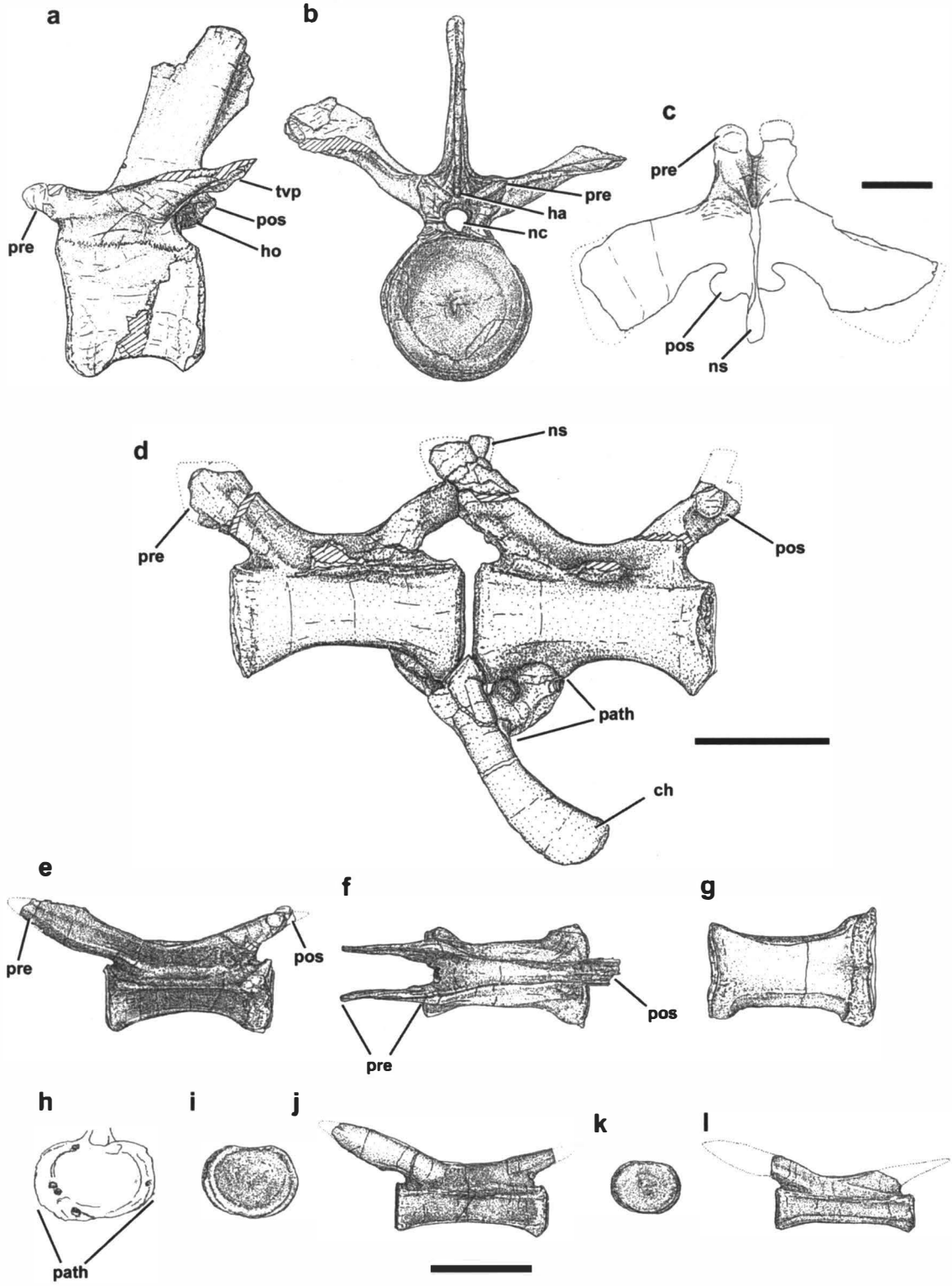

TEXT-FIG. 16. *Neovenator salerii* Hutt, Martill & Barker, 1996; caudal vertebrae (MIWG 6348): **a**, caudal A (3) in left lateral view; **b**, caudal A (3) in anterior view; **c**, caudal A (3) in dorsal view; **d**, caudals L and M in left lateral view; **e**, caudal P in left lateral view; **f**, caudal P in dorsal view; **g**, caudal P in ventral view; **h**, caudal P in anterior view; **i**, caudal P in posterior view; **j**, caudal S in left lateral view; **k**, caudal S in anterior view; **l**, caudal V in left lateral view. Abbreviations: **ch**, chevron; **ha**, hypantrum; **ho**, hyposphene; **nc**, neural canal; **ns**, neural spine; **path**, pathology; **pos**, postzygapophysis; **pre**, prezygapophysis; **tvp**, transverse process. Scale bars represent 50 mm.

rotated to the left. Both prezygapophyses and the anterior portion of the base of the neural spine have been broken off. Only the base of the right transverse process remains and it has been sheared ventrally relative to the left transverse process. The left transverse process is incomplete distally and has been deformed so that it curves dorsally. The seventh caudal vertebra (caudal E) has a well-preserved bone surface and is undistorted. The centrum is complete but the anterior tips of the prezygapophyses, the distal (= dorsal) portion of the neural spine and the right transverse process have been broken off and are missing.

The ?ninth caudal vertebra (caudal F) is represented only by the neural arch, which has a poorly preserved, heavily pitted surface texture but is almost complete with only small parts of the extremities broken away. The ?fourteenth caudal vertebra (caudal G) is undistorted but is missing the anterior portion of the neural arch, including the prezygapophyses, which has been broken away. The ?seventeenth caudal vertebra (caudal H) has a well-preserved and undistorted centrum. The anterior tips of the prezygapophyses and distal portions of the neural spine and transverse processes have been broken from the neural arch and the right transverse process has been sheared ventrally relative to the left. Only the centrum of the ?eighteenth vertebra (caudal I) is preserved. It is well-preserved and almost complete; the ventral portion of the anterior articular surface has been abraded. The ?twenty-first caudal vertebra (caudal J) is preserved. The distal portions of the transverse processes and neural spines have been broken away. A rugose pathological swelling surrounds the base of the left transverse process. The ?twenty-second caudal vertebra (caudal K) is missing the prezygapophyses and the distal portions of the transverse processes and neural arch. The right transverse process has been sheared ventrally relative to the right. The left-hand portion of the anterior articular face is damaged. The ?twenty-fifth (caudal L) and ?twenty-sixth (caudal M) vertebrae are well-preserved and in articulation with each other and their shared chevron. They are both missing the distal portions of the transverse processes and the more anterior of the two elements is missing the anterior tips of the prezygapophyses. A pathological swelling is present on the posterior portion of the right side of the more anterior element which laps onto the proximal portion of the chevron and anterior portion of the more posterior vertebra, uniting the three (Text-figs 16d, 27i, j). The ?twenty-seventh caudal vertebra (caudal N) is undistorted but is missing both postzygapophyses and the right prezygapophysis, which have been broken away. A pathological swelling is present posteriorly on the right side of the centrum. The ?twenty-eighth caudal vertebra (caudal O) is well-preserved and almost complete, missing only the posterior tips of the postzygapophyses and the anterior tip of the right prezygapophysis, which have been broken away. A pathological swelling surrounds the posterior articular surface distorting its size, particularly the transverse dimension.

The remaining distal caudal vertebrae are well-preserved and undistorted. Several are complete or missing only the tips of the zygapophyses (caudals S, T, R). Others are missing the zygapophyses, which have been broken away (caudals P, Q, U).

The articular surfaces of the anterior caudal centra are suboval. The posterior surface is smaller than the anterior surface up until the ?twenty-second caudal vertebra (caudal K), in which, in common with more distal elements, the anterior and posterior articular surfaces are subequal in size. Both articular surfaces of the caudal centra are gently concave. In anterior caudal vertebrae the posterior surface is more deeply concave than the anterior surface. In the ?eighteenth caudal vertebra (caudal I) and more posterior elements of the series up to the ?twenty-seventh element (caudal N) the articular surfaces are subequally biconcave. In those elements posterior to the ?twenty-seventh the posterior surface is more deeply concave than the anterior surface, similar to the condition in anterior caudal vertebrae.

The centra of anterior caudal vertebrae are higher dorsoventrally than wide mediolaterally, and the posterior articular surfaces are generally higher relative to their width than are the anterior surfaces. In most allosauroids (*Acrocanthosaurus*: OMNH 10146; *Giganotosaurus*: MUCPv-CH-1; *Mapusaurus*: MCF-PVPH-108.81; *Sinraptor*: Currie & Zhao 1993) and *Ceratosaurus* (UMNH VP 5286) the articular surfaces of the anterior caudal vertebrae are also higher than wide, but in *Allosaurus* (Madsen 1976) and *Dubreuillosaurus* (MNHN 1998-13) they are approximately as high as wide and in *Torvosaurus* (Britt 1991) they are wider than high. More posteriorly in the caudal series the articular surfaces become less dorsoventrally elongate. In the ?fourteenth

caudal vertebra (caudal G) and more posterior elements the articular surfaces are wider than high. The ?twenty-seventh, ?twenty-eighth and ?twenty-ninth elements (caudals N, O and P) show the greatest exaggeration of this trend. Posterior to these elements the articular surfaces become progressively less dorsoventrally compressed.

The ventral portion of the posterior (but not anterior) surfaces of the centra of all known caudal vertebrae is bevelled for articulation with the chevron. In common with most allosauroids (*Acrocanthosaurus*: Stovall & Langston 1950; *Allosaurus*: Madsen 1976; *Giganotosaurus*: MUCPv-CH-1), the posterior surfaces of the centra of anterior caudal vertebrae are offset ventrally relative to the anterior surface. In *Sinraptor* the posterior surface is offset dorsally relative to the anterior surface (Currie & Zhao 1993).

The ventral surface of the first caudal vertebra bears a thick longitudinal ridge. A weak longitudinal cleft marks the apex of this ridge, though it is present only centrally and does not extend far either anteriorly or posteriorly. A gentle longitudinal ridge is present on the ventral surface of the second caudal vertebra. The ventral surface of the third caudal vertebra is only weakly raised into a ridge. The fourth (caudal B) through ?eighteenth (caudal I) elements have ventral surfaces that are gently rounded transversely with a slightly flattened median longitudinal strip. In the ?twenty-fifth and more posterior elements the ventral surface is broad and flattened. In some of the middle and posterior caudal vertebrae systems of weak ridges or depressions are present on the ventral surface of the centrum.

In most basal tetanurans and neoceratosaurs (*Acrocanthosaurus*: OMNH 10146; *Allosaurus*: Madsen 1976; *Ceratosaurus*: UMNH VP 5286; *Condorraptor*: Rauhut 2005; *Dubreuillosaurus*: MNHN 1998-13; *Monolophosaurus*: IVPP 84019, Zhao & Currie 1993; *Torvosaurus*: Britt 1991), as well as in coelophysoids (Rauhut 2003), the ventral surfaces of the anterior caudal centra bear distinct longitudinal grooves. These grooves often become weaker in more posterior elements of the caudal series. In *Sinraptor* the groove is absent in the first caudal vertebra but particularly strong in subsequent anterior elements, and in the second centrum divides the ventral surface into a 'double keel' (Currie & Zhao 1993, p. 2064). In common with *Neovenator*, ventral grooves are not present on the anterior caudal centra of derived carcharodontosaurids (*Giganotosaurus*: MUCPv-CH-1; *Mapusaurus*: MCF-PVPH-108.81), in which a stout longitudinal ridge is instead expressed.

Large oval pleurocentral depressions are present on the lateral surfaces of the anterior caudal vertebrae, straddling the centrum and the portion of the neural arch ventral to the transverse process. They are deepest and most prominent in the second caudal vertebra and are shallower and more poorly expressed in more posterior elements. They are absent in the ?twenty-first (J) element and more posterior elements of the caudal series. Several irregularly placed small foramina of variable size are present within these depressions as well as a few ventral to them on the lateral faces of the centrum in the first and second caudal vertebrae. In most instances between the third (A) and seventh (E) elements two small foramina are present, one anteriorly and one posteriorly, within the pleurocentral depressions. Foramina are generally absent from the lateral surfaces of more posterior elements of the caudal series.

The prezygapophyses of anterior caudal vertebrae emerge anteriorly from the anterior surface of the neural arch. They diverge slightly across the midline and have dorsomedially facing facets comparable in size to those of the dorsal vertebrae. Long, teardrop-shaped prespinal fossae originate between the prezygapophyses and continue a short distance dorsally along the narrow anterior surface of the neural spine. In the fourth caudal vertebra (B) and more posterior elements of the series the prespinal fossa does not continue dorsally and is reduced to a small circular recess that penetrates the anterior surface of the base of the neural spine. In the ?twenty-eighth (O) and more distal elements the prespinal fossa is absent. No prezygapophyses are preserved between the fifth (C) and ?twenty-first (J) caudal vertebrae. The prezygapophyses of the ?twenty-fifth element (L) emerge dorsally from the anterior portion of the neural arch. The prezygapophyseal facets face dorsomedially with slight anterior inclination and are slightly concave dorsoventrally. In more posterior elements of the caudal series (?twenty-fifth [L] and ?twenty-sixth [M] caudal vertebrae) the prezygapophyses emerge anterodorsally, with progressively more anterior inclination. In the distal caudal elements the prezygapophyses

emerge anteriorly with a slight dorsal inclination and are extremely elongate, up to 70% (caudal T) of the centrum length.

The postzygapophyses of anterior caudal vertebrae are set into the posteroventral portion of the neural spine, as they are in the dorsal vertebrae. They have ventrolaterally directed facets of comparable size to those of the dorsal vertebrae. Pairs of postzygapophyseal facets are in contact at their ventromedial corners, from where a hyposphene extends ventrally in anterior caudal vertebrae. The hyposphenes are similar to those of the dorsal vertebrae, consisting of paired parallel sheets, but are much shorter dorsoventrally. They become progressively shorter posteriorly in the anterior portion of the caudal series and are absent in the sixth (D) and more posterior caudal vertebrae. The postspinal fossa is a long suboval cleft originating between the postzygapophyses and continuing for a short distance dorsally along the posterior surface of the neural spine. The fossa becomes progressively shorter, and is absent in the ?twenty-eighth (O) and more posterior elements. The postzygapophyseal facets face increasingly more strongly laterally and less strongly ventrally along the caudal series posteriorly.

The transverse processes of the anterior caudal vertebrae are dorsoventrally thin sheets with anteroposteriorly narrow bases that expand distally. Broad, but very low centrodiapophyseal laminae support the transverse processes ventrally but are absent in the ?seventeenth (H) and more posterior caudal elements. The degree of dorsal and posterior inclination, the length, and the anteroposterior breadth of the transverse processes decrease posteriorly in the caudal series. In the ?twenty-second (K) element of the series the processes are laterally directed with only a slight distal expansion. In the ?twenty-sixth (M) caudal vertebra the transverse processes are reduced to stout, anteroposteriorly short, laterally directed posts. Posterior to the ?twenty-sixth (M) vertebra the transverse processes are absent and a low but sharp longitudinal ridge is present on the lateral surfaces of each centrum, giving the centrum a subhexagonal transverse cross section.

The neural spines of the anterior caudal vertebrae are transversely thin sheets. They are inclined posteriorly and are composed of a central body that is slightly thickened mediolaterally, particularly in the posterior portion of the base, and distally, where they have a suboval cross section. Thin accessory sheets are appended to the anterior and posterior margins of the body of the spine. In the second caudal vertebra the posterior sheet continues almost to the dorsalmost level of the central rod and the anterior sheet terminates about a third of spine height from the central part. This results in a conspicuous kink in the anterior outline of the spine in lateral view. Such a kink is present in some allosauroids (*Acrocanthosaurus*: Stovall & Langston 1950; *Allosaurus*: Madsen 1976; *Mapusaurus* Coria & Currie 2006). However, these taxa differ from *Neovenator* in that the kink develops into an anterodorsal spike-like process in more posterior elements of the caudal series.

The dorsal extent of the anterior and posterior sheets of the neural spine becomes reduced in successively more posterior caudal vertebrae. In the ?fourteenth (G) caudal vertebra the anterior sheet is anteroposteriorly long and forms a low shoulder in the outline of the neural arch in lateral view anterior to the spine body. The posterior flange is developed as a slight posterior projection from the mid-part of the spine. In the ?fourteenth (G) and more posterior elements of the caudal series the neural spine is anteroposteriorly narrow and rod-like. It emerges posterodorsally from the dorsal surface of the neural arch and curves dorsally along its length so that the anterior margin of the spine is concave in lateral view. The neural spine is progressively reduced in more posterior vertebrae of the caudal series. In the ?twenty-fifth (L) and ?twenty-sixth (M) elements it is only just visible in lateral view above the postzygapophyses. In more posterior caudal vertebrae it is absent.

Chevrons. Five chevrons from a range of positions in the tail are known from the holotype (MIWG 6348), including proximal, middle and distal elements (Pl. 24; Text-fig. 17). A single partial chevron from MIWG 6352 is also known (Pl. 28; Text-fig. 17).

The proximal chevrons are large with rod-like haemal spines, almost as thick transversely as they are broad anteroposteriorly. The distal (= ventral) end of the proximal chevron of the holotype is not preserved. Chevrons from the middle part of the caudal series have transversely

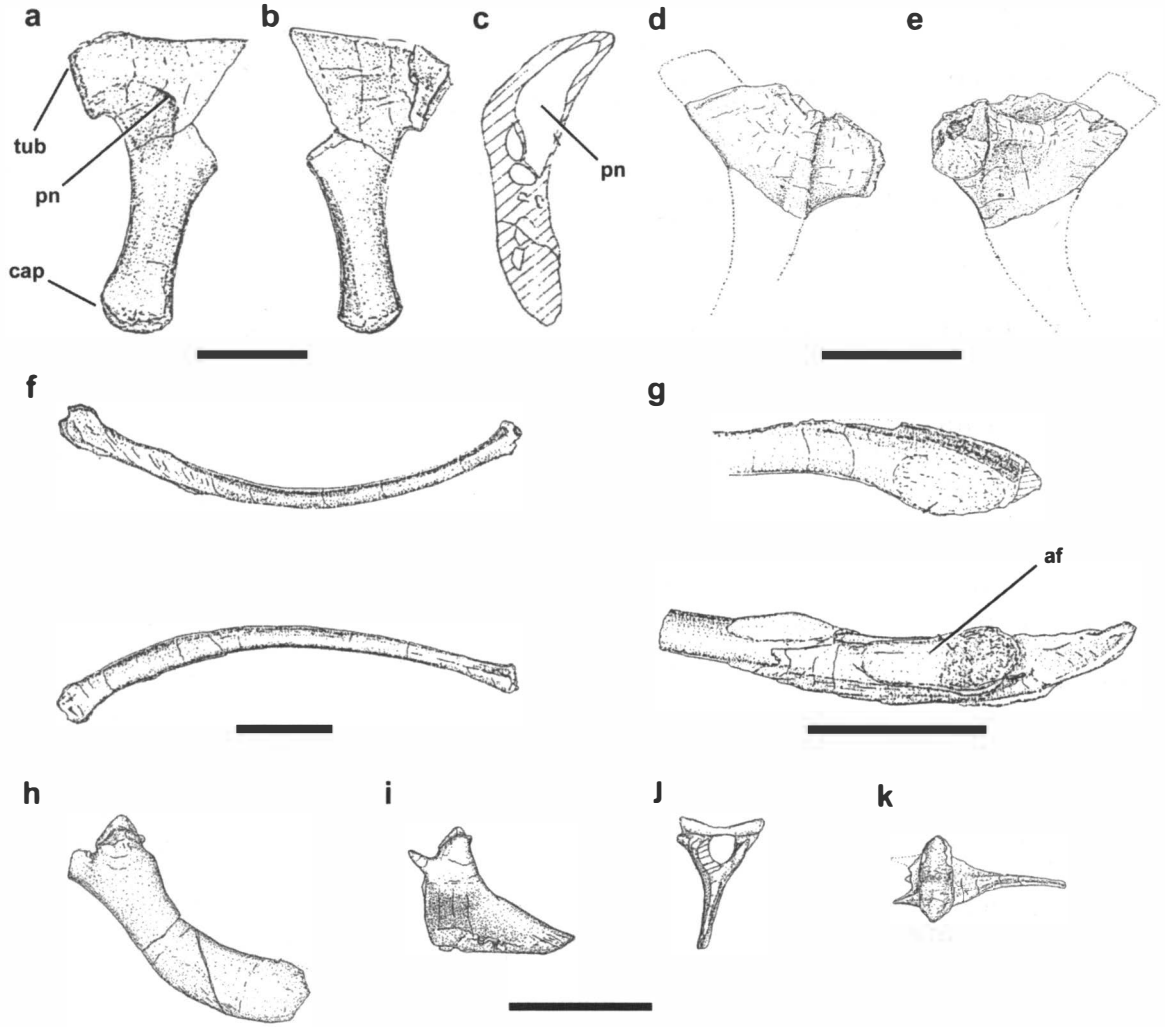

TEXT-FIG. 17. *Neovenator salerii* Hutt, Martill & Barker, 1996; ribs, gastralia, and chevrons (MIWG 6348): **a**, dorsal rib head in anterior view; **b**, dorsal rib head in posterior view; **c**, dorsal rib head in cross sectional view; **d**, cervical rib head in anterior view; **e**, cervical rib head in posterior view; **f**, gastral element in ventral and dorsal views; **g**, medial gastral element in ventral and dorsal views; **h**, middle chevron in left lateral view; **i**, distal chevron in left lateral view; **j**, distal chevron in dorsal view; **k**, distal chevron in dorsal view. Abbreviations: **af**, articular facet; **cap**, capitulum; **pn**, pneumatic cavity; **tub**, tuberculum. Scale bars represent 50 mm.

thin and posteroventrally curved haemal spines, with anteroposteriorly expanded distal portions. Distal chevrons are also transversely thin. The outline of the distal chevrons in lateral view is strongly inflected posteriorly to form an L-shape that extends farther posteriorly than it does ventrally. All chevrons bear prominent paired anterior proceses on both sides of the anterior opening of the haemal canal. These are present in the majority of theropods (Rauhut 2003). Much less prominent posterior processes are also present. The surface for articulation with the caudal centrum has a transversely elongate, eye-shaped outline in proximal view. This surface is divided into two facets by a prominent and angular transverse ridge; one faces anteroproximally, the other posteroproximally.

Ribs. Fragments of several ribs are known from the holotype (MIWG 6348), although most of these are highly eroded and damaged (Pl. 25; Text-fig. 17). However, three large fragments reveal details of the cervical and dorsal ribs. Several rib fragments are also known from MIWG 6352.

A fragment of a cervical rib preserves part of the proximal region, including a complete tuberculum and the bases of the capitulum and shaft. The tuberculum is 32 mm deep dorsoventrally and 24 mm long anteroposteriorly at its terminal expansion. Laterally, a robust ridge separates the shaft from the tuberculum. Medially, a wide web of bone stretches from the tuberculum to the base of the capitulum. The dorsal surface of this web is excavated by a small pneumatopore, as is the medial surface of the proximal end of the shaft below this web. There is no distinct pneumatic opening on the lateral surface.

Two large fragments are known from the dorsal rib series. The larger fragment is from a left element and includes a complete tuberculum and capitulum, but only the very proximal portion of the shaft. The second fragment is from a right element and includes the tuberculum, a distal portion of the neck of the capitulum, and the proximal region of the shaft. The tuberculum of the left element is 26 mm long anteroposteriorly and 34 mm deep dorsoventrally, and the capitulum is 22 mm long and 31 mm deep. The capitulum is slightly expanded and rugose at its proximal end, with a smooth, oval articular surface for the parapophysis. The articular surface on the tuberculum is excavated by a deep sinuous notch which would have received the diapophysis. Medially, a ridge extends across the ventromedial margin of the capitulum, while the region between the capitulum and tuberculum is broadly concave and smooth.

Both fragments exhibit a web of bone between the tuberculum and capitulum, which is excavated by a deep pneumatopore. Pneumatic openings are seen in the ribs of some theropods, and are extensively developed and widespread across the series in *Ceratosaurus* and some abelisaurids (*Carnotaurus*: Bonaparte *et al.* 1990; not *Majungasaurus*: O'Connor 2007). In contrast, pneumatic openings are more limited in allosauroids, being restricted to the fifth right rib in *Sinraptor* (Currie & Zhao 1993) and apparently absent in *Allosaurus* (Gilmore 1920; Madsen 1976) and *Acrocanthosaurus* (Stovall & Langston 1950; Harris 1998). External pneumatic openings are also absent in the potential allosauroid *Monolophosaurus* (Zhao & Currie 1993) and all preserved dorsal ribs of the basal tetanuran *Dubreuillosaurus* (MNHN 1998-13). Dorsally the pneumatopore is overhung by a ridge that continues onto the tuberculum. Broken surfaces in several fragments of the holotype and MIWG 6352 show that the shafts and capitula were hollow, a feature that likely extended across the series due to its prevalence in numerous specimens.

Gastralia. Several fragments of the gastral basket are preserved in the holotype (MIWG 6348), although none was found articulated (Pl. 25; Text-fig. 17). The fragments appear to represent 10–15 discrete elements, many of which are broken into additional fragments. Hutt (1999) referred to several of these as sternal ribs, but it is apparent that he was referring to gastralia. None of the preserved fragments appears to represent furculae, elements that are frequently mistaken for gastralia and vice-versa (Claessens 2004).

Most of these pieces are too fragmentary to describe, but a nearly complete element is preserved and is used here to describe the basic features of the gastral basket. This specimen is a left midline element, 260 mm long. The shaft is strongly bowed and proximally expanded, with a ventral surface that bears a flat but rugose region for articulation with the opposing right midline element. A preserved proximal portion of a right midline element shows the same general morphology, but with a flat articular surface on its dorsal margin, indicating that the right element would have overlapped the left element in ventral view, as in *Allosaurus* (Chure 2000). Proximal to this articulation the proximal end develops a proximally directed hook, while distal to the articulation the posterior edge of the shaft is marked by an elongate groove for articulation with the lateral gastral element. The shaft is generally oval in cross section medially (= proximally) but becomes circular laterally (= distally). The shafts of all preserved medial elements taper laterally, as they do in *Allosaurus* and *Sinraptor*, and do not terminate in a club-like expansion as they do in *Acrocanthosaurus* (Harris 1998), *Carcharodontosaurus* (Stromer 1934) and *Giganotosaurus* (MUCPv-CH-1). There is no sign of any fused medial elements as occur in many theropods, but this is likely due to poor preservation.

APPENDICULAR SKELETON

Scapula-coracoid. The left scapula and coracoid of the holotype (MIWG 6348) are almost complete

(Table 4; Pl. 30; Text-fig. 18). They are fused together, and the suture is marked by rugose bone texture on both elements on the lateral and medial surfaces. The suture is slightly open medially, but this may be exaggerated by post-mortem deformation. The articulation is sinuous as in most theropods: a convex projection of the scapula articulates with a concave depression in the coracoid to form the majority of the contact, but the scapula becomes slightly concave dorsally to receive a convex projection from the coracoid.

The glenoid fossa is 53 mm long in lateral view, with the scapula contributing two thirds of its length. It faces ventrally on the coracoid and ventrally and slightly laterally on the scapula,

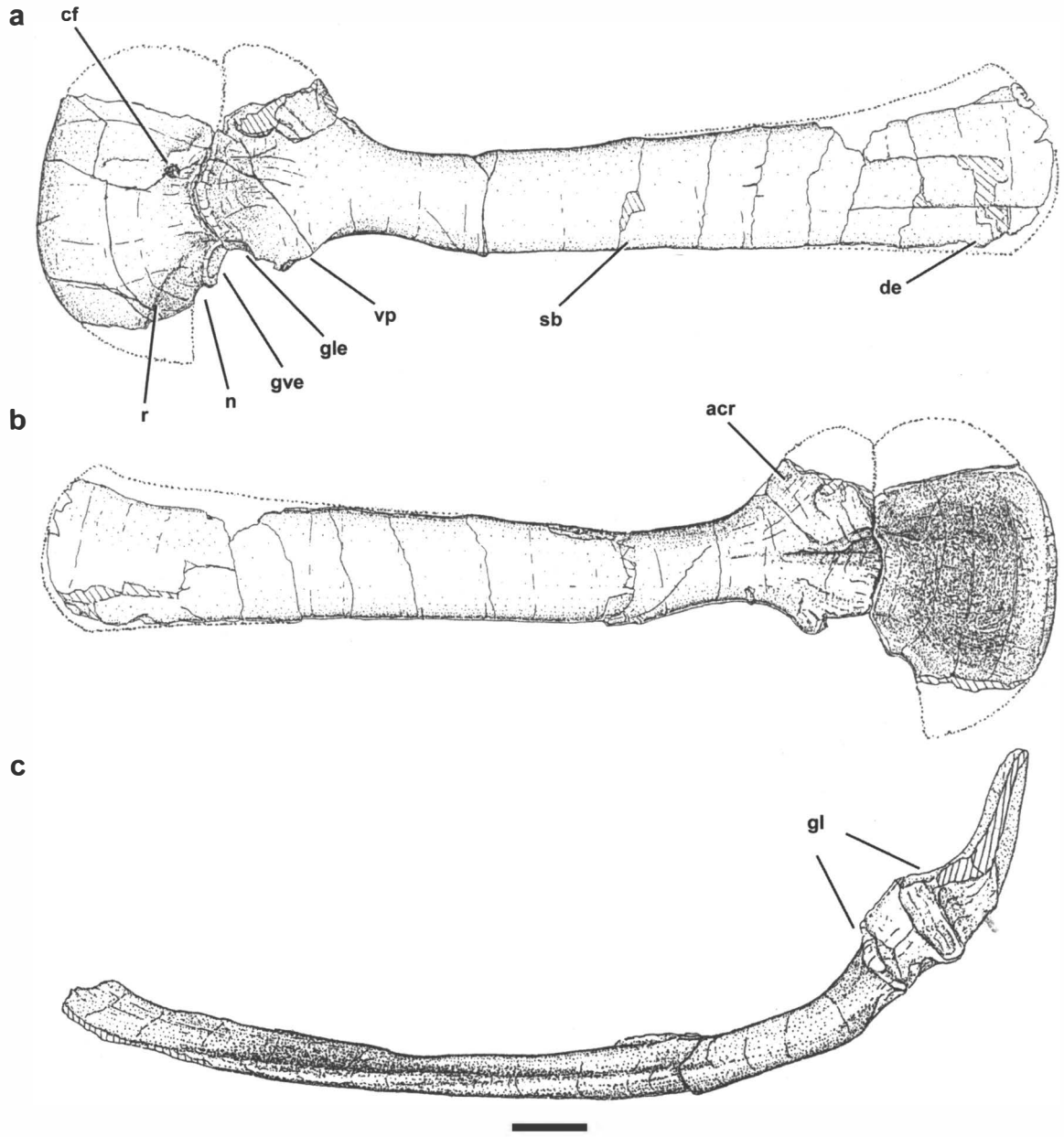

TEXT-FIG. 18. *Neovenator salerii* Hutt, Martill & Barker, 1996; scapula and coracoid (MIWG 6348): **a**, left scapula and coracoid in lateral view; **b**, left scapula and coracoid in medial view; **c**, left scapula and coracoid in ventral view. Abbreviations: **acr**, acromion; **cf**, coracoid foramen; **de**, distal expansion; **gl**, glenoid; **gle**, lateral expression of the glenoid; **gve**, ventral expression of the glenoid; **n**, notch; **r**, ridge (?biceps tubercle); **sb**, scapular blade; **vp**, ventral process. Scale bar represents 50 mm

with the ventral and lateral surfaces separated by a prominent ridge of bone. Lateral exposure of the fossa is much more extensive in *Mapusaurus*, in which the scapular glenoid faces as much laterally as it does ventrally (Coria & Currie 2006). The glenoid is wider mediolaterally (63 mm) than long anteroposteriorly. This differs from the condition in *Allosaurus* (Madsen 1976) and most theropods in which the glenoid is longer than wide, and represents an autapomorphy of *Neovenator* (Pl. 30; Text-fig. 18). The coracoid contribution to the glenoid is divided into a slightly concave lateral portion and a flat medial region, which are equal in size and separated by a caudomedially trending ridge. The ventral scapula contribution is slightly distorted but is flat and does not bear any ridge.

Coracoid. The coracoid is broken dorsally and ventrally, and lacks most of the posteroventral process and the dorsal margin where the scapula and coracoid join. Thus, it is not possible to determine whether there was a dorsal notch between the elements (contra Holtz 2000; Holtz *et al*. 2004). Although the distal region of the posteroventral process is broken, the broad base of this structure suggests that it was elongate and strongly hooked posteriorly as in all allosauroids except *Sinraptor* (Gao 1998). This process is separated from the glenoid by a smooth, concave notch as in all allosauroids and spinosauroids. A shallow sinuous ridge extends anteroventrally onto the lateral surface of the posteroventral process from the anterodorsal border of the glenoid. This ridge is possibly homologous to the biceps tubercle, which is located in the same region but expressed as a more discrete mound in most theropods. Consistent with this interpretation is the condition seen in *Allosaurus*, in which the tubercle is a raised mound near the midline of a similar

TABLE 4. Girdle measurements.

Coracoid (MIWG 6348, left element)

Length (anteroposterior): 140 mm
Depth (dorsoventral) anterior to glenoid: 132 mm*
Thickness (mediolateral) at anterior end: 9.5 mm
Thickness (mediolateral) at coracoid foramen: 14.5 mm
Thickness (mediolateral) at glenoid: 31.5 mm

Scapula (MIWG 6348, left element)

Length (anteroposterior)[1]: 505 mm
Minimum blade depth (dorsoventral): 67 mm
Maximum blade depth (dorsoventral): 90 mm
Thickness (mediolateral) at level of minimum depth[2]: 35 mm
Thickness (mediolateral) at level of maximum depth[2]: 14 mm

Ilium (MIWG 6352, left element)

Length (anteroposterior)[3]: 570 mm
Acetabular margin, length of curve: 190 mm
Pubic peduncle, length (anteroposterior): 135 mm
Pubic peduncle, width (mediolateral): 67 mm
Ischial peduncle, length (anteroposterior): 34 mm
Ischial peduncle, width (mediolateral): 42 mm

Pubis (MIWG 6352, left element)

Length of shaft: 560 mm
Anteroposterior length of proximal projection[4]: 160 mm
Ischial peduncle, depth (dorsoventral): 67 mm
Ischial peduncle, width (mediolateral): 49 mm
Iliac peduncle, length (anteroposterior): 68 mm
Iliac peduncle, width (mediolateral): 51 mm
Distal boot, length (anteroposterior): 364 mm

[1]: Measured along outside curve, missing posterior margin
[2]: Measured at midpoint of blade
[3]: Measured from preserved anterior end of preacetabular process to posterior margin of postacetabular process
[4]: Measured from anterior margin of iliac peduncle to posterior margin of ischial peduncle
*denotes incomplete measurement due to broken surfaces

sinuous ridge (Madsen 1976, fig. 23). The coracoid foramen is located 38 mm above the dorsal margin of the glenoid and immediately anteriorly. It is small, with a diameter of 11 mm, and extends posterodorsally into the interior of the coracoid. However, unlike the condition in most theropods (e.g. *Allosaurus*: Madsen 1976; *Ceratosaurus*: Madsen & Welles 2000; *Mapusaurus*: Coria & Currie 2006), the coracoid foramen does not penetrate completely through the bone and consequently is not expressed on the medial surface of the coracoid as a foramen or fossa.

Scapula. This element is broken dorsally in the region of the acromion process and is abraded around the periphery of the distal expansion of the blade. The blade is broadly convex laterally, with a dorsal margin that is shallowly concave. This dorsal margin rises strongly dorsally to form a deep plate that meets the coracoid, but details of the dorsal portion of this plate cannot be determined due to breakage. Regardless, it is evident that the acromion process was prominent and distinctly offset from the dorsal margin of the blade as it is in allosauroids and *Megaraptor* (Calvo *et al.* 2004), not smoothly continuous with the dorsal margin as it is in *Carnotaurus* (Bonaparte *et al.* 1990), *Ceratosaurus* (Madsen & Welles 2000) and *Torvosaurus* (Britt 1991). The shape of the ventral margin of the base of the scapula is more complicated. Immediately posterior to the glenoid this margin is marked by a small notch, which is bordered posteriorly by a slight ventral protuberance. The ventral margin then sweeps dorsally to form a concave region which gradually straightens out distally. There is no notch between the concave and straight regions as in *Giganotosaurus* (MUCPv-CH-1). The ventral margin of the blade is approximately at the same level as the glenoid region, similar to the condition in most allosauroids but differing from the state in *Allosaurus* (Madsen 1976) and *Sinraptor* (Gao 1998) in which the blade is located far dorsal to the glenoid.

On the medial surface, a poorly pronounced ridge buttresses the glenoid and extends posteroventrally before fanning out and merging with the ventral margin of the blade. A similar ridge is seen in other allosauroids, and results in a triangular cross section anteriorly (apex representing the ridge pointing medially). As the blade continues posteriorly and the ridge dissipates the cross section assumes the shape of an elongate teardrop. The medial surface of the dorsal margin of the blade is marked by a pathological raised rugosity, which is described further in the pathology section below.

Pelvic girdle

Ilium. Portions of both ilia are known for the holotype (BMNH R10001), but these elements are fragmentary and highly eroded (Pls 31–32; Text-fig. 19). Additionally, an incomplete ilium is known from the referred specimen MIWG 6352 (Pl. 33). This specimen is substantially more complete than the holotype ilia, and forms the basis for the majority of the following description. However, the holotype specimens do preserve important anatomical features that are not observable on the referred specimen, and these are discussed below.

The referred ilium (MIWG 6352) is incomplete dorsally, missing most of the iliac blade, but the pubic and ischial peduncles, acetabular margin, and the ventral portions of the preacetabular and postacetabular processes are well-preserved (Table 4). The ilium is 87 mm wide mediolaterally at the dorsal margin of the acetabulum. The preacetabular process (70 mm wide mediolaterally at its edge) and postacetabular process (30 mm) both thin substantially as they project away from the acetabular margin. The pubic peduncle appears to be divided into two articular surfaces (Pl. 33), but this is an artefact of breakage, and only one articular facet would have been present, as is clear in the holotype (BMNH R10001).

Only the ventral region of the preacetabular process is preserved, and it is slightly broken anteriorly. The preserved ventral margin is crossed by a prominent ridge on the lateral surface that dissipates posteriorly as it nears the acetabulum. This ridge is oriented almost horizontally as in *Mapusaurus* (Coria & Currie 2006), unlike the condition in *Sinraptor* (Currie & Zhao 1993) where it curves strongly anterodorsally. In this latter taxon the ridge continues anterodorsally, extends across the preacetabular process, and terminates at the anterodorsal corner of the ilium.

The pubic peduncle is generally flat and smooth laterally, but ventrally is rugose near its articulation with the pubis. A narrow crescentric fossa, the cuppedicus fossa, occupies the region

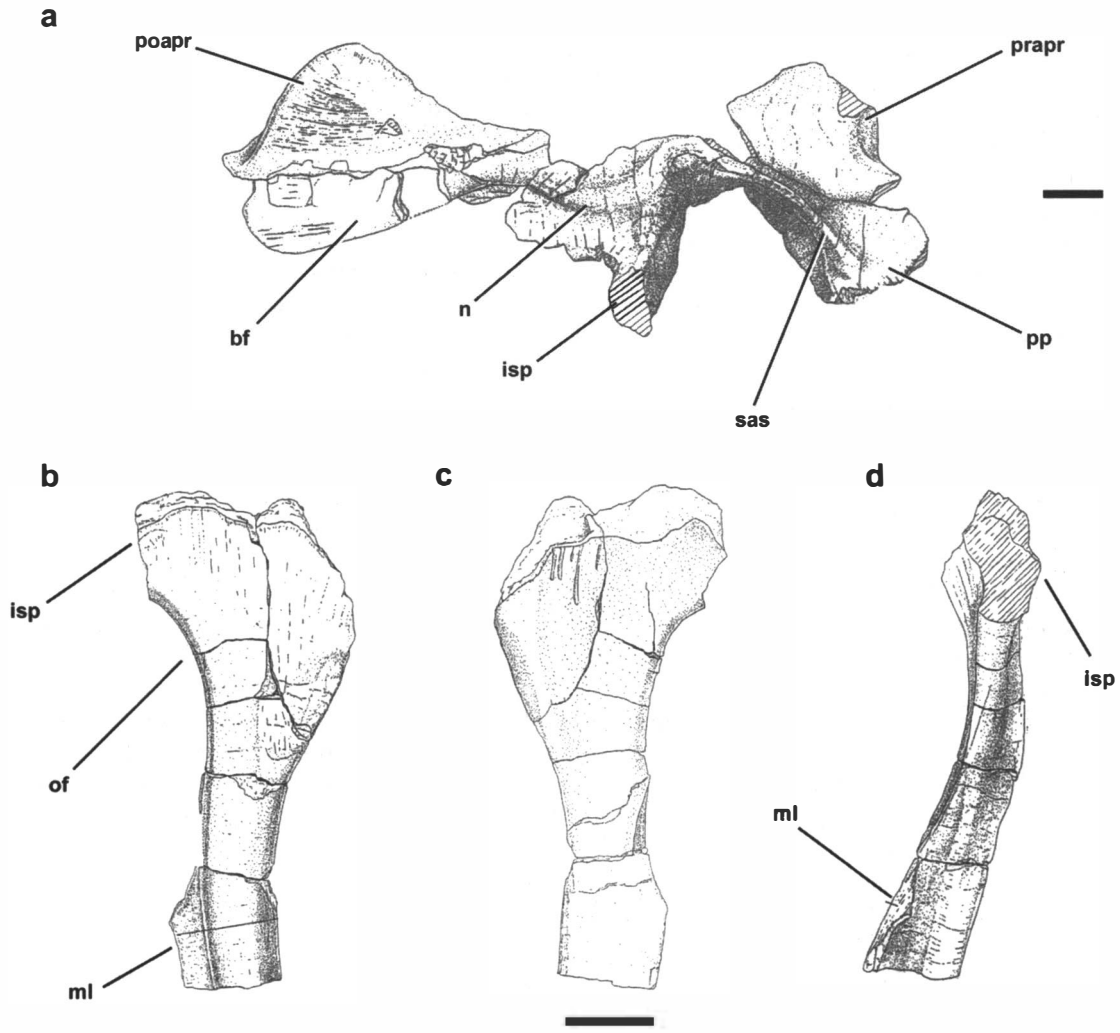

TEXT-FIG. 19. *Neovenator salerii* Hutt, Martill & Barker, 1996; ilium and pubis (BMNH R10001): **a**, right ilium in lateral view; **b**, right pubis in lateral view; **c**, right pubis in medial view; **d**, right pubis in posterior view. Abbreviations: **bf**, brevis fossa; **isp**, ischial peduncle; **ml**, medial lamina; **n**, notch; **of**, obturator flange; **poapr**, postacetabular process; **pp**, pubic peduncle; **prapr**, preacetabular process; **sas**, supracetabular shelf. Scale bars represent 50 mm.

where the pubic peduncle and preacetabular process diverge, as is characteristic of tetanurans (Hutchinson 2001). The pubic peduncle terminates posterior to the anterior edge of the preacteabular process as in most basal theropods. In contrast, in *Allosaurus* (Madsen 1976) and *Sinraptor* (Currie & Zhao 1993) this peduncle is enlarged and curved somewhat anteriorly such that it terminates anterior to the preacetabular process. The supracetabular shelf originates on the posterolateral surface of the pubic peduncle, and extends posteriorly as a prominent, ventrolaterally oriented shelf that overhangs the anterodorsal region of the acetabulum. A laterally projecting supracetabular shelf has often been regarded as a synapomorphy of Tetanurae (e.g. Gauthier 1986; Carrano *et al.* 2002; Holtz *et al.* 2004; Sereno *et al.* 2004), but in many basal tetanurans (e.g. *Allosaurus*: UMNH VP 8246; *Sinraptor*: IVPP 10600; *Torvosaurus*: Britt 1991) it projects ventrolaterally as it does in *Neovenator*. In *Neovenator* the supracetabular shelf is not continuous with the ventral margin of the postacetabular process. Instead, the two are separated by a smooth concavity on the lateral surface of the ilium at the base of the ischial peduncle as in other tetanurans and abelisaurids (e.g. *Carnotaurus*: Bonaparte *et al.* 1990; MNN GAD1: Sereno & Brusatte 2008).

The ischial peduncle is much smaller than the pubic peduncle (Table 4), as is the case in most allosauroids (e.g. *Allosaurus*: Madsen 1976) and basal tetanurans generally (e.g. *Afrovenator*, *Torvosaurus*: Rauhut 2003). However, the ischial peduncle in *Sinraptor* (Currie & Zhao 1993), although somewhat smaller than the pubic peduncle, is not nearly as reduced and tapered ventrally as in *Allosaurus*, *Neovenator* and most other basal tetanurans. In *Neovenator* the posterior surface of the ischial peduncle is smoothly rounded. Posterior to the peduncle, separate lateral and medial laminae of the postacetabular process, measuring 23 mm and 14 mm in mediolateral width respectively, define a deeply inset brevis fossa. In lateral view the fossa is visible anteriorly but it is concealed posteriorly by the overhanging lateral lamina, which extends farther ventrally in this region of the ilium. In ventral view the brevis fossa widens posteriorly, as the result of divergent lateral and medial laminae. A narrow brevis fossa that does not widen posteriorly is sometimes regarded as diagnostic of tetanurans (Holtz 2000; Hutchinson 2001; Rauhut 2003), and is present in *Sinraptor* (Currie & Zhao 1993), *Torvosaurus* (Britt 1991) and coelurosaurs (Rauhut 2003). However, an expanding fossa is also seen in *Allosaurus* (UMNH VP 8246; BYU 5164) and *Giganotosaurus* (MUCPv-CH-1), which like *Neovenator* exhibit a condition comparable to basal theropods such as *Ceratosaurus* (BYU 13024) and coelophysoids (Rauhut 2003).

Medially, the surface of the ilium is highly eroded and few details of the sacral rib articulations are visible.

The holotype material includes a left ilium preserving the acetabular region and base of the preacetabular process and a right element preserving the acetabular region and base of the postacetabular process (BMNH R10001). These specimens are similar in overall morphology to MIWG 6352. However, three additional anatomical observations are apparent, which are not necessarily absent, only unobservable, on the otherwise more complete referred ilium. First, the right element is pierced by a small, 3 mm foramen in the cuppedicus fossa. This foramen is teardrop-shaped, opens anteriorly, and is similar in position and form to a foramen known in *Allosaurus* (Madsen 1976) and many other basal tetanurans. Second, the left ilium possesses a robust medial shelf that arises from the anterodorsal margin of the pubic peduncle and delimits the cuppedicus fossa dorsally. This shelf is horizontal and mediolaterally wide posteriorly but curves ventrally and becomes mediolaterally narrower as it extends anteriorly before merging with the medial surface of the preacetabular process. A similar feature is present in many tyrannosauroids and is sometimes regarded as a diagnostic feature of this group (Holtz 2001; Holtz *et al.* 2004). However, this shelf is absent in other allosauroids (*Allosaurus*: Madsen 1976; *Giganotosaurus*: MUCPv-CH-1; *Sinraptor*: Currie & Zhao, 1993) and is consequently an autapomorphy of *Neovenator* among allosauroid theropods.

Third, the medial surface of the right element is marked by a caved-in region immediately dorsal to the acetabulum. The rim of this region is clearly broken but the internal space exhibits finished bone surface that indicates the presence of a chamber in life. This chamber is elongate anteroposteriorly and divided into two cavities: a smaller, 10 mm long anterior cavity and a larger, 65 mm posterior cavity. This posterior cavity is further divided by an anteroposteriorly trending ridge and is penetrated by what appears to be at least one accessory foramen. Although some of these features may simply be the result of breakage, it is possible that they represent iliac pneumaticity, as has also been reported in *Mapusaurus* (Coria & Currie 2006).

Pubis. The holotype includes fragments of the pubis, including several portions of the shaft and the proximal region of the right element (BMNH R10001; Pls 34, 35; Text-fig. 19). This element is much better preserved in a referred specimen (MIWG 6352), in which complete conjoined left and right pubes are known (Pl. 36; Table 4). Unfortunately, this specimen is heavily abraded and has been crushed dorsoventrally, but most anatomical details are observable. This element forms the basis for the description.

The curvature of the shaft in lateral view cannot be determined due to crushing. However, it is apparent that the pubis was expanded proximally for articulation with the ilium and ischium. Distal to this expanded region the pubis narrows into the shaft, which gives rise to a medial lamina approximately 175 mm distal to the acetabular margin. This lamina would have made contact with a corresponding lamina on the opposite pubis to form the pubic apron

medially. Details of this apron and the degree of contact between the opposing pubes are also obscured by crushing.

Distally, the pubis expands into a large 'boot', which is extensively developed posterior to the shafts but also includes an anterior portion that projects 70 mm anteriorly. Among other theropods with a large pubic boot a similar expansion is seen in many allosauroids (e.g. *Allosaurus*: Madsen 1976; *Acrocanthosaurus*: Stovall & Langston 1950; Harris 1998; *Giganotosaurus*: MUCPv-CH-1), as well as tyrannosaurids (Brochu 2002) and the potential allosauroid *Siamotyrannus* (Buffetaut *et al.* 1996). In contrast, *Sinraptor* (Currie & Zhao 1993), compsognathids (including *Aristosuchus* from the Isle of Wight: Naish *et al.* 2001), and some basal tyrannosauroids (*Dilong*: Xu *et al.* 2004) do not have an anterior expansion. The pubic boot in *Neovenator* is enormous, measuring 65% of the length of the shaft (Table 4). Similarly expanded pubic boots are seen only in carcharodontosaurids (e.g. *Giganotosaurus*), in which they measure more than 60% of the length of shaft, in contrast to 30–50% in other allosauroids and basal tetanurans. In ventral view the boot is relatively flat with raised lateral margins. It is shaped like an elongate triangle that tapers to a point posteriorly, as in allosauroids and other basal tetanurans (e.g. *Streptospondylus*: Allain 2001; *Torvosaurus*: Britt 1991). In contrast, most coelurosaurs exhibit a narrow, parallel-sided pubic boot (Rauhut 2003). The cross section of the boot in *Neovenator* is rectangular anteriorly, whereas the posterior projection is triangular. The dorsal surface of the posterior projection is sharp and slopes ventrally as it extends posteriorly.

Laterally, the posterodorsal corner of the pubis between the ischial peduncle and the shaft is broadly rounded, resulting in a completely open obturator foramen as in most allosauroids (e.g. *Acrocanthosaurus*: Stovall & Langston 1950; *Allosaurus*: Madsen 1976; *Giganotosaurus*: MUCPv-CH-1). Basal theropods such as coelophysoids, *Ceratosaurus*, and abelisaurids possess an enclosed obturator foramen completely surrounded by a web of bone, which projects posteriorly to meet a similar flange from the ischium, forming a deep plate below the acetabulum (Tykoski & Rowe 2004). This condition also characterizes many basal tetanurans, including *Lourinhanosaurus* (Mateus 1998), *Monolophosaurus* (Zhao & Currie 1993), *Sinraptor hepingensis* (Gao 1998) and *Torvosaurus* (Britt 1991). *Sinraptor dongi* shows an intermediate morphology in which the foramen is open posteriorly, but nearly enclosed by projections of bone extending ventrally from the ischial peduncle and posterodorsally from the main shaft (Currie & Zhao 1993). *Neovenator* and other allosauroids possess a small flange that extends ventrally from the ischial peduncle, but it is much smaller than in *Sinraptor*.

Ischium. The holotype includes fragments of the ischium, among them a proximal portion of the left element (MIWG 6348), fragments of the shaft of the left element (BMNH R10001), and the conjoined distal region of both elements (BMNH R10001) (Pls 37–39; Text-fig. 20). The proximal region of the left ischium is known also in MIWG 6352 (Pl. 37; Text-fig. 20).

The proximal fragment of MIWG 6348 includes the entire pubic and iliac peduncles and the acetabular margin, but only the most proximal region of the ischial shaft. This fragment measures 179 mm from the anterior edge of the pubic peduncle to the posterior margin of the iliac peduncle, and includes an 88 mm long acetabular margin that is preserved on the dorsal and lateral surfaces as a smooth fossa. The pubic peduncle, which is broken slightly anteriorly, is 31 mm wide mediolaterally and 54 mm deep dorsoventrally, and the iliac peduncle is 49 mm wide and 79 mm long anteroposteriorly. Only 90 mm of the shaft is preserved distal to the margin of the acetabulum, and at the broken surface it is 18 mm wide and 73 mm long.

In lateral view, the posterolateral surface immediately distal to the iliac peduncle is marked by a broad fossa, which is homologous to the ischial tubercle of Hutchinson (2001). This fossa is expressed as a more robust tubercle in many archosaurs, including several basal coelurosaurs. In allosauroids and other basal tetanurans it is expressed as a groove, which often extends distally along the ischial shaft. Anteriorly there is no ventral lamina extending from the pubic peduncle distally to join with the shaft, which differs from the condition in many basal theropods, including *Torvosaurus* (Britt 1991) and *Monolophosaurus* (Zhao & Currie 1994). Instead, there would have been a distinct obturator notch separating the obturator process from the pubic peduncle as in other neotetanurans. The proximal portion of this notch is visible as the smoothly rounded

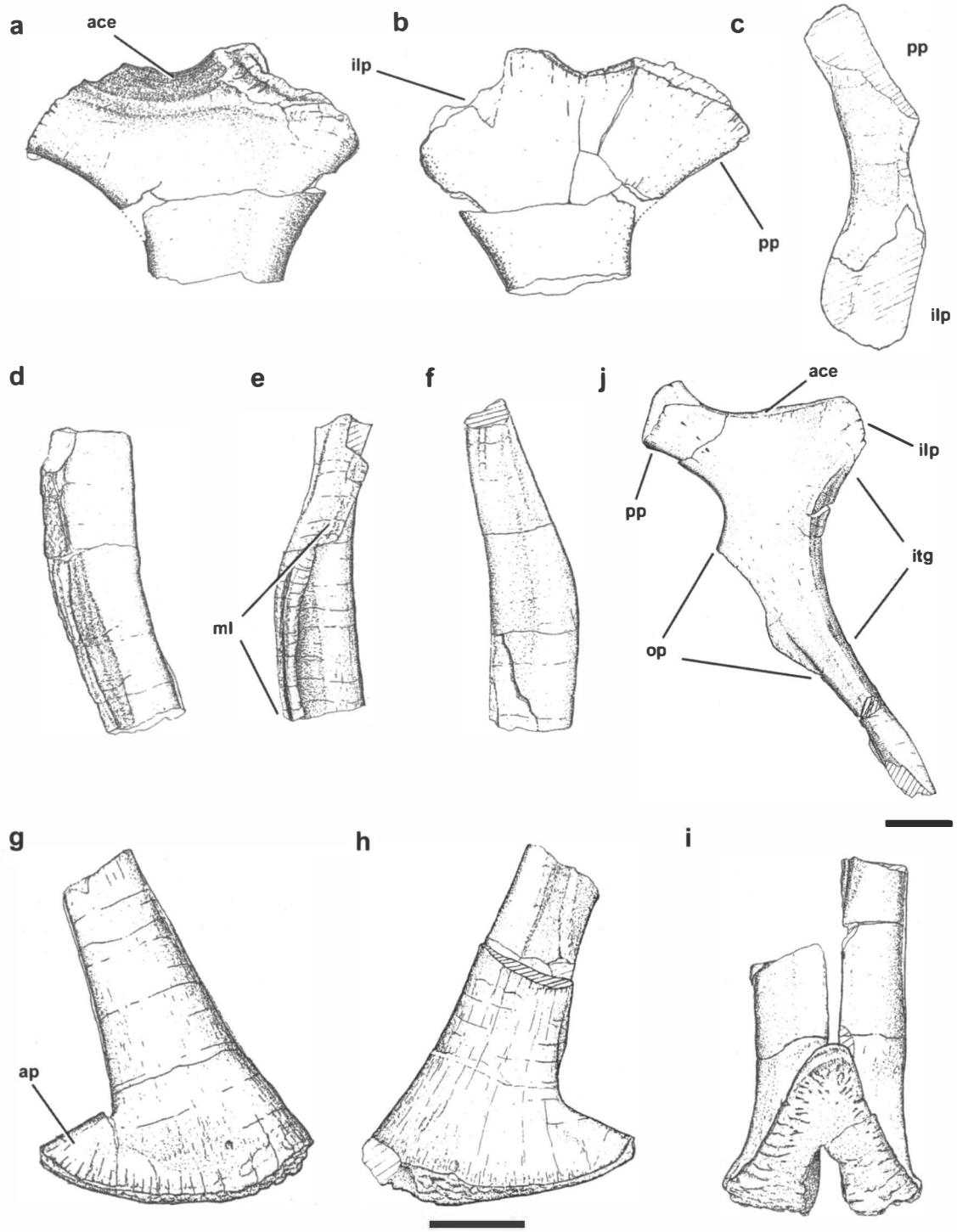

TEXT-FIG. 20. *Neovenator salerii* Hutt, Martill & Barker, 1996; ischium (BMNH R10001 and MIWG 6352): **a**, left ischium in lateral view; **b**, left ischium in medial view; **c**, left ischium in dorsal view; **d**, left ischium mid shaft region (BMNH R10001) in lateral view; **e**, left ischium mid shaft region (BMNH R10001) in anterior view; **f**, left ischium mid shaft region (BMNH R10001) in posterior view; **g**, left ischium boot (BMNH R10001) in left lateral view; **h**, left ischium boot (BMNH R10001) in right lateral view; **i**, left ischium boot (BMNH R10001) in anterior view; **j**, left ischium (MIWG 6352) in lateral view. Abbreviations: **ace**, acetabulum; **ap**, anterior process; **ilp**, iliac peduncle; **itg**, ischial tubercle groove; **ml**, medial lamina; **op**, obturator process; **pp**, pubic peduncle. Scale bars represent 50 mm. Bottom scale bar for all figures except **j**.

anterior margin of the shaft below the pubic peduncle, but the obturator process itself is not visible due to breakage distally.

In dorsal view, the pubic peduncle is divided into a laterally positioned semicircle, which is shallowly concave and rugose, and a medially positioned crescentic region that is flat (Pl. 37, fig. 1). The articular surface of the iliac peduncle is semicircular and medially excavated by a deep sinuous notch (Pl. 37, fig. 2), as in *Allosaurus* (Madsen 1976) and *Giganotosaurus* (MUCPv-CH-1). Immediately anterior to the articular surface is a broad, anterolaterally facing antritrochanter, which measures 26 mm in anteroposterior length. An antitrochanter is seen also in *Giganotosaurus* (MUCPv-CH-1) and *Sinraptor* (IVPP 10600). In lateral view the posterior edge of the iliac peduncle is smoothly confluent with the ischial shaft as in *Sinraptor*, as well as *Monolophosaurus*, *Torvosaurus*, and most other theropods. However, in most allosauroids, including *Acrocanthosaurus*, *Allosaurus*, *Carcharodontosaurus* (Stromer 1931), *Giganotosaurus* and *Mapusaurus*, the iliac peduncle develops a posteriorly directed flange that is distinctly set off from the posterior margin of the shaft (Brusatte & Sereno 2008).

As revealed by several fragments, the shaft of the ischium possesses an extensive medial lamina, which is excavated by a deep groove for articulation with the opposing ischium. This lamina is strongly pronounced and wide proximally. Proximally the shaft is rectangular in cross section, but it becomes progressively oval distally as presumably the opposing ischial shafts lose medial contact. The shafts remain separate as they continue distally, but the cross section becomes D-shaped as the medial surface of the shaft flattens. At its distal termination the shaft develops an anterior process, which conjoins with its opposite to form an ischial boot. The main bodies of the shafts are not in contact distally and are widely separated. However, they are marked medially with numerous striations and ridges, which have been interpreted by previous authors (e.g. Harris 1998; Coria & Currie 2006) as the unfused contact between the opposing ischia. As this is clearly not the case in *Neovenator*, this interpretation should be reconsidered. Instead, this scarring may represent attachment for the fibrous pubo-ischiadic membrane (Hutchinson 2001). The presence of scarring on both left and right ischia and the lack of contact between the opposing elements for much of their length indicates that separate lateral membranes were present in *Neovenator*, not the single medial membrane characteristic of more basal theropods and other archosaurs. This medial membrane is retained as an atrophied structure distal to the larger lateral membranes in some theropods (Hutchinson 2001), and may have been anchored to the ischial boot in *Neovenator*.

The distal ischial boot is prominent and has a rugose lateral surface, which is heavily marked by striations and small foramina on its lateral and ventral surfaces. This structure is 140 mm long anteroposteriorly and V-shaped in ventral view (87 mm mediolaterally wide posteriorly and 40 mm wide anteriorly at the conjoined anterior processes) (Pl. 39). However, this triangle is excavated by a posteriorly opening notch, as only the anterior processes of the individual shafts are conjoined. This differs from other theropods, which either exhibit unfused, closely appressed, or completely fused distal ischia (e.g. Madsen 1976; Currie & Zhao 1993; Holtz *et al.* 2004). Therefore, the anteriorly fused and posteriorly divergent condition of the distal expansion of the ischium is an autapomorphy of *Neovenator* (Pl. 39). Additionally, the anterior process of *Neovenator* is rare among theropods, as it is seen in *Acrocanthosaurus* (Harris 1998) but absent in most other theropods, including all other allosauroids, which exhibit a spatula-shaped (e.g. *Allosaurus*: Madsen 1976) or poorly expanded (e.g. *Sinraptor*: Currie & Zhao 1993) distal ischium.

The ischial fragment of MIWG 6352 is similar to the corresponding element in MIWG 6348, although it is from a smaller individual (anteroposterior length = 167 mm). The only major difference is in the acetabular margin, which is expressed on the dorsal and lateral surfaces of the proximal shaft in the holotype but restricted to the dorsal surface in the referred specimen. It is possible that this difference represents intraspecific variation, or potentially ontogenetic variation in light of the size difference.

Importantly, this referred ischium reveals details of the shaft that are not preserved in the holotype, which is missing this region. The ischial tubercle groove extends posteriorly along the posterolateral margin of the shaft. It is shallow as in most allosauroids, not deep as in

Acrocanthosaurus, a condition described by Harris (1998) as an autapomorphy of this genus. The obturator process is set off from the shaft by a distinct notch proximally, but distally it becomes smoothly confluent with the shaft, not discretely offset by a notch as in *Acrocanthosaurus*, *Allosaurus* and *Sinraptor*, and many other basal tetanurans (Holtz *et al.* 2004). *Mapusaurus* exhibits a possibly unique condition in which a distinctly offset and notched obturator process is followed distally by a small subsidiary process (Coria & Currie 2006). It is possible that this additional process is present in *Neovenator*, but this is indeterminate due to breakage. Distally the shaft is oval in cross section, measuring 24 mm in anteroposterior length and 31 mm in mediolateral width at its termination 311 mm distal to the acetabular margin.

Femur. Both femora are preserved in the holotype (MIWG 6348; Table 5; Pl. 40; Text-fig. 21). The right femur was found with the right tibia during the second excavation at Grange Chine, and the left was found subsequently by one of us (SH). They are both well-preserved and almost complete, although the head of the left element is abraded and the posterior flange on the caput of the right element is broken off. The shaft is almost straight in anterior view, curving only weakly medially. It is broader mediolaterally than thick anteroposteriorly and it has a flat posterior surface. In lateral view the distal half of the shaft curves posteriorly.

TABLE 5. Hind leg measurements (MIWG 6348) in mm; * = incomplete measurements.

Element	Length	Minimum circumference	Proximal antpost.	Proximal mediolat.	Midshaft antpost.	Midshaft mediolat.	Distal antpost.	Distal mediolat.
Left Femur	730	270	80*	195	76	90	155	180
Right Femur	730	275	87*	190	75	96	150	175
Left Tibia	680	225	225	107*	63	77	79	180
Right Tibia	685	230	160*	117	66	79	75	180
Left Fibula	618	98	139	39	36	23	69	40

The femoral head is angled dorsomedially as in carcharodontosaurids (*Acrocanthosaurus*: OMNH 10147; *Carcharodontosaurus*: Stromer, 1931; *Giganotosaurus*: MUCPv-CH-1; *Mapusaurus*: Coria & Currie 2006) and some tyrannosauroids (Carr *et al.* 2005). In contrast, those of *Allosaurus* (Madsen 1976) and *Sinraptor* (Currie & Zhao 1993) emerge horizontally. Additionally, the femoral head of *Neovenator* is directed anteromedially in proximal view (Pl. 40, figs 5, 7; Text-fig. 21e), whereas it is strictly medially directed in other allosauroids (*Allosaurus*: Madsen 1976; *Giganotosaurus*: MUCPv-CH-1; *Mapusaurus*: Coria & Currie 2006; *Sinraptor*: Currie & Zhao 1993). Although the femoral head is directed anteromedially in many other basal tetanurans (e.g. *Afrovenator*: UC OBA 1; *Eustreptospondylus*: OUMNH J.13558), in these taxa the long axis of the femoral head is horizontal. Thus, an anteroproximomedially oriented femoral head can be considered an autapomorphy of *Neovenator*. The posterior flange of the caput is missing from both femora. The ventral surface of the head forms a distinct shelf that overhangs the shaft proximally. This shelf originates medially under the caput, anterior to the posterior flange, and extends laterally onto the anterior surface of the head, where it curves distolaterally, becoming progressively weaker. The shelf contacts the proximal portion of the posteromedial surface of the lesser trochanter as a weak ridge.

The head is of subequal transverse width for the medial two thirds of its length and only the lateral portion of the head narrows towards the greater trochanter, which is narrower than the rest of the head (Text-fig. 21e). In some basal tetanurans the head narrows progressively along its entire length as it approaches the greater trochanter. However, while some femora of *Allosaurus* display the latter condition (BYU 951), others show a condition more similar to that in *Neovenator* (UMNH VP 7908). The same variability seems to be present between femora of *Fukuiraptor* (Currie & Azuma 2006).

A gentle longitudinal ridge originates proximally on the posterior surface of the femoral head of *Neovenator*, dividing that surface into anterior and posterior regions of anteroposterior concavity. This ridge merges with the femoral shaft at the level of the ventral surface of the caput. The greater trochanter forms an oval platform on the lateral surface of the shaft proximally. It is anteroposteriorly wide compared to those of *Acrocanthosaurus*, *Allosaurus* and

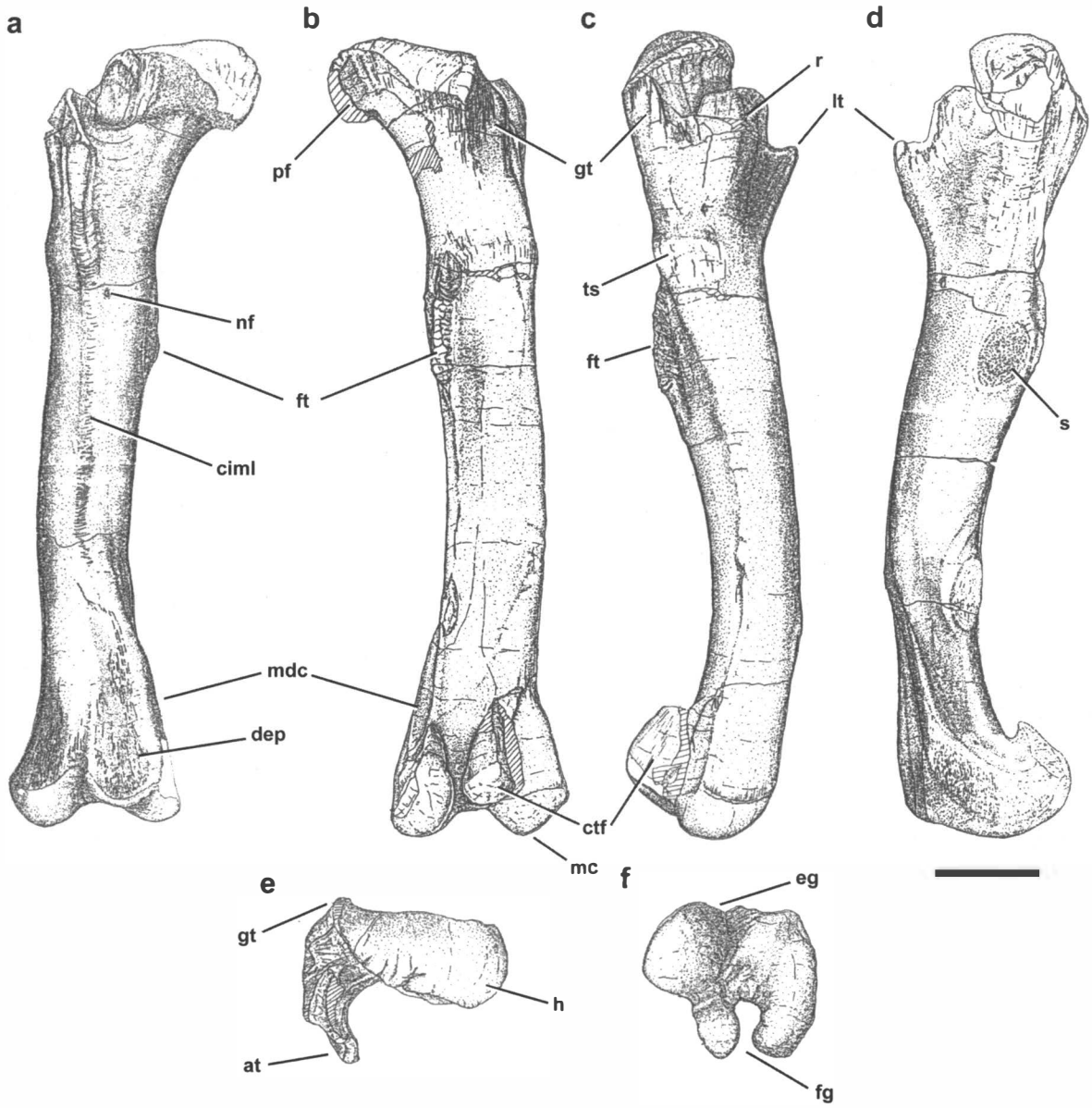

TEXT-FIG. 21. *Neovenator salerii* Hutt, Martill & Barker, 1996; femur (MIWG 6348): **a**, left femur in anterior view; **b**, left femur in posterior view; **c**, left femur in lateral view; **d**, left femur in medial view; **e**, left femur in proximal view; **f**, left femur in distal view. Abbreviations: **at**, accessory trochanter; **ciml**, cranial intermuscular line; **ctf**, crista tibiofibularis; **dep**, depression; **eg**, extensor groove; **fg**, flexor groove; **ft**, fourth trochanter; **gt**, greater trochanter; **h**, head; **lt**, lesser trochanter; **mc**, medial condyle; **mdc**, medial distal crest; **nf**, nutrient foramen; **pf**, posterior flange of caput; **r**, ridge; **s**, scar; **ts**, trochanteric shelf. Scale bar represents 100 mm.

Sinraptor, which have a greater trochanter that is narrow relative to its proximodistal height. The greater trochanters of derived carcharodontosaurids (e.g. *Giganotosaurus*: MUCPv-CH-1) are comparably wider than that of *Neovenator*.

The lesser trochanter is wing-like and extremely robust. It rises dorsally to midheight of the head, and is separated from the greater trochanter by a deep cleft that continues a short distance distally as a shallow groove on the lateral surface of the shaft. A robust suboval eminence is present on the external surface of the lesser trochanter proximally (Pl. 40, figs 5, 7; Text-fig. 21e). This eminence is not present in any other allosauroid (*Allosaurus*: Madsen 1976;

Giganotosaurus: MUCPv-CH-1; *Sinraptor*: IVPP 10600) and thus is diagnostic of *Neovenator*. A pronounced large triangular accessory trochanter emerges anteromedially from the lesser trochanter as in all allosauroids (e.g. *Giganotosaurus*: MUCPv-CH-1; *Mapusaurus*: MCF-PVPH 108.203; *Sinraptor*: IVPP 10600). The accessory trochanter of *Carcharodontosaurus* is developed as a broad flange oriented transverse to the plane of the lesser trochanter (Stromer 1931), a condition that seems to be autapomorphic. The trochanteric shelf of *Neovenator* is a low mound on the lateral surface of the shaft at the base of the lesser trochanter. A crescentic rugose region, roughened by proximodistal striations, surrounds the proximal portion of the shelf. A robust longitudinal buttress extends distally from the base of the lesser trochanter, and migrates distomedially, merging with the shaft just distal to midlength of the bone. The cranial intermuscular line is expressed as closely packed, transversely oriented striations along the top of this buttress, extending proximally along the anterior surface of the accessory trochanter. The primary nutrient foramen is located on the shaft anterodistal to the base of the lesser trochanter.

The fourth trochanter emerges posteriorly from the medial surface of the shaft as a wedge-shaped flange. In some carcharodontosaurids (*Giganotosaurus*: MUCPv-CH-1; *Mapusaurus*: Coria & Currie 2006) the fourth trochanter is reduced, but in most allosauroids it is comparable in size and shape to that of *Neovenator* (*Acrocanthosaurus*: Harris 1998; *Allosaurus*: Madsen 1976; *Sinraptor*: Currie & Zhao 1993). The lateral surface of this trochanter is highly rugose. Additionally, a large oval rugosity straddles the medial surfaces of the femoral shaft and fourth trochanter. Lateral to the proximal end of the fourth trochanter is a thumbprint-shaped depression that is absent in other theropods and is therefore an autapomorphy of *Neovenator* (Text-fig. 21b).

The distal end of the femoral shaft expands mediolaterally and posteriorly to accommodate the condyles. A large oval depression is present distally on the medial half of the anterior surface of the femur and extends to the distal end of the bone as in *Allosaurus* (Madsen 1976) and *Sinraptor* (Currie & Zhao 1993). A smaller depression is present in *Acrocanthosaurus* (OMNH 10146), in which it does not extend to the distal end of the femur. The depression is flanked medially by a strong medial distal crest, which ends 220 mm from the distal end of the right femur, at 30% of femoral length, similar to those of other allosauroids except *Sinraptor*, in which the crest is much shorter.

In most allosauroids and in basal tetanurans in general, the anterior surface of the medial condyle slopes posterolaterally to form a wide extensor groove bounded laterally by the convex anterior surface of the lateral condyle (e.g. *Acrocanthosaurus*: OMNH 10146; *Allosaurus*: Madsen 1976; *Piatnitzkysaurus*: PVL 4073). In *Neovenator* the morphology of the extensor groove is autapomorphic: the anterior surface of the medial condyle is planar and that of the lateral condyle is rounded but does not project anteriorly, such that the anterior surface of the distal femur is almost flat. The extensor groove is developed as a narrow groove on the posterior surface between the condyles that extends only a short distance proximally (Text-fig 21a).

In anterior view, the lateral condyle extends farther distally and is more highly convex than the medial condyle, which resembles a rounded cone, as is seen in *Carcharodontosaurus* (Stromer 1931) and possibly *Giganotosaurus* (MUCPv-CH-1, P.C. Sereno, pers. comm.), although breakage in the latter taxon renders this observation ambiguous. This condition differs from the less projecting and smoothly rounded lateral condyle of *Acrocanthosaurus* (OMNH 10146), *Allosaurus* (Madsen 1976) and *Sinraptor* (Currie & Zhao 1993). The distal surface of the medial condyle of *Neovenator* curves posteroproximally to become its posterior surface, which extends proximally as a hook-shaped process. A stout crista tibiofibularis is present on the posterior surface of the lateral condyle. The crista tibiofibularis is separated from the floor of the flexor groove distally by a notch that extends onto the distal surface of the femur as a groove laterally flanking the depressed intercondylar region. Medial to this notch a pair of short longitudinal grooves marks the spaces between two proximodistally short, raised ridges in the central region of the flexor groove. Weak ridges extend from the proximal ends of the crista tibiofibularis and the posterior expansion of the medial condyle. These ridges continue proximally and meet in the lateral region of the posterior surface of the shaft.

Tibia. Both tibiae are known from the holotype (MIWG 6348; Table 5; Pl. 41; Text-fig. 22). The left tibia was found during the second excavation at Grange Chine and the right was found later with the left femur by one of us (SH). In the right tibia the anterior portion of the cnemial crest is broken off but the bone is undistorted and otherwise well-preserved. The proximal end of the left tibia is crushed transversely, and consequently the head is transversely compressed and the medial face is caved in.

The shaft is almost straight, curving only slightly anteriorly and medially. The plane of the distal expansion is twisted relative to the proximal end so that the anterior surface faces anteromedially. The shaft is flat anteriorly and convex posteriorly; it is wider mediolaterally than

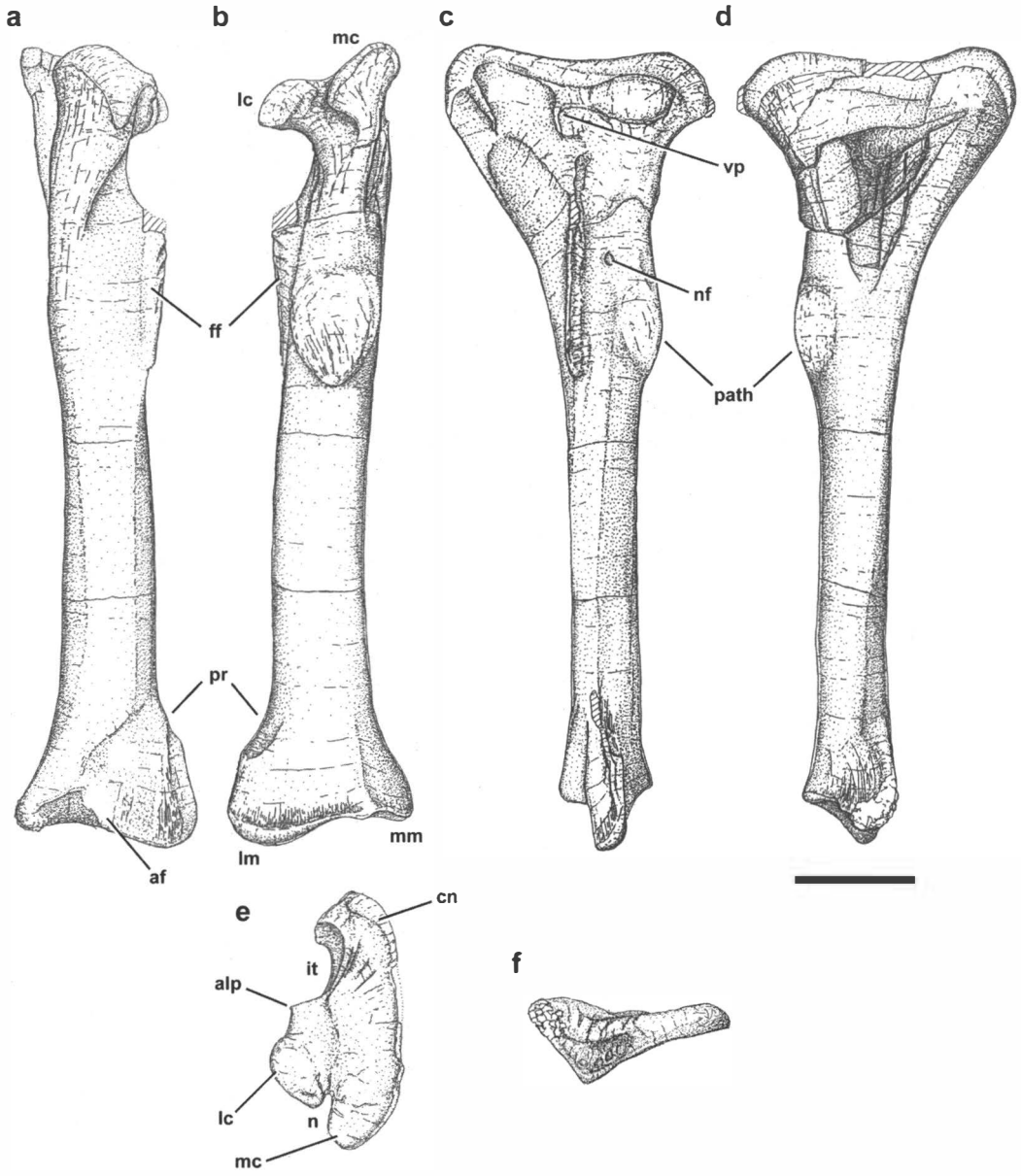

TEXT-FIG. 22. *Neovenator salerii* Hutt, Martill & Barker, 1996; tibia (MIWG 6348): **a**, left tibia in anterior view; **b**, left tibia in posterior view; **c**, left tibia in lateral view; **d**, left tibia in medial view; **e**, left tibia in proximal view; **f**, left tibia in distal view. Abbreviations: **af**, astragalar facet; **alp**, anterolateral process; **cn**, cnemial crest; **ff**, fibular flange; **it**, incisura tibialis; **lc**, lateral condyle; **lm**, lateral malleolus; **mc**, medial condyle; **mm**, medial malleolus; **n**, notch; **nf**, nutrient foramen; **path**, pathology; **pr**, pinched region; **vp**, ventral spine-like process. Scale bar represents 100 mm.

thick anteroposteriorly at midlength and becomes increasingly compressed towards the distal expansion. The primary nutrient foramen is located posterior to midpoint of the fibular flange.

The medial condyle extends further proximally than the lateral (fibular) condyle, as is usual for theropods, giving the impression that the head has been tilted laterally in posterior view. The proximal surface of the lateral condyle is more strongly convex than that of the medial condyle, and the condyles are subequal in transverse width. They are separated by a wide notch posteriorly that extends onto the posterior surface of the shaft as a shallow ovate depression.

In proximal view the shape of the lateral condyle is subrectangular. The medial condyle is lobate and extends posteriorly beyond the lateral condyle, curving slightly laterally as is seen in some tibiae of *Allosaurus* (Madsen 1976; BYU 13864). However, in other *Allosaurus* tibiae the medial condyle is subrectanglar and does not extend past the lateral condyle (UMNH VP 7928). In basal tetanurans generally the medial condyle is subrectangular (*Afrovenator*: UC OBA 1; *Torvosaurus*: BYU 2016; *Sinraptor*: Currie & Zhao 1993), and only in *Torvosaurus* does it extend posteriorly past the lateral condyle. In *Lourinhanosaurus* (ML 370) the medial condyle is lobate but does not extend posteriorly beyond the lateral condyle. In the enigmatic theropod *Erectopus* from the Aptian–Albian of France the medial condyle is subrectangular but does extend posteriorly beyond the lateral condyle (MNHN 2001-4).

The lateral condyle is expanded posteriorly and laterally, overhanging the tibial shaft. This overhanging morphology does not extend to the anterior region of the condyle, which is unexpanded and flush with the lateral surface of the tibia. In proximal view an anterolateral process with a triangular outline projects into the incisura tibialis from the anterior surface of the lateral condyle. A similar anterolateral process is present in *Allosaurus* (Madsen 1976), but is absent in *Sinraptor* (Currie & Zhao 1993). The base of a smoothly rounded anterolateral projection is visible in *Erectopus* (MNHN 2001-4). Unlike the anterolateral process of *Allosaurus*, this projection develops into a ventral spine (broken off in the left tibia) that overhangs the lateral surface of the shaft (Text-fig. 22e); this spine is also absent in other basal tetanurans (e.g. *Piatnitzkysaurus*: PVL 4073; *Sinraptor*: Currie & Zhao 1993) and is an autapomorphy of *Neovenator*. The lateral condyle and anterolateral process are separated from the cnemial crest by a strong incisura tibialis, as is seen in tetanurans and *Ceratosaurus*, as well as some specimens of *Coelophysis* (Rauhut 2003).

In lateral view the cnemial crest has a rounded subrectangular anterior end that extends slightly above the condyles proximally and curves laterally to the level of the lateral condyle. A strong, posteroventrally oriented ridge extends from the lateral surface of the crest. In most other basal tetanurans a distinct ridge is present in this position, but it is much less pronounced than in *Neovenator* (e.g. *Allosaurus*: Madsen 1976; *Erectopus*: MNHN 2001-4; *Sinraptor*: Currie & Zhao 1993; *Torvosaurus*: BYU 2016).

The fibular flange is a vertical ridge on the lateral surface of the shaft, measuring 140 mm in length. It is developed as a narrow lamina, with a rugose posterior surface. The flange continues proximally as a low and weakly rugose ridge that widens progressively before merging with the shaft. The lateral surface of the shaft is gently flattened distal to the fibular flange. Distally the flattened surface migrates around the shaft to the lateral part of the anterior surface.

The shaft is transversely expanded distally, and has a triangular outline in distal view. A shallow fossa is present posteriorly on the distal surface that would have articulated with a raised posterior eminence on the astragalus. A weak triangular facet for the ascending process of the astragalus is present on the anterior surface of the distal expansion. A low, rounded, suprastragalar buttress (= medial buttress) extends proximolaterally from the ventromedial corner of the medial malleolus to the apex of the facet. This buttress is weak in comparison to the step-like suprastragalar buttresses of other basal tetanurans (e.g. *Allosaurus*: Madsen 1976; *Erectopus*: MNHN 2001-4; *Sinraptor*: Currie & Zhao 1993; *Streptospondylus*: MNHN 8607; *Torvosaurus*: BYU 2016).

In anterior view the lateral malleolus of the distal expansion is large and projects farther distally than the medial malleolus, as it does in *Acrocanthosaurus* (OMNH 10146) and *Mapusaurus* (Coria & Currie 2006). In contrast, the lateral malleolus ends at the same level as the medial

malleolus or projects only slightly distally in *Allosaurus* (Madsen 1976), *Giganotosaurus* (MUCPv-CH-1), and *Sinraptor* (Currie & Zhao 1993). The lateral margin of the lateral malleolus is marked by a kink, which forms a low shoulder in anterior view. Proximal to this kink the lateral expansion takes the form of an anteroposteriorly thin lamina (Text-fig. 22a–c), pinched between a recess on the posterior surface and a gentle longitudinal groove on the anterior surface that extends distally parallel to the lateral margin of the distal end of the bone. This condition is absent in other allosauroids (*Acrocanthosaurus*: OMNH 10146; *Allosaurus*: Madsen 1976; *Giganotosaurus*: MUCPv-CH-1; *Sinraptor*: Currie & Zhao 1993) and thus it is an autapomorphy of *Neovenator*. The remainder of the lateral malleolus is anteroposteriorly thick as is usual for theropods.

The medial malleolus of the distal tibia extends distomedially and is similar in form to those of *Allosaurus* and *Sinraptor*, but is unlike the more medially projecting medial malleolus of *Acrocanthosaurus* (OMNH 10146) and *Mapusaurus* (Coria & Currie 2006). An intensely rugose area is present proximally on the medial surface of the medial malleolus (Text-fig. 22d) (obscured by the formation of pyrite crystals in the left tibia), a condition that is absent in other allosauroids, including *Acrocanthosaurus* (NCSM 14345), *Allosaurus* (Madsen 1976), *Mapusaurus* (Coria & Currie 2006) and *Sinraptor* (Currie & Zhao 1993), and is therefore an autapomorphy of *Neovenator*.

Fibula. The left fibula of the holotype (MIWG 6348) is complete and well-preserved (Pl. 41; Text-fig. 23; Table 5). This element is expanded proximally into an anteroposteriorly broad plate, which comprises the upper one quarter of the bone. Distally the plate tapers into the thin shaft, which has a relatively constant anteroposterior length until narrowing to a minimum of 34 mm immediately before expanding distally into a terminal swelling. This distal expansion is twisted slightly relative to the shaft so that it is positioned anterior to the tibia (with its 'medial' surface instead facing posteromedially); it has a rugose, teardrop-shaped distal articular surface for contact with the astragalus and calcaneum. In this region, *c.* 20 mm dorsal to the articulation with the tarsals, the lateral surface of the distal end of the fibula is marked by a rugose pathology, which is described below. The proximal articular surface tapers posteriorly to a point in proximal view, and is shallowly concave anteroposteriorly for articulation with the femur.

The lateral surface of the fibula is generally smooth. The lateral surface of the proximal expansion is traversed by a posteroventrally inclined ridge that straightens out distally and becomes confluent with the posterior margin of the shaft (Text-fig. 23b). Posterior to this ridge, the lateral surface of the proximal expansion adjacent to its posterior margin is excavated by a deep fossa which continues down the length of the projection, before thinning and joining the shaft. The anterior margin of the lateral surface of the shaft anterior to the ridge is concave, but not nearly as deep as the fossa posterior to the ridge.

Medially, the proximal expansion is invaded by a large oval fossa, which measures 97 mm in proximodistal height and 41 mm in anteroposterior width. This fossa is deep and rugose proximally, and becomes shallower and smoother distally before dissipating. The anterior margin of the fossa nearly abuts the anterior margin of the fibula itself, but is demarcated by a flange of bone oriented mediolaterally. Thus, the anterior margin of the fossa ends abruptly, whereas more posteriorly the fossa slopes gently to merge with the medial surface of the fibula. Immediately distal to the fossa the medial surface is heavily rugose with thick swellings anteriorly and posteriorly for the interosseum tibiofibulare ligaments (Currie & Zhao 1993). This region serves to separate the deep proximal fossa from a more distal groove that extends down the length of the shaft, which becomes gradually shallower until flattening immediately proximal to where the shaft swells into the distal expansion. The medial surface of the distal expansion is flat but heavily striated and rugose for articulation with the tibia. There is no oblique ridge separating the tibial contact from the remainder of the medial shaft as in *Sinraptor*.

Pes. The left pes of the holotype (MIWG 6348) is relatively complete, and includes metatarsals II–V and phalanges of the second (II-1, II-2), third (III-4) and fourth (IV-1–IV-5) digits (Pls 42–45; Text-figs 24, 25). Left pedal phalanx IV-3 is pathological, as described in the pathology section below. Isolated material from the right pes of the holotype is also known, and includes a complete phalanx IV-3 and a highly eroded proximal segment of the ungual of digit

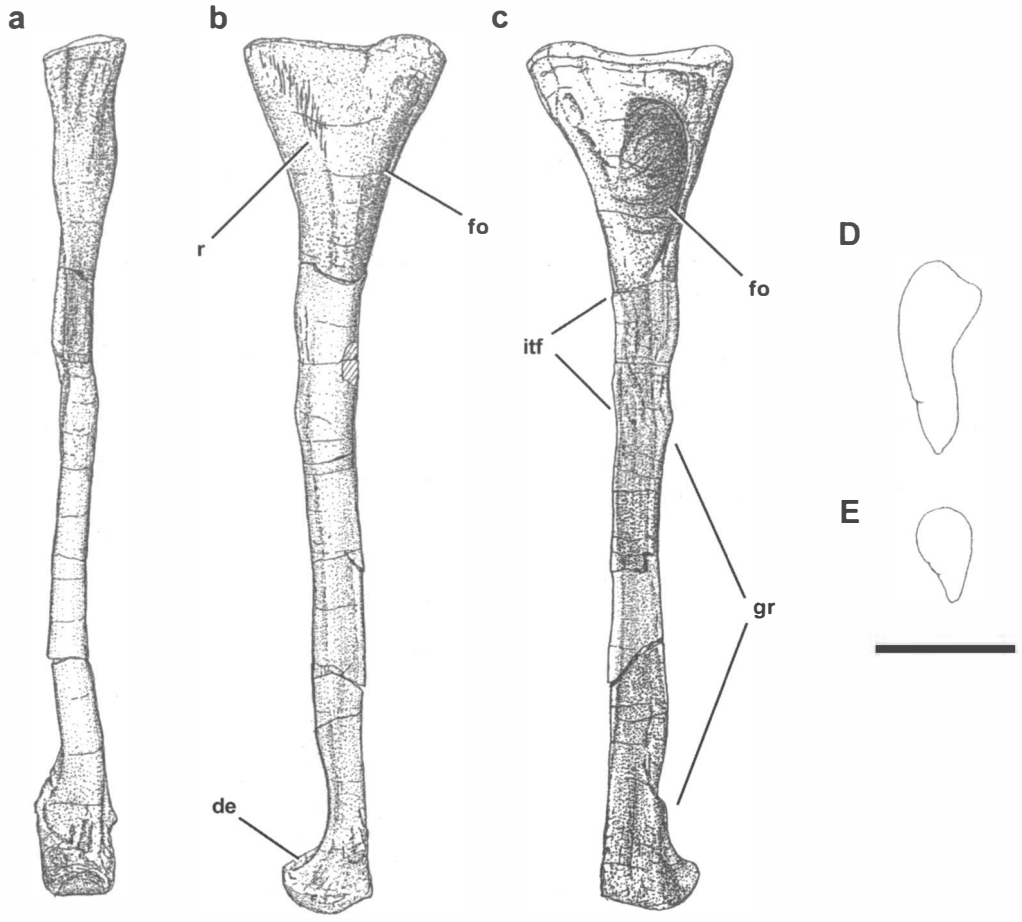

TEXT-FIG. 23. *Neovenator salerii* Hutt, Martill & Barker, 1996; fibula (MIWG 6348): **a**, left fibula in anterior view: **b**, left fibula in lateral view; **c**, left fibula in medial view; **d**, left fibula in proximal view; **e**, left fibula in distal view. Abbreviations: **de**, distal expansion; **fo**, fossa; **gr**, groove; **itf**, attachment area for interosseum tibiofibulare ligaments; **r**, ridge. Scale bar represents 100 mm.

III (III-4). A cast (MIWG 5470) of a pedal phalanx collected with two referred vertebrae appears to represent phalanx III-1, and agrees in general size and form with the pedal elements of *Neovenator*. The original is in a private collection and this element will not be discussed further.

Metatarsals. The preserved metatarsals include complete left metatarsals II, IV and V and the proximal half of left metatarsal III (Table 6; Pls 42–45; Text-figs 24, 25). Metatarsals II and IV are approximately equal in length as in most large theropods, whereas metatarsal V is a small sigmoidal splint that would have been closely appressed to the posterolateral surface of metatarsal IV in life. Metatarsals II–IV are closely appressed proximally and diverge only slightly from each other as they continue distally, due to curvature in metatarsals II and IV. This is similar to the condition in *Acrocanthosaurus* (Stovall & Langston 1950; Currie & Carpenter 2000), *Allosaurus* (Madsen 1976) and *Sinraptor* (Currie & Zhao 1993).

The shaft of metatarsal II is approximately straight and only curved slightly medially away from the axis of metatarsal III. Metatarsal II is trapezoid in proximal view, with a slightly concave lateral surface for articulation with metatarsal III. This concave excavation extends distally as a smoothly rounded surface on the proximal region of the lateral surface, where a series of fine striations mark the articular surface for metatarsal III. The broadly concave lateral articulation for metatarsal III is unique among large theropods, as the surface is flat in *Acrocanthosaurus* (Currie & Carpenter 2000), *Allosaurus* (Madsen 1976), *Dilophosaurus* (UCMP 37302), *Fukuiraptor* (Azuma & Currie 2000), *Mapusaurus* (MCF-PVPH-108.35), *Sinraptor* (Currie & Zhao 1993) and

TABLE 6. Metatarsal measurements (MIWG 6348, left elements) in mm; * = incomplete measurements.

	Length	Proximal length[1]	Proximal width[2]	Midshaft antpost.	Midshaft mediolat.	Distal length[3]	Distal width	Minimum circum.
Metatarsal II	315	72	50	43	41	67	55	130
Metatarsal III	268*	?	41	42	32	?	?	126
Metatarsal IV	325	95	37	46	37	62	41	129
Metatarsal V	150	25	16	21	16	14	7	61

[1]: maximum anteroposterior length of proximal articular surface
[2]: mediolateral width of proximal articular surface at midpoint
[3]: maximum axis of distal articular surface

Torvosaurus (Britt 1991). The posterior surface of metatarsal II is marked by an elongate, shallow groove at midshaft for articulation with a small metatarsal I.

Distally, the lateral collateral ligament pit is deeply excavated and surrounded by a broad fossa that terminates against the smooth distal articular surface. In contrast, the medial ligament pit does not take the form of a deep excavation, but is expressed rather as a shallow fossa. This is the case in many large theropods, but differs from *Acrocanthosaurus* (Harris 1998), in which lateral and medial pits are both deeply excavated. In distal view, the articular surface for the first phalanx is divided into two condyles: a large bulbous anterior condyle that is subrectangular in distal view, and a much smaller finger-like posterior condyle. These condyles diverge from each other at *c.* 90 degrees, and are separated by a cleft that becomes confluent with a deep flexor groove posteriorly. The posterior condyle of *Neovenator* is much smaller relative to the anterior condyle than it is in *Acrocanthosaurus*, *Fukuiraptor*, *Torvosaurus* and basal tyrannosauroids (*Appalachiosaurus*: Carr *et al.* 2005), but is similar to the condition in *Mapusaurus*.

In addition to missing its distal half, metatarsal III is also broken on the posterior margin of its proximal surface. This obscures the shape of the proximal articular surface, but it appears as if this face was roughly triangular. This surface is mediolaterally broad anteriorly, constricted around its midpoint, and ends in a narrow posterior lobe (Pl. 42, fig. 11; Pl. 44, fig. 3). This is a consequence of constriction of the posterior portion of the proximal end of metatarsal III between metatarsals II and IV in proximal view (Pl. 44, fig. 3). Such strong constriction is not apparent in *Acrocanthosaurus* (Currie & Carpenter 2000), *Allosaurus* (Madsen 1976), *Mapusaurus* (Coria & Currie 2006) and *Sinraptor* (Currie & Zhao 1993). Unfortunately, breakage obscures details of the distal articular surface and much of the shaft, but it appears as if metatarsal III was generally straight throughout its length.

The shaft of metatarsal IV diverges laterally as it extends distally as it does in many large theropods. The degree of curvature is similar to that in other allosauroids (e.g. *Allosaurus*: Madsen 1976). Proximally, the articular surface gives rise to a prominent posteromedial lobe, which is largely responsible for constriction of the posterior portion of the proximal surface of metatarsal III (Pl. 44, fig. 3). Consequently, there is a deep concavity in the dorsomedial region of the outline of this surface in metatarsal IV, which is much deeper than the concavity for articulation with metatarsal IV on metatarsal II. Distally, the medial collateral ligament pit is a distinct and deep excavation set into a broad fossa that extends to the smooth articular surface. This fossa is marked by several fine striations that radiate outward from the pit. The lateral collateral ligament pit is not deeply excavated but instead expressed as an anteroposteriorly inclined shallow fossa.

The distal articular surface is complex. One large oval condyle dominates the anterior region of the surface, and posteriorly gives rise to two smaller processes. These processes diverge from each other at *c.* 30 degrees and are separated by a sharp cleft. The lateral accessory process extends farther posteriorly than the medial process and is a wing-like flange with subparallel lateral and medial sides that do not taper to a point. This flange is nearly identical to that of *Sinraptor* (Currie & Zhao 1993, fig. 27), but differs greatly from the condition in many other large theropods. Separate medial and lateral posterior projections are present in *Afrovenator* (UC OBA 1), *Condorraptor* (Rauhut 2005), *Dilophosaurus* (Welles 1984), *Megaraptor* (Calvo *et al.* 2004), *Torvosaurus* (Britt 1991) and basal coelurosaurs (e.g. *Appalachiosaurus*: Carr *et al.* 2005), but the

lateral process is very different in form. In these taxa the lateral projection tapers to a point, extends to the same posterior level as the medial accessory process, and is separated from the medial process by an obtuse angle and a shallow groove.

Metatarsal V is much shorter and thinner than the other metatarsals. It lacks a well-formed distal articular surface and thus supported no phalanges. The shaft is gently curved in lateral view and tapers slightly distally. This is broadly similar to the condition in *Allosaurus* (Madsen

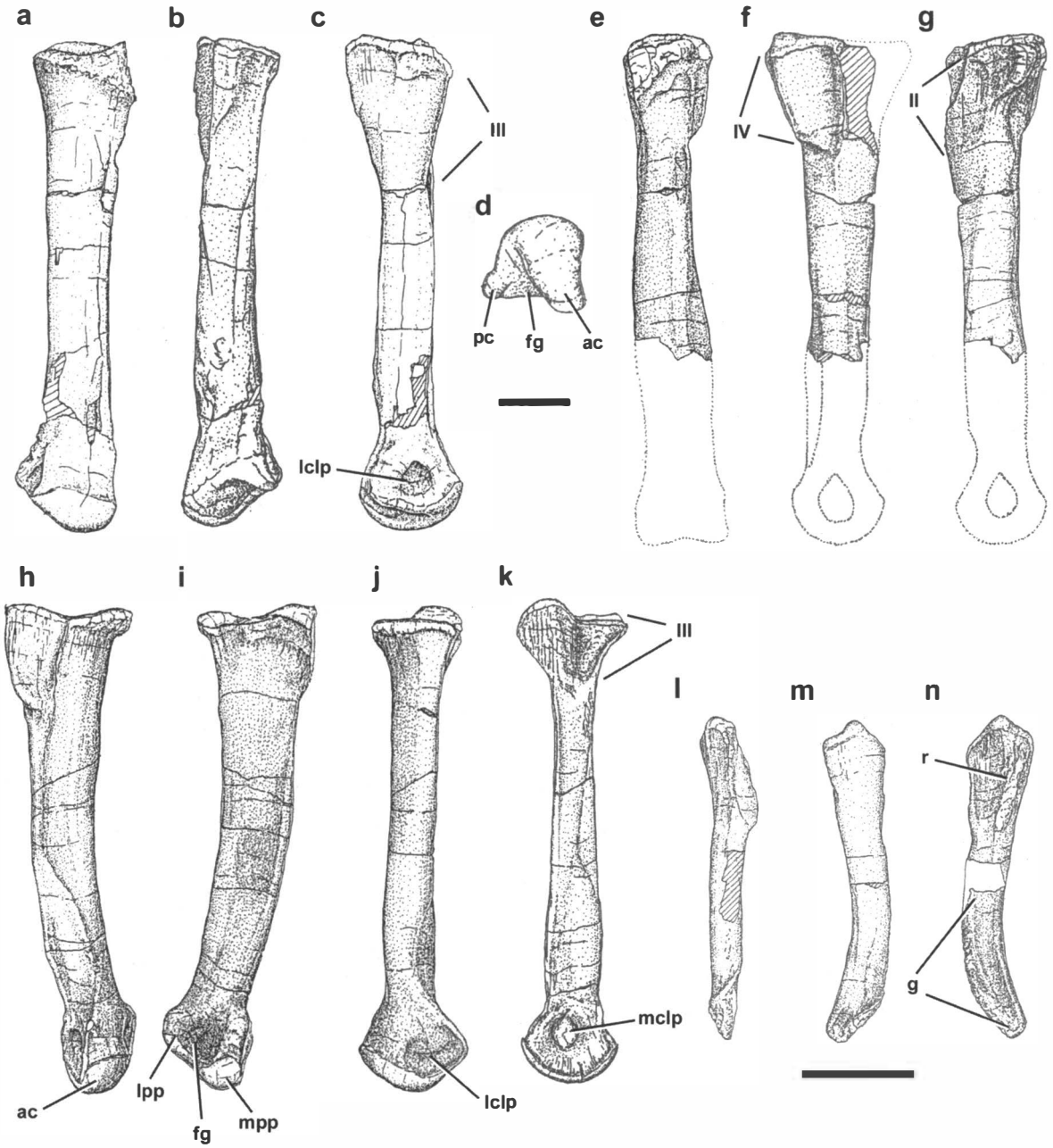

TEXT-FIG. 24. *Neovenator salerii* Hutt, Martill & Barker, 1996; metatarsals (MIWG 6348): **a**, left mt II in anterior view; **b**, left mt II in posterior view; **c**, left mt II in lateral view; **d**, left mt II in distal view; **e**, left mt III in anterior view; **f**, left mt III in posterior view; **g**, left mt III in medial view; **h**, left mt IV in anterior view; **i**, left mt IV in posterior view; **j**, left mt IV in lateral view; **k**, left mt IV in medial view; **l**, left mt V in posterior view; **m**, left mt V in lateral view; **n**, left mt V in medial view. Abbreviations: **II, III, IV**: articular surfaces for metatarsals II, III, IV; **ac**, anterior condyle; **fg**, flexor groove; **g**, groove; **lclp**, lateral collateral ligament pit; **lpp**, lateral posterior process; **mclp**, medial collateral ligament pit; **mpp**, medial posterior process; **pc**, posterior condyle; **r**, ridge. Scale bars represent 50 mm.

1976) and *Sinraptor* (Currie & Zhao 1993), but unlike that in the spinosauroid *Dubreuillosaurus*, in which metatarsal V is straight and tapers strongly distally. The lateral surface is flat proximally but gradually becomes slightly convex as it continues distally. In medial view, a strong, rugose ridge extends from the proximal articular head for approximately one third of the length of the shaft. This ridge likely braced against the surface of metatarsal IV, and is much more prominent than that of *Allosaurus* (Madsen 1976) and *Sinraptor*. Farther distally there is a sharp groove along the distal third of the medial surface of the shaft that Currie & Zhao (1993) interpreted as a canal for tendons of the flexor musculature in *Sinraptor*. Alternatively, it may have articulated against a sharp crest on metatarsal IV in *Neovenator*. Immediately posterior to this groove is a hightly rugose surface which clearly articulated with metatarsal IV. In proximal view the articular surface is broadly rectangular, but with a thin concave flange projecting posterodistally to cup a projection on metatarsal IV. This flange continues distally as a sharp ridge that separates the lateral and medial surfaces of the shaft.

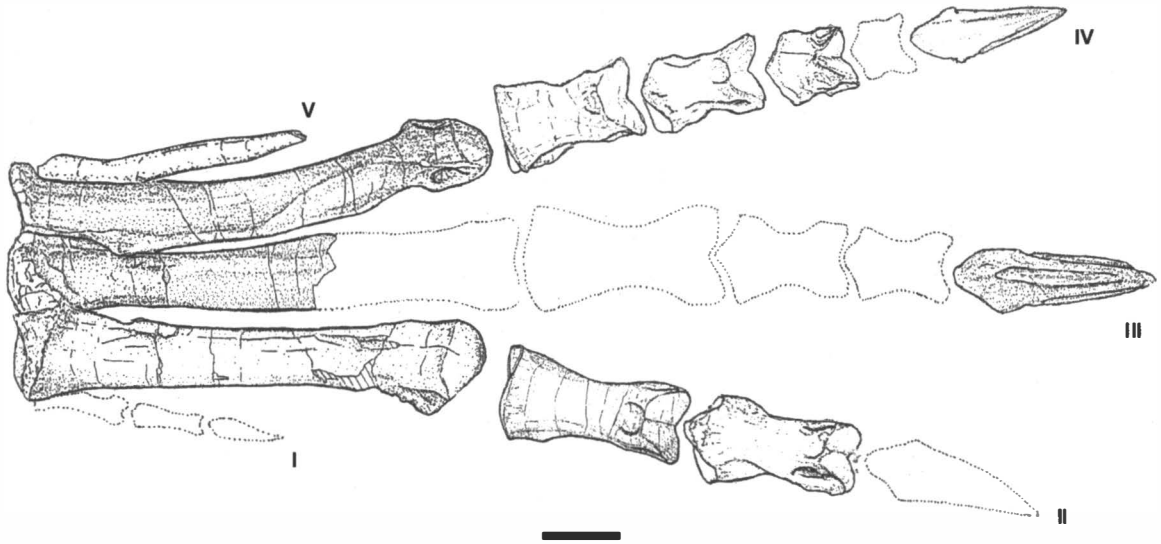

TEXT-FIG. 25. *Neovenator salerii* Hutt, Martill & Barker, 1996; left pes (MIWG 6348). Abbreviations: **I, II, III, IV, V**: digit number. Scale bar represents 50 mm.

Phalanges. The extensor surfaces of all non-ungual phalanges with the exception of II-2 and IV-4 are marked by a deep excavation immediately proximal to the distal articular condyles (Table 7; Pls 43–45; Text-fig. 25). These structures would have received the superior margin of the proximal articular surface of the following phalanx, and thus would have acted to limit digit extension. The excavations become smaller both absolutely and relative to phalanx length in more distal phalanges. They also change shape from an anteroposteriorly expanded oval to a mediolaterally expanded triangle along the digit. *Sinraptor* also lacks an excavation on II-2 (Currie & Zhao 1993, fig. 25L), but details of the pedal phalanges of many large theropods are poorly described.

The flexor surfaces of all non-ungual phalanges are ornamented with strong ridges that begin at the medial and lateral margins of the proximal articular surface and extend diagonally inwards before merging into the midregion of the smooth ventral surface. A slightly different condition is present on phalanx II-1, in which the medial ridge does not continue diagonally toward the centre of the bone. Instead, it begins to extend inwards (anterolaterally) toward the centre but then curves medially halfway along its length before gradually terminating on the medial edge of the bone. The curved shape of this ridge defines a broad area on the proximomedial corner of the flexor surface that includes a pronounced raised rugosity surrounded by a smooth margin. This rugosity is unknown in other theropods and is probably pathological, but it is unclear whether the medial curvature of the ridge is an original feature. The lateral ridge on this element runs inward as in all other non-ungual phalanges.

TABLE 7. Pedal phalanx measurements (MIWG 6348, left elements*) in mm.

	Length	Proximal height	Proximal width	Midshaft height	Midshaft width	Distal height	Distal width	Min. circum.
II-1	109	60	62	37	38	37	50	122
II-2	88	52	37	30	34	29	34	116
III-4	117	49	36	32	27	-	-	-
IV-1	83	56	54	29	38	28	51	118
IV-2	69	41	46	29	35	24	47	110
IV-3*	52	38	39	25	35	22	36	111
IV-4	34	34	37	28	37	20	31	113
IV-5	82	35	28	24	22	-	-	-

*-since left IV-3 pathological, the undistorted right IV-3 was measured; height = measurement from flexor to extensor surface; width is mediolateral.

The proximal articular surfaces of proximal phalanges (II-1, IV-1) are concave, whereas those of more distal phalanges are saddle-shaped, as they are divided medially by a dorsoventrally oriented ridge (Pl. 45). These surfaces have a broadly trapezoidal outline in proximal view, with medial and lateral surfaces that are slightly concave as in *Sinraptor* (Currie & Zhao 1993), not straight as in *Allosaurus* (Madsen 1976). Rugosities for the collateral ligaments and digit flexors are present around the periphery of the proximal surface on all adjacent surfaces (Currie & Zhao 1993)

The distal articular surfaces are saddle-shaped, with two bulbous condyles separated by a smooth depression that continues onto the flexor and extensor surfaces as sulci for the flexor and extensor tendons. The phalanges of digit II are characterized by a medial condyle that is slightly taller than the lateral condyle and angled medially. Those of digit IV are also characterized by a slightly taller and medially angled medial condyle, although the angle is not as strong as in the phalanges of digit II.

The collateral ligament pits on the phalanges of digit II are distinct on both medial and lateral sides but stronger medially, where the excavation is large in diameter, much deeper, and surrounded by a broader fossa. In digit IV the pits are generally stronger medially and more weakly expressed laterally. In phalanx IV-2 the lateral pit does not form any excavation but is expressed only as a shallow fossa. This is unlike the state in *Sinraptor*, which shows a well-developed pit on the lateral surface of this phalanx (Currie & Zhao 1993, fig. 28). In phalanx IV-4 the medial and lateral pits are approximately equal in size and depth, and are located much closer to the extensor surface than in preceding phalanges, as is characteristic of the penultimate phalanx of many large theropods.

Unguals are known for digits III and IV. Both unguals are characterized by a single groove on both the lateral and medial surfaces. This groove is deep and distinctly demarcated by sharp edges, and is located closer to the flexor margin of the bone than in *Allosaurus*, *Sinraptor*, and an isolated ungual of *Mapusaurus* of unknown position (Coria and Currie 2006, fig. 34). The extensor surface of the left ungual III is excavated by a single median shallow groove. This structure is not present on ungual IV, and is not evident on a more fragmentary and eroded right ungual III. We follow Hutt *et al.* (1996) and Naish *et al.* (2001) in regarding the extensor surface groove as an autapomorphy, but consider this interpretation as tentative due to limited comparative material in other allosauroids and basal tetanurans in general.

DISCUSSION

PHYLOGENETIC RELATIONSHIPS OF *NEOVENATOR*

Neovenator salerii is the most complete large theropod known from Europe, and is one of the best preserved Early Cretaceous theropods worldwide. Thus, it is of considerable importance for phylogenetic studies of theropods in general and allosauroids and basal tetanurans in particular. Unfortunately, *Neovenator* has often been excluded from cladistic analyses and studies of theropod evolution (e.g. Currie & Carpenter 2000; Allain 2002; Novas *et al.* 2005) despite its completeness and potential to yield important information on a poorly known time period in large theropod

evolution. Those cladistic analyses that have included *Neovenator* agree that it is a member of Allosauroidea, a cosmopolitan and long-lived clade of basal tetanuran theropods that includes the well-known *Allosaurus* from the Upper Jurassic of North America and Europe, *Sinraptor* from the Middle Jurassic of China, and Carcharodontosauridae, a subgroup that produced some of the largest terrestrial predators to have ever lived. The more precise relationships of *Neovenator* have proven controversial: it has been suggested that it is the sister taxon to *Allosaurus* (Holtz 2000); others, however, place it as a basal member of Carcharodontosauridae, but often with weak character support (Harris 1998; Rauhut 2003; Holtz *et al.* 2004).

We do not include a complete phylogenetic analysis here, but information gleaned from the present study has been included in a separate study by Brusatte & Sereno (2008), which constitutes the largest and most complete phylogenetic analysis of allosauroid theropods yet undertaken (Text-fig. 26). This analysis places *Sinraptor* as the basalmost allosauroid, followed successively by *Allosaurus* and Carcharodontosauridae (the latter is defined phylogenetically as the most inclusive clade containing *Carcharodontosaurus saharicus*, but not *Sinraptor dongi*, *Allosaurus fragilis* or *Passer domesticus*). *Neovenator* is recovered as more closely related to *Carcharodontosaurus*

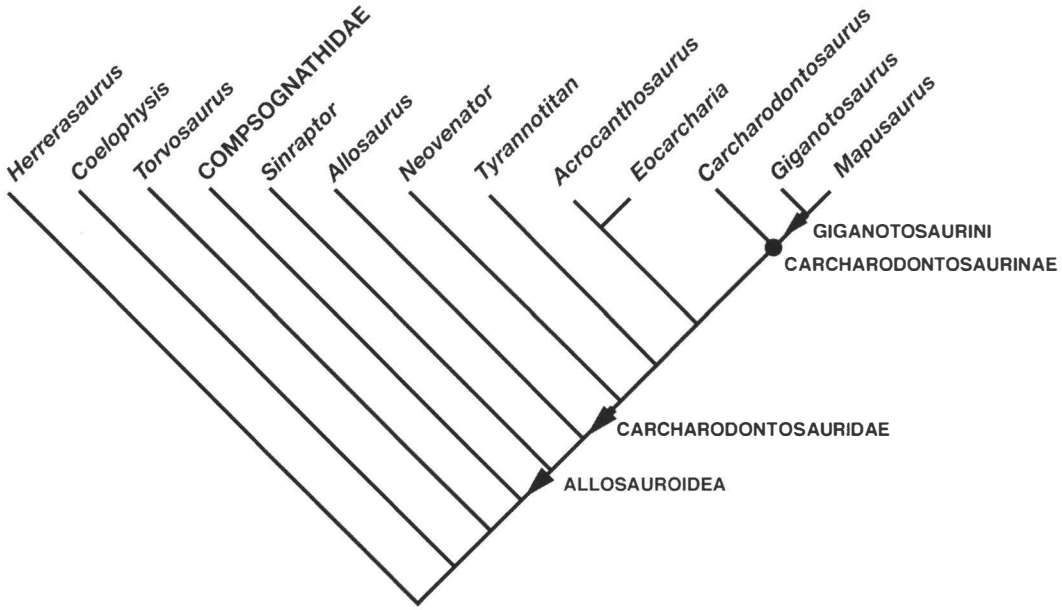

TEXT-FIG. 26. Cladogram of allosauroid theropod phylogeny from the analysis of Brusatte & Sereno (2008). *Neovenator salerii* is recovered as the basalmost member of Carcharodontosauridae, an allosauroid subgroup that includes some of the largest theropods to have ever evolved. Circles denote clades defined with node-based definitions, and arrows denote those clades defined by stem-based definitions.

and other carcharodontosaurids than it is to *Allosaurus* or *Sinraptor*, and thus is a carcharodontosaurid by definition (Sereno 1998; Sereno *et al.* 2005; Brusatte & Sereno 2008). However, it is found to be the basalmost member of the group, and lacks the synapomorphies that characterize more derived members of the clade, which are much larger and distinguished by extremely apomorphic skulls. Below we discuss several of the characters used in this phylogenetic analysis, but we limit our discussion to those characters that can be observed in *Neovenator*. For a more complete list of characters, including those pertaining to parts of the skull not preserved in *Neovenator*, see Brusatte & Sereno (2008).

Neovenator was originally described by Hutt *et al.* (1996) as a close relative of *Allosaurus* among allosauroid theropods, a conclusion not based on a phylogenetic analysis or a discussion of derived characters but instead on an overall comparison of skeletal morphology. It is true that *Neovenator* shares a limited number of derived characters with *Allosaurus*, including a subvertical premaxilla-maxilla articulation, five teeth in the premaxilla, and a lateral lamina of the maxilla that strongly overlaps the anteroventral corner of the antorbital fossa (which also appears to be

present in *Carcharodontosaurus* and *Mapusaurus*; contra Holtz *et al.* 2004 and Brusatte & Sereno 2008). These derived states are not present in any other allosauroids (with the possible exception of a vertical premaxilla-maxilla articulation, which is present in the potential allosauroid *Monolophosaurus*), nor in proximate outgroups to Allosauroidea. However, these characters are few in number, restricted to the skull, and are outweighed by a number of cranial and postcranial characters uniquely shared by *Neovenator* and carcharodontosaurids to the exclusion of *Allosaurus* and *Sinraptor*. These characters include several used in the analysis of Brusatte & Sereno (2008).

Principal row of dentary neurovascular foramina curving ventrally. Many theropods have a principal row of neurovascular foramina on the lateral surface of the dentary. This row is located immediately ventral to the tooth row throughout its entire length (a horizontally 'straight' longitudinal row) in some allosauroids, including *Allosaurus* (Madsen 1976) and *Sinraptor* (Currie & Zhao 1993). This condition also predominates in many allosauroid outgroups (e.g. *Herrerasaurus*: Sereno & Novas 1993; *Ceratosaurus*: Madsen & Welles 2000; *Torvosaurus*: Britt 1991; basal tyrannosauroids; abelisaurids) and the potential allosauroid *Monolophosaurus* (Zhao & Currie 1993). In contrast, the dentaries of *Neovenator*, *Carcharodontosaurus* (Brusatte & Sereno 2007) and *Giganotosaurus* (Calvo & Coria 2000) are characterized by a principal row that curves sharply ventrally as it continues posteriorly, such that the posterior principal foramina are several centimetres below the tooth row and the anterior foramina. This condition is also infrequently seen in some outgroups, such as *Dubreuillosaurus* (MNHN 1998-13 RJN 22; Allain 2002).

Camellate interior structure of cervical vertebrae. The internal structure of the cervical vertebrae of some carcharodontosaurids is extremely complex, and consists of an extensive network of small interconnected pneumatic chambers known as camellae. Britt (1993) defines camellae as small, thin-walled chambers separated internally by thin bony trabeculae and contained within relatively thin external walls. This internal architecture contrasts with that of basal tetanurans generally, which consists of a much smaller number of larger chambers, called camerae, separated by discrete bony laminae internally and held within thick external walls (Britt 1993). A complex camellate internal texture is present in the presacral vertebrae of *Neovenator*, and is present also in *Acrocanthosaurus* (Harris 1998) and *Giganotosaurus* (MUCPv-CH-1). It is not present in *Allosaurus* and *Sinraptor*, which have a camerate internal structure (Britt 1993). The condition in *Carcharodontosaurus* has been treated as uncertain in some cladistic analyses (Harris 1998; Currie & Carpenter 2000). Our observation of numerous elements from Morocco (SGM-Din 3, UCRC uncatalogued) and Niger (MNN IGU11) suggests that camellate structure may be present in *Carcharodontosaurus*, but is often masked by poor preservation. However, poor preservation aside, it is also apparent that the degree of camellate pneumaticity in *Carcharodontosaurus* is not as developed as in *Acrocanthosaurus* and *Giganotosaurus*, in which the cervicals are extensively divided into numerous camellae.

Multiple pleurocoels on postaxial cervical vertebrae. Pleurocoels excavate the lateral surfaces of the cervical vertebrae in many theropod taxa. In most taxa only a single pleurocoel is present on each side of the vertebral centrum, a condition seen in *Allosaurus* (Madsen 1976) and *Sinraptor* (Currie & Zhao 1993), as well as *Carcharodontosaurus* (SGM-Din 3, MNN IGU11, UCRC uncatalogued). However, some carcharodontosaurids possess pleurocoels that are divided in two by a prominent internal lamina or twinned pleurocoels located very close to each other anteriorly on the lateral surface of the centrum (*Acrocanthosaurus*: Harris 1998; *Giganotosaurus*: MUCPv-CH-1; *Tyrannotitan*: Novas *et al.* 2005). A similar condition is present in some cervical vertebrae of *Neovenator*. Some other theropods (traditionally referred to as 'ceratosaurs') possess multiple pleurocoels (e.g. *Ceratosaurus*: UMNH VP 5278; *Dilophosaurus*: UCMP 37302), but in these taxa the pleurocoels are widely separated, with the more posterior opening situated near the posterior articular surface of the centrum. Thus, the condition in *Neovenator* is most similar to that in some carcharodontosaurids.

Pleurocoels extending throughout the dorsal vertebral column. Pleurocoels excavate the lateral surfaces of the dorsal vertebrae in many theropod taxa, but are usually restricted to the anterior dorsals

and absent on more posterior elements. This condition is seen in *Allosaurus* and *Sinraptor*; the potential allosauroids *Fukuiraptor* (Azuma & Currie 2000), *Monolophosaurus* (Zhao & Currie 1993) and *Siamotyrannus* (Buffetaut *et al.* 1996); and many allosauroid outgroup taxa (e.g. *Ceratosaurus*: Madsen and Welles 2000; *Coelophysis*: Colbert 1989; compsognathids: Currie & Chen 2001). However, in all carcharodontosaurids for which posterior dorsal vertebrae are known, the pleurocoels are seen to extend throughout the length of the column, and are present even on posterior elements. This condition is seen in *Acrocanthosaurus* (Harris 1998), *Giganotosaurus* (MUCPv-CH-1), *Mapusaurus* (Coria & Currie 2006) and *Tyrannotitan* (Novas *et al.* 2005). In *Neovenator* the pleurocoels also extend throughout the dorsal column, and are clearly present on posterior elements, including the last dorsal vertebra (Pl. 13).

Greatly enlarged pubic boot. A distal expansion of the conjoined pubes, commonly referred to as a 'pubic boot,' characterizes many theropods. The pubic boots of carcharodontosaurids are especially hypertrophied, measuring greater than 60% of the length of the pubic shaft. Such greatly enlarged pubic boots are seen in *Acrocanthosaurus* (OMNH 10146; Stovall & Langston 1950) and *Giganotosaurus* (MUCPv-CH-1). The state in other carcharodontosaurids (*Carcharodontosaurus*, *Mapusaurus*, *Tyrannotitan*) is unknown. In contrast, the pubic boots of other allosauroids (*Allosaurus*: *c.* 55%; *Sinraptor*: *c.* 30%), as well as many allosauroid outgroup taxa (e.g. *Herrerasaurus*: 45%) are much shorter. Other outgroup taxa (e.g., *Ceratosaurus*: Madsen & Welles 2000; *Coelophysis*: Colbert 1989; *Torvosaurus*: Britt 1991; compsognathids: Ostrom 1978, Peyer 2006) possess only a small distal pubic expansion. The pubic boot of *Neovenator* is greatly hypertrophied, measuring 65% of the length of the pubic shaft, a similar proportion to that of carcharodontosaurids. It is also worth noting that the enlarged pubic boot of *Allosaurus*, which is nearly as hypertrophied as those of carcharodontosaurids, is consistent with its position as the closest outgroup to Carcharodontosauridae (Brusatte & Sereno 2008).

Morphology of ischial boot. The distal end of the ischium is unexpanded or moderately expanded in most theropods, including *Allosaurus* (Madsen 1976), *Giganotosaurus* (MUCPv-CH-1), *Mapusaurus* (Coria & Currie 2006), *Sinraptor* (Currie & Zhao 1993) and *Tyrannotitan* (Novas *et al.* 2005), as well as *Monolophosaurus* (Zhao & Currie 1993) and several allosauroid outgroups (e.g. *Herrerasaurus*: Novas 1993; *Ceratosaurus*: Madsen and Welles 2000; *Coelophysis*: Colbert 1989; *Torvosaurus*: Britt 1991; compsognathids: Ostrom 1978; Currie & Chen 2001; Hwang *et al.* 2004; Peyer 2006). In contrast, the distal ischium of *Acrocanthosaurus* shows a moderately expanded boot with an anterior projection (Harris 1998). This taxon is reconstructed as lacking a boot by Stovall & Langston (1950), but this region is missing in the specimen they describe (OMNH 10146). *Neovenator* also possesses a distal boot on the ischium that is expanded anteriorly. Details of the ischial boot of *Neovenator* are clearly autapomorphic (see above), but the presence of an ischial boot with an anterior expansion may link *Neovenator* and *Acrocanthosaurus*, which is a strongly supported member of Carcharodontosauridae (Brusatte & Sereno 2008).

Dorsally inclined femoral head. A femoral head that emerges horizontally and is perpendicular to the shaft is a well-established synapomorphy of Dinosauria (Benton 2004; Langer & Benton 2006). This condition is seen in most dinosaur ingroup taxa, including the allosauroids *Allosaurus* (Madsen 1976) and *Sinraptor* (Currie & Zhao 1993), the potential allosauroid *Fukuiraptor* (Azuma & Currie 2000) and several allosauroid outgroup taxa (e.g. *Herrerasaurus*: Novas 1993; *Ceratosaurus*: Madsen & Welles 2000; *Coelophysis*: Colbert 1989; compsognathids: Currie & Chen 2001; Naish *et al.* 2004). However, a different condition is seen in carcharodontosaurids, in which the femoral head is inclined dorsally, and as a result is raised relative to the greater trochanter. This derived state is present in *Acrocanthosaurus* (OMNH 10147), *Carcharodontosaurus* (Stromer 1931), *Giganotosaurus* (MUCPv-CH-1), *Mapusaurus* (Coria & Currie 2006) and *Tyrannotitan* (Novas *et al.* 2005). This condition is also present in *Neovenator*.

Lateral distal condyle of femur highly convex and projecting distally. In most theropods the lateral and medial distal condyles of the femur are broadly convex and extend to the same level distally. This condition is present in *Acrocanthosaurus* (Harris 1998; Currie & Carpenter 2000), *Allosaurus*

(Madsen 1976) and *Sinraptor* (Currie & Zhao 1993), as well as the potential allosauroid *Fukuiraptor* (Azuma & Currie 2000) and several allosauroid outgroup taxa (e.g. *Herrerasaurus*: Novas 1993; *Ceratosaurus*: Madsen and Welles 2000; *Coelophysis*: Colbert 1989). In contrast, some carcharodontosaurids possess a highly convex lateral condyle that resembles a cone, which projects farther distally than the medial condyle. This apomorphic condition is seen in *Carcharodontosaurus* (Stromer 1931) and is also present in *Neovenator*. It may also be present in *Giganotosaurus* (P. C. Sereno, pers. comm.), although breakage on the holotype femora (MUCPv-CH-1) renders comparison difficult. Although the occurrence of the primitive condition in *Acrocanthosaurus* renders the conical and projecting condyle an equivocal synapomorphy of Carcharodontosauridae, its shared presence in *Neovenator* and more derived carcharodontosaurids is striking.

Lateral malleolus of tibia extending far distal to the medial malleolus. In most theropods the lateral malleolus of the tibia extends to the same level or only projects slightly farther distally than the medial malleolus. This is the case in the allosauroids *Allosaurus* (Madsen 1976) and *Sinraptor* (Currie & Zhao 1993), as well as several allosauroid outgroups (e.g. *Herrerasaurus*: Novas 1993; *Ceratosaurus*: Madsen and Welles 2000; *Coelophysis*: Cobert 1989; compsognathids: Hwang *et al.* 2004). However, in some carcharodontosaurids the lateral malleolus projects far distally to the level of the medial malleolus. This character can be quantified as the ratio of the length of the expansion distal to the distal end of the medial malleolus to the length of the tibia as a whole. The expansion is greater than 5% of the length of the tibia in *Acrocanthosaurus* (8%: Stovall & Langston 1950) and *Mapusaurus* (7%: Coria & Currie 2006), whereas the expansion is usually 2–3% of tibial length in other allosauroids. In *Neovenator* the expansion measures 5% of the length of the tibia. Unfortunately, tibiae are unknown for *Carcharodontosaurus* and *Tyrannotitan*, and the holotype left tibia of *Giganotosaurus* (MUCPv-CH-1) is too damaged for comparison. The condition in *Neovenator* may be intermediate between the poorly expanded lateral malleolus of basal allosauroids and the well-expanded condition of more derived carcharodontosaurids, which is consistent with the placement of *Neovenator* as a basal carcharodontosaurid.

Two additional characters, one modified and the other not used in the analysis of Brusatte & Sereno (2008), also link *Neovenator* with carcharodontosaurids.

Heavily textured facial bones. The facial bones (premaxilla, maxilla, nasal, dentary) of most theropods are generally smooth. Neurovascular foramina and tracts are often present, but deep ridges, grooves, and excresences are usually absent or restricted to the region immediately near the tooth row (Currie & Zhao 1993; Currie & Carpenter 2000). However, in abelisaurids (e.g. *Carnotaurus*: Bonaparte *et al.* 1990; *Majungasaurus*: Sampson & Witmer 2007) and carcharodontosaurids (e.g. *Carcharodontosaurus*: Sereno *et al.* 1996; Brusatte & Sereno 2007; *Giganotosaurus*: MUCPv-CH-1; *Mapusaurus*: Coria & Currie 2006) the facial bones are much more heavily textured, with rugose, mottled surfaces. The premaxilla, maxilla, and nasal of *Neovenator* are also heavily textured, more similar to the rugose condition of carcharodontosaurids than the smoother facial bones of *Acrocanthosaurus* (Currie & Carpenter 2000), *Allosaurus* (Madsen 1976) and *Sinraptor* (Currie & Zhao 1993; Gao 1998). In some cases, derived carcharodontosaurids possess more extreme texturing of certain facial elements, which can be atomized into distinct autapomorphies of *Carcharodontosaurus* (deep grooves and ridges on maxilla) and *Giganotosaurus* + *Mapusaurus* (nasal excresences). Overall, the facial texturing of *Neovenator* is not as extreme as in derived carcharodontosaurids, and may be an intermediate condition. However, the absence of extreme texturing in *Acrocanthosaurus* renders this character homoplastic, and further study of cranial bone texture, such as that outlined by Sampson & Witmer (2007) for abelisaurids, is needed for carcharodontosaurids.

Reduced nasal contribution to antorbital fossa. The nasal contributes to the antorbital fossa in most allosauroid theropods (*Allosaurus*, *Carcharodontosaurus*, *Giganotosaurus*, *Mapusaurus*, *Sinraptor*, the potential allosauroid *Monolophosaurus*), a condition not seen in other basal tetanurans but rarely in non-tetanuran theropods (e.g. *Cryolophosaurus*, *Dilophosaurus*: Smith *et al.* 2007). This

contribution is wide in *Allosaurus* (Madsen 1976), *Monolophosaurus* (Zhao & Currie 1993) and *Sinraptor* (Currie & Zhao 1993; Gao 1998) in which it is broadly visible in lateral view. A more limited nasal antorbital fossa is characteristic of carcharodontosaurids, including *Carcharodontosaurus* (SGM-Din 1), *Giganotosaurus* (MUCPv-CH-1) and *Mapusaurus* (Coria & Currie 2006). The state in other carcharodontosaurids is unknown. The polarity of these character states is unclear since outgroup taxa do not possess a nasal contribution to the fossa, but the basal position of *Sinraptor* and *Allosaurus* among allosauroids (Brusatte & Sereno 2008) suggests that a limited contribution is the derived state. In *Neovenator*, the nasal contribution to the fossa is reduced in extent similar to those of carcharodontosaurids, but much reduced compared to *Allosaurus*, *Monolophosaurus* and *Sinraptor*.

Carcharodontosaurids are also characterized by a nasal contribution to the fossa that is only visible in ventral view, which is not necessarily correlated with the reduced extent of the fossa (SGM-Din 1; MUCPv-CH-1; Coria & Currie 2006). The nasal antorbital fossa of *Neovenator* is visible in lateral view but only slightly, suggesting that this taxon may exhibit an intermediate condition between the broadly laterally exposed fossa of basal allosauroids and the ventrally restricted fossa of carcharodontosaurids. However, transverse crushing in *Neovenator* renders comparison problematical.

As is clear, *Neovenator* shares several derived character states with carcharodontosaurids to the exclusion of *Allosaurus* and *Sinraptor*. However, *Neovenator* also lacks a number of synapomorphies that unite more derived carcharodontosaurids (*Carcharodontosaurus*, *Giganotosaurus*, *Mapusaurus*). Some of these synapomorphies are seen also in *Acrocanthosaurus*, and support its placement as a carcharodontosaurid more derived than *Neovenator* but basal to the 'derived carcharodontosaurids' (herein used to refer to *Carcharodontosaurus*, *Giganotosaurus* and *Mapusaurus*).

Synapomorphies of *Acrocanthosaurus* and derived carcharodontosaurids not present in *Neovenator* include: an anteriorly squared dentary, a dentary with an anteroventral projection, anterior and posterior articular faces of the midcervical vertebrae at approximately the same level, sacral pleurocoels, medial gastral elements expanded distally into club-shaped projections, and a femur:fibula ratio of less than 0.70.

Synapomorphies of derived carcharodontosaurids not present in *Neovenator* and *Acrocanthosaurus* include: reduced recurvature of the maxillary and dentary teeth and possibly the degree of facial bone rugosity (especially in the premaxilla, maxilla, nasal, and dentary).

Somewhat equivocal synapomorphies of more derived carcharodontosaurids not present in *Neovenator* include: dorsoventrally deep interdental plates (condition uncertain in *Acrocanthosaurus*) and posterior articular faces of the mid cervicals at least 20% broader than tall (present in *Acrocanthosaurus* and *Carcharodontosaurus*, but not *Giganotosaurus*).

Based on the distribution of the aforementioned characters, as well as the numerical phylogenetic analysis of Brusatte & Sereno (2008), we regard *Neovenator salerii* as a basal carcharodontosaurid (Text-fig. 26). Most characters supporting a carcharodontosaurid affinity are axial or appendicular, and *Neovenator* lacks many cranial synapomorphies that characterize less inclusive groups within Carcharodontosauridae. These cranial characters include highly apomorphic features of the facial region, lower jaw, and dentition that are unknown in all or nearly all other theropod clades. Thus, the basal position of *Neovenator* within Carcharodontosauridae suggests that the highly apomorphic skull of this group evolved after changes to the axial and appendicular skeleton. Additionally, these postcranial changes, including increased pneumaticity throughout the axial column and several hind limb characters that may indicate a change in stance and musculature, did not necessarily evolve as a direct consequence of increasing body size, as they are present in *Neovenator*, which is much smaller (*c.* 7 m body length) than derived carcharodontosaurids (*c.* 12–14 m) and similar in size to the basal allosauroids *Allosaurus* and *Sinraptor*.

Although certainly somewhat simplistic, a literal reading of character change across allosauroid phylogeny can illuminate the major anatomical transitions within this group. Based on our current understanding of allosauroid phylogeny (Text-fig. 26), it appears as if basal carcharodontosaurids were similar in body size to *Allosaurus* and *Sinraptor* and possessed a skull

that was similar to that of *Allosaurus*, based on the shared possession of three synapomorphies (subvertical premaxilla-maxilla articulation, five teeth in the premaxilla, and a lamina lateralis of the maxilla that strongly overlaps the anteroventral corner of the antorbital fossa). Few unique carcharodontosaurid cranial characters are present in *Neovenator*, and additional cranial synapomorphies arose piecemeal throughout carcharodontosaurid evolution, culminating in the distinctive, heavily textured crania of derived carcharodontosaurids. Unfortunately, extensive missing data in several basal carcharodontosaurids preclude a more detailed node-by-node mapping of cranial synapomorphies, but it is clear that synapomorphies of the dentary (squared-off anterior end, ventral process) arose prior to certain features of cranial texturing (such as the autapomorphic texture of the maxilla and nasal in some taxa), thin and unrecurved lateral teeth, and numerous braincase characters that are only seen in *Carcharodontosaurus*, *Giganotosaurus* and *Mapusaurus* (although a braincase is unknown from this latter taxon).

In the postcranial skeleton, many carcharodontosaurid characters are already present in *Neovenator*, and these form the most important source of shared character data linking this taxon to the younger and larger derived carcharodontosaurids. However, many of these characters do not show a uniform distribution within Carcharodontosauridae, indicating that homoplasy is widespread within the group. In fact, of the eight postcranial characters linking *Neovenator* with carcharodontosaurids discussed above, only four (camellate cervicals, dorsal pleurocoels extending throughout the column, hypertrophied pubic boot, dorsally directed femoral head) are present in every carcharodontosaurid for which the pertinent region of the anatomy is preserved ('codable' taxa). The other four characters are present in some but not all carcharodontosaurids, and thus require reversals or independent acquisition within Carcharodontosauridae.

In the axial skeleton, several synapomorphies of Carcharodontosauridae and less inclusive clades relate to pneumaticity, including the presence, form, and distribution of pleurocoels in different regions of the axial column and the form of internal chambers. Multiple pleurocoels on postaxial cervical vertebrae are seen in all codable carcharodontosaurids except *Carcharodontosaurus*. The lack of this feature is most parsimoniously interpreted as a loss in this taxon, due to its derived position within carcharodontosaurid phylogeny. Pleurocoels extending throughout the dorsal column are seen in all codable carcharodontosaurids, while sacral pleurocoels and caudal pleurocoels are absent in *Neovenator* and seen only in less inclusive groups. Although missing data render any conclusion uncertain, and homoplasy in other regions of the skeleton give reason for caution, a literal reading of these characters suggests that axial pneumaticity in carcharodontosaurids advanced caudally throughout carcharodontosaurid evolution, and that more derived carcharodontosaurids lost some of these features.

In the appendicular skeleton, the shift from a medially directed femoral head in basal allosauroids to a dorsally inclined head in carcharodontosaurids (including *Neovenator*) probably involved a change in stance and possibly limb musculature. Although a more rigorous myological or biomechanical study is outside the scope of this monograph, it is possible that some of the other numerous hindlimb and pelvic synapomorphies of carcharodontosaurids may be related to a restructuring of hindlimb musculature, which in turn may have affected centre of mass, stance, gait and speed. This hypothesis deserves further study.

Biogeographical and stratigraphical implications

The interpretation of *Neovenator* as a basal carcharodontosaurid extends both the temporal and geographical ranges of this widespread clade. *Neovenator* is the oldest known member of Carcharodontosauridae, and extends the temporal range of this group into the Barremian. The existence of early Early Cretaceous carcharodontosaurids is implied by the presence of *Allosaurus*, the sister taxon to Carcharodontosauridae, in the Upper Jurassic (Kimmeridgian–Tithonian). Thus, interpretation of *Neovenator* as a basal carcharodontosaurid partially fills a major gap in the allosauroid fossil record, as previously the oldest known member of Carcharodontosauridae was the Aptian *Tyrannotitan* (Novas *et al.* 2005). Currently, a gap of about 25 million years remains between *Allosaurus* and *Neovenator*. This gap, which comprises most of the early Early Cretaceous,

is poorly sampled (Weishampel *et al.* 2004), and further fieldwork should uncover older and potentially more basal carcharodontosaurids.

Neovenator is also the first carcharodontosaurid from Europe and the only European member of this clade known from fossils other than shed teeth. Carcharodontosaurid teeth have previously been reported from Spain (Canudo & Ruiz-Omeñaca 2003) and France (Vullo *et al.* 2007), but some of these referrals are tentative and little can be said about the phylogeny, biology or evolutionary importance of these animals. With the exception of *Acrocanthosaurus* from the Aptian–Albian of North America, all other known carcharodontosaurids are from the former Gondwanan landmasses of South America and Africa (Novas *et al.* 2005; Brusatte & Sereno 2008). In contrast, basal allosauroids are known from China (*Sinraptor*, *Yangchuanosaurus*), North America (*Allosaurus*) and Europe (*Allosaurus*). The presence of a basal carcharodontosaurid in Europe not only increases the geographical range of this clade, but also suggests that carcharodontosaurids may have been major components of Early Cretaceous ecosystems in Europe, along with spinosaurids (e.g. *Baryonyx*) and possibly abelisaurids (Buffetaut *et al.* 1988; Accarie *et al.* 1995). Although yet to be discovered together in a single European fossil assemblage, this triumvirate of taxa is known from upper Lower Cretaceous units in Africa (Brusatte & Sereno 2007) and South America (Medeiros & Schultz 2002), and may represent an ecological grouping that existed for much of the Cretaceous in these regions.

Additionally, interpretation of *Neovenator* as a basal carcharodontosaurid makes it plausible (although definitely not certain) that this clade arose in Europe, and argues against the hypothesis that Carcharodontosauridae was a mostly Gondwanan group that originated in South America (Naish & Martill 2007; contra Allain 2002; Novas *et al.* 2005). A literal reading of the currently known fossil record and phylogeny of Allosauroidea suggests that carcharodontosaurids became restricted to Gondwana later in their evolution, as the derived carcharodontosaurids *Carcharodontosaurus*, *Giganotosaurus* and *Mapusaurus* are known only from Africa and South America. While intense sampling renders the presence of Late Cretaceous carcharodontosaurids highly unlikely in North America, the absence of this clade in post-Barremian units in Europe may be an artefact of poor sampling. Finally, the identification of European and North American carcharodontosaurids weakens Allain's (2002) hypothesis that Middle–Late Jurassic theropod faunas were characterized by marked provincialism, with unique Asian (Sinraptoridae), Laurasian (Allosauridae, including *Acrocanthosaurus* and *Neovenator*), and Gondwanan (Carcharodontosauridae) allosauroid subgroups.

Comparison with other Wealden Group theropods

Several other theropods are known from the Wealden Group of England, including potential allosauroids. However, none of these other taxa is synonymous with *Neovenator*. Although based on fragmentary material, the potential allosauroids *Becklespinax altispinax* (BMNH R1828) and *Valdoraptor oweni* (BMNH R2559) are both diagnosed by autapomorphies that are demonstrably absent on elements represented in the holotype and referred specimens of *Neovenator*. These autapomorphies, which include the tall and robust neural spines of *Becklespinax* and the short metatarsus with a mediolaterally compressed metatarsal II of *Valdoraptor*, are absent in *Neovenator* (Naish & Martill 2007). Naish (2003) described an isolated tibia from the Hastings Beds Group (HASMG G.378) that probably belongs to an allosauroid but is clearly different from *Neovenator*. This tibia may be referable to *Becklespinax* (Naish 2003; Naish & Martill 2007), but such a conclusion is difficult to evaluate since the holotype of this taxon consists of only three articulated dorsal vertebrae, and the tibia was found unassociated with additional material. As the holotype dorsal vertebrae of *Becklespinax* are highly autapomorphic, additional material of this taxon should be recognizable, and future discoveries may shed light on the skeletal anatomy of this taxon.

Several non-allosauroid theropods are also known from the Wealden Group, and include the spinosaurid *Baryonyx* (BMNH R9951; Charig & Milner 1986, 1997; Martill & Hutt 1996; Hutt & Newbery 2004), the basal tyrannosauroid *Eotyrannus* (IWCMS 1997.550; Hutt *et al.* 2001), the compsognathid *Aristosuchus* (BMNH R178; Owen 1876; Naish *et al.* 2001), and the indeterminate coelurosaurs *Calamospondylus* (Fox, *in* Anon. 1866), *Calamosaurus* (BMNH R901; Lydekker 1881),

Ornithodesmus (BMNH R178; Seeley 1887; Howse & Milner 1993), and *Thecocoelurus* (BMNH R181; von Huene 1923; Naish & Martill 2002). All of these taxa are known from regions of the skeleton that overlap with *Neovenator*, and the presence of autapomorphies not seen in *Neovenator*, the lack of *Neovenator* autapomorphies, and overall morphological and size differences with *Neovenator* clearly show that none of these theropods represents the same taxon as *Neovenator*. Additionally, among this assemblage of theropods, only *Baryonyx* and possibly *Eotyrannus* (Naish, pers. comm.) are of a similar body size to *Neovenator*, and the others represent much smaller coelurosaurs. Unfortunately, most taxa are based on fragmentary remains that often include only one or a few fragments of the skeleton, thus obscuring information on the anatomy, phylogeny, and ecology of these animals. Therefore, speculation on the taxonomic and ecological composition of theropod faunas in the Wealden Group is currently premature, but it is apparent that at least two (and possibly three) large bodied theropods (*Neovenator*, *Baryonyx*, *Eotyrannus*) occurred together (Hutt & Newbery 2004).

It is worth noting that diagnostic remains of *Neovenator* are currently known only from the Isle of Wight, and have not yet been discovered in the Wealden Group on the mainland of England. As autapomorphies are known from all regions of the skeleton, recognizing even fragmentary remains of *Neovenator* should be possible. Although the lack of specimens from the mainland may be an artefact of sampling, the fact that intense collection within the Wealden Group over the past century and half has yet to yield additional specimens is noteworthy. This may indicate that *Neovenator*, as well as other theropod taxa also known from few specimens, were rare components of Wealden faunas, at least compared to herbivorous taxa such as *Hypsilophodon*, *Iguanodon* and *Polacanthus* that are represented by numerous specimens (Hutt 2001). Such a discrepancy between herbivorous and predatory taxa is not unexpected, but collecting records alone indicate that theropods were especially rare in the Wealden.

Pathologies of *Neovenator*

Several pathological features are present across the skeleton of *Neovenator*, including bony calluses, exostotic bone growth (formation of new bone on the surface of an element), vertebral fusion, and possibly healed fractures (Text-fig. 27). As the pathologies of *Neovenator* are the subject of a separate study (by Naish, Cooper & Martill), we do not fully describe these features here. However, below is a brief list and description of the most noticeable pathological features (all of which are known from the holotype skeleton MIWG 6348/BMNH R10001), as well as comments on their likely sources and comparison with well-studied pathologies in the closely related *Allosaurus* (Petersen *et al.* 1972; Chure 2000; Hanna 2002).

In the axial skeleton, pathologies are present on several vertebrae, ribs, chevrons and gastralia. One cervical vertebra exhibits a crushed ventral surface that does not appear to be the result of deformation during fossilization. In the caudal series, vertebra I is marked by a fractured transverse process, vertebra K exhibits a pathological depression on the right side of the centrum, and vertebra O has a posterior face covered with exostotic bone growth, which is especially prevalent around the margins. The most noticeable pathology in the caudal series involves vertebrae L and M and their associated chevron, which are fused together into a single mass. A similar condition has been noted in *Allosaurus*, which Petersen *et al.* (1972) ascribed to neoplastic ankylosis (fusion of multiple elements by new, abnormal bone formation). Hanna (2002) also noted several instances of fused caudal vertebrae in *Allosaurus*. Additionally, one fragment of a dorsal rib shaft of *Neovenator* exhibits an enlarged rugose callus, similar to injuries reported in *Allosaurus* (Hanna 2002). The gastral basket of *Neovenator* is characterized by abundant pathologies, including one element with a bulbous callus at midlength, one with an expanded and rugose distal end, and another with evidence of bone damage and regrowth across its entire length. Similar gastral pathologies have been described in *Allosaurus* (Chure 2000; Hanna 2002), and are thought to indicate traumatic injuries such as falls or defensive blows by prey species.

In the appendicular skeleton, pathologies are seen on the scapula, tibia, fibula, and a pedal phalanx. The medial surface of the dorsal margin of the scapular blade is marked by a rugose raised area approximately one third of the distance posteriorly along the element. Scapular

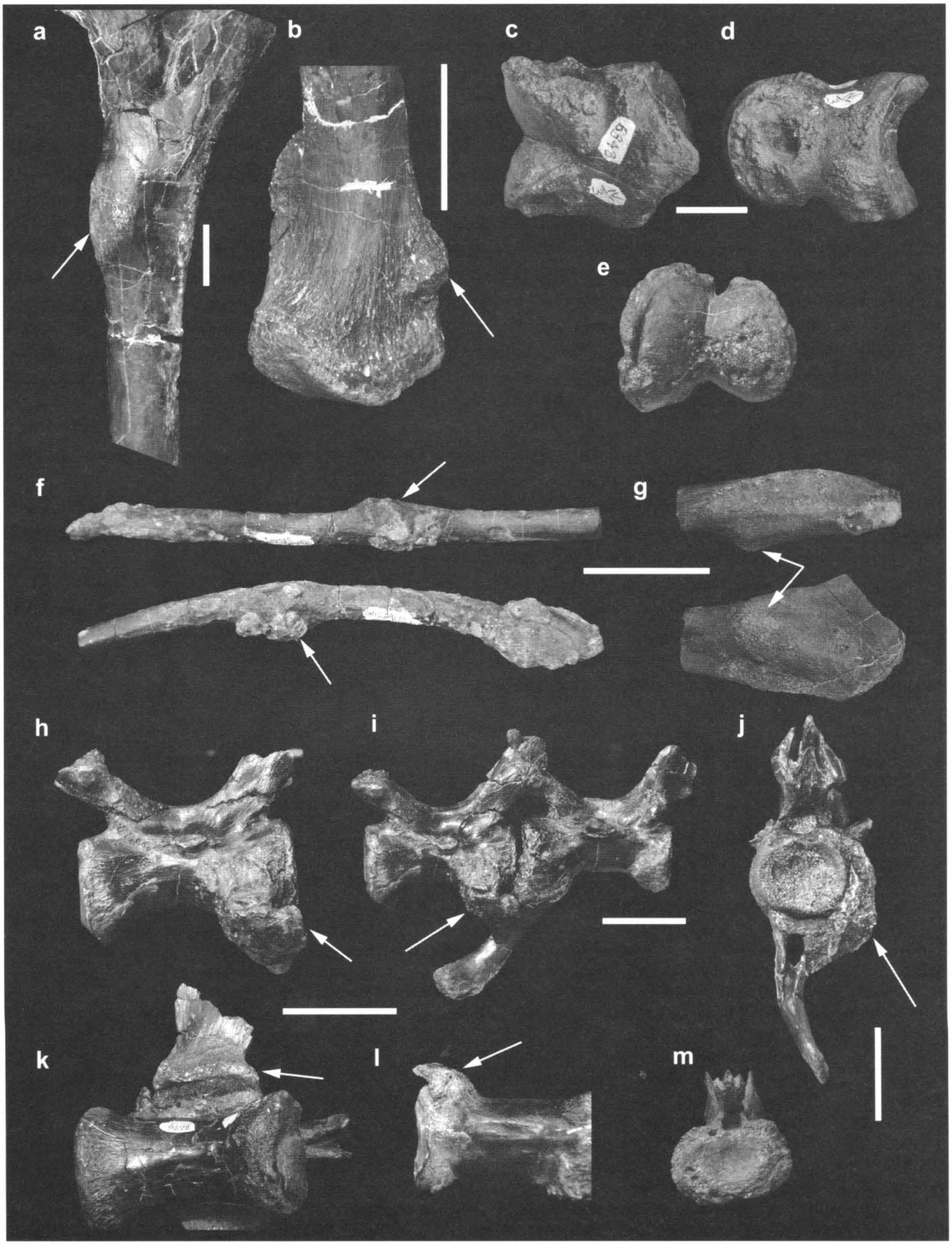

TEXT-FIG. 27. *Neovenator salerii* Hutt, Martill & Barker, 1996; pathologies (MIWG 6348). **a**, left tibia in medial view; **b**, left fibula in anterior view; **c**, left phalanx IV-3 in extensor view; **d**, left phalanx IV-3 in lateral view; **e**, left phalanx IV-3 in distal view; **f**, gastralia; **g**, dorsal rib shaft fragment; **h**, caudal vertebra L in left lateral view; **i**, caudal vertebrae L and M in left lateral view; **j**, caudal vertebrae L and M in anterior view; **k**, caudal vertebra I in ventral view; **l**, caudal vertebra K in ventral view; **m**, caudal vertebra O in posterior view. Scale bars represent 50 mm. Arrows indicate pathologies.

pathologies have been described in *Allosaurus*, but these are small depressions that occur on the lateral surface of the plate-like anterior region of the bone (Hanna 2002). In the hind limb, the tibia sports one of the most noticeable pathologies on the skeleton: an enlarged bulbous swelling on the posterior surface of the shaft. This was originally regarded as a potentially unique character of *Neovenator* by Hutt *et al.* (1996) but reinterpreted by Hutt (1999) as a pathology, a conclusion supported here. The lateral surface of the distal end of the fibula is marked by a rugose knob *c.* 20 mm dorsal to the smooth articular surface for the astragalus and calcaneum. Finally, one of the most extensive pathologies is seen on left pedal phalanx IV-3. This element is almost completely covered by exostotic bone growth, which is punctured by randomly positioned small lesions. Compared to the non-pathological right IV-3, this element is wider and shorter, with slightly expanded proximal and distal ends. Notably, although this exostoic bone growth has completely enveloped this phalanx there are no signs of exostosis or other pathologies on adjacent phalanges. Exostotic bone growth on the pedal phalanges is present in one specimen of *Allosaurus* (Hanna 2002), but in this element the proximal articular surface is greatly expanded and the distal surface is unaffected. However, the rugose, irregular texture and small lesions of the *Allosaurus* phalanx are similar to the condition in *Neovenator*, and suggest a bone infection such as osteomyelitis.

Pathologies are not evident on any of the skull bones. This suggests that *Neovenator* may not have engaged in intraspecific agonistic behaviour such as that reported in the allosauroid *Sinraptor*, tyrannosaurids and other large theropods (Tanke & Currie 2000). Such behaviour is apparently also absent in *Allosaurus* (Tanke & Currie 2000), but a larger sample size is needed to assess more confidently possible agonistic activity in *Neovenator*.

The presence of so many pathologies across the skeleton of *Neovenator* begs the question of whether trauma, infection, or some other injury caused the death of MIWG 6348/BMNH R10001. This question is difficult to answer, as it is not apparent exactly what types and even how many separate injuries this individual suffered. We leave further interpretation of the pathologies to the detailed study of Naish, Cooper & Martill.

REFERENCES

ACCARIE, H., BEAUDOIN, B., DEJAZ, J., FRIÈS, G., MICHARD, J.-G. & TAQUET, P. 1995. Découverte d'un dinosaure théropode nouveau (*Genusaurus sisteronis* n. g., n. sp.) dans l'Albien marin de Sisteron (Alpes de Haute-Provence, France) et extension au Crétacé inférieur de la lignée cératosaurienne. *Compte Rendus de l'Academie des Sciences, Paris, Série IIa*, **320**, 327–334.

ALCOBER, O., SERENO, P. C., LARSSON, H. C. E., MARTINEZ, R. & VARRICCHIO, D. 1998. A Late Cretaceous carcharodontosaurid (Theropoda: Allosauroidea) from Argentina. *Journal of Vertebrate Paleontology*, **15**, 16A.

ALLAIN, R. 2001. Redescription de *Streptospondylus altdorfensis*, le dinosaure théropode de Cuvier, du Jurassique de Normandie. *Geodiversitas*, **23**, 349–367.

—— 2002. Discovery of megalosaur (Dinosauria, Theropoda) in the middle Bathonian of Normandy (France) and its implications for the phylogeny of basal Tetanurae. *Journal of Vertebrate Paleontology*, **22**, 548–563.

ALLEN, P. 1975. Wealden of the Weald: a new model. *Proceedings of the Geologists' Association*, **86**, 389–437, 3 pls.

—— 1981. Pursuit of Wealden models. *Journal of the Geological Society of London*, **138**, 375–405.

—— 1998. Purbeck–Wealden (early Cretaceous) climates. *Proceedings of the Geologists' Association*, **109**, 197–236.

BENSON, R. B. J., BARRETT, P. M., POWELL, H. P. & NORMAN, D. B. 2008. The taxonomic status of *Megalosaurus bucklandii* (Dinosauria, Theropoda) from the Middle Jurassic of Oxfordshire, UK. *Palaeontology*, **51**, 419–424.

BENTON, M. J. 2004. Origin and relationships of Dinosauria. Pp. 7–19. *In* WEISHAMPEL, D. B., DODSON, P. & OSMOLSKA, H. (Eds). *The Dinosauria* (2nd edition). University of California Press, Berkeley, California.

BONAPARTE, J. F., NOVAS, F. E. & CORIA, R. A. 1990. *Carnotaurus sastrei* Bonaparte, the horned, lightly built carnosaur from the Middle Cretaceous of Patagonia. *Contributions in Science, Natural History Museum of Los Angeles County*, **416**, 1–41.

BRITT, B. B. 1991. Theropods of Dry Mesa Quarry (Morrison Formation, Late Jurassic), Colorado, with emphasis on the osteology of *Torvosaurus tanneri*. *Brigham Young University Geology Studies*, **37**, 1–72.

[—— 1993. *Pneumatic postcranial bones in dinosaurs and other archosaurs*. Unpublished Ph.D. Thesis, University of Calgary.]

BROCHU, C. A. 2002. Osteology of *Tyrannosaurus rex*: insights from a nearly complete skeleton and high-resolution computed tomographic analysis of the skull. *Society of Vertebrate Paleontology Memoir*, **7**, 1–138.

BRUSATTE, S. L. BENSON, R. B. J., CARR, T. D., WILLIAMSON, T. E. & SERENO, P. C. 2007. The systematic utility of theropod enamel wrinkles. *Journal of Vertebrate Paleontology*, **24**, 1052–1056.

—— & SERENO, P. 2006. Basal abelisaurid and carcharodontosaurid theropods from the Elrhaz Formation (Aptian–Albian) of Niger. *Journal of Vertebrate Paleontology*, **26**(3), 46A.

—— & —— 2007. A new species of *Carcharodontosaurus* (Dinosauria: Theropoda) from the Cenomanian of Niger and a revision of the genus. *Journal of Vertebrate Paleontology*, **24**, 902–916.

—— & —— 2008. Phylogeny of Allosauroidea (Dinosauria: Theropoda): comparative analysis and resolution. *Journal of Systematic Palaeontology*, **6**, 155–182.

BUFFETAUT, E., SUTEETHORN, V. & TONG, H. 1996. The earliest known tyrannosaur from the Lower Cretaceous of Thailand. *Nature*, **381**, 689–691.

——, MECHIN, P. & MECHIN-SALESSY, A. 1988. Un dinosaure théropode d'affinités gondwaniennes dans le Crétacé supérieur de Provence. *Comptes Rendus de l'Academie des Sciences Paris, Série II*, **306**, 153–158.

CALVO, J. O. & CORIA, R. 2000. New specimen of *Giganotosaurus carolinii* (Coria & Salgado, 1995), supports it as the largest theropod ever found. *Gaia*, **15**, 117–122.

——, PORFIRI, J. D., VERALLI, C., NOVAS, F. & POBLETE, F. 2004. Phylogenetic status of *Megaraptor namunhuaiquii* Novas based on a new specimen from Neuquén, Patagonia, Argentina. *Ameghiniana*, **41**, 565–575.

CANUDO, J. I. & RUIZ-OMEÑACA, J. I. 2003. Los restos directos de dinosaurios terópodos (excluyendo Aves) en España. Pp. 347–374. *In* PÉREZ-LORENTE, F. (Ed.). *Dinosaurios y otros reptiles Mesozoicos en España*. Instituto de Estudios Riojanos, Logroño.

CARR, T. D., WILLIAMSON, T. E. & SCHWIMMER, D. R. 2005. A new genus and species of tyrannosauroid from the Late Cretaceous (Middle Campanian) Demopolis Formation of Alabama. *Journal of Vertebrate Paleontology*, **25**, 119–143.

CARRANO, M. T., SAMPSON, S. D. & FORSTER, C. A. 2002. The osteology of *Masiakasaurus knopfleri*, a small abelisauroid (Dinosauria: Theropoda) from the Late Cretaceous of Madagascar. *Journal of Vertebrate Paleontology*, **22**, 510–534.

CHARIG, A. J. & MILNER, A. C. 1986. *Baryonyx*, a remarkable new theropod dinosaur. *Nature*, **324**, 359–361.

—— & —— 1997. *Baryonyx walkeri*, a fish-eating dinosaur from the Wealden of Surrey. *Bulletin of the Natural History Museum, Geology Series*, **53**, 11–70.

[CHURE, D. J. 2000. *A new species of* Allosaurus *from the Morrison Formation of Dinosaur National Monument (UT-CO) and a revision of the theropod family Allosauridae*. Unpublished Ph.D. thesis, Columbia University, New York.]

CLAESSENS, L. P. A. M. 2004. Dinosaur gastralia: origin, morphology, and function. *Journal of Vertebrate Paleontology*, **24**, 89–106.

CORIA, R. A. & CURRIE, P. J. 2006. A new carcharodontosaurid (Dinosauria, Theropoda) from the Upper Cretaceous of Argentina. *Geodiversitas*, **28**, 71–118.

—— & SALGADO, L. 1995. A new giant carnivorous dinosaur from the Cretaceous of Patagonia. *Nature*, **377**, 224–226.

CURRIE, P. J. & AZUMA, Y. 2006. New specimens, including a growth series, of *Fukuiraptor* (Dinosauria, Theropoda) from the Lower Cretaceous Kitadani Quarry of Japan. *Journal of the Paleontological Society of Korea*, **22**, 173–193.

—— & CARPENTER, K. 2000. A new specimen of *Acrocanthosaurus atokensis* (Theropoda, Dinosauria) from the Lower Cretaceous Antlers Formation (Lower Cretaceous, Aptian) of Oklahoma, USA. *Geodiversitas*, **22**, 207–246.

—— & CHEN, P.-J. 2001. Anatomy of *Sinosauropteryx prima* from Liaoning, northeastern China. *Canadian Journal of Earth Sciences*, **38**, 1705–1727.

—— & ZHAO, X.-J. 1993. A new large theropod (Dinosauria, Theropoda) from the Jurassic of Xinjiang, People's Republic of China. *Canadian Journal of Earth Sciences*, **30**, 2037–2081.

EDMUND, A. G. 1960. Tooth replacement phenomena in lower vertebrates. *Royal Ontario Museum, Life Science Division, Contributions*, **52**, 1–190.

EZCURRA, M. D. 2007. The cranial anatomy of the coelophysoid theropod *Zupaysaurus rougieri* from the Upper Triassic of Argentina. *Historical Biology*, **19**, 185–202.

FOX, W. IN ANON. 1866. Another Wealden reptile. *Athenaeum*, **2014**, 740.

GALLOIS, R. W. 1965. *British regional geology. The Wealden distict*. Geological Survey and Museum. xii + 101 pp, 12 pls. H.M.S.O., London.

GAO, Y. 1998. *Complete carnosaur skeleton from Zigong, Sichuan* Yangchuanosaurus hepingensis. 100 pp., Zigong Dinosaur Museum.

GAUTHIER, J. 1986. Saurischian monophyly and the origin of birds. *Memoirs of the California Academy of Sciences*, **8**, 1–55.

GILMORE, C. W. 1920. Osteology of the carnivorous Dinosauria in the United States National Museum, with special reference to the genera *Antrodemus* (*Allosaurus*) and *Ceratosaurus*. *Bulletin of the United States National Museum*, **110**, 1–154.

GRADSTEIN, F., OGG, J. & SMITH A. 2004. *A geologic time scale 2004*. Cambridge University Press, Cambridge.

HANNA, R. R. 2002. Multiple injury and infection in a sub-adult theropod dinosaur *Allosaurus fragilis* with comparisons to allosaur pathology in the Cleveland-Lloyd Dinosaur Quarry collection. *Journal of Vertebrate Paleontology*, **22**, 76–90.

HARRIS, J. D. 1998. A reanalysis of *Acrocanthosaurus atokensis*, its phylogenetic status, and paleobiogeographic implications, based on a new specimen from Texas. *New Mexico Museum of Natural History and Science Bulletin*, **13**, 1–75.

HOLTZ, T. R. 2001. The phylogeny and taxonomy of the Tyrannosauridae. Pp. 64–83. *In* CARPENTER, K. & TANKE, D. (Eds). *Mesozoic vertebrate life*. Indiana University Press, Bloomington, Indiana.

——, MOLNAR, R. E. & CURRIE, P. J. 2004. Basal Tetanurae. Pp. 71–110. *In* WEISHAMPEL, D. B., DODSON, P. & OSMOLSKA, H. (Eds). *The Dinosauria* (2nd edition). University of California Press, Berkeley, California.

HOWSE, S. C. B. & MILNER, A. C. 1993. *Ornithodesmus* – a maniraptoran theropod dinosaur from the Lower Cretaceous of the Isle of Wight, England. *Palaeontology*, **36**, 425–438.

HUENE, F. VON 1923. Carnivorous Saurischia in Europe since the Triassic. *Bulletin of the Geological Society of America*, **34**, 449–458.

HUGHES, N. F. & MCDOUGALL, A. B. 1989. New Wealden correlation for the Wessex Basin. *Proceedings of the Geologists' Association*, **100**, 85–90.

HUTCHINSON, J. R. 2001. The evolution of pelvic osteology and soft tissues on the line to extant birds (Neornithes). *Zoological Journal of the Linnean Society*, **131**, 123–168.

[HUTT, S. 1999. Neovenator salerii: *a new theropod dinosaur from the Wealden of the Isle of Wight: its status and significance for theropod evolution.* Unpublished M.Phil. thesis, University of Portsmouth.]

—— 2001. Appendix: catalogue of Wealden Group Dinosauria in the Museum of Isle of Wight Geology. Pp. 411–422. *In* MARTILL, D. M. & NAISH, D. (Eds). *Dinosaurs of the Isle of Wight*. Palaeontological Association Field Guides to Fossils, **10**. 433 pp., London.

——, MARTILL, D. M. & BARKER, M. J. 1996. The first European allosaurid dinosaur (Lower Cretaceous, Wealden Group, England). *Neues Jahrbuch für Geologie und Paläontologie, Monatshefte*, **1996**, 635–644.

——, NAISH, D. W., MARTILL, D. M., BARKER, M. J. & NEWBERY, P. 2001. A preliminary account of a new tyrannosauroid theropod from the Wessex Formation (Early Cretaceous) of southern England. *Cretaceous Research*, **22**, 227–242.

—— & NEWBERY, P. 2004. An exceptional theropod vertebra from the Wessex Formation (Lower Cretaceous), Isle of Wight, England. *Proceedings of the Isle of Wight Natural History and Archaeological Society*, **20**, 61–76.

——, SIMMONDS, K. & HULLMAN, G. 1990. Predatory dinosaurs from the Isle of Wight. *Proceedings of the Isle of Wight Natural History and Archaeological Society*, **9**,137–146.

HWANG, S. H., NORELL, M. A., JI, Q. & GAO, K. 2004. A large compsognathid from the Early Cretaceous Yixian Formation of China. *Journal of Systematic Palaeontology*, **2**, 13–30.

INSOLE, A. N. & HUTT, S. 1994. Palaeoecology of the dinosaurs of the Wessex Formation (Wealden Group, Early Cretaceous), Isle of Wight, southern England. *Zoological Journal of the Linnean Society*, **112**, 197–215.

IRMIS, R. 2007. Axial skeleton ontogeny in the Parasuchia (Archosauria: Pseudosuchia) and its implications for ontogenetic determination in archosaurs. *Journal of Vertebrate Paleontology*, **27**, 350–361.

LAMANNA, M. C., MARTINEZ, R. D. & SMITH, J. B. 2002. A definitive abelisaurid theropod dinosaur from the Early Cretaceous of Patagonia. *Journal of Vertebrate Paleontology*, **22**, 58–69.

LANGER, M. C. & BENTON, M. J. 2006. Early dinosaurs: a phylogenetic study. *Journal of Systematic Palaeontology*, **4**, 309–358.

LYDEKKER, R. 1891. On certain ornithosaurian and dinosaurian remains. *Quarterly Journal of the Geological Society of London*, **47**, 41–44.

MADSEN, J. H. 1976. *Allosaurus fragilis*: a revised osteology. *Utah Geological Survey Bulletin*, **109**, 1–163.

—— & WELLES, S. P. 2000. *Ceratosaurus* (Dinosauria, Theropoda) a revised osteology. *Utah Geological Survey Miscellaneous Publication*, **00-2**, 1–80.

MANTELL, G. A. 1825. Notice on the *Iguanodon*, a newly discovered fossil reptile, from the sandstone of Tilgate Forest. *Philosophical Transactions of the Royal Society of London*, **115**, 179–186.

—— 1841. Memoir on a portion of the lower jaw of the *Iguanodon*, and on the remains of the *Hylaeosaurus* and other saurians, discovered in the strata of Tilgate Forest, in Sussex. *Philosophical Transactions of the Royal Society of London*, **131**, 131–151.

—— 1848. On the structure of the jaws and teeth of the *Iguanodon*. *Philosophical Transactions of the Royal Society of London*, **138**, 183–202.

—— 1849. Additional observations on the osteology of the *Iguanodon* and *Hylaeosaurus*. *Philosophical Transactions of the Royal Society of London*, **139**, 271–305.

MARSH, O. C. 1878. Principal characters of American Jurassic dinosaurs. Pt. 1. *American Journal of Science, Series 3*, **16**, 411–416.

—— 1881. Principal characters of American Jurassic dinosaurs. Part V. *American Journal of Science, Series 3*, **21**, 417–423.

MARTILL, D. M. & HUTT, S. 1996. Possible baryonychid teeth from the Wessex Formation (Lower Cretaceous, Barremian) of the Isle of Wight, England. *Proceedings of the Geologists' Association*, **107**, 81–84.

—— & NAISH, D. 2001. The geology of the Isle of Wight. Pp. 25–43. *In* MARTILL, D. M. & NAISH, D. (Eds). *Dinosaurs of the Isle of Wight*. Palaeontological Association Field Guides to Fossils, **10**. 433 pp, London.

——, —— & HUTT, S. 2001. Introduction. Pp. 11–24. *In* MARTILL, D. M. & NAISH, D. (Eds). *Dinosaurs of the Isle of Wight*. Palaeontological Association Field Guides to Fossils, **10**. 433 pp, London.

MARTIN, P. J. 1828. *A geological memoir on a part of West Sussex*. London.

MATEUS, O. 1998. *Lourinhanosaurus antunesi*, a new Upper Jurassic allosauroid (Dinosauria: Theropoda) from Lourinhã (Portugal). *Memórias da Academia de Ciências de Lisboa*, **37**, 111–124.

MEDEIROS, M. A. & SCHULTZ, C.L. 2002. A fauna dinossauriana da "Laje do Coringa", Cretáceo médio do nordeste do Brasil. *Arquivos do Museu Nacional, Rio de Janeiro*, **60**, 155–162.

NAISH, D. 2003. A definitive allosauroid (Dinosauria; Theropoda) from the Lower Cretaceous of East Sussex. *Proceedings of the Geologists' Association*, **114**, 319–326.

——, HUTT, S. & MARTILL, D. M. 2001. Saurischian dinosaurs 2: theropods. Pp. 242–309. *In* MARTILL, D. M. & NAISH, D. (Eds). *Dinosaurs of the Isle of Wight*. Palaeontological Association Field Guides to Fossils, **10**. 433 pp, London.

—— & MARTILL, D. M. 2002. A reappraisal of *Thecocoelurus daviesi* (Dinosauria: Theropoda) from the Early Cretaceous of the Isle of Wight. *Proceedings of the Geologists' Association*, **113**, 23–30.

—— & —— 2007. Dinosaurs of Great Britain and the role of the Geological Society of London in their discovery: basal Dinosauria and Saurischia. *Journal of the Geological Society, London*, **164**, 493–510.

——, —— & FREY, E. 2004. Ecology, systematics, and biogeographical relationships of dinosaurs, including a new theropod, from the Santana Formation (?Albian, Early Cretaceous) of Brazil. *Historical Biology*, **16**, 57–70.

NORELL, M. A. & HWANG, S. H. 2004. A troodontid dinosaur from Ukhaa Tolgod (Late Cretaceous Mongolia). *American Museum Novitates*, **3446**, 1–9.

NOVAS, F. E. 1993. New information on the systematics and postcranial skeleton of *Herrerasaurus ischigualastensis* (Theropoda: Herrerasauridae) from the Ischigualasto Formation (Upper Triassic) of Argentina. *Journal of Vertebrate Paleontology*, **13**, 400–423.

——, VALAIS, S. DE, VICKERS-RICH, P., & RICH, T. 2005. A large Cretaceous theropod from Patagonia, Argentina, and the evolution of carcharodontosaurids. *Naturwissenschaften*, **92**, 226–230.

O'CONNOR, P. M. 2007. The postcranial axial skeleton of *Majungasaurus crenatissimus* (Theropoda: Abelisauridae) from the Late Cretaceous of Madagascar. Pp. 127–162. *In* SAMPSON, S. D. & KRAUSE, D. W. (Eds). *Majungasaurus crenatissimus* (Theropoda: Abelisauridae) from the Late Cretaceous of Madagascar. *Society of Vertebrate Paleontology Memoir*, **8**, 1–184.

OSTROM, J. H. 1978. The osteology of *Compsognathus longipes* Wagner. *Zitteliana*, **4**, 73–118.

OWEN, R. 1842. Report on British fossil reptiles. *Report of the British Association for the Advancement of Science*, **11** (1841), 60–294.

—— 1858. Monograph on the fossil Reptilia of the Wealden and Purbeck formations. Pt. IV. Dinosauria (*Hylaeosaurus*) [Wealden]. *Monograph of the Palaeontographical Society*: 8–26, pls 4–11. (Publ. No. 43, part of Vol. 10 for 1856).

—— 1859. Monograph on the fossil Reptilia of the Wealden and Purbeck formations. Supplement No. 2. Crocodilia (*Streptospondylus*, & c.). *Monograph of the Palaeontographical Society*: 20–44, pls 5–12. (Publ. No. 48, part of Vol. 11 for 1857).

—— 1864. Monograph on the fossil Reptilia of the Wealden and Purbeck formations. Supplement No. 3. Dinosauria (*Iguanodon*) [Wealden]. *Monograph of the Palaeontographical Society*: 19–21, pl. 10. (Publ. No. 71, part of Vol. 16 for 1862).

—— 1876. Monograph of the fossil Reptilia of the Wealden and Purbeck formations. Supplement No. 7. Crocodilia (*Poekilopleuron*), Dinosauria (*Chondrosteosaurus*). *Monograph of the Palaeontographical Society*: 1–7, pls 1–6. (Publ. No. 136, part of Vol. 30 for 1876).

PAUL, G. S. 2007. Turning the old into the new: a separate genus for the gracile iguanodont from the Wealden of England. Pp. 69–77. *In* CARPENTER, K. (Ed.). *Horns and beaks: ceratopsian and ornithopod dinosaurs*. Indiana University Press, Bloomington.

PETERSEN, K., ISAKON, J. I. & MADSEN, JR, J. H. 1972. Preliminary study of paleopathologies in the Cleveland-Lloyd dinosaur collection. *Utah Academy Proceedings*, **49**, 44–47.

PEYER, K. 2006. A reconsideration of *Compsognathus* from the Upper Tithonian of Canjuers, southeastern France. *Journal of Vertebrate Paleontology*, **26**, 879–896.

RADLEY, J. D. 2004. Demystifying the Wealden of the Weald (Lower Cretaceous, south-east England). *OUGS Journal*, **25**, 6–16.

—— 2006a. A Wealden guide I: the Weald sub-basin. *Geology Today*, **22**(3), 109–118.

—— 2006b. A Wealden guide II: the Wessex sub-basin. *Geology Today*, **22**(5), 187–193.

—— & BARKER, M. J. 1998. Stratigraphy, palaeontology and correlation of the Vectis Formation (Wealden Group, Lower Cretaceous) at Compton Bay, Isle of Wight, southern England. *Proceedings of the Geologists' Association*, **105**, 187–196.

RAUHUT, O. W. M. 2003. The interrelationships and evolution of basal theropod dinosaurs. *Special Papers in Palaeontology*, **69**, 1–213.

—— 2005. Osteology and relationships of a new theropod dinosaur from the Middle Jurassic of Patagonia. *Palaeontology*, **48**, 87–110.

RAWSON, P. F., CURRY, D., DILLEY, F. C., HANCOCK, J. M., KENNEDY, W. J., NEALE, J. W., WOOD, C. J. & WORSSAM, B. C. 1978. *A correlation of Cretaceous rocks in the British Isles*. Geological Society of London, Special Report, **9**, 1–70.

SAMPSON, S. D. & WITMER, L. M. 2007. Craniofacial anatomy of *Majungasaurus crenatissimus* (Theropoda: Abelisauridae) from the Late Cretaceous of Madagascar. Pp. 32–102. *In* SAMPSON, S. D. & KRAUSE, D. W. (Eds). *Majungasaurus crenatissimus* (Theropoda: Abelisauridae) from the Late Cretaceous of Madagascar. *Society of Vertebrate Paleontology Memoir*, **8**, 1–184.

SEELEY, H. G. 1887. On a sacrum apparently indicating a new type of bird, *Ornithodesmus cluniculus* Seeley. *Quarterly Journal of the Geological Society of London*, **43**, 206–211.

—— 1888. On the classification of the fossil animals commonly named Dinosauria. *Proceedings of the Royal Society of London*, **43**, 165–171.

SERENO, P.C. 1991. Basal archosaurs: phylogenetic relationships and functional implications. *Society of Vertebrate Paleontology Memoir*, **2**, 1–53.

—— 1998. A rationale for phylogenetic definitions, with application to the higher-level phylogeny of Dinosauria. *Neues Jahrbuch für Geologie und Paläontologie Abhandlungen*, **210**, 41–83.

——, BECK, A. L., DUTHEIL, D. B., GADO, B., LARSSON, H. C. E., LYON, G. H., MARCOT, J. D., RAUHUT, O. W. M., SADLEIR, R. W., SIDOR, C. A., VARRICCHIO, D. J., WILSON, G. P. & WILSON, J. A. 1998. A long-snouted predatory dinosaur from Africa and the evolution of spinosaurids. *Science*, **282**, 1298–1302.

—— & BRUSATTE, S. L. 2008. Basal abelisaurid and carcharodontosaurid theropods from the Lower Cretaceous Elrhaz Formation of Niger. *Acta Palaeontologica Polonica*, **53**, 15–46.

——, DUTHEIL, D. B., IAROCHENE, M., LARSSON, H. C. E., LYON, G. H., MAGWENE, P. M., SIDOR, C. A., VARRICCHIO, D. J. & WILSON, J. A. 1996. Predatory dinosaurs from the Sahara and Late Cretaceous faunal differentiation. *Science*, **272**, 986–991.

——, MCALLISTER, S. & BRUSATTE, S. L. 2005. TaxonSearch: a relational database for suprageneric taxa and phylogenetic definitions. *PhyloInformatics*, **8**, 1–21.

—— & NOVAS, F. E. 1993. The skull and neck of the basal theropod *Herrerasaurus ischigualastensis*. *Journal of Vertebrate Paleontology*, **13**, 451–476.

——, WILSON, J. A. & CONRAD, J. L. 2004. New dinosaurs link southern landmasses in the Mid-Cretaceous. *Proceedings of the Royal Society, Series B*, **271**, 1325–1330.

——, ——, LARSSON, H. C .E., DUTHEIL, D. B. & SUES, H.- D. 1994. Early Cretaceous dinosaurs from the Sahara. *Science*, **266**, 267–271.

SMITH, J. B. 2007. Dental morphology and variation in *Majungasaurus crenatissimus* (Theropoda: Abelisauridae) from the Late Cretaceous of Madagascar. Pp. 103–126. *In* SAMPSON, S. D. & KRAUSE, D. W. (Eds). *Majungasaurus crenatissimus* (Theropoda: Abelisauridae) from the Late Cretaceous of Madagascar. *Society of Vertebrate Paleontology Memoir*, **8**, 1–184.

SMITH, N. D., MAKOVICKY, P. J., HAMMER, W. R. & CURRIE, P. J. 2007. Osteology of *Cryolophosaurus ellioti* (Dinosauria: Theropoda) from the Early Jurassic of Antarctica and implications for early theropod evolution. *Zoological Journal of the Linnean Society*, **151**, 377–421.

[STEWART, D. J. 1978. *The sedimentology and palaeoenvironment of the Wealden Group of the Isle of Wight, southern England*. Unpublished Ph.D. Thesis, Portsmouth Polytechnic.]

—— 1981. Chapter 3. A field guide to the Wealden Group of the Hastings area and the Isle of Wight. Pp. 3.1–3.31. *In* ELLIOT, T. (Ed.). *Field guides to modern and ancient fluvial systems in Britain and Spain*. Proceedings of the Second International Conference on Fluvial Sediments: 'Modern and Ancient Fluvial Systems: Sedimentology and Processes'. 188 pp, University of Keele.

——, RUFFELL, A., WACH, G. & GOLDRING, R. 1991. Lagoonal sedimentation and fluctuating salinities in the Vectis Formation (Wealden Group, Lower Cretaceous) of the Isle of Wight, southern England. *Sedimentary Geology*, **72**, 117–134.

STOVALL, J. W. & LANGSTON, W. 1950. *Acrocanthosaurus atokensis*, a new genus and species of Lower Cretaceous Theropoda from Oklahoma. *American Midland Naturalist*, **43**, 696–728.

STROMER, E. 1931. Ergebnisse der Forschungsrisen Prof. E. Stromers in den Wüsten Ägyptens. II. Wirbeltierreste der Baharje-Stufe (unterstes Cenoman). 10. Ein Skelett-Rest von Carcharodontosaurus no. gen. *Abhandlungen der Bayerischen Akademie der Wissenschaften, Mathematisch-Naturwissenschaftliche Abteilung, Neue Folge*, **9**, 1–23.

—— 1934. Ergebnisse der Forschungsreisen Prof. E. Stromers in den Wüsten Ägyptens. II. Wirbeltierreste der Baharje-Stufe (unterstes Cenoman). 13. Dinosauria von E. Stromer. *Abhandlungen der Bayerischen Akademie der Wissenschaften, Mathematisch-Naturwissenschaftliche Abteilung, Neue Folge*, **22**, 1–79.

SUES, H.-D., FREY, E., MARTILL, D. M. & SCOTT, D. M. 2002. *Irritator challengeri*, a spinosaurid (Dinosauria: Theropoda) from the Lower Cretaceous of Brazil. *Journal of Vertebrate Paleontology*, **22**, 535–547.

SWEETMAN, S. C. 2004. The first record of velociraptorine dinosaurs (Saurischia, Theropoda) from the Wealden (Early Cretaceous, Barremian) of southern England. *Cretaceous Research*, **25**, 353–364.

VULLO, R., NERAUDEAU, D. & LENGLET, T. 2007. Dinosaur teeth from the Cenomanian of Charentes, Western France: evidence for a mixed Laurasian-Gondwanan assemblage. *Journal of Vertebrate Paleontology*, **27**, 931–943

WALDMAN, M. 1974. Megalosaurids from the Bajocian Middle Jurassic of Dorset. *Palaeontology*, **17**, 325–340.

WATSON, J. & ALVIN, K. L. 1996. An English Wealden floral list, with comments on possible environmental indicators. *Cretaceous Research*, **17**, 5–26.

WELLES, S. P. 1984. *Dilophosaurus wetherilli* (Dinosauria, Theropoda) osteology and comparisons. *Palaeontographica, Abteilung A, Palaeozoologie-Stratigraphie*, **185**, 85–180.

WEISHAMPEL, D. B., BARRETT, P. M., CORIA, R. A., LE LOEUFF, J., XU, X., ZHAO, X., SAHNI, A., GOMANI, E. M. P. & NOTO, C. R. 2004. Dinosaur distribution. Pp. 517–606. *In* WEISHAMPEL, D. B., DODSON, P. & OSMOLSKA, H. (Eds). *The Dinosauria* (2nd edition). University of California Press, Berkeley, California.

WITMER, L. M. 1997. The evolution of the antorbital cavity of archosaurs: a study in soft-tissue reconstruction in the fossil record with analysis of the function of pneumaticity. *Society of Vertebrate Paleontology Memoir*, **3**, 1–73.

XU, X., NORELL, M. A., KUANG, X., WANG, X., ZHAO, Q. & JIA, C. 2004. Basal tyrannosauroids from China and evidence for protofeathers in tyrannosauroids. *Nature*, **431**, 680–684.

ZHAO, X.-J. & CURRIE, P. J. 1993. A large crested theropod from the Jurassic of Xinjiang, People's Republic of China. *Canadian Journal of Earth Sciences*, **30**, 2027–2036.

Stephen L. Brusatte
Division of Paleontology
American Museum of Natural History
Central Park West at 79th Street
New York, NY 10024
USA
e-mail: sbrusatte@amnh.org

Roger B. J. Benson
Department of Earth Sciences
University of Cambridge
Downing Street
Cambridge CB2 3EQ
UK
e-mail: rbb27@cam.ac.uk

and

The Natural History Museum
Cromwell Road
London SW7 5BD
UK

Stephen Hutt
Dinosaur Isle Museum
Culver Parade
Sandown PO36 8QA
UK
e-mail: Stephen.Hutt@iow.gov.uk

PLATE 1

Fig.

Neovenator salerii Hutt, Martill & Barker, 1996

1 Left premaxilla (MIWG 6348) in lateral view.

2 Left premaxilla (MIWG 6348) in medial view.

3 Left and right premaxillae (MIWG 6348) in anterior view.

4 Left premaxilla (MIWG 6348) in posterior view.

5 Left and right premaxillae (MIWG 6348) in ventral view.

Scale bar represents 50 mm.

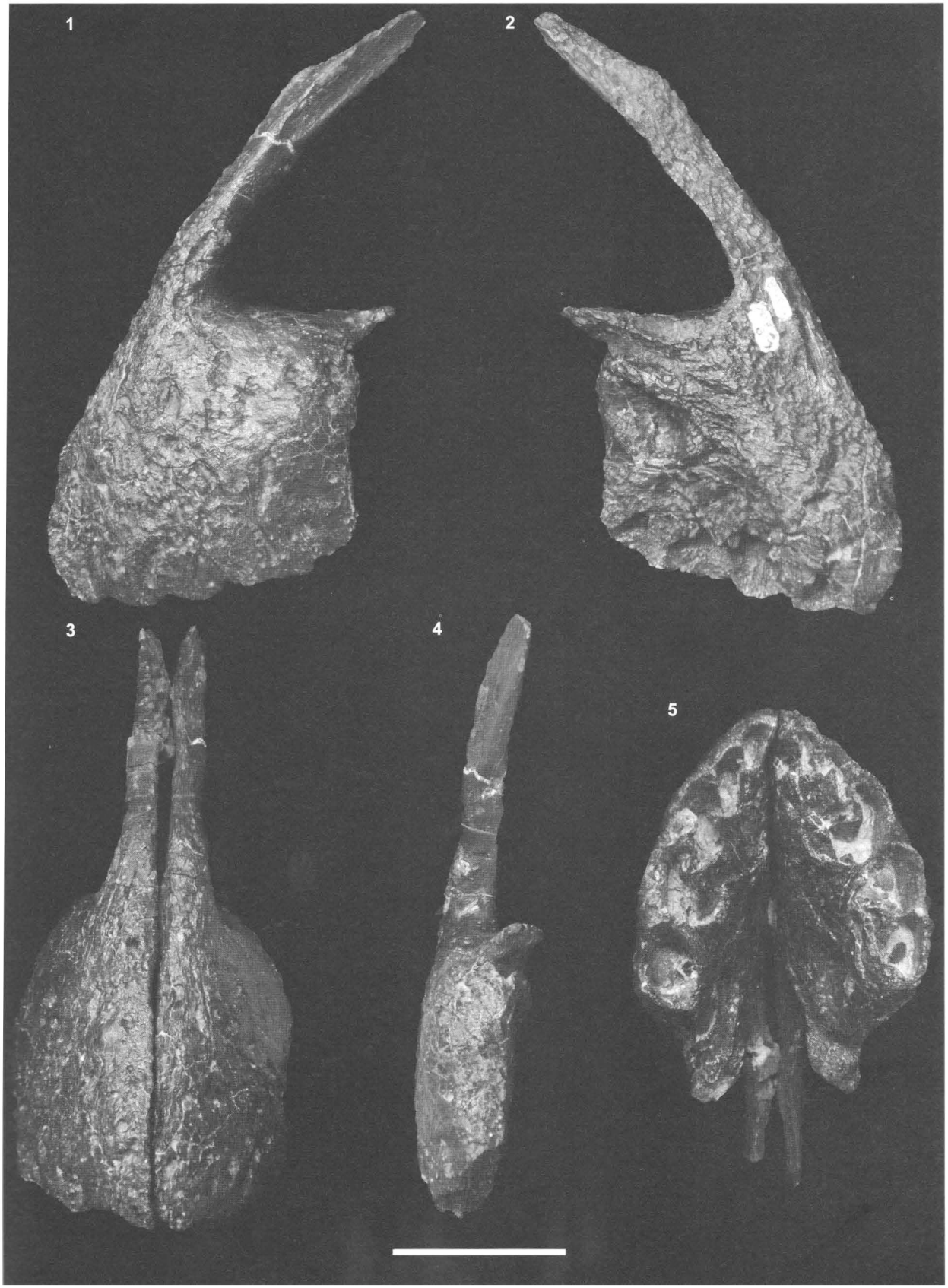
1
2
3
4
5

PLATE 2

Fig.

Neovenator salerii Hutt, Martill & Barker, 1996

1 Left maxilla (MIWG 6348) in lateral view.

2 Left maxilla (MIWG 6348) in medial view.

3 Left maxilla (MIWG 6348) in ventral view.

4 Left maxilla (MIWG 6348) in dorsal view.

Scale bar represents 50 mm.

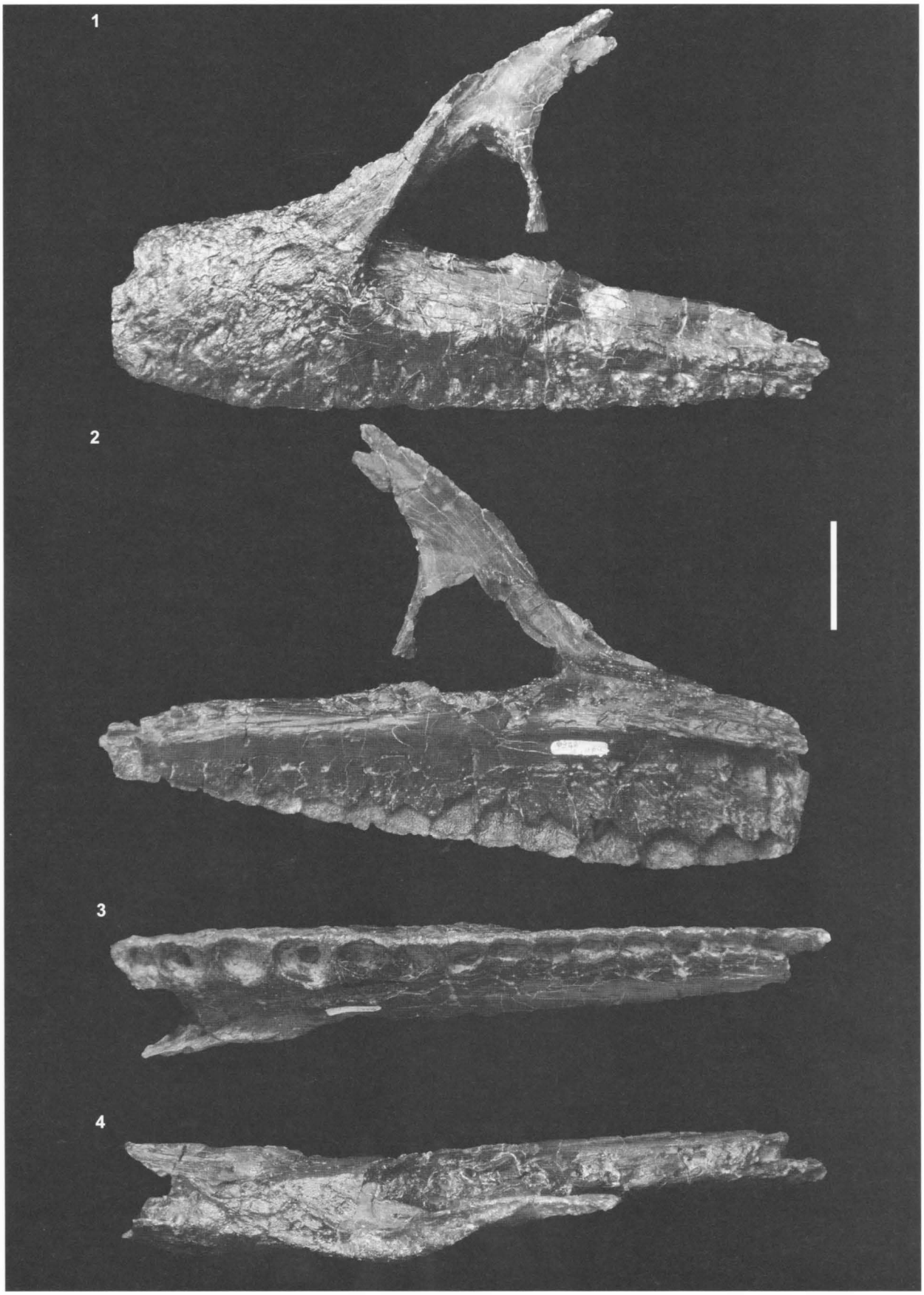
1
2
3
4

PLATE 3

Fig.

Neovenator salerii Hutt, Martill & Barker, 1996

1 Right nasal (MIWG 6348) in lateral view.

2 Right nasal (MIWG 6348) in medial view.

3 Right nasal (MIWG 6348) in dorsal view.

4 Right nasal (MIWG 6348) in ventral view.

5 Right palatine (MIWG 6348) in lateral view.

6 Right palatine (MIWG 6348) in medial view.

7 Right palatine (MIWG 6348) in dorsal view.

Scale bars represent 50 mm.

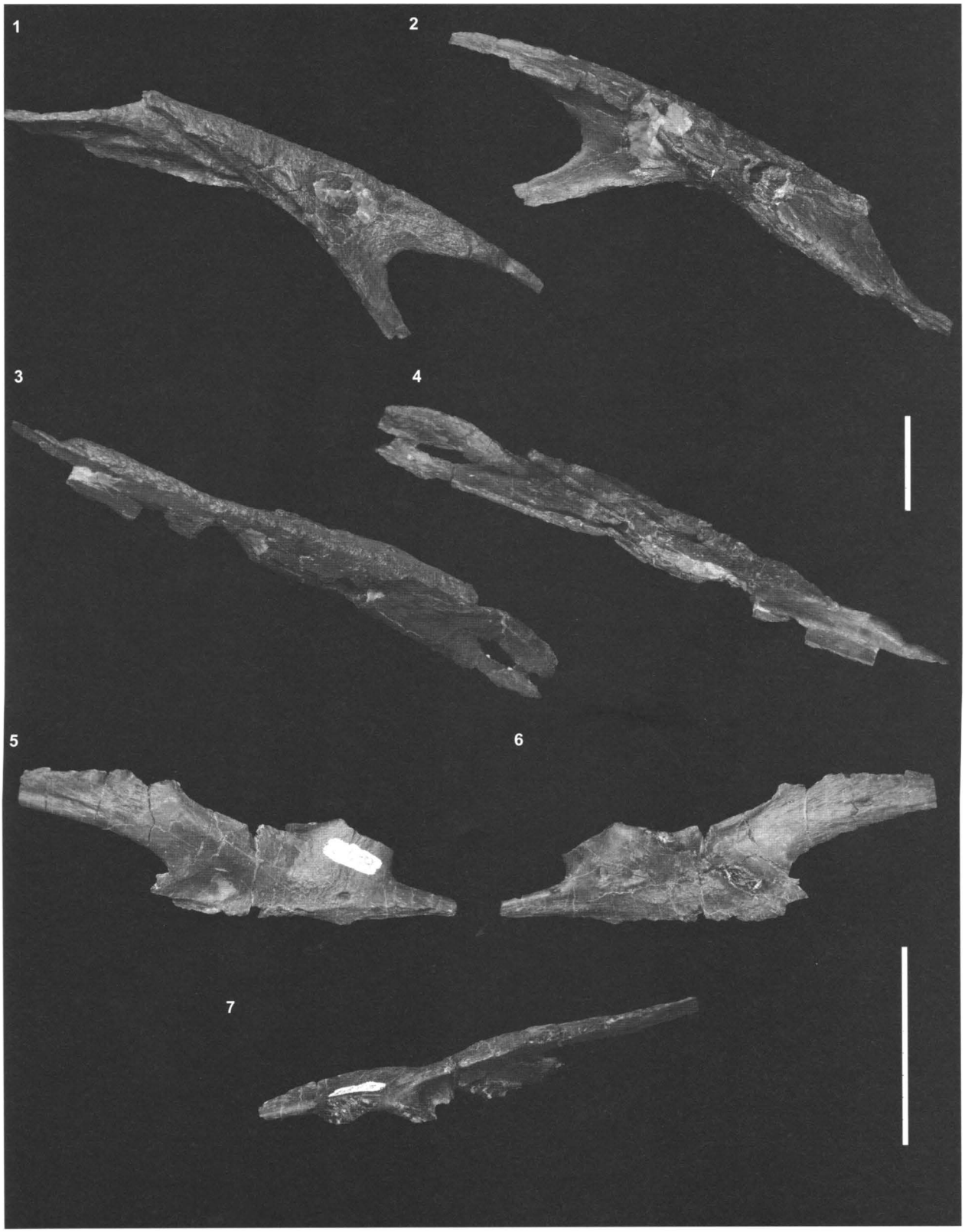
1
2
3
4
5
6
7

PLATE 4

Fig.

Neovenator salerii Hutt, Martill & Barker, 1996

1 Small replacement tooth (MIWG 6348) in labial or lingual view.

2 Small replacement tooth (MIWG 6348) in posterior view.

3 Small replacement tooth (MIWG 6348) in labial or lingual view with magnified (4x) portion of the mesial carina.

4 Small replacement tooth (MIWG 6348) in labial or lingual view with magnified (4x) portion of the distal carina.

5 Adult tooth tip (MIWG 6348) in labial or lingual view.

6 Adult tooth tip (MIWG 6348) in distal view.

7 Large replacement tooth (MIWG 6348) in labial or lingual view.

8 Large replacement tooth (MIWG 6348) in labial or lingual view.

9 Adult tooth tip (MIWG 6348) in mesial view.

10 Adult tooth tip (MIWG 6348) in labial or lingual view.

11 Adult tooth tip (MIWG 6348) in labial or lingual view with magnified (4x) portions of the distal (left) and mesial (right) carinae.

12 Adult tooth (MIWG 6348) in distal view with magnified (4x) portion of the distal carina.

13 Adult tooth (MIWG 6348) in mesial view.

14 Adult tooth (MIWG 6348) in labial or lingual view.

Scale bar represents 20 mm.

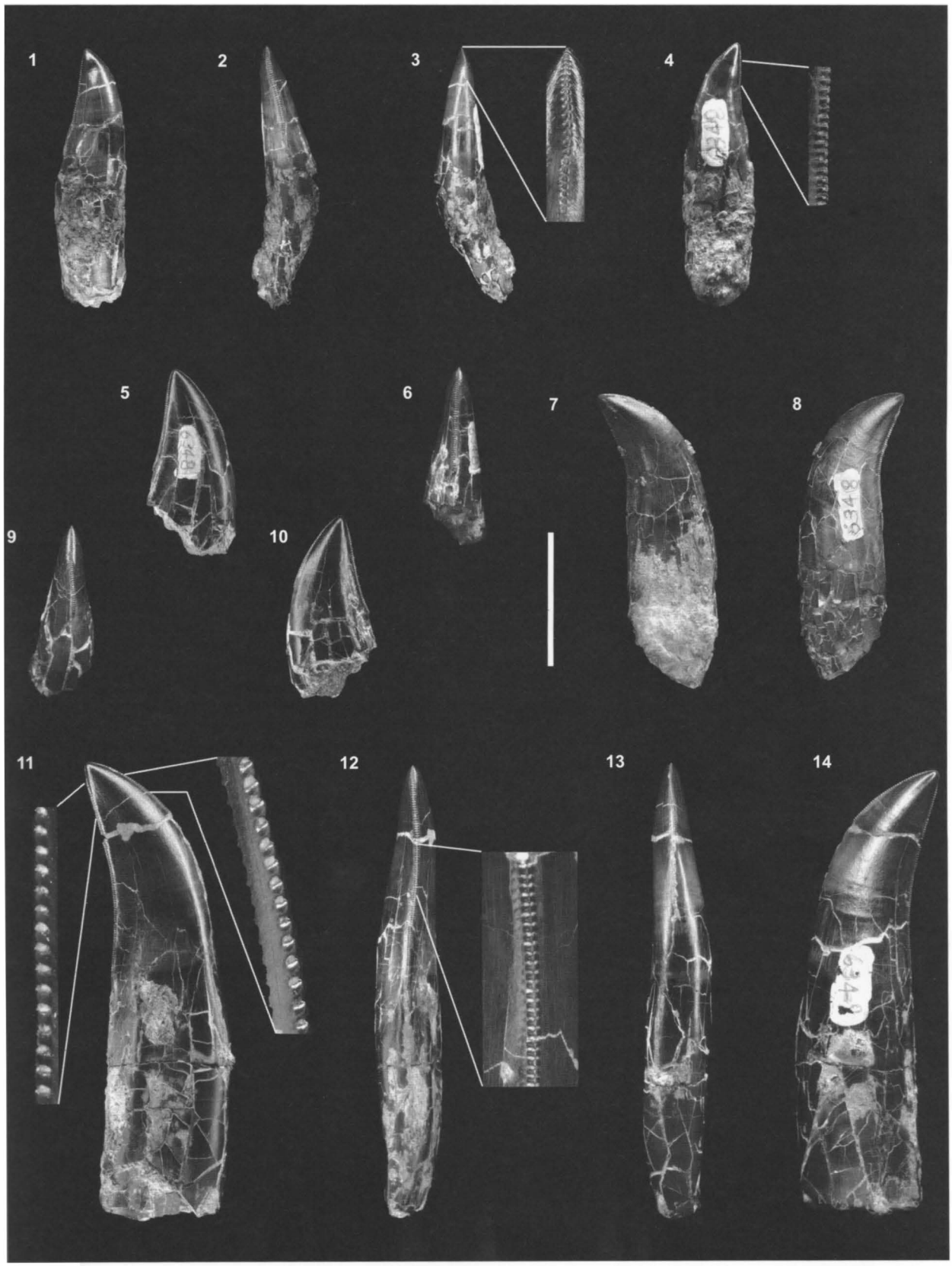
1
2
3
4
5
6
7
8
9
10
11
12
13
14

PLATE 5

Fig.

Neovenator salerii Hutt, Martill & Barker, 1996

1 Axis (MIWG 6348) in left lateral view.

2 Axis (MIWG 6348) in anterior view.

3 Axis (MIWG 6348) in right lateral view.

4 Axis (MIWG 6348) in posterior view.

5 Axis (MIWG 6348) in ventral view.

6 Axis (MIWG 6348) in dorsal view.

7 Cervical vertebra 5 (BMNH R10001) in left lateral view.

8 Cervical vertebra 5 (BMNH R10001) in anterior view.

9 Cervical vertebra 5 (BMNH R10001) in right lateral view.

10 Cervical vertebra 5 (BMNH R10001) in posterior view.

11 Cervical vertebra 5 (BMNH R10001) in ventral view.

12 Cervical vertebra 5 (BMNH R10001) in dorsal view.

Scale bar represents 100 mm.

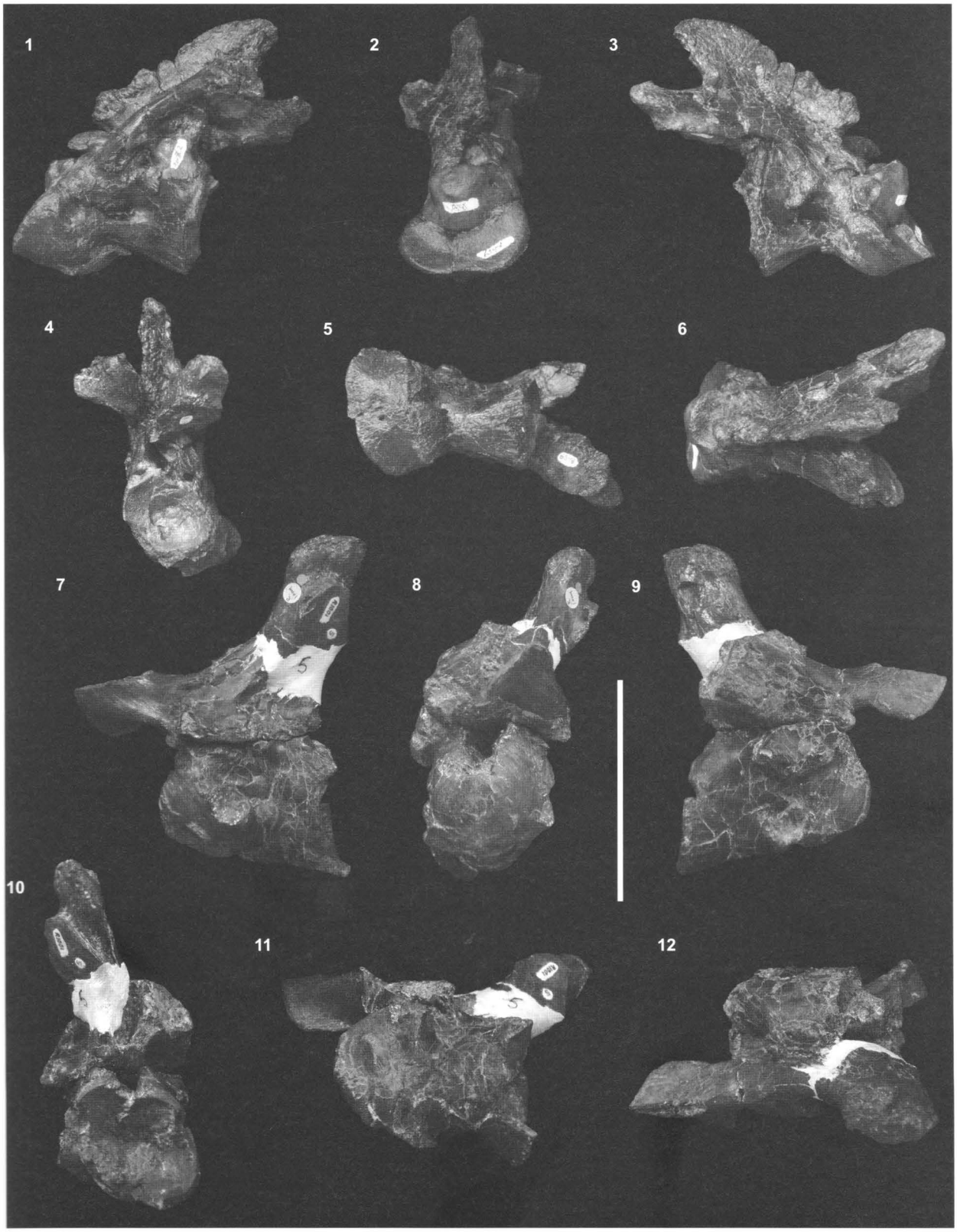
1
2
3
4
5
6
7
8
9
10
11
12

PLATE 6

Fig.

Neovenator salerii Hutt, Martill & Barker, 1996

1 Cervical vertebra 6 (MIWG 6348) in left lateral view.

2 Cervical vertebra 6 (MIWG 6348) in anterior view.

3 Cervical vertebra 6 (MIWG 6348) in right lateral view.

4 Cervical vertebra 6 (MIWG 6348) in posterior view.

5 Cervical vertebra 6 (MIWG 6348) in ventral view.

6 Cervical vertebra 6 (MIWG 6348) in dorsal view.

7 Cervical vertebra 7 (BMNH R10001) in left lateral view.

8 Cervical vertebra 7 (BMNH R10001) in anterior view.

9 Cervical vertebra 7 (BMNH R10001) in right lateral view.

10 Cervical vertebra 7 (BMNH R10001) in posterior view.

11 Cervical vertebra 7 (BMNH R10001) in ventral view.

12 Cervical vertebra 7 (BMNH R10001) in dorsal view.

Scale bar represents 100 mm.

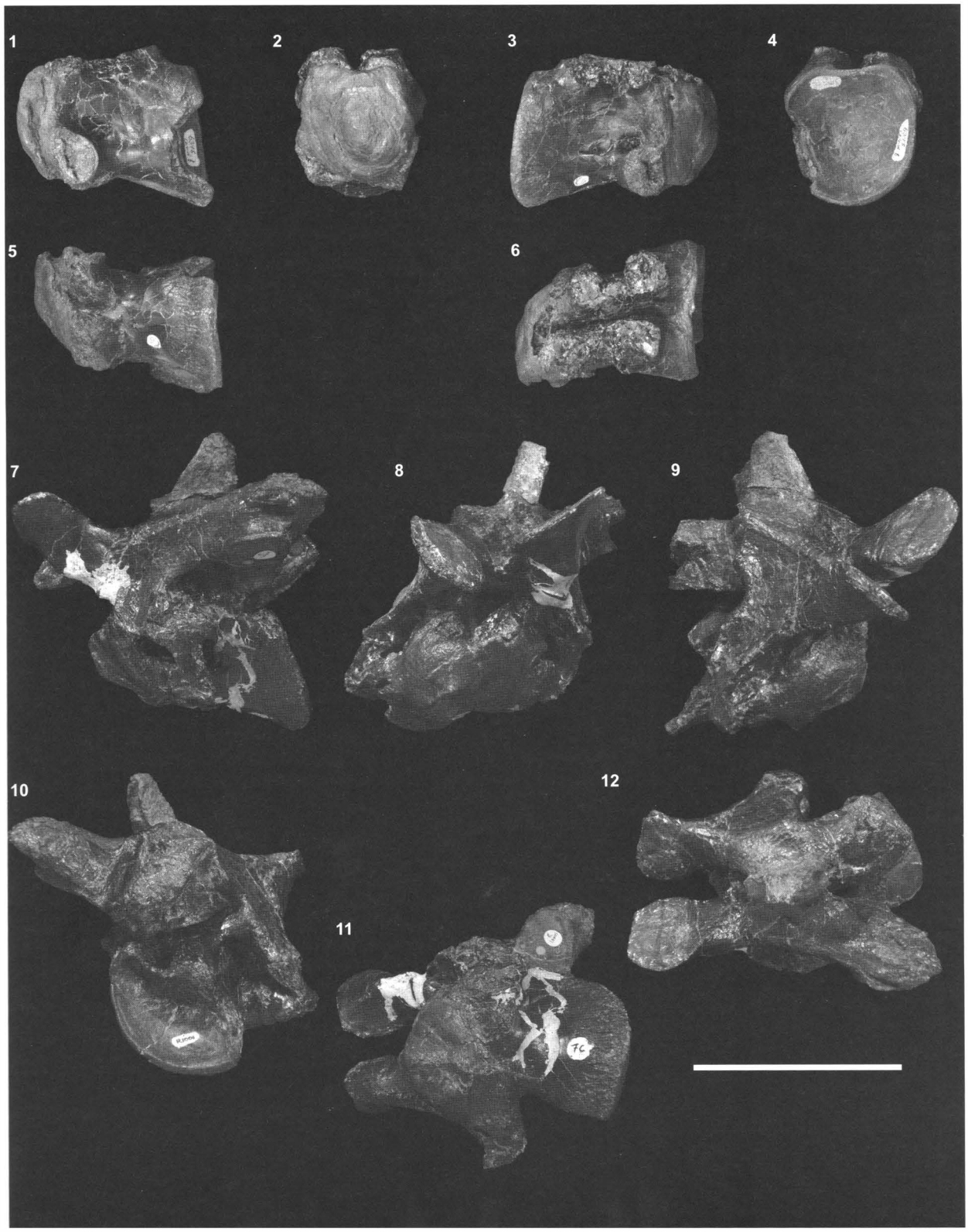
1
2
3
4
5
6
7
8
9
10
11
12

PLATE 7

Fig.

Neovenator salerii Hutt, Martill & Barker, 1996

1 Cervical vertebra 8 (MIWG 6348) in left lateral view.

2 Cervical vertebra 8 (MIWG 6348) in anterior view.

3 Cervical vertebra 8 (MIWG 6348) in right lateral view.

4 Cervical vertebra 8 (MIWG 6348) in ventral view.

5 Cervical vertebra 8 (MIWG 6348) in posterior view.

6 Cervical vertebra 8 (MIWG 6348) in dorsal view.

7 Cervical vertebra 9 (MIWG 6348) in left lateral view.

8 Cervical vertebra 9 (MIWG 6348) in anterior view.

9 Cervical vertebra 9 (MIWG 6348) in right lateral view.

10 Cervical vertebra 9 (MIWG 6348) in posterior view.

11 Cervical vertebra 9 (MIWG 6348) in ventral view.

12 Cervical vertebra 9 (MIWG 6348) in dorsal view.

Scale bar represents 100 mm.

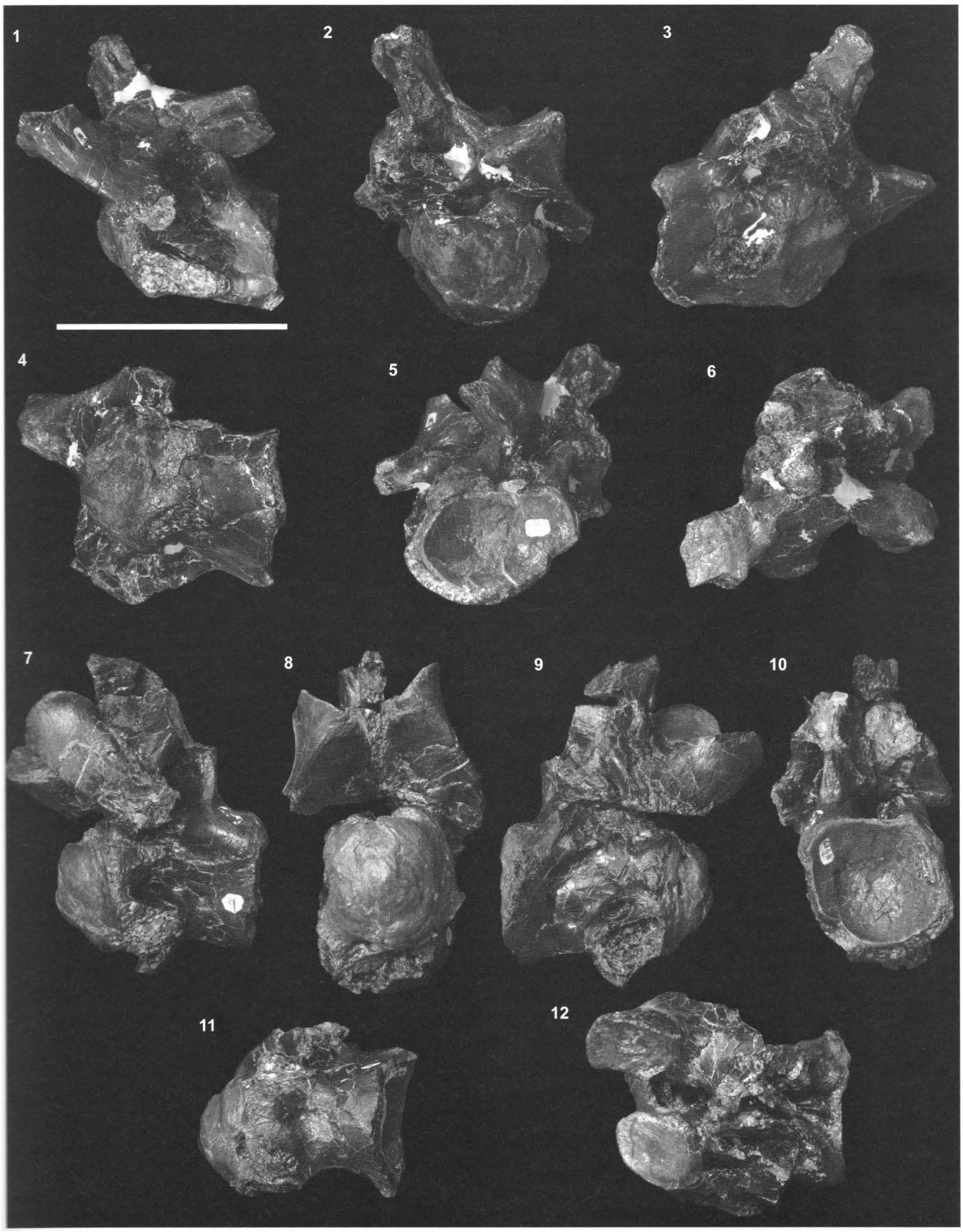
1
2
3
4
5
6
7
8
9
10
11
12

PLATE 8

Fig.

Neovenator salerii Hutt, Martill & Barker, 1996

1 Dorsal vertebra 1 (BMNH R10001) in left lateral view.

2 Dorsal vertebra 1 (BMNH R10001) in anterior view.

3 Dorsal vertebra 1 (BMNH R10001) in right lateral view.

4 Dorsal vertebra 1 (BMNH R10001) in posterior view.

5 Dorsal vertebra 1 (BMNH R10001) in ventral view.

6 Dorsal vertebra 1 (BMNH R10001) in dorsal view.

7 Dorsal vertebra 2 (BMNH R10001) in left lateral view.

8 Dorsal vertebra 2 (BMNH R10001) in anterior view.

9 Dorsal vertebra 2 (BMNH R10001) in right lateral view.

10 Dorsal vertebra 2 (BMNH R10001) in posterior view.

11 Dorsal vertebra 2 (BMNH R10001) in ventral view.

12 Dorsal vertebra 2 (BMNH R10001) in dorsal view.

Scale bar represents 100 mm.

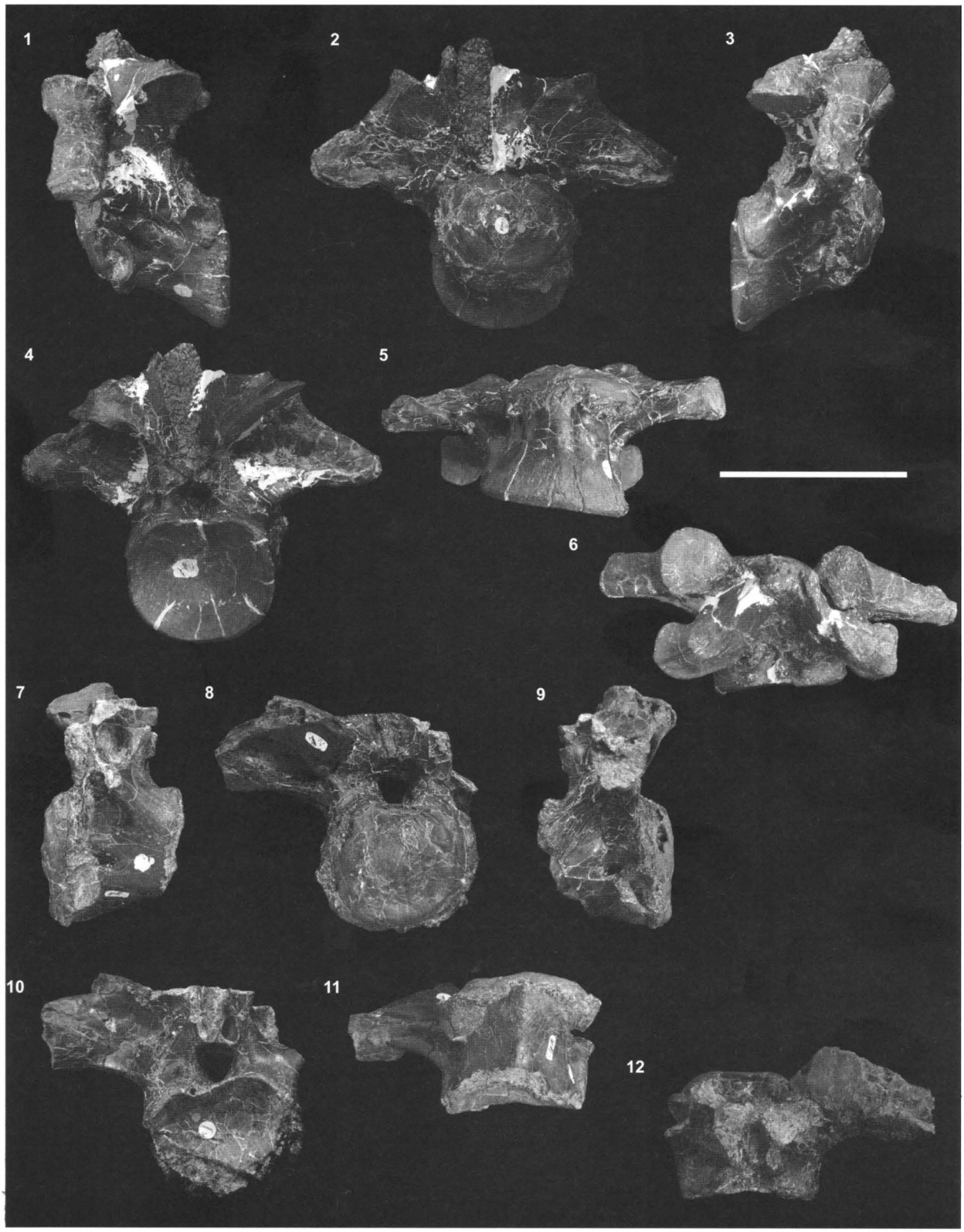
1
2
3
4
5
6
7
8
9
10
11
12

PLATE 9

Fig.

Neovenator salerii Hutt, Martill & Barker, 1996

1 Dorsal vertebra 5 (BMNH R10001) in left lateral view.

2 Dorsal vertebra 5 (BMNH R10001) in anterior view.

3 Dorsal vertebra 5 (BMNH R10001) in right lateral view.

4 Dorsal vertebra 5 (BMNH R10001) in posterior view.

5 Dorsal vertebra 5 (BMNH R10001) in ventral view.

6 Dorsal vertebra 5 (BMNH R10001) in dorsal view.

7 Dorsal vertebra 6 (BMNH R10001) in left lateral view.

8 Dorsal vertebra 6 (BMNH R10001) in ventral view.

9 Dorsal vertebra 6 (BMNH R10001) in dorsal view.

10 Dorsal vertebra 6 (BMNH R10001) in anterior view.

11 Dorsal vertebra 6 (BMNH R10001) in right lateral view.

12 Dorsal vertebra 6 (BMNH R10001) in posterior view.

Scale bar represents 100 mm.

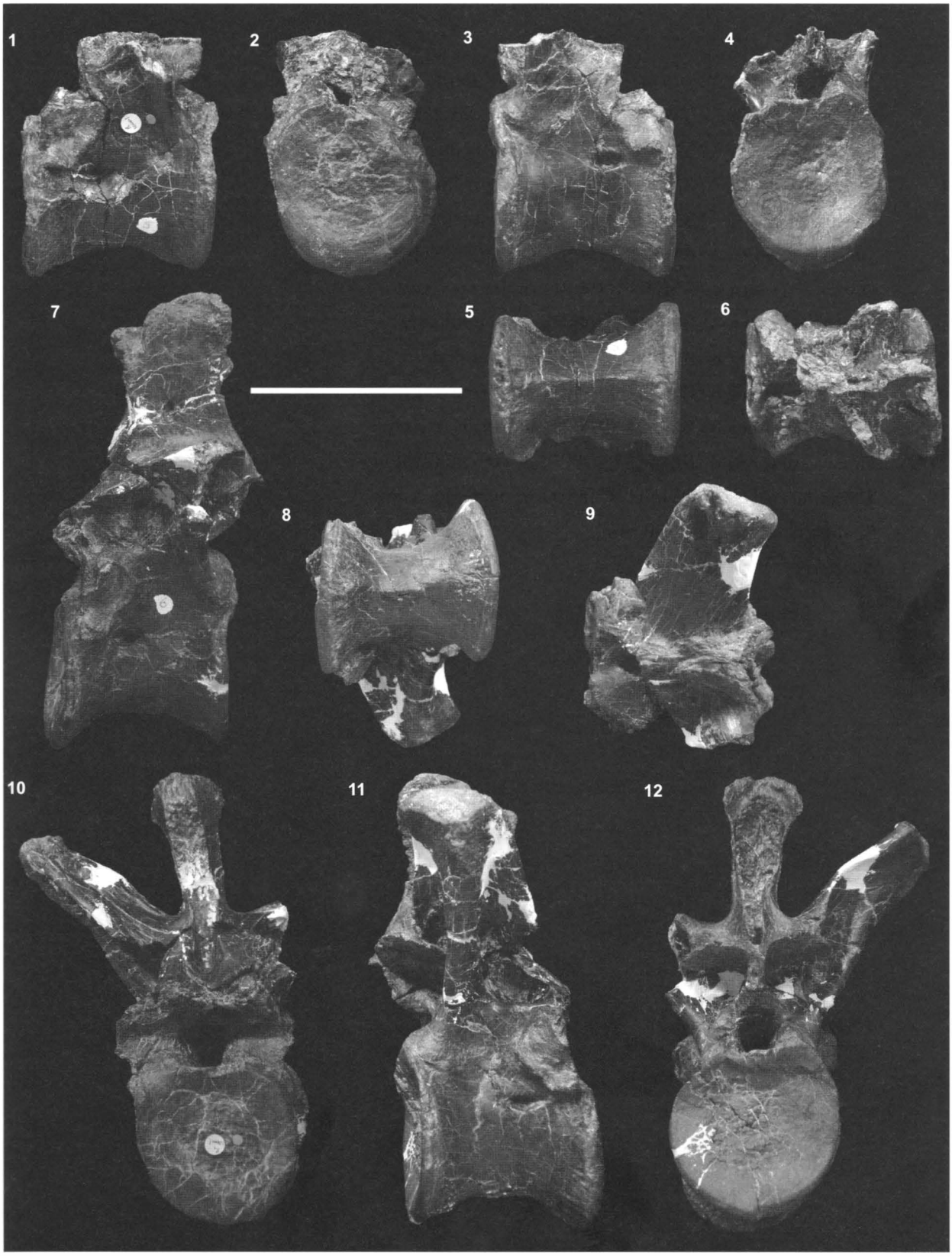
1
2
3
4
7
5
6
8
9
10
11
12

PLATE 10

Fig.

Neovenator salerii Hutt, Martill & Barker, 1996

1 Dorsal vertebra 7 (BMNH R10001) in left lateral view.

2 Dorsal vertebra 7 (BMNH R10001) in anterior view.

3 Dorsal vertebra 7 (BMNH R10001) in right lateral view.

4 Dorsal vertebra 7 (BMNH R10001) in posterior view.

5 Dorsal vertebra 7 (BMNH R10001) in ventral view.

6 Dorsal vertebra 7 (BMNH R10001) in dorsal view.

7 Dorsal vertebra 8 (BMNH R10001) in ventral view.

8 Dorsal vertebra 8 (BMNH R10001) in dorsal view.

9 Dorsal vertebra 8 (BMNH R10001) in left lateral view.

10 Dorsal vertebra 8 (BMNH R10001) in anterior view.

11 Dorsal vertebra 8 (BMNH R10001) in right lateral view.

12 Dorsal vertebra 8 (BMNH R10001) in posterior view.

Scale bar represents 100 mm.

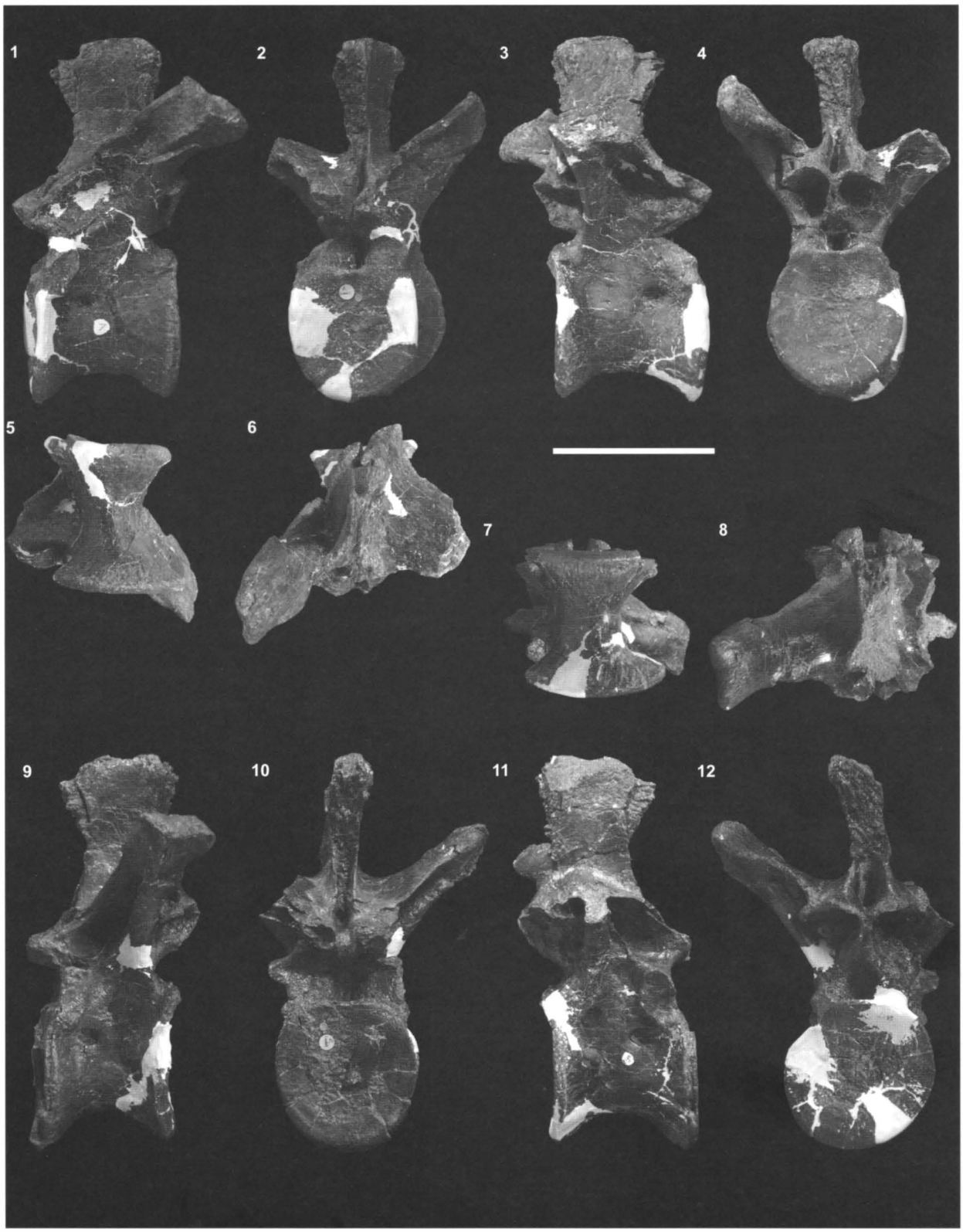
1
2
3
4
5
6
7
8
9
10
11
12

PLATE 11

Fig.

Neovenator salerii Hutt, Martill & Barker, 1996

1 Dorsal vertebra 9 (MIWG 6348) in left lateral view.

2 Dorsal vertebra 9 (MIWG 6348) in anterior view.

3 Dorsal vertebra 9 (MIWG 6348) in right lateral view.

4 Dorsal vertebra 9 (MIWG 6348) in posterior view.

5 Dorsal vertebra 9 (MIWG 6348) in ventral view.

6 Dorsal vertebra 9 (MIWG 6348) in dorsal view.

7 Dorsal vertebra 10 (MIWG 6348) in left lateral view.

8 Dorsal vertebra 10 (MIWG 6348) in anterior view.

9 Dorsal vertebra 10 (MIWG 6348) in right lateral view.

10 Dorsal vertebra 10 (MIWG 6348) in posterior view.

11 Dorsal vertebra 10 (MIWG 6348) in ventral view.

12 Dorsal vertebra 10 (MIWG 6348) in dorsal view.

Scale bar represents 100 mm.

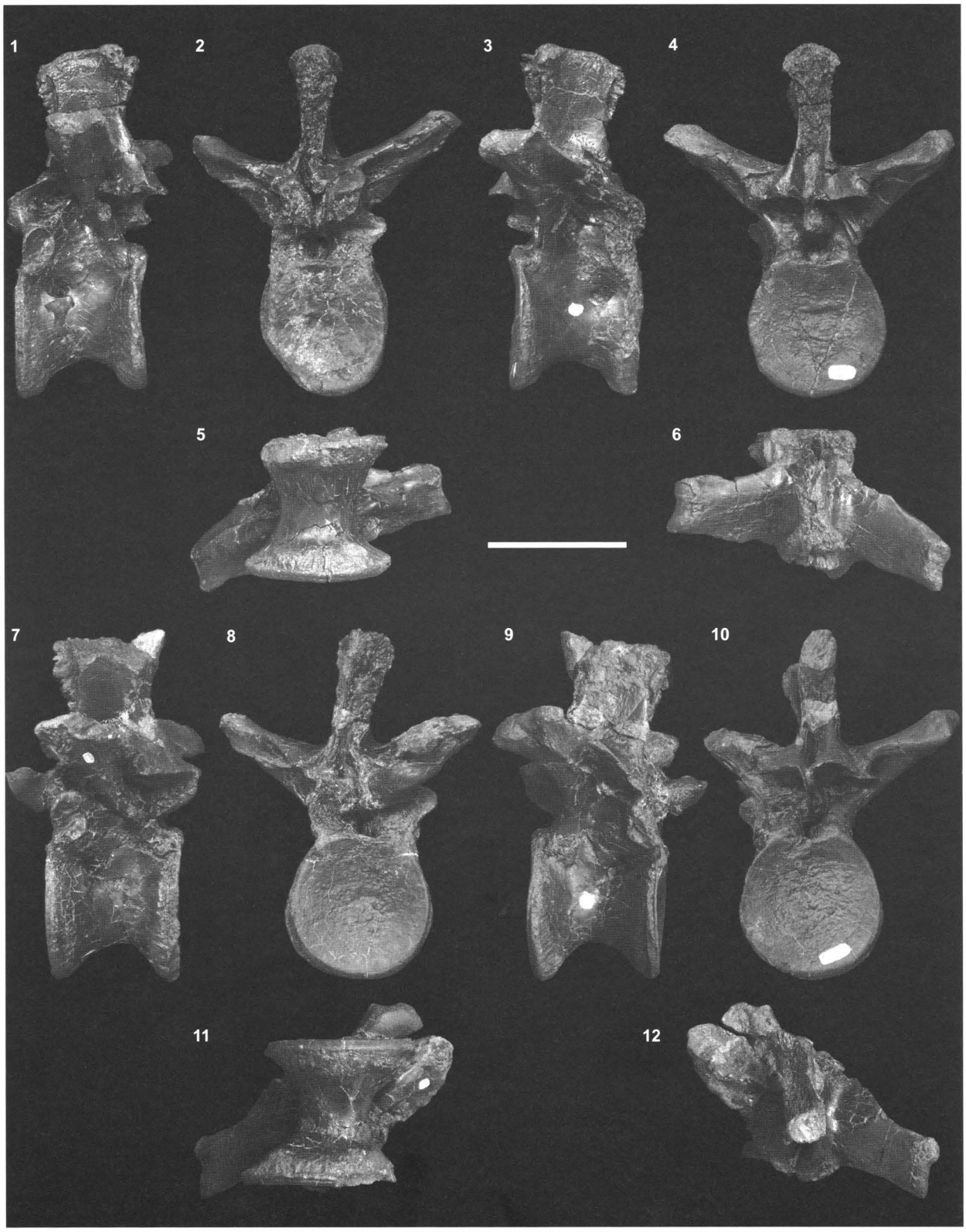
1
2
3
4
5
6
7
8
9
10
11
12

PLATE 12

Fig.

Neovenator salerii Hutt, Martill & Barker, 1996

1 Dorsal vertebra 12 (BMNH R10001) in left lateral view.

2 Dorsal vertebra 12 (BMNH R10001) in anterior view.

3 Dorsal vertebra 12 (BMNH R10001) in right lateral view.

4 Dorsal vertebra 12 (BMNH R10001) in ventral view.

5 Dorsal vertebra 12 (BMNH R10001) in dorsal view.

6 Dorsal vertebra 12 (BMNH R10001) in posterior view.

7 Dorsal vertebra 13 (BMNH R10001) in ventral view.

8 Dorsal vertebra 13 (BMNH R10001) in dorsal view.

9 Dorsal vertebra 13 (BMNH R10001) in left lateral view.

10 Dorsal vertebra 13 (BMNH R10001) in anterior view.

11 Dorsal vertebra 13 (BMNH R10001) in right lateral view.

12 Dorsal vertebra 13 (BMNH R10001) in posterior view.

Scale bar represents 100 mm.

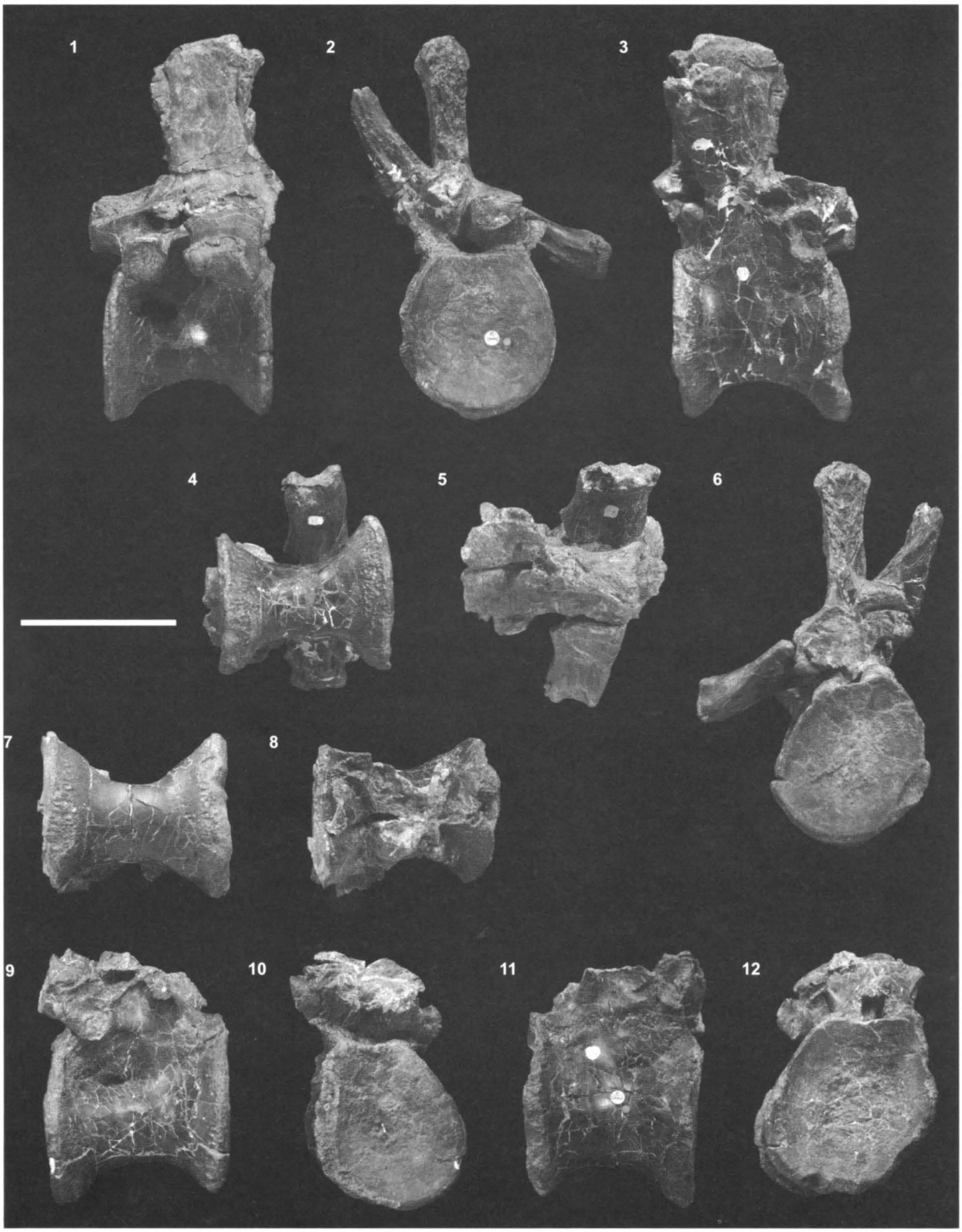
1
2
3
4
5
6
7
8
9
10
11
12

PLATE 13

Fig.

Neovenator salerii Hutt, Martill & Barker, 1996

1 Dorsal vertebra 14 (MIWG 6348) in left lateral view.

2 Dorsal vertebra 14 (MIWG 6348) in anterior view.

3 Dorsal vertebra 14 (MIWG 6348) in right lateral view.

4 Dorsal vertebra 14 (MIWG 6348) in ventral view.

5 Dorsal vertebra 14 (MIWG 6348) in posterior view.

6 Dorsal vertebra 14 (MIWG 6348) in dorsal view.

Scale bar represents 100 mm.

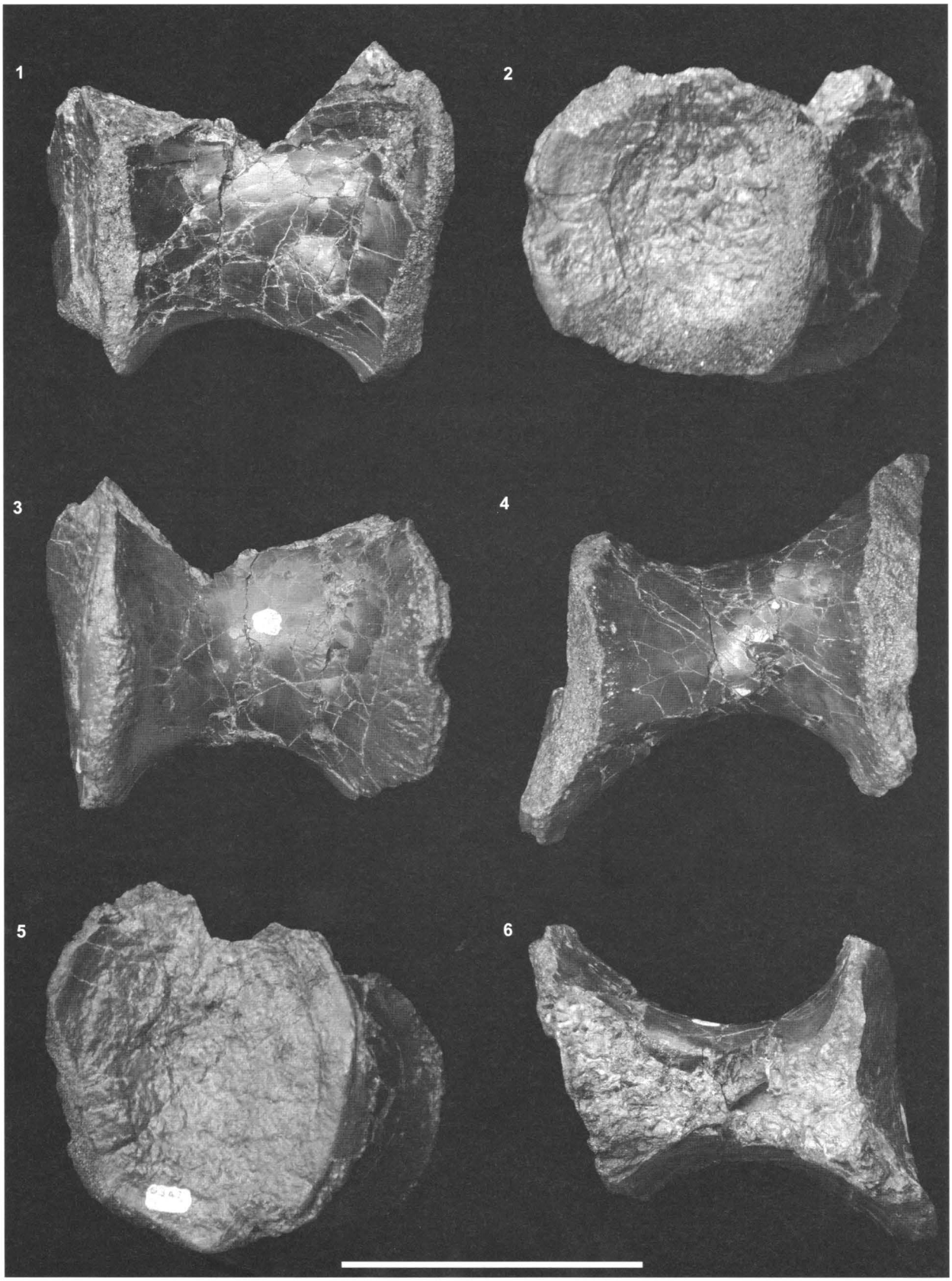
1
2
3
4
5
6

PLATE 14

Fig.

Neovenator salerii Hutt, Martill & Barker, 1996

1 Sacral block 1 (BMNH R10001) in lateral view.

2 Sacral block 1 (BMNH R10001) in opposing lateral view.

3 Sacral block 1 (BMNH R10001) in ventral view.

4 Sacral block 1 (BMNH R10001) in anterior/posterior view.

5 Sacral block 1 (BMNH R10001) in anterior/posterior view.

6 Sacral block 2 (BMNH R10001) in lateral view.

7 Sacral block 2 (BMNH R10001) in opposing lateral view.

8 Sacral block 2 (BMNH R10001) in ventral view.

9 Sacral block 2 (BMNH R10001) in anterior/posterior view.

10 Sacral block 2 (BMNH R10001) in anterior/posterior view.

Scale bar represents 50 mm. Uncertain identity of the isolated sacral blocks precludes definitive identification of left/right lateral and anterior/posterior views.

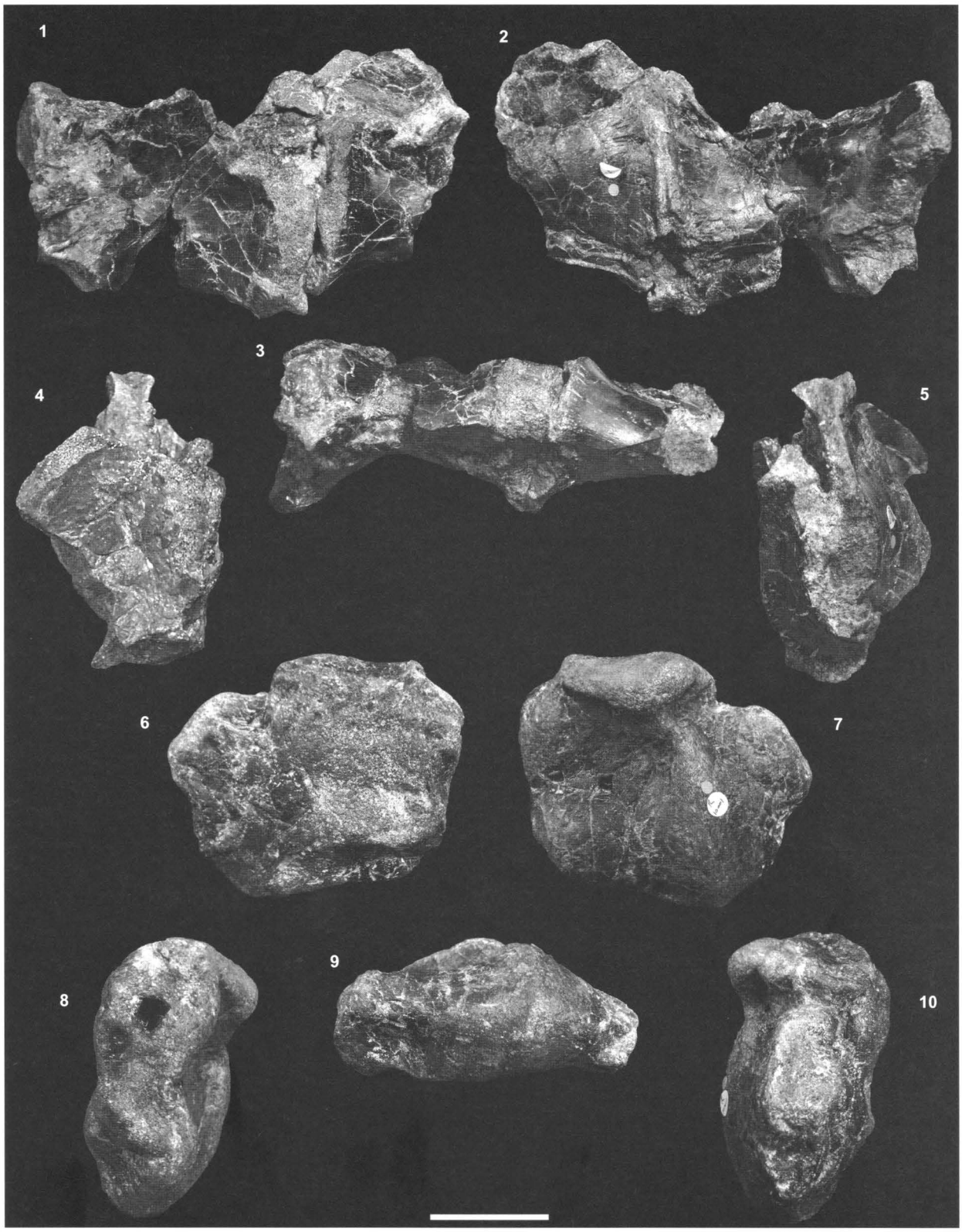
1
2
3
4
5
6
7
8
9
10

PLATE 15

Fig.

Neovenator salerii Hutt, Martill & Barker, 1996

1 Caudal vertebra 1 (MIWG 6348) in left lateral view.

2 Caudal vertebra 1 (MIWG 6348) in anterior view.

3 Caudal vertebra 1 (MIWG 6348) in right lateral view.

4 Caudal vertebra 1 (MIWG 6348) in posterior view.

5 Caudal vertebra 1 (MIWG 6348) in ventral view.

6 Caudal vertebra 1 (MIWG 6348) in dorsal view.

7 Caudal vertebra 2 (MIWG 6348) in left lateral view.

8 Caudal vertebra 2 (MIWG 6348) in anterior view.

9 Caudal vertebra 2 (MIWG 6348) in right lateral view.

10 Caudal vertebra 2 (MIWG 6348) in posterior view.

11 Caudal vertebra 2 (MIWG 6348) in ventral view.

12 Caudal vertebra 2 (MIWG 6348) in dorsal view.

Scale bar represents 100 mm.

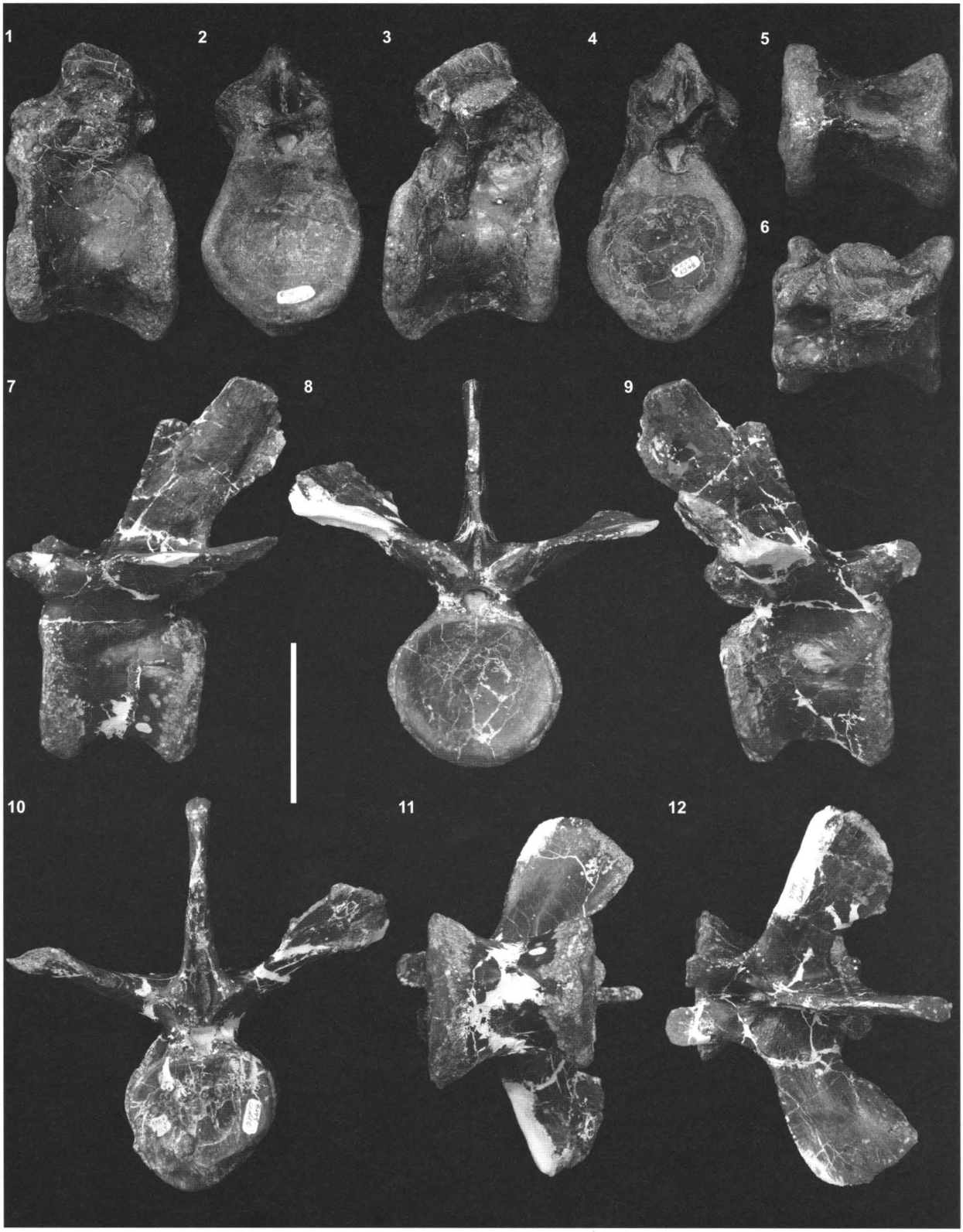
1
2
3
4
5
6
7
8
9
10
11
12

PLATE 16

Fig.

Neovenator salerii Hutt, Martill & Barker, 1996

1 Caudal vertebra 'A' (MIWG 6348) in left lateral view.

2 Caudal vertebra 'A' (MIWG 6348) in anterior view.

3 Caudal vertebra 'A' (MIWG 6348) in right lateral view.

4 Caudal vertebra 'A' (MIWG 6348) in ventral view.

5 Caudal vertebra 'A' (MIWG 6348) in posterior view.

6 Caudal vertebra 'A' (MIWG 6348) in dorsal view.

7 Caudal vertebra 'B' (MIWG 6348) in left lateral view.

8 Caudal vertebra 'B' (MIWG 6348) in anterior view.

9 Caudal vertebra 'B' (MIWG 6348) in right lateral view.

10 Caudal vertebra 'B' (MIWG 6348) in posterior view.

11 Caudal vertebra 'B' (MIWG 6348) in ventral view.

12 Caudal vertebra 'B' (MIWG 6348) in dorsal view.

Scale bar represents 100 mm.

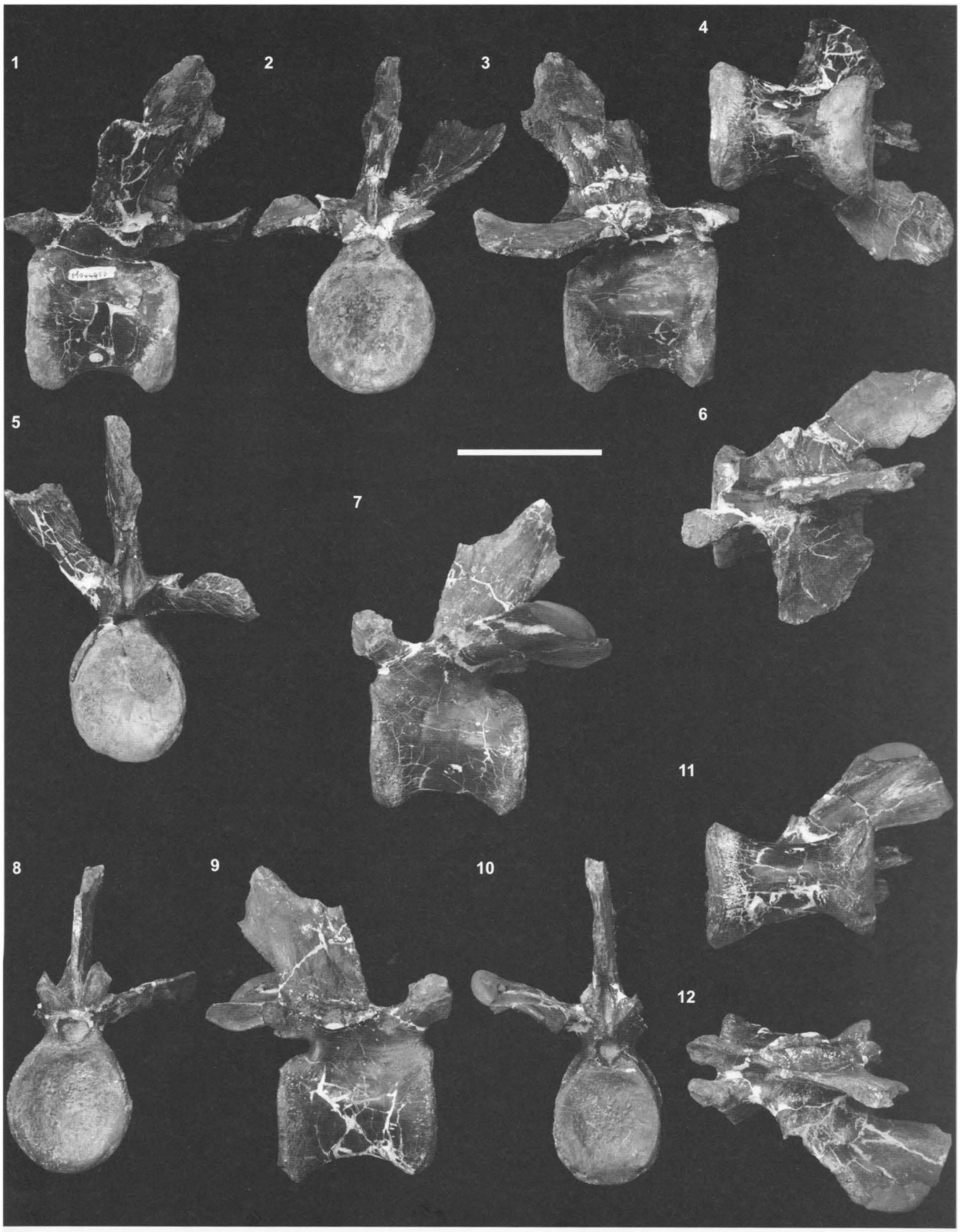
1
2
3
4
5
6
7
8
9
10
11
12

PLATE 17

Fig.

Neovenator salerii Hutt, Martill & Barker, 1996

1 Caudal vertebra 'C' (MIWG 6348) in left lateral view.

2 Caudal vertebra 'C' (MIWG 6348) in anterior view.

3 Caudal vertebra 'C' (MIWG 6348) in right lateral view.

4 Caudal vertebra 'C' (MIWG 6348) in posterior view.

5 Caudal vertebra 'C' (MIWG 6348) in ventral view.

6 Caudal vertebra 'C' (MIWG 6348) in dorsal view.

7 Caudal vertebra 'D' (MIWG 6348) in left lateral view.

8 Caudal vertebra 'D' (MIWG 6348) in anterior view.

9 Caudal vertebra 'D' (MIWG 6348) in right lateral view.

10 Caudal vertebra 'D' (MIWG 6348) in posterior view.

11 Caudal vertebra 'D' (MIWG 6348) in ventral view.

12 Caudal vertebra 'D' (MIWG 6348) i n dorsal view.

Scale bar represents 100 mm.

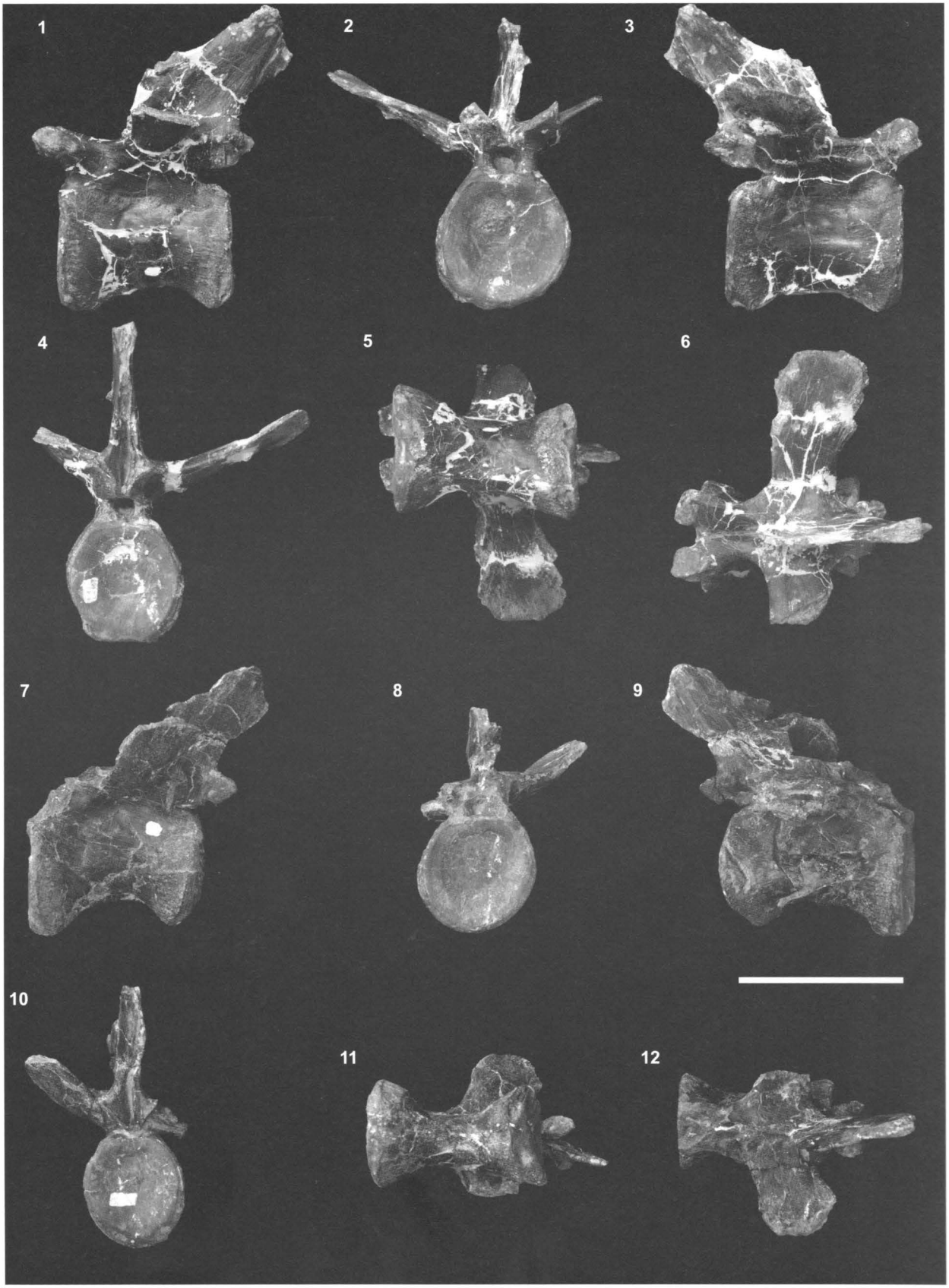
1
2
3
4
5
6
7
8
9
10
11
12

PLATE 18

Fig.

Neovenator salerii Hutt, Martill & Barker, 1996

1 Caudal vertebra 'E' (MIWG 6348) in left lateral view.

2 Caudal vertebra 'E' (MIWG 6348) in anterior view.

3 Caudal vertebra 'E' (MIWG 6348) in right lateral view.

4 Caudal vertebra 'E' (MIWG 6348) in posterior view.

5 Caudal vertebra 'E' (MIWG 6348) in ventral view.

6 Caudal vertebra 'E' (MIWG 6348) in dorsal view.

7 Caudal vertebra 'F' (MIWG 6348) in left lateral view.

8 Caudal vertebra 'F' (MIWG 6348) in anterior view.

9 Caudal vertebra 'F' (MIWG 6348) in right lateral view.

10 Caudal vertebra 'F' (MIWG 6348) in posterior view.

11 Caudal vertebra 'F' (MIWG 6348) in dorsal view.

12 Caudal vertebra 'G' (MIWG 6348) in left lateral view

13 Caudal vertebra 'G' (MIWG 6348) in anterior view.

14 Caudal vertebra 'G' (MIWG 6348) in right lateral view.

15 Caudal vertebra 'G' (MIWG 6348) in ventral view.

16 Caudal vertebra 'G' (MIWG 6348) in posterior view.

17 Caudal vertebra 'G' (MIWG 6348) in dorsal view.

Scale bar represents 100 mm.

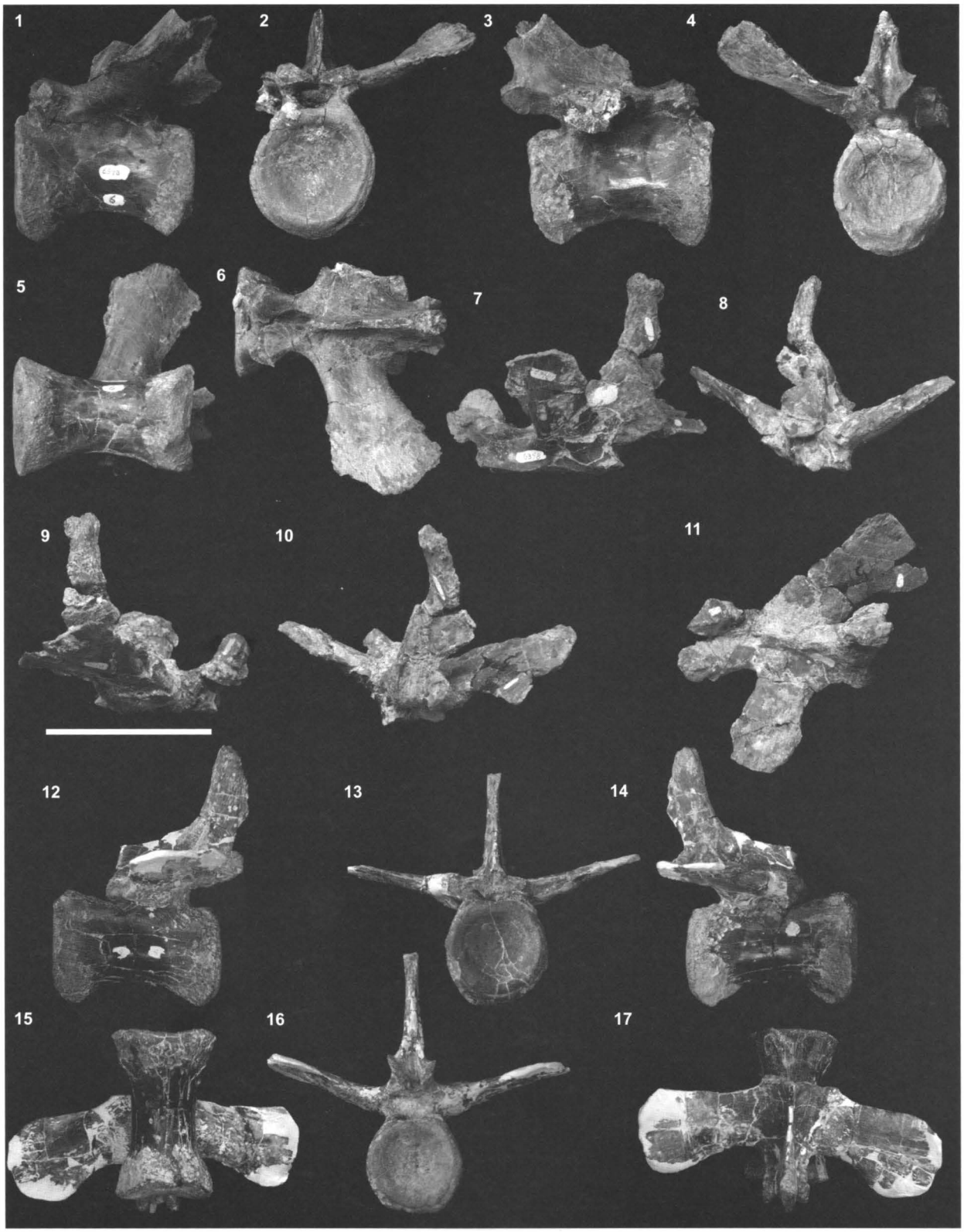
1
2
3
4
5
6
7
8
9
10
11
12
13
14
15
16
17

PLATE 19

Fig.

Neovenator salerii Hutt, Martill & Barker, 1996

1 Caudal vertebra 'H' (MIWG 6348) in left lateral view.

2 Caudal vertebra 'H' (MIWG 6348) in anterior view.

3 Caudal vertebra 'H' (MIWG 6348) in right lateral view.

4 Caudal vertebra 'H' (MIWG 6348) in posterior view.

5 Caudal vertebra 'H' (MIWG 6348) in ventral view.

6 Caudal vertebra 'H' (MIWG 6348) in dorsal view.

7 Caudal vertebra 'I' (MIWG 6348) in left lateral view.

8 Caudal vertebra 'I' (MIWG 6348) in anterior view.

9 Caudal vertebra 'I' (MIWG 6348) in right lateral view.

10 Caudal vertebra 'I' (MIWG 6348) in posterior view.

11 Caudal vertebra 'I' (MIWG 6348) in ventral view.

12 Caudal vertebra 'I' (MIWG 6348) in dorsal view.

13 Caudal vertebra 'J' (MIWG 6348) in left lateral view.

14 Caudal vertebra 'J' (MIWG 6348) in anterior view.

15 Caudal vertebra 'J' (MIWG 6348) in right lateral view.

16 Caudal vertebra 'J' (MIWG 6348) in posterior view.

17 Caudal vertebra 'J' (MIWG 6348) in ventral view.

18 Caudal vertebra 'J' (MIWG 6348) in dorsal view.

Scale bar represents 100 mm.

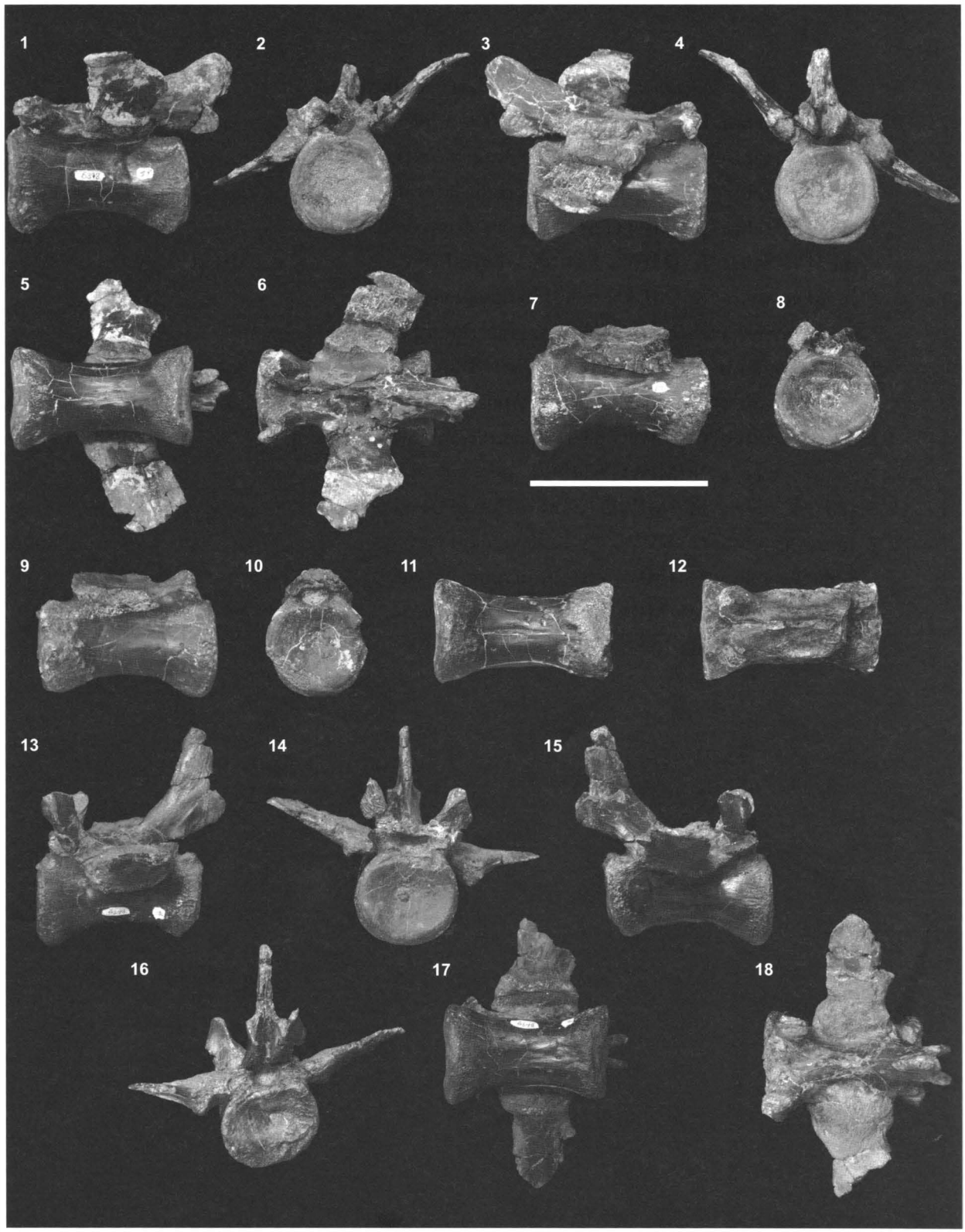
1
2
3
4
5
6
7
8
9
10
11
12
13
14
15
16
17
18

PLATE 20

Fig.

Neovenator salerii Hutt, Martill & Barker, 1996

1 Caudal vertebra 'K' (MIWG 6348) in left lateral view.

2 Caudal vertebra 'K' (MIWG 6348) in anterior view.

3 Caudal vertebra 'K' (MIWG 6348) in right lateral view.

4 Caudal vertebra 'K' (MIWG 6348) in posterior view.

5 Caudal vertebra 'K' (MIWG 6348) in ventral view.

6 Caudal vertebra 'K' (MIWG 6348) in dorsal view.

7 Caudal vertebra 'L' (MIWG 6348) in anterior view.

8 Caudal vertebrae 'L' and 'M' (MIWG 6348) in left lateral view.

9 Caudal vertebra 'M' (MIWG 6348) in posterior view.

10 Caudal vertebra 'L' (MIWG 6348) in anterior view

11 Caudal vertebra 'L' (MIWG 6348) in dorsal view.

12 Caudal vertebra 'M' (MIWG 6348) in dorsal view.

13 Caudal vertebra 'L' (MIWG 6348) in ventral view.

14 Caudal vertebra 'M' (MIWG 6348) in anterior view.

15 Caudal vertebra 'M' (MIWG 6348) in ventral view.

Scale bar represents 100 mm.

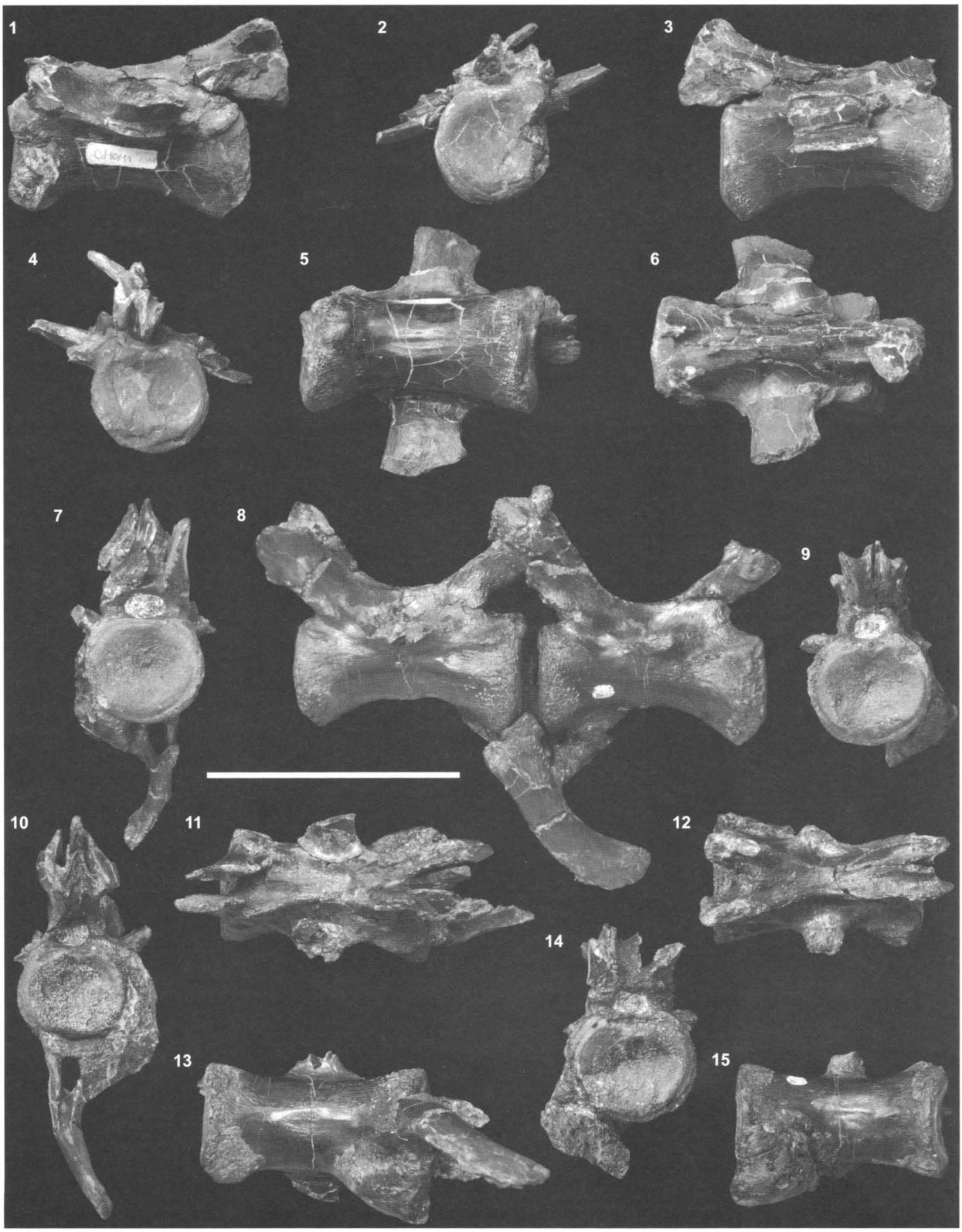
1
2
3
4
5
6
7
8
9
10
11
12
13
14
15

PLATE 21

Fig.

Neovenator salerii Hutt, Martill & Barker, 1996

1 Caudal vertebra 'N' (MIWG 6348) in left lateral view.

2 Caudal vertebra 'N' (MIWG 6348) in anterior view.

3 Caudal vertebra 'N' (MIWG 6348) in right lateral view.

4 Caudal vertebra 'N' (MIWG 6348) in posterior view.

5 Caudal vertebra 'N' (MIWG 6348) in ventral view.

6 Caudal vertebra 'N' (MIWG 6348) in dorsal view.

7 Caudal vertebra 'O' (MIWG 6348) in left lateral view.

8 Caudal vertebra 'O' (MIWG 6348) in anterior view.

9 Caudal vertebra 'O' (MIWG 6348) in right lateral view.

10 Caudal vertebra 'O' (MIWG 6348) in posterior view.

11 Caudal vertebra 'O' (MIWG 6348) in ventral view.

12 Caudal vertebra 'O' (MIWG 6348) in dorsal view.

13 Caudal vertebra 'P' (MIWG 6348) in left lateral view.

14 Caudal vertebra 'P' (MIWG 6348) in anterior view.

15 Caudal vertebra 'P' (MIWG 6348) in right lateral view.

16 Caudal vertebra 'P' (MIWG 6348) in posterior view.

17 Caudal vertebra 'P' (MIWG 6348) in ventral view.

18 Caudal vertebra 'P' (MIWG 6348) in dorsal view.

Scale bar represents 100 mm.

1
2
3
4
5
6
7
8
9
10
11
12
13
14
15
16
17
18

PLATE 22

Fig.

Neovenator salerii Hutt, Martill & Barker, 1996

1 Caudal vertebra 'Q' (MIWG 6348) in left lateral view.

2 Caudal vertebra 'Q' (MIWG 6348) in anterior view.

3 Caudal vertebra 'Q' (MIWG 6348) in right lateral view.

4 Caudal vertebra 'Q' (MIWG 6348) in posterior view.

5 Caudal vertebra 'Q' (MIWG 6348) in ventral view.

6 Caudal vertebra 'Q' (MIWG 6348) in dorsal view.

7 Caudal vertebra 'R' (MIWG 6348) in left lateral view.

8 Caudal vertebra 'R' (MIWG 6348) in anterior view.

9 Caudal vertebra 'R' (MIWG 6348) in right lateral view.

10 Caudal vertebra 'R' (MIWG 6348) in posterior view.

11 Caudal vertebra 'R' (MIWG 6348) in ventral view.

12 Caudal vertebra 'R' (MIWG 6348) in dorsal view.

13 Caudal vertebra 'S' (MIWG 6348) in left lateral view.

14 Caudal vertebra 'S' (MIWG 6348) in anterior view.

15 Caudal vertebra 'S' (MIWG 6348) in right lateral view.

16 Caudal vertebra 'S' (MIWG 6348) in posterior view.

17 Caudal vertebra 'S' (MIWG 6348) in ventral view.

18 Caudal vertebra 'S' (MIWG 6348) in dorsal view.

Scale bar represents 100 mm.

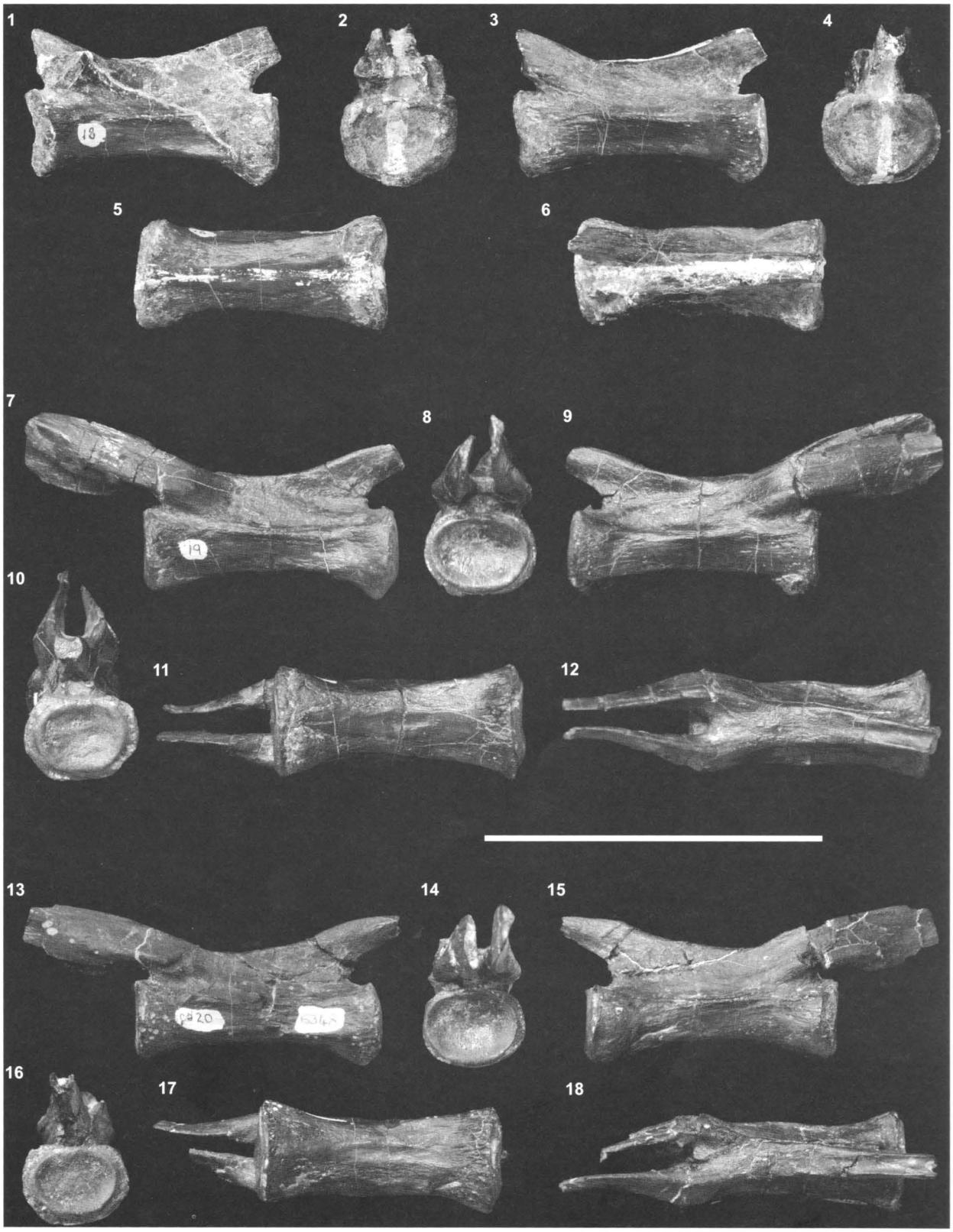
1
2
3
4
5
6
7
8
9
10
11
12
13
14
15
16
17
18

PLATE 23

Fig.

Neovenator salerii Hutt, Martill & Barker, 1996

1 Caudal vertebra 'T' (MIWG 6348) in left lateral view.

2 Caudal vertebra 'T' (MIWG 6348) in anterior view.

3 Caudal vertebra 'T' (MIWG 6348) in posterior view.

4 Caudal vertebra 'T' (MIWG 6348) in right lateral view.

5 Caudal vertebra 'T' (MIWG 6348) in ventral view.

6 Caudal vertebra 'T' (MIWG 6348) in dorsal view.

7 Caudal vertebra 'U' (MIWG 6348) in left lateral view.

8 Caudal vertebra 'U' (MIWG 6348) in anterior view.

9 Caudal vertebra 'U' (MIWG 6348) in right lateral view.

10 Caudal vertebra 'U' (MIWG 6348) in posterior view.

11 Caudal vertebra 'U' (MIWG 6348) in ventral view.

12 Caudal vertebra 'U' (MIWG 6348) in dorsal view.

Scale bar represents 100 mm.

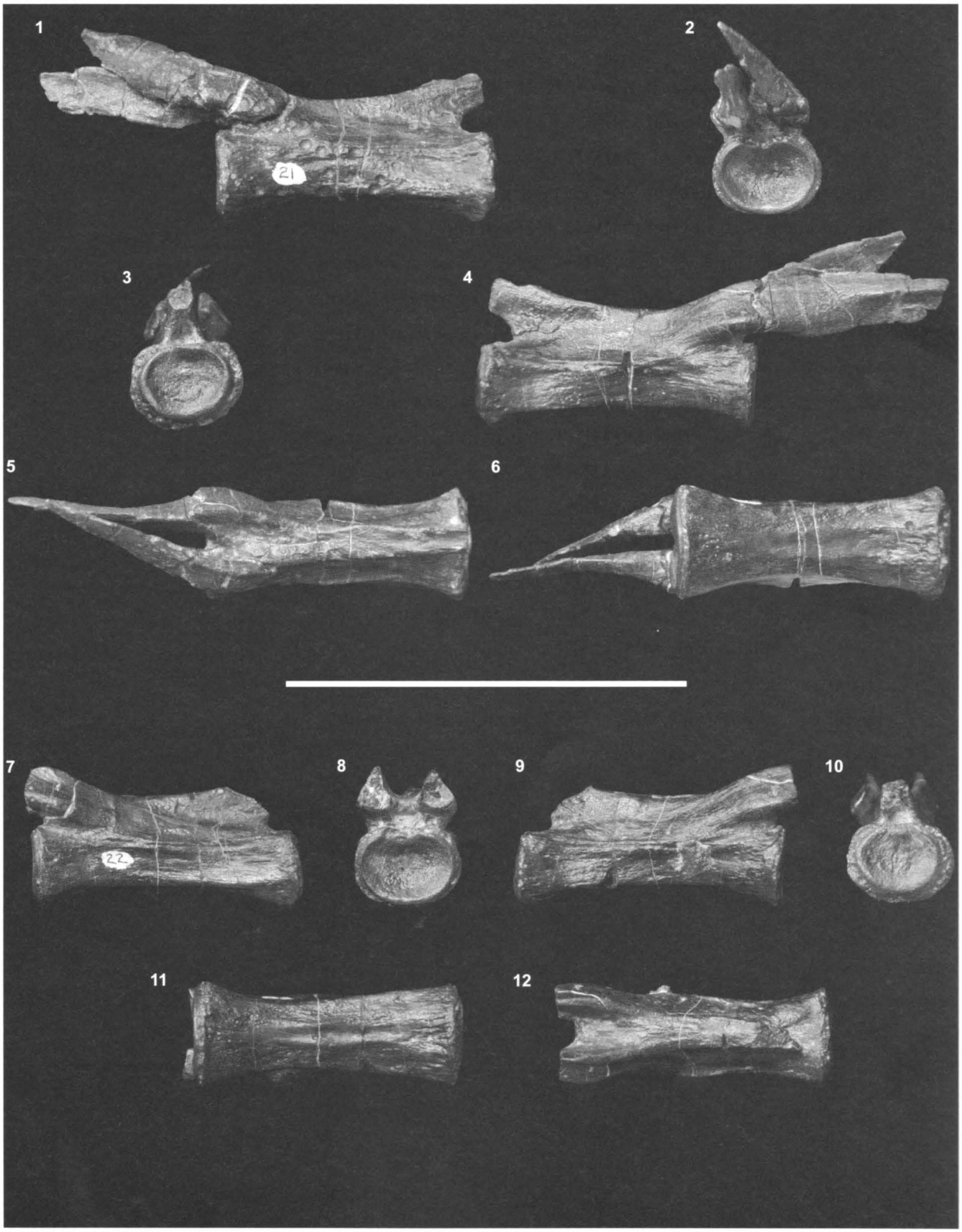
1
2
3
4
5
6
7
8
9
10
11
12

PLATE 24

Fig.

Neovenator salerii Hutt, Martill & Barker, 1996

1 Proximal caudal chevron (MIWG 6348) in anterior view.

2 Proximal caudal chevron (MIWG 6348) in left lateral view.

3 Proximal caudal chevron (MIWG 6348) in posterior view.

4 Proximal caudal chevron (MIWG 6348) in right lateral view.

5 Middle caudal chevron one (MIWG 6348) in anterior view.

6 Middle caudal chevron one (MIWG 6348) in left lateral view.

7 Middle caudal chevron one (MIWG 6348) in posterior view.

8 Middle caudal chevron one (MIWG 6348) in right lateral view.

9 Middle caudal chevron one (MIWG 6348) in proximal view.

10 Middle caudal chevron two (MIWG 6348) in proximal view.

11 Middle caudal chevron two (MIWG 6348) in anterior view.

12 Middle caudal chevron two (MIWG 6348) in left lateral view.

13 Middle caudal chevron two (MIWG 6348) in posterior view.

14 Middle caudal chevron two (MIWG 6348) in right lateral view.

15 Distal caudal chevron (MIWG 6348) in anterior view.

16 Distal caudal chevron (MIWG 6348) in left lateral view.

17 Distal caudal chevron (MIWG 6348) in posterior view.

18 Distal caudal chevron (MIWG 6348) in right lateral view.

Scale bar represents 50 mm.

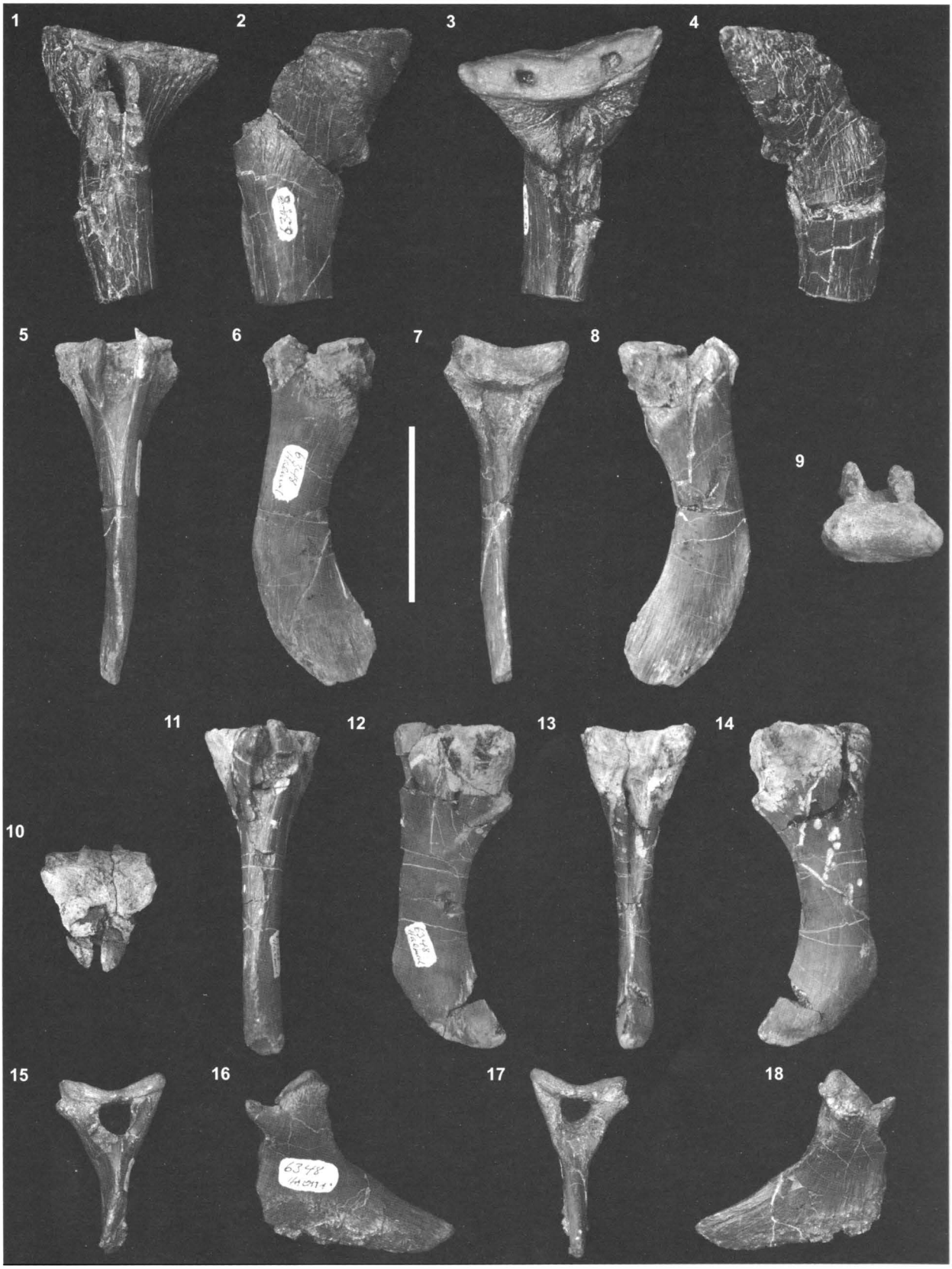
1
2
3
4
5
6
7
8
9
10
11
12
13
14
15
16
17
18

PLATE 25

Fig.

Neovenator salerii Hutt, Martill & Barker, 1996

1 Cervical rib (MIWG 6348) in lateral view.

2 Cervical rib (MIWG 6348) in medial view.

3 Cervical rib (MIWG 6348) in anterior view.

4 Cervical rib (MIWG 6348) in posterior view.

5 Dorsal rib (MIWG 6348) in lateral view.

6 Dorsal rib (MIWG 6348) in medial view.

7 Dorsal rib (MIWG 6348) in lateral view.

8 Dorsal rib (MIWG 6348) in medial view.

9 Dorsal rib capitulum (MIWG 6348) in cross sectional view.

10 Dorsal rib capitulum (MIWG 6348) in lateral view.

11 Gastral element (MIWG 6348).

12 Proximal end of medial gastral element (MIWG 6348) in ventral view.

13 Proximal end of medial gastral element (MIWG 6348) in dorsal view.

14 Distal end of medial gastral element (MIWG 6348).

Scale bars represent 20 mm.

1
2
3
4
5
6
9
10
7
8
11
12
13
14

PLATE 26

Fig.

Neovenator salerii Hutt, Martill & Barker, 1996

1 Dorsal vertebra 1 (MIWG 5470) in left lateral view.

2 Dorsal vertebra 1 (MIWG 5470) in anterior view.

3 Dorsal vertebra 1 (MIWG 5470) in right lateral view.

4 Dorsal vertebra 1 (MIWG 5470) in posterior view.

5 Dorsal vertebra 1 (MIWG 5470) in ventral view.

6 Dorsal vertebra 1 (MIWG 5470) in dorsal view.

7 Dorsal vertebra 8 (MIWG 5470) in left lateral view.

8 Dorsal vertebra 8 (MIWG 5470) in ventral view.

9 Dorsal vertebra 8 (MIWG 5470) in dorsal view.

10 Dorsal vertebra 8 (MIWG 5470) in anterior view.

11 Dorsal vertebra 8 (MIWG 5470) in right lateral view.

12 Dorsal vertebra 8 (MIWG 5470) in posterior view.

Scale bar represents 100 mm.

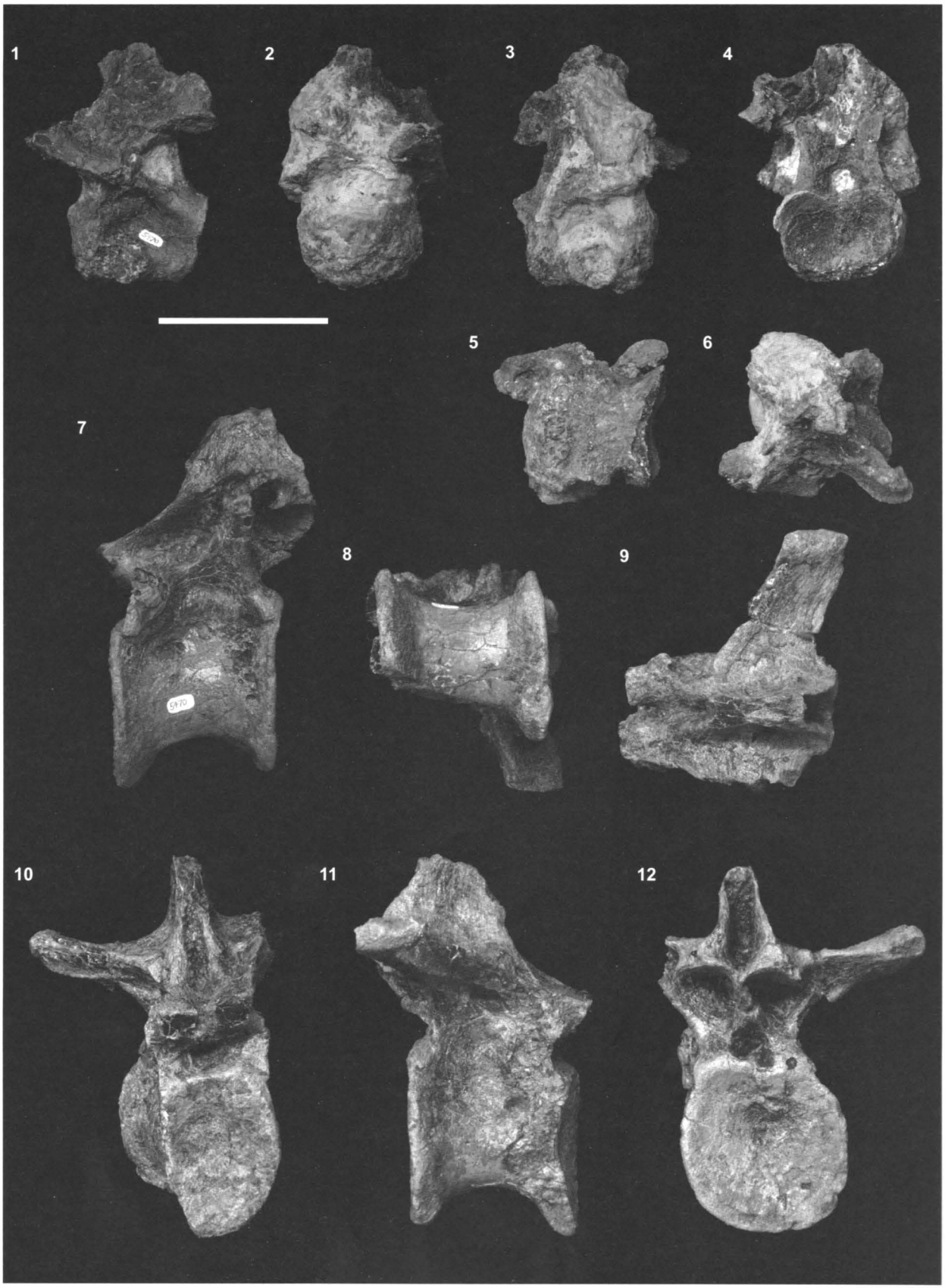
1
2
3
4
5
6
7
8
9
10
11
12

PLATE 27

Fig.

Neovenator salerii Hutt, Martill & Barker, 1996

1 Dorsal vertebra 2 (MIWG 6352) in left lateral view.

2 Dorsal vertebra 2 (MIWG 6352) in anterior view.

3 Dorsal vertebra 2 (MIWG 6352) in right lateral view.

4 Dorsal vertebra 2 (MIWG 6352) in ventral view.

5 Dorsal vertebra 2 (MIWG 6352) in posterior view.

6 Dorsal vertebra 2 (MIWG 6352) in dorsal view.

7 Dorsal vertebra 5 (MIWG 6352) in left lateral view.

8 Dorsal vertebra 5 (MIWG 6352) in anterior view.

9 Dorsal vertebra 5 (MIWG 6352) in right lateral view.

10 Dorsal vertebra 5 (MIWG 6352) in ventral view.

11 Dorsal vertebra 5 (MIWG 6352) in posterior view.

12 Dorsal vertebra 5 (MIWG 6352) in dorsal view.

Scale bar represents 100 mm.

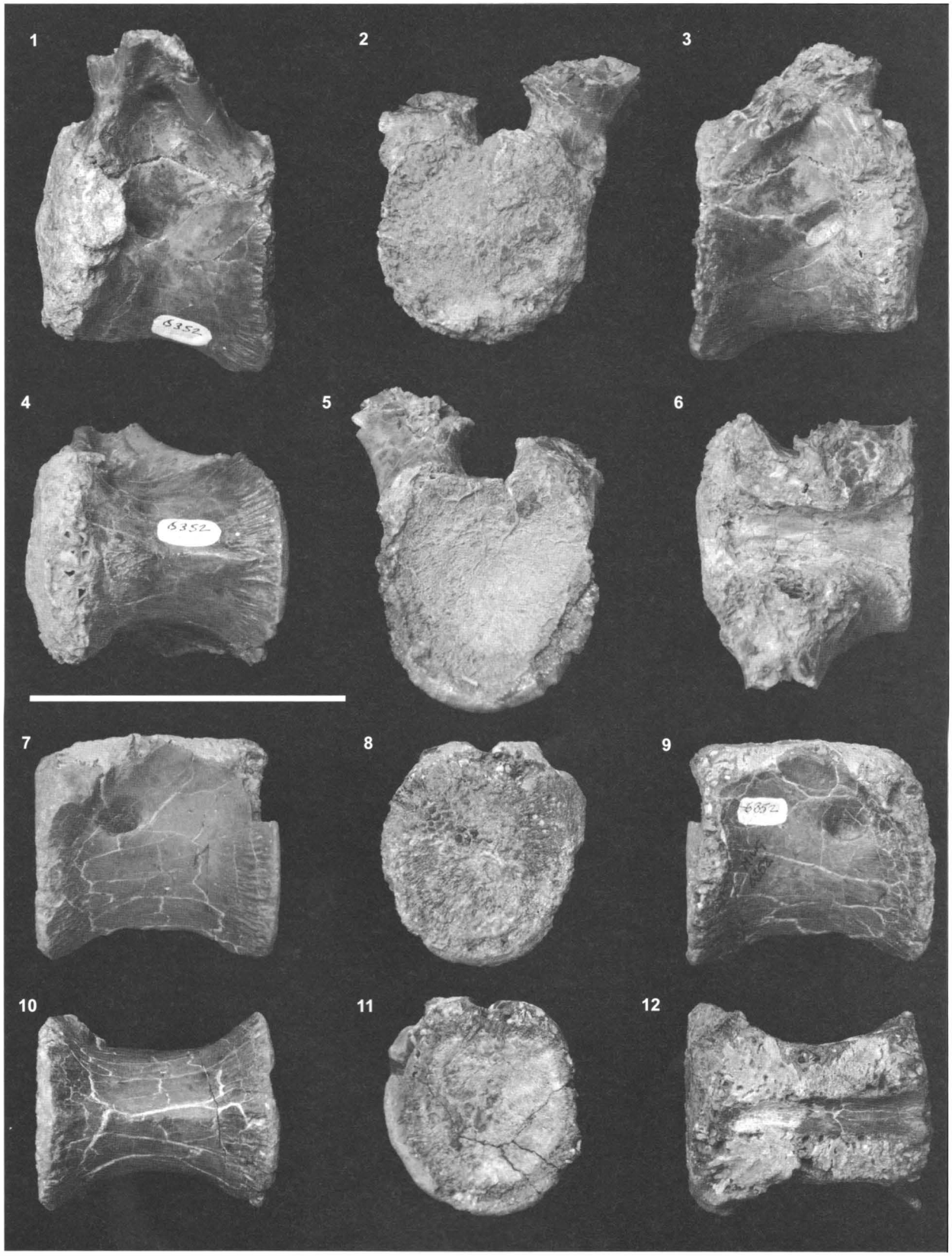
1
2
3
4
5
6
7
8
9
10
11
12

PLATE 28

Fig.

Neovenator salerii Hutt, Martill & Barker, 1996

1 Dorsal vertebra 6 (MIWG 6352) neural arch in left lateral view.

2 Dorsal vertebra 6 (MIWG 6352) neural arch in anterior view.

3 Dorsal vertebra 6 (MIWG 6352) neural arch in right lateral view.

4 Dorsal vertebra 6 (MIWG 6352) neural arch in ventral view.

5 Dorsal vertebra 6 (MIWG 6352) neural arch in posterior view.

6 Dorsal vertebra 6 (MIWG 6352) neural arch in dorsal view.

7 Chevron (MIWG 6352) in left lateral view.

8 Chevron (MIWG 6352) in anterior view.

9 Chevron (MIWG 6352) in right lateral view.

10 Chevron (MIWG 6352) in posterior view.

Scale bar represents 100 mm.

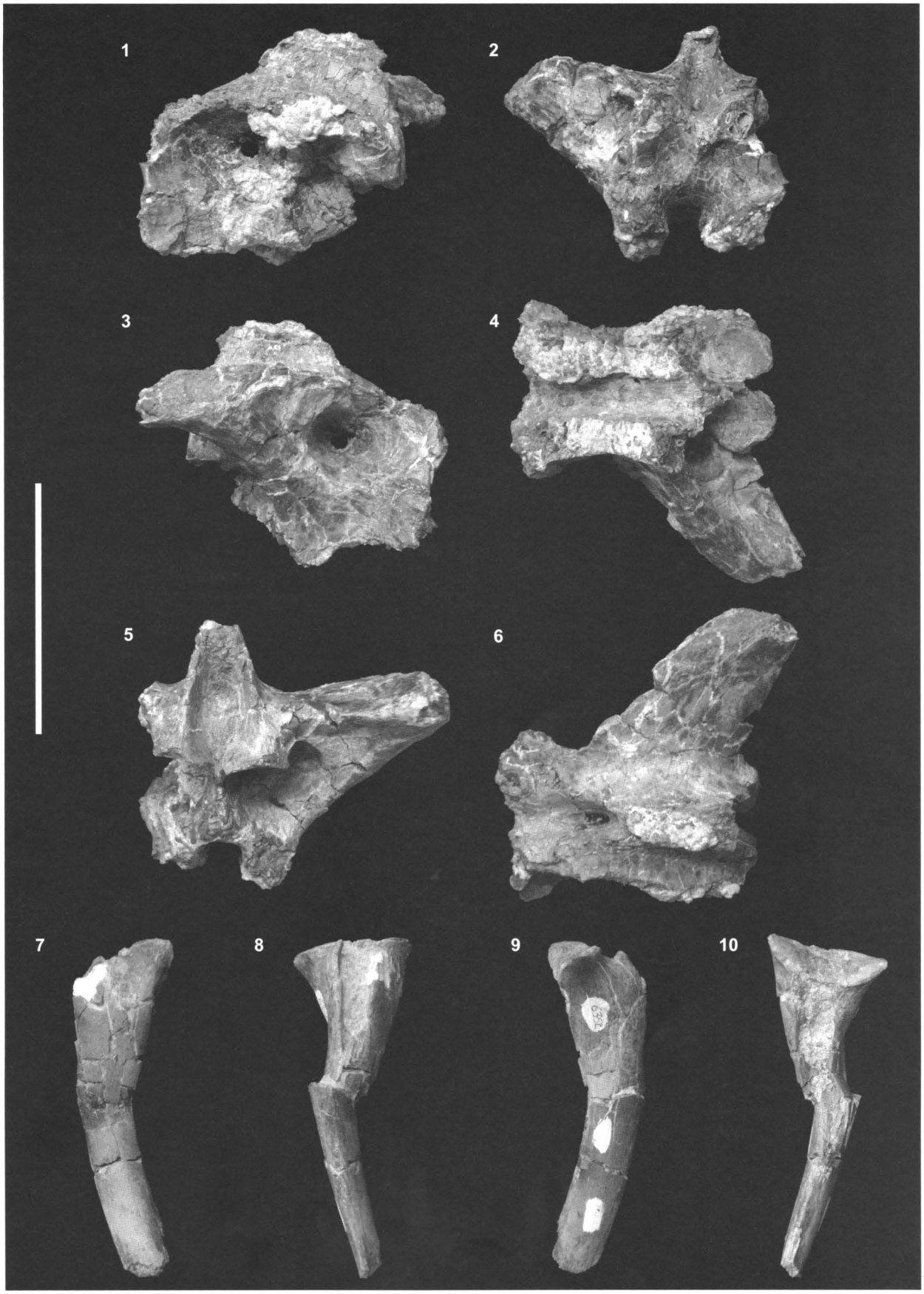
1
2
3
4
5
6
7
8
9
10

PLATE 29

Fig.

Neovenator salerii Hutt, Martill & Barker, 1996

1 Sacral vertebrae 2–4 (MIWG 6352) in left lateral view.

2 Sacral vertebrae 2–4 (MIWG 6352) in right lateral view.

3 Sacral vertebrae 2–4 (MIWG 6352) in dorsal view.

4 Sacral vertebra 2 (MIWG 6352) in anterior view.

5 Sacral vertebra 3 (MIWG 6352) in posterior view.

6 Sacral vertebra 4 (MIWG 6352) in anterior view.

7 Sacral vertebra 4 (MIWG 6352) in posterior view.

8 Isolated sacral (?) (MIWG 6352) in lateral view.

9 Isolated sacral (?) (MIWG 6352) in lateral view.

10 Isolated sacral (?) (MIWG 6352) in ventral view.

11 Isolated sacral (?) (MIWG 6352) in dorsal view.

12 Isolated sacral (?) (MIWG 6352) in anterior/posterior view.

13 Isolated sacral (?) (MIWG 6352) in anterior/posterior view.

14 Isolated sacral neural arch (MIWG 6352) in anterior view.

15 Isolated sacral neural arch (MIWG 6352) in posterior view.

16 Isolated sacral neural arch (MIWG 6352) in left lateral view.

17 Isolated sacral neural arch (MIWG 6352) in right lateral view.

18 Isolated sacral neural arch (MIWG 6352) in ventral view.

Scale bars represent 50 mm. Uncertain identity of isolated sacral precludes definitive identification of left/right lateral and anterior/posterior views.

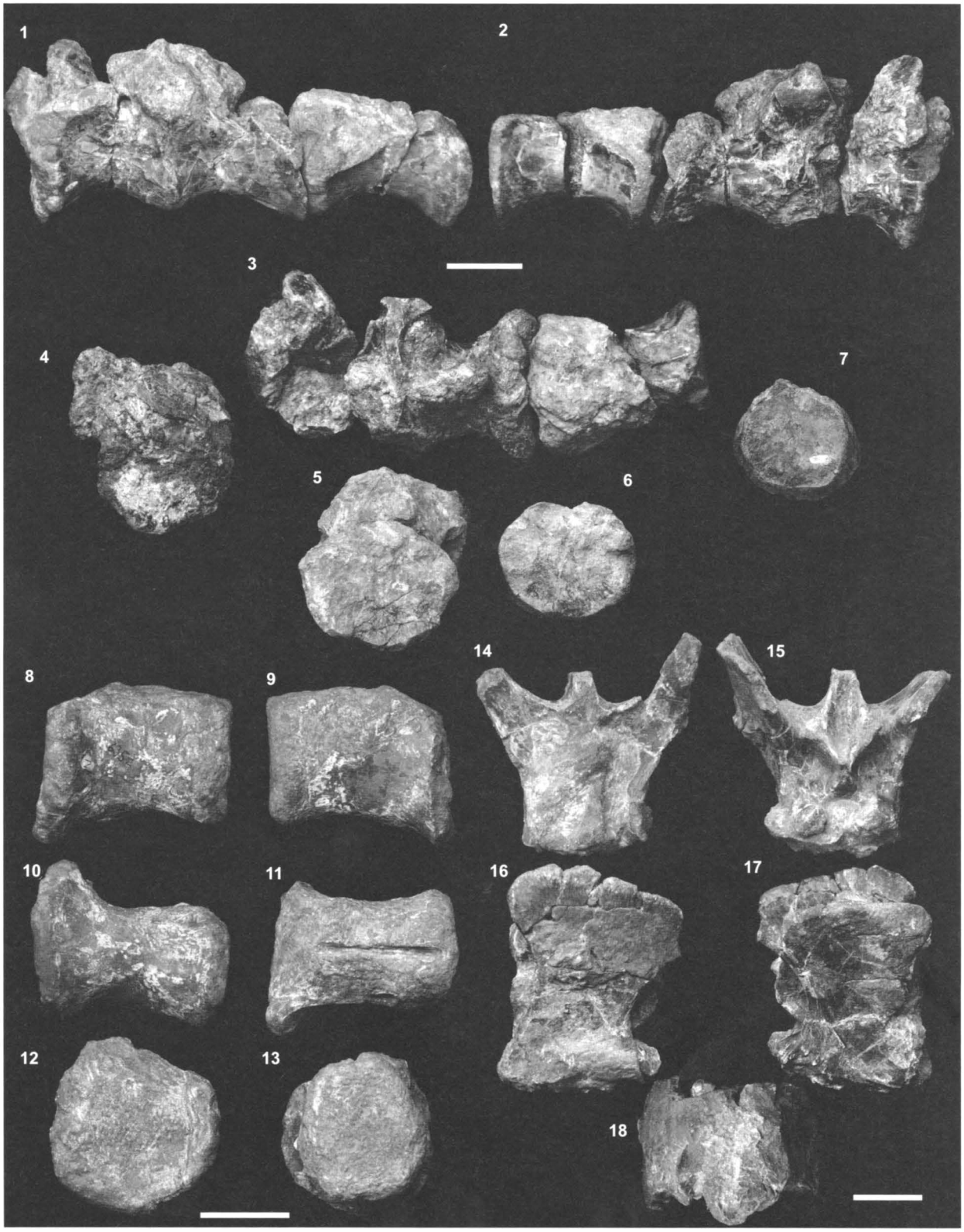
1
2
3
4
5
6
7
8
9
10
11
12
13
14
15
16
17
18

PLATE 30

Fig.

Neovenator salerii Hutt, Martill & Barker, 1996

1 Left scapula and coracoid (MIWG 6348) in lateral view.

2 Left scapula and coracoid (MIWG 6348) in medial view.

3 Left scapula and coracoid (MIWG 6348) in dorsal view.

4 Left scapula and coracoid (MIWG 6348) in ventral view.

5 Left coracoid and anterior scapula (MIWG 6348) in lateral view.

6 Left coracoid and anterior scapula (MIWG 6348) in medial view.

Scale bars represent 100 mm.

1
2
3
4
5
6

PLATE 31

Fig.

Neovenator salerii Hutt, Martill & Barker, 1996

1 Right ilium (BMNH R10001) in lateral view.

2 Right ilium (BMNH R10001) in medial view.

3 Right ilium (BMNH R10001) in ventral view.

4 Acetabular region of right ilium (BMNH R10001) in dorsal view.

5 Right ilium (BMNH R10001) in posterior view.

Scale bar represents 100 mm.

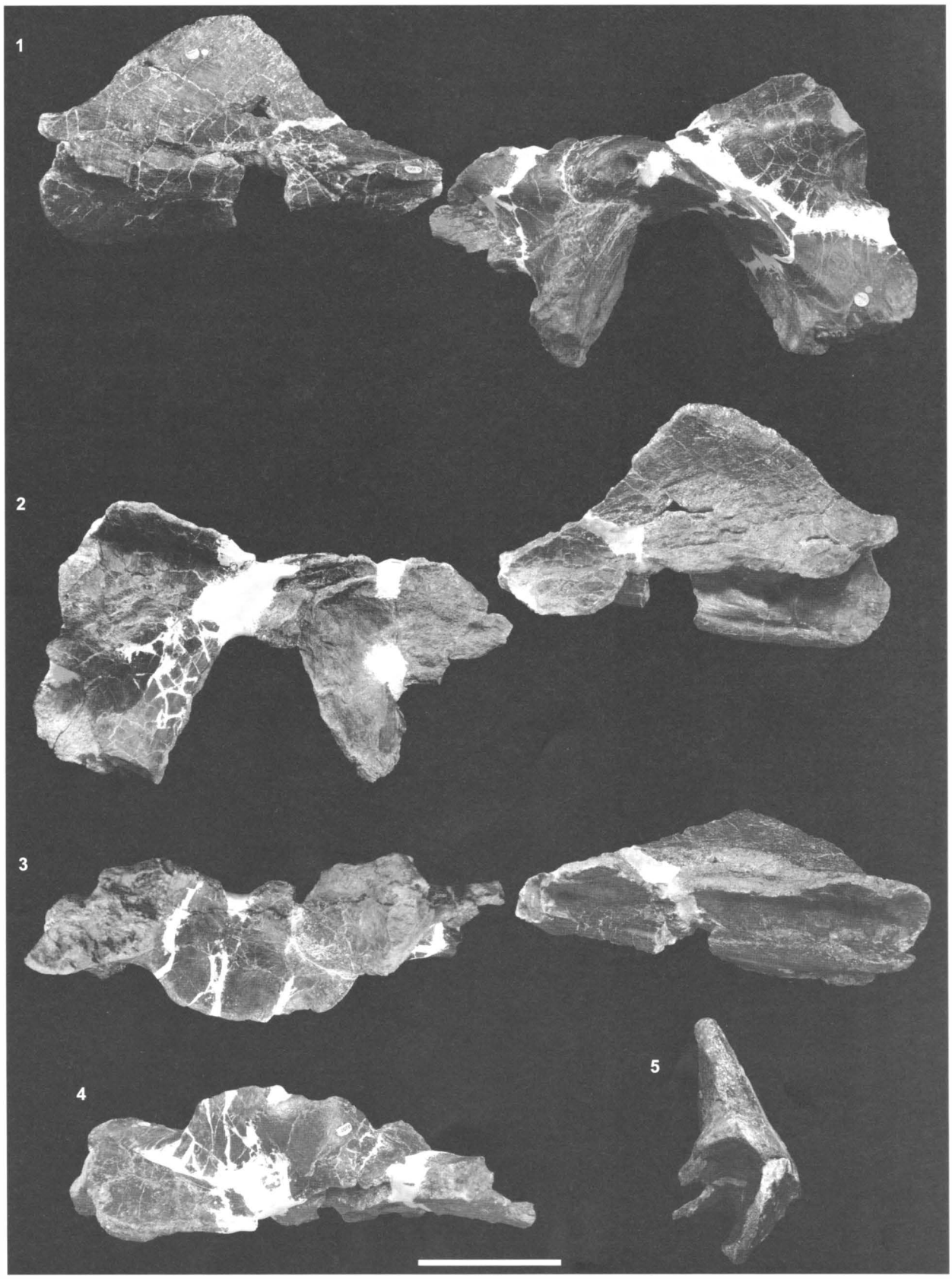
1
2
3
4
5

PLATE 32

Fig.

Neovenator salerii Hutt, Martill & Barker, 1996

1 Left ilium (BMNH R10001) in lateral view.

2 Left ilium (BMNH R10001) in medial view.

3 Left ilium (BMNH R10001) in ventral view.

Scale bar represents 100 mm.

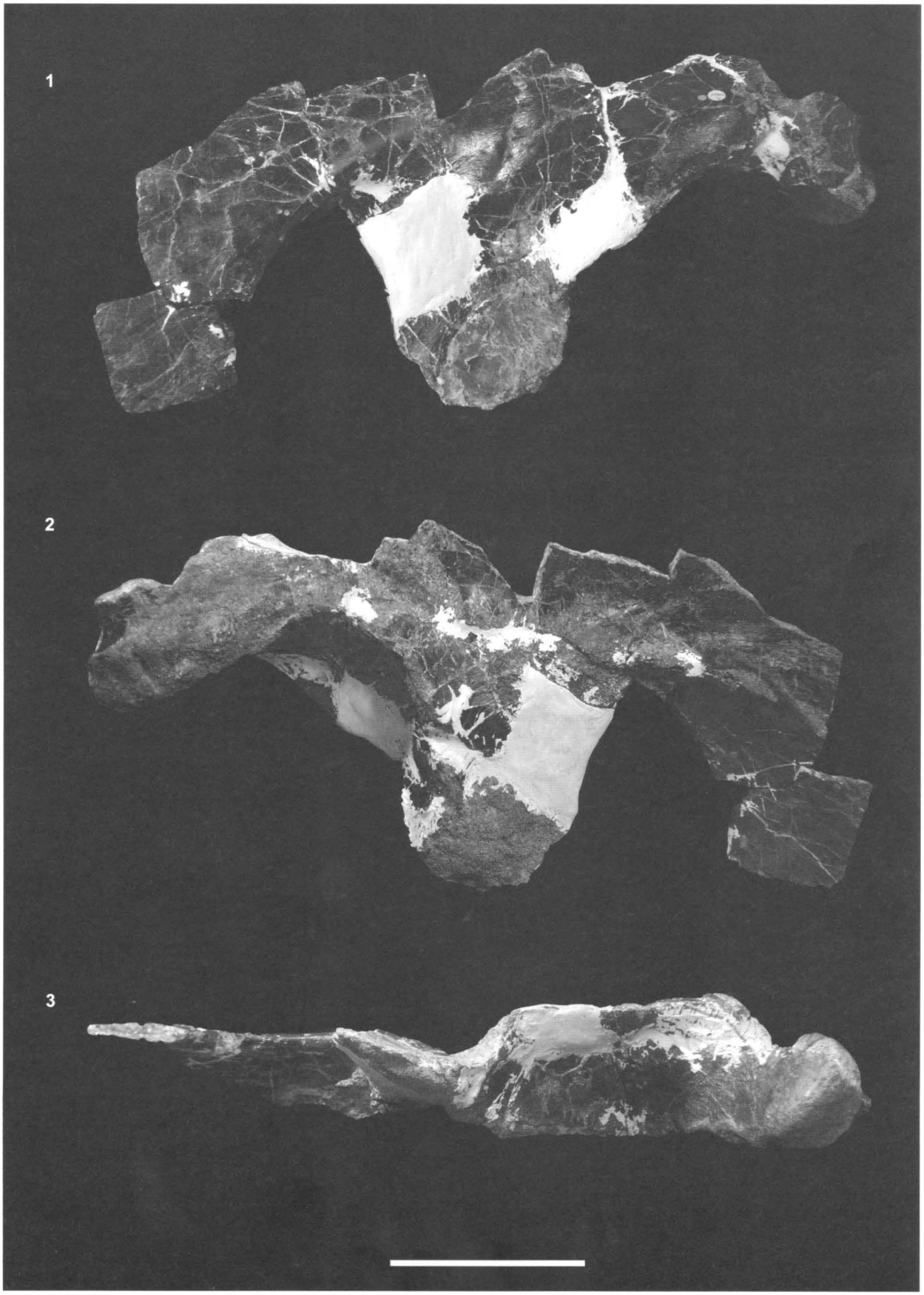
1
2
3

PLATE 33

Fig.

Neovenator salerii Hutt, Martill & Barker, 1996

1 Left ilium (MIWG 6348) in lateral view.

2 Left ilium (MIWG 6348) in medial view.

3 Left ilium (MIWG 6348) in dorsal view.

4 Left ilium (MIWG 6348) in ventral view.

Scale bar represents 100 mm.

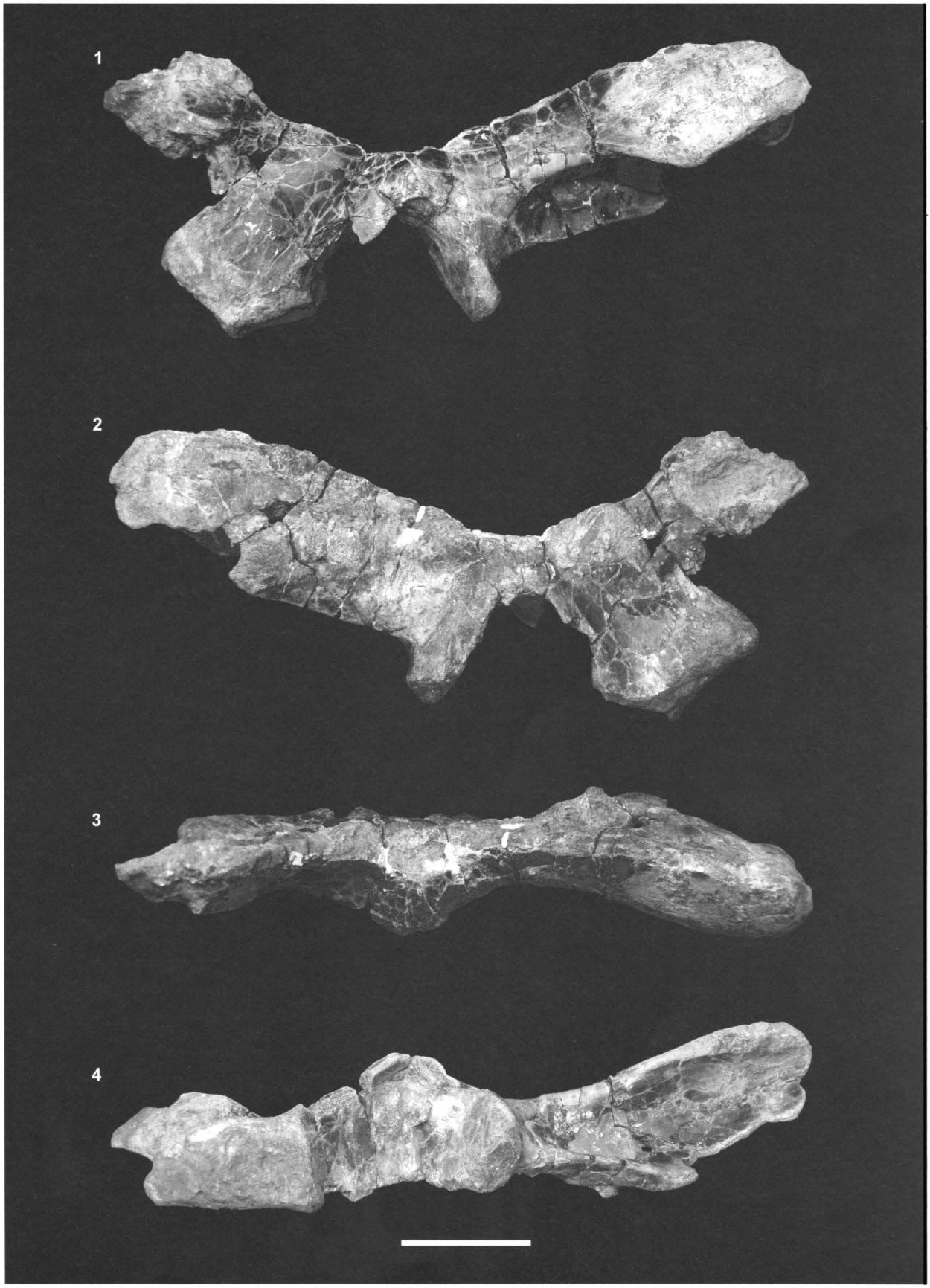
1
2
3
4

PLATE 34

Fig.

Neovenator salerii Hutt, Martill & Barker, 1996

1 Pubis (BMNH R10001) shaft fragment 1 in standard (anterior, posterior, lateral, medial) and cross sectional views of each broken end.

2 Pubis (BMNH R10001) shaft fragment 2.

3 Pubis (BMNH R10001) shaft fragment 3.

4 Pubis (BMNH R10001) shaft fragment 4.

Scale bars represent 100 mm; right scale bar refers to cross sections only.

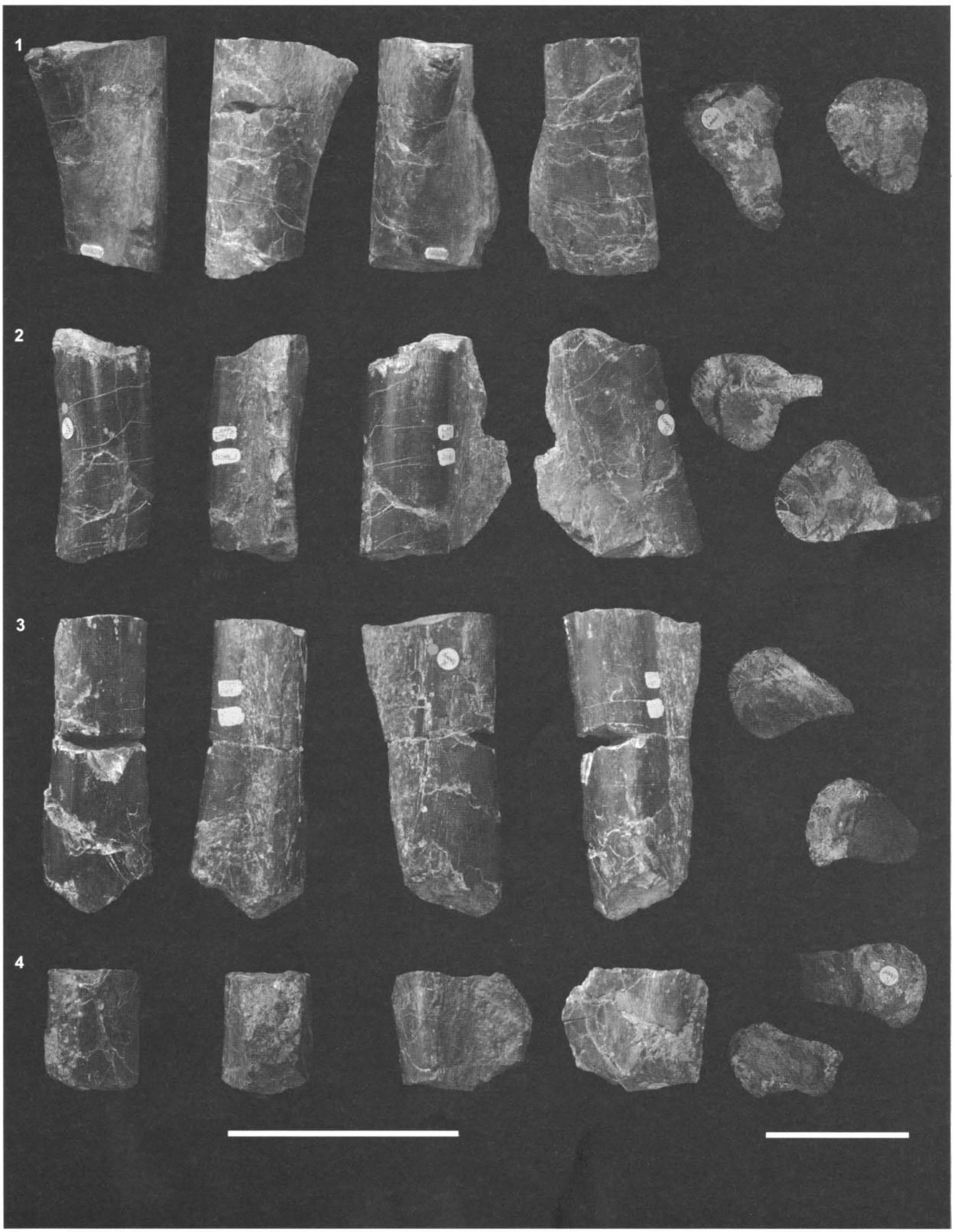
1
2
3
4

PLATE 35

Fig.

Neovenator salerii Hutt, Martill & Barker, 1996

1 Right pubis (BMNH R10001) in anterior view.

2 Right pubis (BMNH R10001) in posterior view.

3 Right pubis (BMNH R10001) in lateral view.

4 Right pubis (BMNH R10001) in medial view.

5 Right pubis (BMNH R10001) in proximal view.

6 Cross section of right pubis (BMNH R10001) at distal broken surface.

Scale bar represents 100 mm.

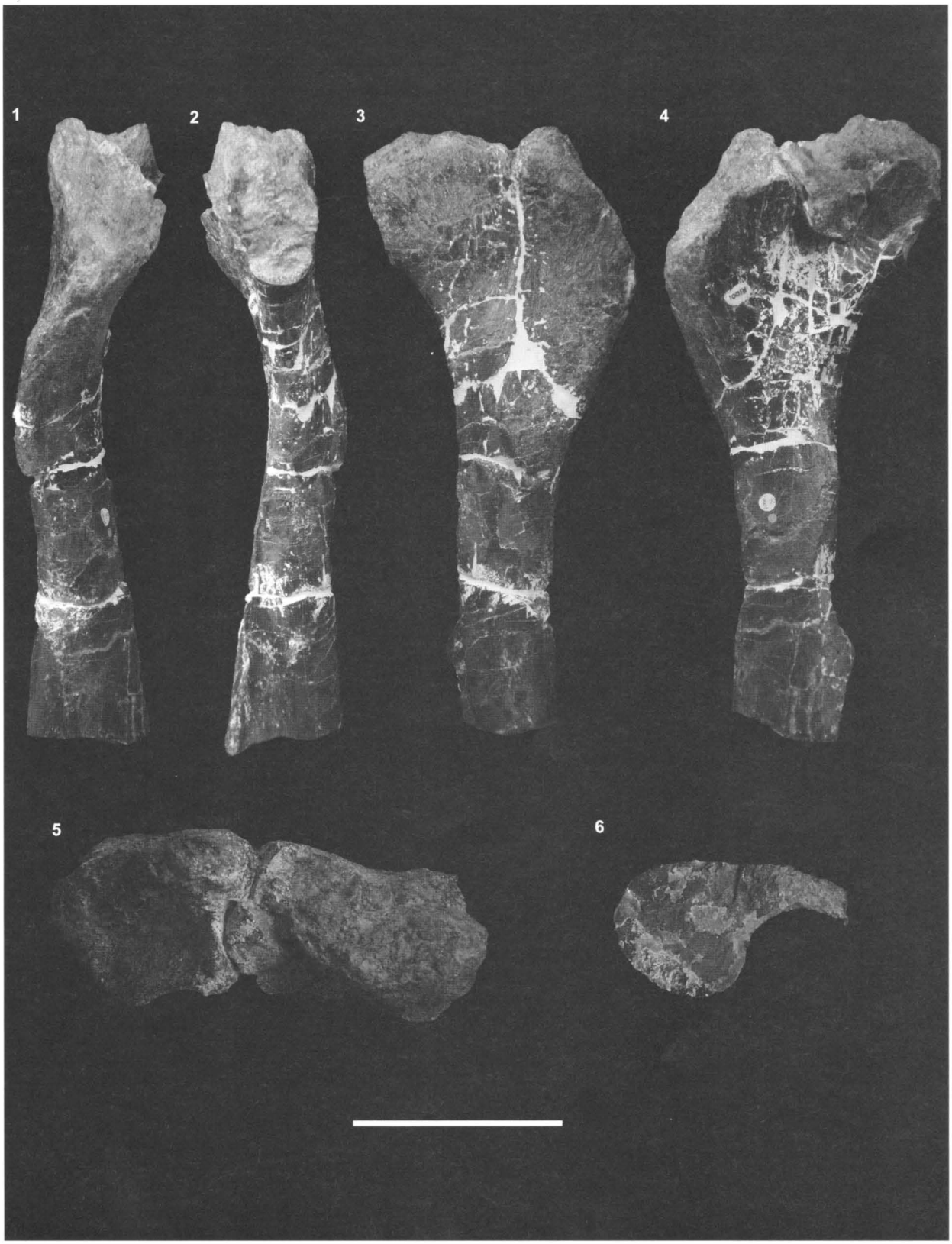
1
2
3
4
5
6

PLATE 36

Fig.

Neovenator salerii Hutt, Martill & Barker, 1996

1 Left pubic shaft (MIWG 6348) in anterior view.

2 Left pubic shaft (MIWG 6348) in posterior view.

3 Left pubic shaft (MIWG 6348) in lateral view.

4 Left pubic shaft (MIWG 6348) in medial view.

5 Left pubic shaft (MIWG 6348) in proximal view.

6 Conjoined pubic boot (MIWG 6348) in left lateral view.

7 Conjoined pubic boot (MIWG 6348) in right lateral view.

8 Conjoined pubic boot (MIWG 6348) in dorsal view.

9 Conjoined pubic boot (MIWG 6348) in ventral view.

Main scale bar represents 100 mm. Scale bar (representing 50 mm) next to figure 5 is for that image only.

1
2
3
4
5
6
7
8
9

PLATE 37

Fig.

Neovenator salerii Hutt, Martill & Barker, 1996

1 Left ischium (MIWG 6348) in anterior view.

2 Left ischium (MIWG 6348) in posterior view.

3 Left ischium (MIWG 6348) in lateral view.

4 Left ischium (MIWG 6348) in medial view.

5 Left ischium (MIWG 6352) in anterior view.

6 Left ischium (MIWG 6352) in posterior view.

7 Left ischium (MIWG 6352) in lateral view.

8 Left ischium (MIWG 6352) in proximal view.

Scale bars represent 50 mm.

1
2
3
4
5
6
7
8

PLATE 38

Fig.

Neovenator salerii Hutt, Martill & Barker, 1996

1 Proximal region of right ischium (BMNH R10001) in lateral view.

2 Proximal region of right ischium (BMNH R10001) in medial view.

3 Ischial shaft fragment (BMNH R10001) in four views (anterior, posterior, lateral, medial) and cross sectional views of both broken surfaces.

4 Ischial shaft fragment (BMNH R10001) in four views (anterior, posterior, lateral, medial).

Scale bar represents 100 mm.

1
2
3
4

PLATE 39

Fig.

Neovenator salerii Hutt, Martill & Barker, 1996

1 Conjoined distal ischia (BMNH R10001) ('boot' region) in left lateral view.

2 Conjoined distal ischia (BMNH R10001) ('boot' region) in right lateral view.

3 Conjoined distal ischia (BMNH R10001) ('boot' region) in anterior view.

4 Conjoined distal ischia (BMNH R10001) ('boot' region) in ventral view, anterior to the left.

Scale bar represents 100 mm.

1
2
3
4

PLATE 40

Fig.

Neovenator salerii Hutt, Martill & Barker, 1996

1 Right femur (MIWG 6348) in anterior view.

2 Right femur (MIWG 6348) in lateral view.

3 Right femur (MIWG 6348) in posterior view.

4 Right femur (MIWG 6348) in medial view.

5 Right femur (MIWG 6348) in proximal view.

6 Right femur (MIWG 6348) in distal view.

7 Left femur (MIWG 6348) in proximal view.

8 Left femur (MIWG 6348) in anterior view.

9 Left femur (MIWG 6348) in lateral view.

10 Left femur (MIWG 6348) in posterior view.

11 Left femur (MIWG 6348) in medial view.

12 Left femur (MIWG 6348) in distal view.

Scale bar represents 200 mm.

1
2
3
4
5
6
7
8
9
10
11
12

PLATE 41

Fig.

Neovenator salerii Hutt, Martill & Barker, 1996

1 Right tibia (MIWG 6348) in anterior view.

2 Right tibia (MIWG 6348) in lateral view.

3 Right tibia (MIWG 6348) in posterior view.

4 Right tibia (MIWG 6348) in medial view.

5 Right tibia (MIWG 6348) in proximal view.

6 Left fibula (MIWG 6348) in proximal view.

7 Left tibia (MIWG 6348) in proximal view.

8 Left tibia (MIWG 6348) in anterior view.

9 Left fibula (MIWG 6348) in anterior view.

10 Left tibia (MIWG 6348) in lateral view.

11 Left fibula (MIWG 6348) in lateral view.

12 Left fibula (MIWG 6348) in posterior view.

13 Left tibia (MIWG 6348) in posterior view.

14 Left fibula (MIWG 6348) in medial view.

15 Left tibia (MIWG 6348) in medial view.

16 Left tibia (MIWG 6348) in distal view.

17 Right tibia (MIWG 6348) in distal view.

Scale bar represents 200 mm.

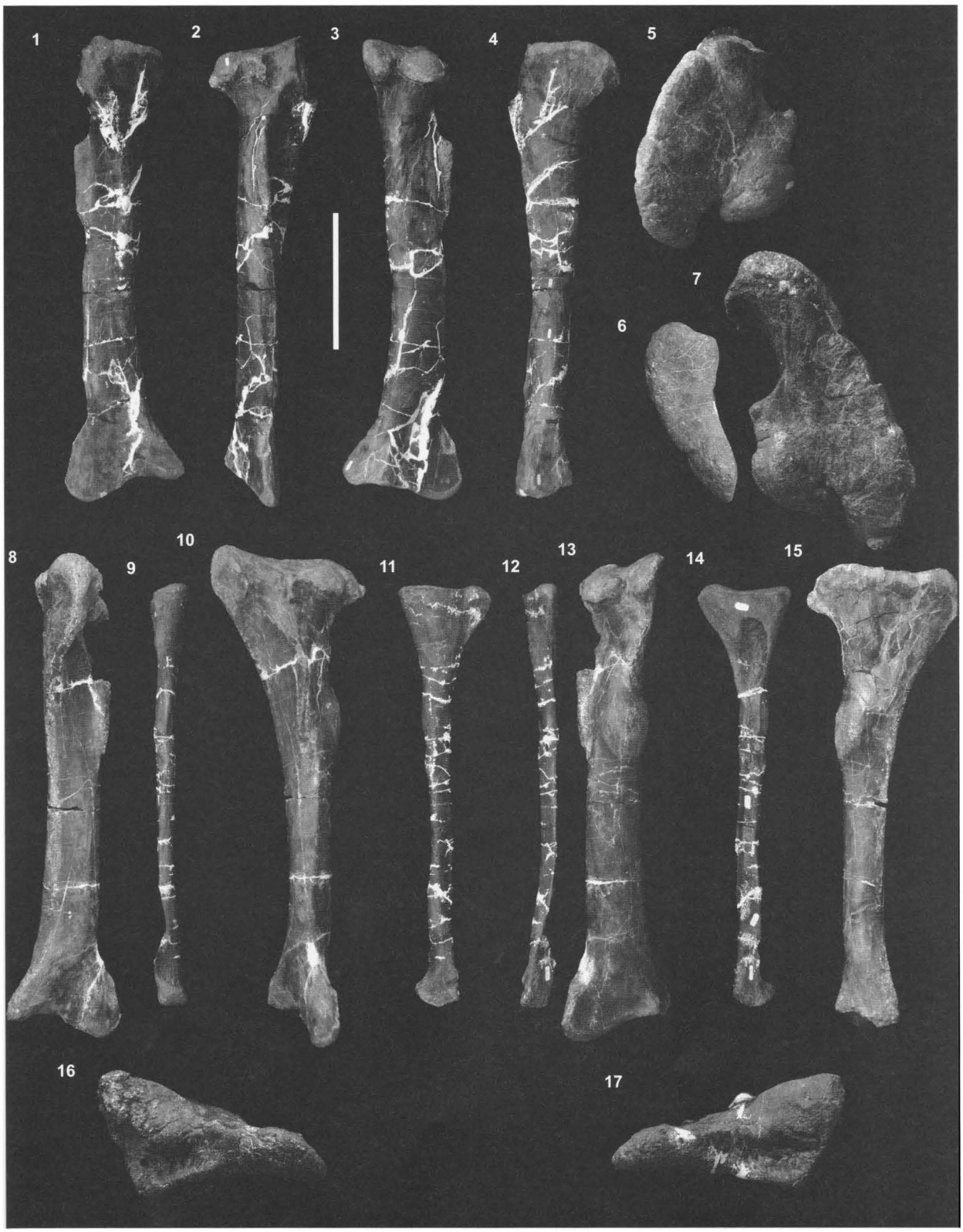
1
2
3
4
5
6
7
8
9
10
11
12
13
14
15
16
17

PLATE 42

Fig.

Neovenator salerii Hutt, Martill & Barker, 1996

1 Left metatarsal II (MIWG 6348) in anterior view.

2 Left metatarsal II (MIWG 6348) in posterior view.

3 Left metatarsal II (MIWG 6348) in lateral view.

4 Left metatarsal II (MIWG 6348) in medial view.

5 Left metatarsal II (MIWG 6348) in proximal view.

6 Left metatarsal II (MIWG 6348) in distal view.

7 Left metatarsal III (MIWG 6348) in anterior view.

8 Left metatarsal III (MIWG 6348) in posterior view.

9 Left metatarsal III (MIWG 6348) in lateral view.

10 Left metatarsal III (MIWG 6348) in medial view.

11 Left metatarsal III (MIWG 6348) in proximal view.

Scale bars represent 50 mm.

1
2
3
4
5
6
7
8
9
10
11

PLATE 43

Fig.

Neovenator salerii Hutt, Martill & Barker, 1996

1 Left metatarsal IV (MIWG 6348) in anterior view.

2 Left metatarsal IV (MIWG 6348) in posterior view.

3 Left metatarsal IV (MIWG 6348) in lateral view.

4 Left metatarsal IV (MIWG 6348) in medial view.

5 Left metatarsal IV (MIWG 6348) in proximal view.

6 Left metatarsal IV (MIWG 6348) in distal view

7 Left metatarsal V (MIWG 6348) in anterior view.

8 Left metatarsal V (MIWG 6348) in posterior view.

9 Left metatarsal V (MIWG 6348) in lateral view.

10 Left metatarsal V (MIWG 6348) in medial view.

11 Right phalanx IV-3 (MIWG 6348) in extensor view.

12 Right phalanx IV-3 (MIWG 6348) in flexor view.

13 Right phalanx IV-3 (MIWG 6348) in lateral view.

14 Right phalanx IV-3 (MIWG 6348) in medial view.

15 Right phalanx IV-3 (MIWG 6348) in distal view.

16 Right phalanx IV-3 (MIWG 6348) in proximal view.

Scale bars represent 50 mm.

1
2
3
4
5
6
7
8
9
10
11
12
13
14
15
16

PLATE 44

Fig.

Neovenator salerii Hutt, Martill & Barker, 1996

1 Left pes (MIWG 6348) in extensor view.

2 Left pes (MIWG 6348) in flexor view.

3 Left pes (metatarsals) (MIWG 6348) in proximal view.

4 Left phalanx II-1 (MIWG 6348) in medial view.

5 Left phalanx II-2 (MIWG 6348) in medial view.

6 Left phalanx III-4 (MIWG 6348) in medial view.

7 Left phalanx IV-1 (MIWG 6348) in medial view.

8 Left phalanx IV-2 (MIWG 6348) in medial view.

9 Left phalanx IV-3 (MIWG 6348) in medial view.

10 Left phalanx IV-4 (MIWG 6348) in medial view.

11 Left phalanx IV-5 (MIWG 6348) in medial view.

Scale bar above represents 50 mm and below represents 20 mm.

1
2
3
4
5
6
7
8
9
10
11

PLATE 45

Fig.

Neovenator salerii Hutt, Martill & Barker, 1996

1 Left phalanx II-1 (MIWG 6348) in lateral, proximal, and distal views.

2 Left phalanx II-2 (MIWG 6348) in lateral, proximal, and distal views.

3 Left phalanx II-4 (MIWG 6348) in lateral and proximal views.

4 Left phalanx IV-5 (MIWG 6348) in lateral and proximal views.

5 Left phalanx IV-4 (MIWG 6348) in lateral, proximal, and distal views.

6 Left phalanx IV-3 (MIWG 6348) in lateral, proximal, and distal views.

7 Left phalanx IV-2 (MIWG 6348) in lateral, proximal, and distal views.

8 Left phalanx IV-1 (MIWG 6348) in lateral, proximal, and distal views.

Scale bars represent 50 mm. Scale bar above is for lateral views; bottom scale bar for proximal and distal views.

1
2
3
4
5
6
7
8